UNIVERSITY OF SOUTHAMPTON

FACULTY OF ENGINEERING, SCIENCE & MATHEMATICS

School of Ocean & Earth Sciences

Nitrogen Nutrition of Harmful Algal Blooms in Upwelling Systems

by

Sophie Seeyave

Thesis for the degree of Doctor of Philosophy

June 2009

UNIVERSITY OF SOUTHAMPTON

ABSTRACT

FACULTY OF ENGINEERING, SCIENCE & MATHEMATICS
SCHOOL OF OCEAN & EARTH SCIENCES

Doctor of Philosophy

NITROGEN NUTRITION OF HARMFUL ALGAL BLOOMS IN UPWELLING SYSTEMS

By Sophie Seeyave

Blooms of toxic, or otherwise harmful phytoplankton species are known to occur in eastern boundary upwelling systems, coincident with the relaxation of upwelling in late summer/autumn. Field studies were carried out in 3 consecutive summers (March/April 06-08) in the Benguela and in the autumn (Sept 06) and summer (June 07) in the Iberian upwelling system (Ría de Vigo), with the aim of identifying common nitrogen nutrition strategies of HAB species that may allow them to succeed in upwelling systems. Two summer field studies were also carried out in the Fal Estuary (UK) to identify possible differences between a UK estuary and these upwelling systems.

In the Benguela, three toxic phytoplankton species were dominant under different nutrient conditions. *Pseudo-nitzschia* spp. were abundant during a period of strong upwelling and high NO_3^-, peaking during short periods of wind relaxation. During these periods, a switch from high nitrate uptake [$\rho(NO_3^-)$] to regenerated nitrogen uptake [$\rho(NH_4^+)$ and ρ(urea)] occurred, with f-ratios dropping from 0.79 to 0.12. *Alexandrium catenella* bloomed during a period of upwelling, displaying high $\rho(NO_3^-)$ and f-ratios up to 0.87. *Dinophysis acuminata* dominated when NO_3^- concentrations were <0.5 μmol l^{-1} and f-ratios <0.1 in 2007, although in 2008 it formed a subsurface maximum, often associated with high NO_3^- concentrations. Nutrient uptake kinetics showed that *Pseudo-nitzschia* spp. displayed the highest maximum specific uptake rates (v_{max}). *D. acuminata* displayed the highest affinity for NH_4^+, as shown by its α values (slope of the nutrient uptake vs. concentration curve). Thus, *A. catenella* was adapted to utilising high NO_3^- concentrations during upwelling pulses, whereas both *Pseudo-nitzschia* and *D. acuminata* were able to acclimate to both high and low NO_3^- concentrations during the upwelling/relaxation cycles.

In the Ría de Vigo, warm water from the stratified shelf entered the ría and downwelled in September, resulting in a well-mixed water column. The phytoplankton assemblage, dominated by *Ceratium* spp., *Dinophysis acuminata* and *Gymnodinium catenatum*, appeared to be advected in to the ría. Nitrate concentrations were consistently low, whereas NH_4^+ concentrations increased towards the head of the ría and with depth. The phytoplankton community was dependent on regenerated nitrogen, with f-ratios <0.2. In contrast, positive circulation in June resulted in strong vertical gradients in temperature, salinity and nutrients and a community dominated by diatoms. Nitrate and NH_4^+ were depleted in surface waters although uptake rates were higher than in September, as were the f-ratios (0.1-0.3).

In both systems, upwelling winds favoured diatoms, although they were able to utilise regenerated nitrogen when NO_3^- was depleted, whereas upwelling relaxation created favourable conditions for HAB development. *Dinophysis* spp. occurred in both systems and were able to grow on recycled nitrogen in the absence of NO_3^-. The Benguela showed high variability in the selection of particular HAB species, perhaps due to greater variability in upwelling-downwelling cycles. In the Ría de Vigo, the occurrence of downwelling and associated nutrient conditions leading to blooms of *Dinophysis* spp. and *Gymnodinium catenatum* seems more predictable.

In the Fal Estuary, *Alexandrium* spp. was favoured by low irradiance and the combination of strong stratification and high nutrient concentrations, and its growth was sustained predominantly by NH_4^+. *A. minutum* strains isolated from both upwelling systems and from a UK Lagoon all displayed higher v_{max} for NH_4^+ relative to NO_3^- but higher growth rates on the latter. This was consistent with field results from all 3 regions, suggesting that the upwelling systems did not display a different order of nitrogen preference, although they did display a higher affinity for NO_3^-.

TABLE OF CONTENTS

FIGURES

TABLES

APPENDIX

DECLARATION OF AUTHORSHIP

I, Sophie Seeyave, declare that the thesis entitled

"Nitrogen Nutrition of Harmful Algal Blooms in Upwelling Systems"

and the work presented in the thesis are both my own, and have been generated by me as the result of my own original research. I confirm that:

- this work was done wholly or mainly while in candidature for a research degree at this University;
- where any part of this thesis has previously been submitted for a degree or any other qualification at this University or any other institution, this has been clearly stated;
- where I have consulted the published work of others, this is always clearly attributed;
- where I have quoted from the work of others, the source is always given. With the exception of such quotations, this thesis is entirely my own work;
- I have acknowledged all main sources of help;
- where the thesis is based on work done by myself jointly with others, I have made clear exactly what was done by others and what I have contributed myself;
- parts of this work (Chapter 3) have been published as:

Seeyave S, Probyn TA, Pitcher GC, Lucas MI, Purdie DA (2009) Nitrogen nutrition in assemblages dominated by *Pseudo-nitzschia* spp., *Alexandrium catenella* and *Dinophysis acuminata* off the west coast of South Africa. Mar Ecol Prog Ser 379: 91-107.

Signed: ……..

Date:…….

Acknowledgements

I would like to thank my supervisors Dr Duncan Purdie (University of Southampton) for his guidance and support throughout the PhD and for his help during the Fal Estuary field trips; Dr Trevor Probyn (Marine & Coastal Management, Cape Town) for sharing his knowledge and ideas during the Lambert's Bay field trips and throughout the PhD, and Dr Michael Lucas (University of Cape Town) for his comments and advice with the thesis writing.

I also thank the Natural Environment Research Council (NERC) for offering me a CASE studentship and Wayne Barnes and the Abalone Farmers' Association of South Africa (AFASA) for their contribution.

This thesis has involved collaborations with scientists from various institutions, to whom I am very grateful for their hospitality and support.

I would like to thank the staff at MCM involved in the Lambert's Bay field trips, in particular Dr Grant Pitcher for organising the trips and for providing phytoplankton counts for 2008, Ms Desiree Calder for the phytoplankton counts and chl-a measurements in 2006 and 2007, Joyce Ntuli for the chl-a measurements in 2008 and Andre duRandt for the CTD and FRRf profiles and sample collection.

For the Ría de Vigo field work, my thanks go to the Oceanología team at the Instituto de Investigaciónes Marinas (IIM) in Vigo: Dr Carmen Castro for much help and kindness before, during and after the field trips; Dr Desmond Barton, for organising CRIA I and II, for allowing me to participate and for sharing his MiniBAT data; Dr Francisco Figueiras, for inviting me to join the field trip and for allowing me to use his chl-a and phytoplankton count data; Dr Xavier Antón (Pepe) Álvarez-Salgado, for logistical support in the lab and for providing me with his nutrient data; Waldo Redondo Caride for operating the CTD and providing the data; and all other IIM staff and students involved, in particular Dr Belén Arbones Fernández, Ms Rosa Bañuelos Fuentes, Ms Vanesa Vieitez Dos Santos, Dr Fernando Alonso Pérez and Dr Oscar Antonio Espinoza González;. I also wish to thank Dr Ricardo Torres (Plymouth Marine Laboratory), for helping to transport my equipment to and from Vigo.

For the Fal Estuary work, I wish to thank Dr Simon Boxall for allowing me to join the student field trips and to use the students' data. I am also grateful to Mr Bob Wilkie for his help on-board *RV Bill Conway*.

I also thank Mike Bolshaw for teaching me to use the stable isotope mass spectrometer and for his help with the instrument.

Finally, I would like to thank my husband Paul Lucas for his love and support over the years and over the world, and for his efforts not to distract me (too much) when I was writing at home. I also thank my parents Clément and Dominique Seeyave for steering me in the right direction throughout my childhood and teenage years, and for selflessly supporting me in all my decisions. I would also like to acknowledge all the friends and family who have brought comfort, fun and happiness to my life over the years. In particular, I thank my late friend Keith Pallett who was always passionate about science and was one of the rare people who loved discussing phytoplankton with me.

LIST OF ABBREVIATIONS

ASP: Amnesic Shellfish Poisoning

At %: % isotopic enrichment

AZP: Azaspiracid Shellfish Poisoning

CEFAS: Centre for Environment, Fisheries and Aquaculture Science

CFP: Ciguatera Fish Poisoning

chl-a: chlorophyll-a

CTD: Conductivity Temperature Depth

CO_2: carbon dioxide

CV: coefficient of variation

DA: Domoic Acid

DO: Dissolved Oxygen

DO_{Sat}: saturated DO concentration

DIN: Dissolved Inorganic Nitrogen

DON: Dissolved Organic Nitrogen

DSP: Diarrhetic Shellfish Poisoning

ENACW: Eastern North Atlantic Central Water

F_m: maximum fluorescence

F_0: initial fluorescence

FSA: Food Standards Agency

F_v/F_m: variable fluorescence divided by maximum fluorescence, a measure of photochemical efficiency of photosystem II

GC: Gas Chromatograph

GF/F: Glass Fibre Filtre

HAB: Harmful Algal Bloom

H': Shannon diversity index

I_{max}: maximum inhibition of NO_3 uptake by NO_2

K_i: half-inhibition constant

K_m: enzyme half-saturation constant

K_Q: nitrogen cell quota below which no cellular growth is observed

K_s: half-saturation constant for nutrient uptake

K_u: half-saturation constant for growth

m/z: mass to charge ratio

LOW: Low Oxygen Water

NH_4^+: ammonium

NiR: Nitrite Reductase

NO_2^-: nitrite

NO_3^-: nitrate

NR: Nitrate Reductase

NSP: Neurotoxic Shellfish Poisoning

OA: Okadaic Acid

PO_4^{3-}: dissolved inorganic phosphate

PN: Particulate Nitrogen

PSP: Paralytic Shellfish Poisoning

PSII : photosystem II

Q: nitrogen cell quota (N $cell^{-1}$)

r: particulate isotopic enrichment

R: aqueous isotopic enrichment (At%)

S: substrate concentration

SACW : South Atlantic Central Water

SD: Standard Deviation

SE: Standard Error

Si (= $Si(OH)_2$): dissolved inorganic silicate (silicic acid)

SIRMS: Stable Isotope Ratio Mass Spectrometry

V_{cell}: cell volume (μm^3)

α: ratio of ν_{max} to K_s, a measure of substrate affinity

δ: excess of ^{15}N relative to natural abundance

μ: cellular growth rate (d^{-1})

μ_{max}: maximum cellular growth rate (d^{-1})

$\rho(N)$: absolute rate of nitrogen uptake (μmol N l^{-1} h^{-1})

ν: PN-specific rate of nitrogen uptake (h^{-1})

σ_{PSII}: functional absorption cross-section of photosystem II

τ: photosynthetic turnover

ν_{max}: maximum PN-specific rate of nitrogen uptake (h^{-1})

$\nu_{max(cell)}$: maximum cell-specific rate of nitrogen uptake (h^{-1})

1 Introduction

1.1. Harmful Algal Blooms

Harmful Algal Blooms (HABs) are proliferations of planktonic algae that cause negative impacts on marine ecosystems, aquaculture resources and human health. They were previously known as "red tides", due to the water discolouration they often cause, however blooms do not need to be visible to cause harm, and conspicuous blooms are not necessarily harmful, hence the term HABs was deemed more appropriate. These blooms occur in coastal waters worldwide, often in harbours, embayments and lagoons which are used for human activities such as aquaculture, tourism and recreation. Their occurrence is thought to have become more frequent and widespread and their impacts more severe in recent years (Hallegraeff, 1993; Chretiennot-Dinet, 1998; Anderson et al., 2002). Some 300 phytoplankton species have been reported to produce "red tides", although only 60-80 species are intrinsically harmful due to biotoxin production, physical damage, anoxia, irradiance reduction or nutritional unsuitability. Among these, 90 % are flagellates and 75 % are dinoflagellates (Smayda, 1997).

Blooms of "benign" (i.e. non-toxic) species can reach extremely high concentrations and may result in water discolouration. Although these blooms often appear as red patches (e.g. *Noctiluca* spp., *Protogonyaulax spinifera*) hence the name "red tides", they can be a variety of different colours, such as the "brown tides" caused by the pelagophyte *Aureococcus anophagefferens* (Bricelj & Lonsdale, 1997). Such blooms are not necessarily harmful, but they can lead to extensive fish and shellfish mortalities when bloom decay causes anoxia and produces hydrogen sulfide. For example, an extensive bloom of *Ceratium furca* and *Prorocentrum micans* at Eland's Bay, on the west coast of South Africa, caused the stranding of 2,000 tonnes of rock lobster and an estimated economic loss of 50 million US dollars (Pitcher & Cockcroft, 1998). They can also negatively impact fauna and flora, such as eel grass and coral reef communities, by reducing light penetration. Other negative effects include mechanical damage to marine organisms, such as clogging of fish gills (e.g. the spiny diatom *Chaetoceros* spp.). The prymnesiophyte *Phaeocystis* spp. is known to form large mucilaginous colonies that can disrupt food-web dynamics and fisheries and have a negative impact on tourism, due to

the production of foam that washes up on beaches (Lancelot et al., 1987; Schoemann et al., 2005).

Blooms of toxic species are of major concern due to their human health and economic impacts. Paralytic (PSP), Diarrhetic (DSP), Amnesic (ASP), Neurotoxic (NSP) and Azaspiracid Shellfish Poisoning (AZP) occur as a result of the accumulation of toxins in filter-feeders, which may cause severe illness or even death to the consumer. *Gymnodinium breve* can cause NSP via shellfish consumption as well as producing aerosols that can cause respiratory problems and skin irritation in humans (Steidinger et al., 1998).

In tropical and subtropical regions, ciguatera toxins can also be bioaccumulated through the food chain to carnivorous fish and result in Ciguatera Fish Poisoning (CFP) from their consumption (Lewis, 1984). Bioaccumulation of the toxin domoic acid also occurs in anchovies on the California coast and has resulted in mortalities of brown pelicans (Work et al., 1992) and sea lions (Scholin et al., 2000). Some phytoplankton species produce toxins that are directly lethal to fish (ichthyotoxic), for example the dinoflagellate *Pfiesteria piscicida* (Morris, 1999) and the raphidophytes *Heterosigma akashiwo* (Honjo, 1993) and *Chattonella* spp.(Toyoshima et al., 1989).

PSP is caused by a group of 21 known closely related water-soluble neurotoxins (tetrahydropurines), comprising 4 sub-groups, (i) carbamate components (saxitoxin STX, neo-saxitoxin neo-STX and gonyautoxins GTX 1-4), (ii) N-sulfo-carbamoyl components (GTX 5-6, C1-C4), (iii) decarbamoyl components (dcSTX, dcneoSTX, dcGTX 1-4) and deoxydecarbamoyl components (doSTX, doneoSTX, doGTX 1) (van Egmond et al., 2004). The effects of PSP range from slight numbness and tingling to complete respiratory paralysis. Many causative organisms of PSP belong to the genus *Alexandrium* (e.g. *A. tamarense*, *A. catenella*, *A. minutum*, *A. fundyense*), while the chain-forming species *Gymnodinium catenatum* is the only athecate dinoflagellate known to produce PSP toxins.

DSP toxins are heat-stable polyether and lipophilic compounds that can be divided into several groups according to their chemical structure. The acidic toxins, which include okadaic acid (OA) and its derivatives dinophysistoxins (DTX 1, 2, 3), are the only group to produce diarrhetic symptoms. Other groups include neutral toxins, consisting of polyether-lactones belonging to the pectenotoxin group, of which 10 have been isolated to date, and yessotoxin (a sulphated polyether) and its derivatives (van Egmond et al., 2004). A related compound causing DSP symptoms was identified in

1995 and later called azaspiracid (Satake et al., 1998). DSP symptoms include diarrhoea, nausea, vomiting and abdominal pain. The main causative organisms of DSP belong to the genus *Dinophysis*, but also include *Protoceratium reticulatum* (Satake et al., 1999), *Lingulodinium polyedrum* and the benthic dinoflagellate *Prorocentrum lima*. *Dinophysis* spp. are known to cause toxicity in shellfish at cell concentrations as low as 200 cells l^{-1} (Lassus et al., 1985).

Several species of the pennate diatom *Pseudo-nitzschia* (e.g. *P. multiseries*, *P. australis, P. pseudodelicatissima*) have been found to produce the toxin domoic acid (DA), responsible for the syndrome ASP (Bates et al., 1989; Buck et al., 1992; Trainer et al., 2002). Domoic acid is an amino acid, which can be transferred through the food chain and can cause illness or death to fish, seabirds and marine mammals as well as humans. Unlike *Dinophysis* spp., high concentrations of cells (at least 100,000 cells l^{-1}) are necessary to produce toxin concentrations in shellfish that exceed the harvestable limit.

1.2. Adaptive strategies of HAB species

HABs are often (quasi-) monospecific, and while in some locations the same species blooms every year in a fairly predictable manner [e.g. *Alexandrium minutum* on the Catalan coast (Bravo et al., 2008), *Alexandrium catenella* in the Thau lagoon (Collos et al., 2007), *Pseudo-nitzschia* spp. on the US west coast (Anderson et al., 2006; Trainer et al., 2007)], in other regions, such as the southern Benguela, a variety of species dominate blooms at different times. In either case, the combination of physical, chemical and ecological factors which may lead to the proliferation of a certain species at the expense of all others is largely unresolved. One approach to improving our understanding of community succession is to study the physiological characteristics of a particular species (e.g. growth response to temperature, salinity, irradiance, nutrient source/ratios/concentrations), which can then be applied to models in an attempt to improve our predictive capability. As most HAB species are dinoflagellates, and diatom blooms are typically considered a “normal” stage in phytoplankton community succession, the characteristics of HAB species are often contrasted with those of diatoms (e.g. Smayda et al., 1997).

1.2.1. Margalef's Mandala

An early model of phytoplankton community succession suggested that the shift from diatoms to dinoflagellates occurred along a gradient of decreasing turbulence and nutrient availability, corresponding to a shift from r (small cell, high growth rate) to K (large cell, low growth rate) growth strategies (Margalef, 1978). Dinoflagellates are thought to thrive under low turbulence conditions for a variety of reasons. At a cellular level, turbulence impairs dinoflagellate growth (White, 1976; Pollingher & Zemel, 1981), disrupts certain cellular processes and behaviour, such as swimming (Thomas & Gibson, 1990), causes physical damage which can lead to cell disintegration (Berdalet & Estrada, 1993) and may even lead to mortality (White, 1976; Pollingher & Zemel, 1981). Furthermore, stratification caused by surface heating, wind relaxation or freshwater input, creates a favourable habitat for dinoflagellate populations. In the case of freshwater input, conditions are improved not only by reduced mixing, but also by increased nutrient concentrations (Smayda, 1997). Reduced wind stress also prevents bloom dispersal once it has formed.

The Mandala was subsequently revised to include a "red tide sequence", which occurred in low turbulence/high nutrient conditions (Figure 1.1), a situation seen as an "anomaly" (Margalef et al., 1979). This agrees with the observed link between HABs and eutrophication (Anderson et al., 2002) and the low affinity for nutrient uptake generally associated with dinoflagellates, indicating that they should thrive under nutrient-enriched conditions (Smayda, 1997; Collos et al., 2005). However, the model remains challenged by the occurrence of extensive blooms in oligotrophic regions such as those of *Gymnodinium breve* in the Gulf of Mexico (Steidinger et al., 1998) and during upwelling relaxation in upwelling systems (Pitcher et al., 1993a; Pitcher & Boyd, 1996; Pitcher et al., 1998; Fawcett et al., 2007).

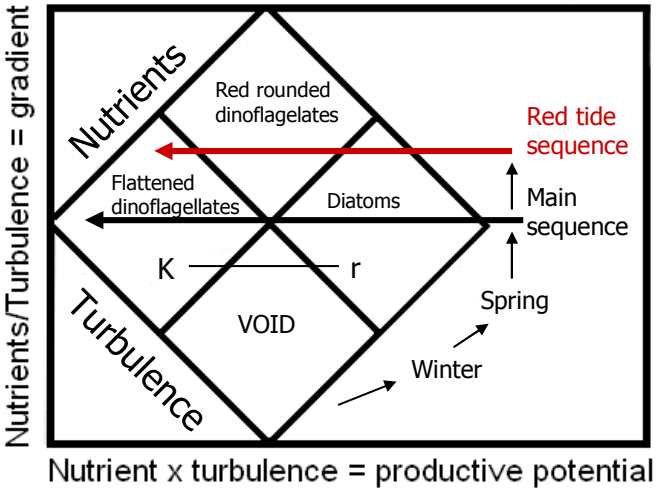

Figure 1.1 Mandala (Margalef, 1979) showing the "main sequence" of diatom dominance in spring to dinoflagellate dominance in summer, along a gradient of decreasing nutrient availability and turbulence, and the "red tide sequence" occurring under the paradoxical combination of high nutrients and low turbulence. r and K growth strategies are explained in the text.

1.2.2. Life forms

The selection of HAB species cannot always be explained by the Mandala, thus Reynolds (1980; 1984) attempted to identify co-occurring freshwater species across a broad spatial and temporal range and to link these "life forms" with the morphological, physiological and ecological traits of their key component species (Reynolds, 1987).

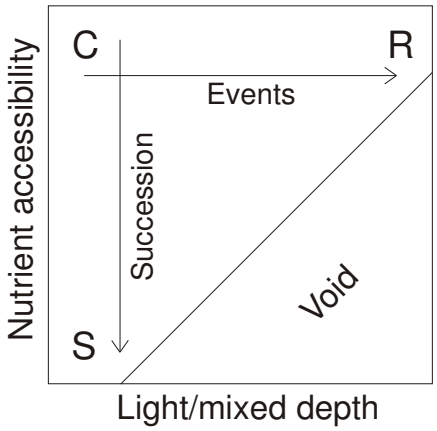

Figure 1.2 Reynolds' Intaglio showing the 3 major strategies devised by Reynolds (1987). See text for explanations.

He identified three primary adaptive strategies (Figure 1.2) in freshwater phytoplankton (Reynolds, 1988; 1995), as adapted from the classification used in terrestrial botany (Grime, 1974):

- Colonist (C strategy), small, r-selected, invasive, fast-growing and with a high surface to volume ratio.
- Nutrient stress-tolerant (S strategy), large, K-selected, acquisitive, slow-growing but biomass-conserving.
- Ruderal (R strategy), attuning, light-harvesting, attenuated, disturbance-tolerant.

Factors other than nutrients and light are also considered to play a minor role, which is represented in the model by a low relief, hence the name “intaglio”.

Smayda & Reynolds (2001) later identified nine life form types that occurred along an onshore-offshore gradient of decreasing nutrients, decreased mixing and increasing mixed layer depth (Figure 1.3).

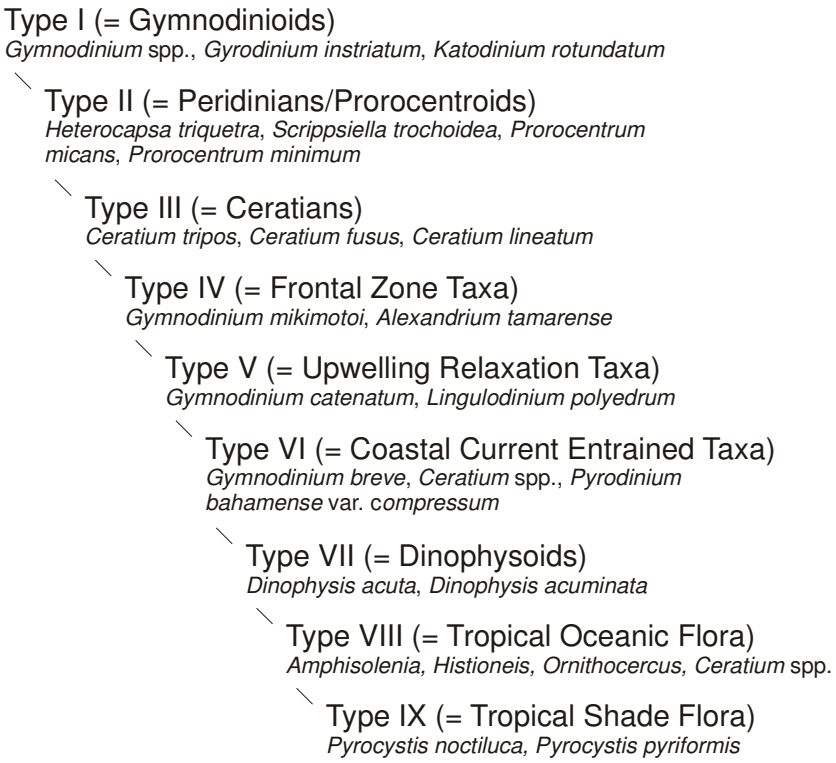

Figure 1.3 Life-form types and representative species, ordered along a gradient of decreasing nutrients, reduced mixing and deepened euphotic zone (from Smayda & Reynolds, 2001)

1.3. HABs in upwelling systems

The California, Humboldt, Canary/Iberian and Benguela currents are the four major eastern boundary upwelling systems worldwide. These are driven by the same physical mechanisms, whereby alongshore, equatorward winds coupled with Ekman transport direct surface currents offshore. This divergence causes upwelling of deep, cold, nutrient-rich water, stimulating primary production that in turn supports fisheries production. As a result, the contribution of upwelling systems to global fish catch is disproportionately high relative to their surface area (Ryther, 1969). Upwelling in these systems is seasonal, occurring during the summer months. Interannual variability in the degree and duration of upwelling is driven by the displacement of high-low pressure dipoles, which causes the reversal of wind direction and transition from upwelling to downwelling. This transition normally occurs between spring and autumn, when downwelling becomes more prevalent. However, synoptic wind patterns can cause short-term variability in upwelling, with upwelling/relaxation cycles occurring on time scales of days.

Traditionally thought to be dominated by fast-growing diatoms, these systems are becoming increasingly impacted by HABs (Smayda, 2000), which now seem to form an integral part of seasonal phytoplankton community succession. As in other temperate coastal environments, diatoms tend to dominate during spring, which in this case corresponds to the upwelling season. As upwelling weakens and thermal insulation increases, the water column becomes increasingly stratified and nutrient depleted and the community becomes increasingly dominated by heterotrophs and flagellates. This pattern is also reflected in the spatial gradient between newly upwelled inshore water dominated by diatoms and aged upwelled offshore water dominated by flagellates (Barlow, 1982; Pitcher & Nelson, 2006).

HABs normally occur towards the end of the upwelling season (late summer/ autumn), although there is no simple pattern in community succession that can account for the high temporal and spatial variability observed in the occurrence of HABs. In fact, HAB species occur over a wide range of nutrient-mixing-advection combinations, which cannot be accounted for by the classical Mandala. In upwelling systems, phytoplankton are subjected to strong physical forcing, such as within upwelling or downwelling fronts and advective currents (Smayda, 2000). The short-term alternations between upwelling

and relaxation create “habitat windows” which may lead to bloom formation if (i) the relaxation period is long enough relative to cellular growth rates, (ii) growth is faster than advective dispersal and mortality losses, and (iii) growth is not impaired by turbulence. Thus, the complexity of upwelling habitats and the rapid fluctuations that occur within them makes it extremely difficult to predict the occurrence of HABs.

In order to increase our understanding of HAB dynamics in upwelling systems, it is useful to draw on the commonalities between these systems, such as the physical and ecological mechanisms involved in HAB development. For example, a link between upwelling relaxation, wind reversal and onshore advection of HABs has been reported for the Benguela (Pitcher & Boyd, 1996; Pitcher et al., 1998), the Iberian (Tilstone et al., 1994) and the Californian (Trainer et al., 2002) upwelling systems.

The occurrence of common species or taxa in the different systems may also indicate common ecological adaptations, although species that bloom in upwelling systems are also found in other coastal habitats (Smayda, 2000). *Alexandrium catenella* has been associated with PSP outbreaks in the Benguela (Pitcher & Calder, 2000), the California current (Nishitani & Chew, 1988) and the Humboldt (Avaria, 1979; Guzman et al., 2002). *Dinophysis acuminata* is responsible for DSP outbreaks in both the Benguela (Pitcher & Calder, 2000) and the Iberian systems (Reguera et al., 1993a; Moita & da Silva, 2000). Toxic *Pseudo-nitzschia* spp. are found in the California, Benguela and Iberian systems but only appear to cause ASP in the former (Adams et al., 2000; Scholin et al., 2000; Trainer et al., 2001). *Protoceratium reticulatum* is common to the Benguela and California systems and is known to produce yessotoxins in the Benguela (Fawcett et al., 2007), although it is relatively poorly studied in both systems and has not been implicated in shellfish poisoning in either case.

Upwelling systems are thus comparable ecosystems, driven by similar hydrographic forcing mechanisms, in which blooms of similar species occur. Therefore, comparison between upwelling systems could be a useful tool to identify mechanisms underlying HAB population and community dynamics, as stated by the IOC programme Global Ecology and Oceanography of Harmful Algal Blooms (GEOHAB, 2001). A better understanding of HABs in upwelling systems could be achieved by comparing the physiological ecology of these species both in the laboratory and in the field.

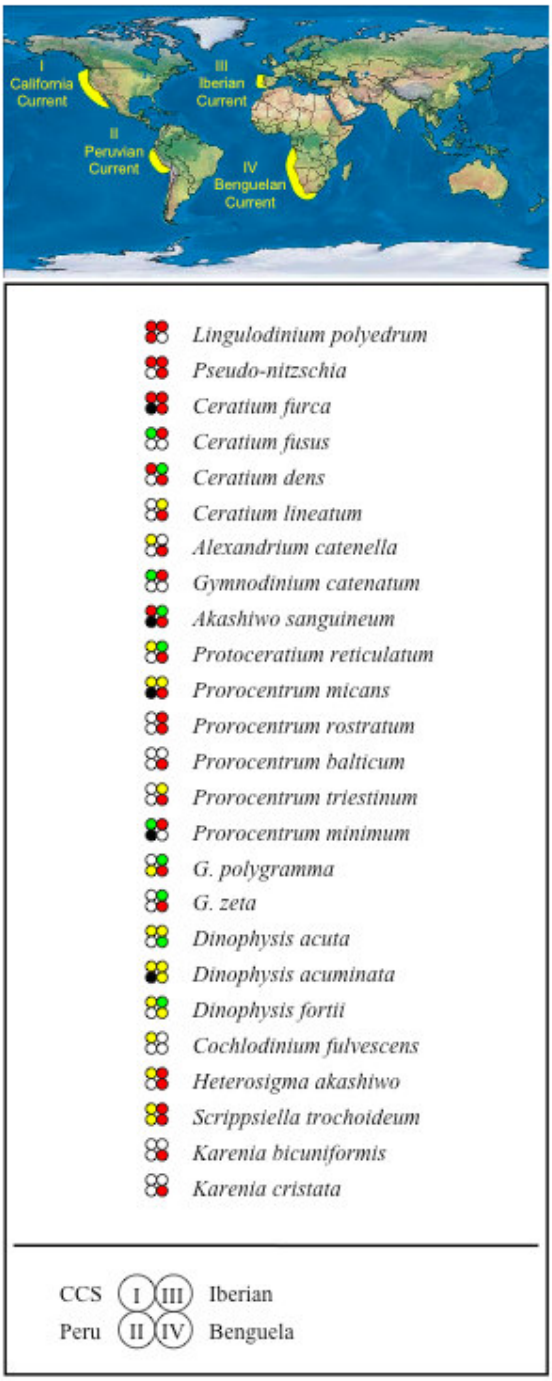

Figure 1.4. Distribution of HAB species in the four major eastern boundary upwelling systems, each of which is represented by a circle (legend in lower panel). Note that the northwest African system is not represented due to insufficient data. Red represents high, yellow moderate and green low biomass. White represents no reported presence and black represents presence but no reported harmful effects. From Smayda & Trainer (submitted).

1.4. The role of nitrogen

1.4.1. Principles of nitrogen uptake

Nitrogen is classically thought to be the nutrient that limits primary production in coastal marine ecosystems (Dugdale & Goering, 1967; Thomas, 1970b;1970a; Ryther & Dunstan, 1971; Goldman et al., 1979; Howarth & Marino, 2006). It is generally taken up as dissolved inorganic nitrogen (DIN): nitrate (NO_3^-), nitrite (NO_2^-) and ammonium (NH_4^+). At least some species also utilise dissolved organic nitrogen (DON), such as the amide urea and some amino acids such as glutamine and asparagine (Syrett, 1981; Palenik & Morel, 1990; Antia et al., 1991). Others may use more complex organic compounds such as polypeptides, proteins and humic acids (Berg et al., 1997; Mulholland et al., 1998; Mulholland et al., 2003). Nitrate is mostly supplied by sources external to the euphotic zone, such as river runoff, atmospheric deposition or upwelling. Ammonium and urea, on the other hand, are supplied by recycling processes, although in some coastal areas NH_4^+ can also be supplied by dust deposition. Uptake of NO_3^- and recycled nitrogen are termed "new" and "regenerated" production, respectively (Dugdale & Goering, 1967) and the ratio of NO_3^- uptake relative to total nitrogen uptake (NO_3^- + NH_4^+ and sometimes urea) is termed the *f*-ratio (Eppley & Peterson, 1979). This has been widely applied as a proxy for nitrogen and carbon export, when based on Redfield stoichiometry, although its application as such is limited because it does not take into account dinitrogen gas (N_2) fixation, which is also a new nitrogen source that can be significant in oligotrophic oceans (Dugdale & Goering, 1967). More recently, Yool et al. (2007) have summarized and discussed euphotic layer nitrification of NH_4^+ to NO_3^-, which renders such NO_3^- no longer "new" in the classical sense, therefore undermining the *f*-ratio as a means of estimating nitrogen or carbon export. However, surface layer nitrification rates are likely to be insignificant in upwelling or other high nutrient oceans where NO_3^- concentrations typically exceed 10-25 μmol l^{-1}.

DIN is actively transported across the cell membrane via "uptake sites" and metabolised within the cell to form amino acids and, in turn, proteins and nucleotides. The conversion of NO_3^- into organic compounds requires first its reduction to NO_2^-, then to NH_4^+. The former reaction is catabolysed by the enzyme nitrate reductase (NR), with NAD(P)H as the electron donor, while the latter requires nitrite reductase (NiR), using ferredoxin as the electron donor (Syrett, 1981).

There are two known pathways of NH_4^+ assimilation, both involving reductive reactions resulting in the production of glutamic acid and/or glutamine. The first known pathway involves the enzyme glutamic dehydrogenase (GDH). Lea and Miflin (1974) later discovered an alternative pathway that involves a combination of glutamine synthetase (GS) and glutamate synthase (also known as GOGAT -glutamine-oxoglutarate aminotransferase). The latter pathway is now known to be more widespread in marine phytoplankton (Zehr & Falkowski, 1988; Charpin & Devaux, 1997), partly because it is has a higher affinity (μM range) relative to GDH (mM range) (Bressler & Ahmed, 1984, and refs therein). Genes encoding glutamine synthetase have recently been identified in marine diatoms and linked with NH_4^+ assimilation (Schnitzler-Parker & Armbrust, 2005), indicating that the latter reaction is more likely.

Urea can be metabolised in 2 ways, involving either the enzyme urease or a combination of urea carboxylase and allophanate hydrolase (Syrett, 1981). Schnitzler-Parker & Armbrust (2005) identified carbamoyl phosphate synthase (CPS) as the enzyme that catalyses the first step in the urea cycle, and arginine and ornithine as intermediates in the cycle .

1.4.2. Ammonium-nitrate interactions

High concentrations of NH_4^+ are thought to inhibit NO_3^- uptake, as shown by the suppression of NO_3^- uptake observed at NH_4^+ concentrations of 0.2-0.3 μmol l^{-1} (Wheeler & Kokkinakis, 1990), 0.5-1.0 μmol l^{-1} (Syrett & Morris, 1963; Goering et al., 1970; Caperon & Meyer, 1972) or 1-2 μmol l^{-1} (Cochlan & Harrison, 1991). The earlier studies assumed that NO_3^- uptake and reduction were tightly coupled, therefore inhibition of NO_3^- uptake could be explained by the suppression of NR activity and/or synthesis. It has since been shown, however, that NO_3^- uptake and reduction are frequently uncoupled during transient situations (Collos, 1982). Furthermore, the suppression of NO_3^- uptake is too rapid to be explained by the inhibition of NR, therefore it was concluded that uptake itself (i.e. transport across the cell membrane) was inhibited as well as, and prior to, NO_3^- reduction (McCarthy, 1981; Syrett, 1981). The exact mechanisms involved in inhibition are still poorly understood, although it appears that a product of NH_4^+ metabolism (glutamine or an organic product of glutamine) suppresses the NO_3^- uptake mechanism (Syrett, 1981). More recently, a study by

Hildebrand & Dahlin (2000) demonstrated that the nitrate transporter gene is suppressed in cultures of the diatom *Cylindrotheca fusiformis* grown on NH_4^+ as sole nitrogen source, showing that a component of inhibition is at the level of gene expression.

Furthermore, phytoplankton are known to express a "preference" for NH_4^+, the theoretical basis for this being the additional energy requirement of NO_3^- assimilation, due to the need for reduction of NO_3^- to NH_4^+ before it can be incorporated into cellular material (Goering et al., 1970; Syrett, 1981). In order to distinguish between inhibition and preference, one needs to measure uptake rates of both nitrogen sources in the presence and absence of one another, a situation that is difficult to achieve in the field. Inhibition and preference involve different mechanisms, one distinction being that inhibition is dependent upon NH_4^+ concentration whereas preference is not (Dortch, 1990).

Preference for a certain form of nitrogen over others can be determined in several ways. A time lag in uptake of one source that is not observed in the other or higher growth rates sustained by one source but not by the other are both indicative of nutritional preference. The Relative Preference Index (RPI) introduced by McCarthy et al. (1977) has been a subject of controversy, as it can be more strongly influenced by ambient concentrations than by actual preference. In areas where NO_3^- concentrations are much higher than NH_4^+ concentrations, such as upwelling systems, this bias can lead to falsely high RPI values for NO_3^- (Stolte & Riegman, 1996). A more reliable method for determining preference is to measure uptake rates at increasing concentrations of a particular nutrient (see following section, Nutrient uptake kinetics). Inhibition of NO_3^- uptake by NH_4^+ can only be properly quantified by comparing the NO_3^- uptake rate in the absence of NH_4^+ with that in the presence of increasing concentrations of NH_4^+ (Dortch, 1990). This results in an inhibition kinetics curve analogous to a "reverse" Michaelis-Menten curve (Varela & Harrison, 1999) following the equation:

$$\nu = \nu_{max} * [1 - I_{max} * [NH_4^-]/ (K_i + [NH_4^-])] \quad (1.1)$$

where ν is specific uptake, ν_{max} is maximum specific uptake in the absence of NH_4^+, I_{max} is maximum inhibition (between 0 and 1) and K_i is the half-inhibition constant (the concentration at which inhibition is half of I_{max}).

Although NH_4^+ inhibition has been widely reported, it is not as universal nor as severe as previously thought (Collos, 1989; Dortch, 1990). Simultaneous uptake of NO_3^-

and NH_4^+ is often observed (McCarthy, 1981) and there is a high variability in the degree to which NH_4^+ affects NO_3^- uptake (Dortch, 1990). The interaction between NO_3^- and NH_4^+ also appears to vary between species and to be influenced by environmental factors such as light, as well as nutritional state. For example, Collos et al. (1989) concluded that NH_4^+ inhibition may not affect nitrogen-sufficient cells and L' Helguen et al. (2008) found that NH_4^+ inhibition was stronger in the <2 μm than in the >2 μm size fraction (Figure 1.5), consistent with the severity of NH_4^+ inhibition observed in the picoflagellate *Micromonas pusilla* (Cochlan & Harrison, 1991) and in the coccolithophore *Emiliania huxleyi* (Varela & Harrison, 1999).

In addition to the inhibition of NO_3^- uptake by NH_4^+, different forms of nitrogen compete for uptake sites on the cell surface, therefore competitive inhibition can be observed between different nitrogen forms. This translates as linear interactions between different forms of nitrogen, whereby the uptake rate of a particular nitrogen source is correlated with the relative concentrations of the two sources competing for the uptake sites. This competitive inhibition has been observed between NO_3^- and NH_4^+, NO_3^- and NO_2^- and between NO_2^- and NH_4^+ (Collos, 1989).

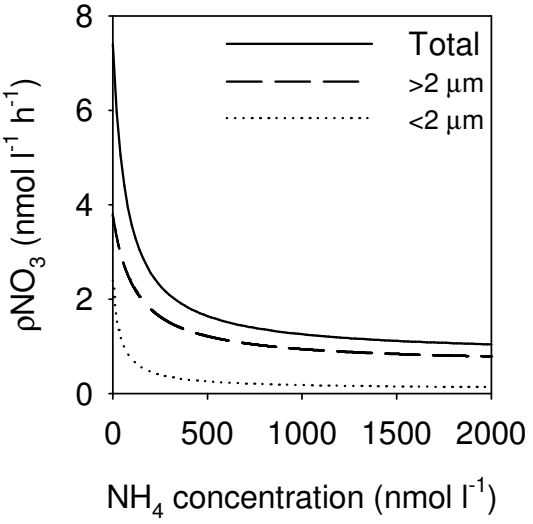

Figure 1.5 Ammonium inhibition kinetics as described by the equation of Varela & Harrison (1999). Note that uptake here is absolute (ρ) rather than specific (v). Here, the smaller size fraction is more severely inhibited, as shown by higher maximum inhibition (I_{max}) values (0.96 vs 0.84), lower maximum uptake ρ_{max} (4.0 vs 3.8) and lower half-inhibition constant K_i (38 vs 117). Adapted from L' Helguen et al. (2008).

1.4.3. Nitrogen uptake kinetics

The Michaelis-Menten equation (illustrated in Fig. 1.6.) was first applied to enzyme-substrate kinetics by Michaelis & Menten (1913) and later to the relationship between bacterial growth rates and limiting concentrations of organic substrate (Monod, 1942). Dugdale (1967) first applied this equation to a mass balance model of phytoplankton nutrient dynamics and the validity of the model was confirmed by MacIsaac & Dugdale (1969) using field data. Since then, nutrient uptake kinetics have been used extensively to analyse preferences for particular nitrogen sources in different species [see reviews by Dortch (1990), Litchman (2007) and Kudela (2008b)] or to predict the outcome of competitive interactions between species (Eppley et al., 1969; Doyle, 1975; Collos et al., 1997).

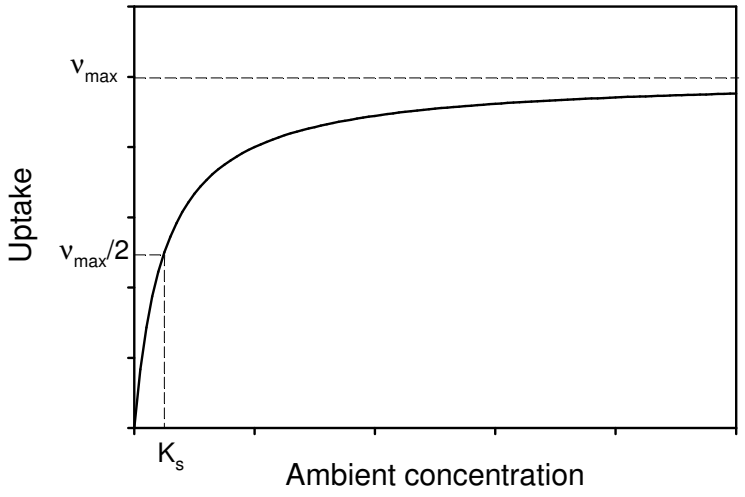

Figure 1.6. Illustration of the Michaelis-Menten equation $\nu = \nu_{max} * S/ (K_s + S)$. Symbols are explained in the text.

The Michaelis-Menten equation is a rectangular hyperbolic function described by:

$$\nu = (\nu_{max} * S)/ (K_s + S) \quad (1.2)$$

where ν is uptake rate, S is substrate concentration and K_s is the substrate concentration at which $\nu = \nu_{max}/2$, known as the half-saturation constant.

Comparison of v_{max} and K_s for NO_3^- and NH_4^+ can provide an indication of preference for either form of nitrogen (Dortch, 1990). The analogous Monod equation applies to growth rates as a function of nutrient concentration:

$$\mu = (\mu_{max} S)/(K_u + S) \quad (1.3)$$

where μ is specific growth rate (d^{-1}), μ_{max} is the maximum specific growth rate and K_u is the half-saturation constant for growth.

Although in the original application of the Michaelis-Menten equation to nutrient uptake kinetics it was assumed that growth and uptake were coupled (Dugdale 1967), it has since been recognised that growth and uptake rates are only coupled during balanced growth, for example in the steady state of a continuous culture (Caperon, 1968), a situation rarely encountered in nature (Maestrini & Bonin, 1981; McCarthy, 1981). Therefore K_s and K_u are usually distinct, as are v_{max} and μ_{max} (McCarthy, 1981; Goldman & Glibert, 1982b).

Uncoupling between v_{max} and μ_{max} is evident during "luxury consumption" in "storage specialists" (Sommer, 1984) as well as during "surge" uptake in nitrogen-starved cells (Conway et al., 1976; Glibert & Goldman, 1981). In the latter case v_{max} is much higher than μ_{max} immediately following nutrient addition, and as nitrogen limitation is lifted and the relative growth rate (μ/μ_{max}) increases, v_{max} decreases and should, in theory, converge with μ_{max} when the relative growth rate reaches 1 ($\mu = \mu_{max}$).

This indicates that nitrogen is stored intracellularly, a strategy that can be particularly important in vertically migrating dinoflagellates (Dugdale & Goering, 1967; Cullen & Horrigan, 1981). Caperon (1968) and Droop (1968) first hypothesised that growth rate was a function of intracellular rather than external nitrogen concentrations and the latter formulated the Droop model:

$$\mu = \mu_\infty (Q - K_Q)/Q \quad (1.4)$$

where μ_∞ is the specific growth rate at which cell quota Q (N $cell^{-1}$) is infinite, and K_Q is the Q below which there is no cellular growth.

Furthermore, the enzymes thought to be involved in nitrogen assimilation have much higher half-saturation constants (K_m) than the K_s values measured for uptake, confirming that nitrogen is pooled internally (Eppley & Rogers, 1970). Subsequent studies have

shown that uptake and NR activity can be regulated by an internal nutrient pool rather than by external nutrient concentrations (Collos & Slawyk, 1976).

Finally, physical processes can be mistaken for biological processes during uptake kinetics experiments. For example, ion adsorption onto dead cell membranes can result in apparent uptake kinetics. Apparent saturation kinetics have also been observed with urea in a diatom species that was not able to grow on that nitrogen source (McCarthy, 1981).

1.4.4. Ecological applications of nitrogen uptake kinetics

It is thought that species are selected on the basis of their ability to compete for the nutrient concentrations typical of their habitat (McCarthy, 1981), and this is reflected in variations in K_s and ν_{max}. Higher K_s values for NO_3^- and NH_4^+ uptake have been reported both in clones and natural populations from eutrophic coastal waters relative to those from the oligotrophic ocean (Eppley et al., 1969; MacIsaac & Dugdale, 1969), and Collos et al. (2005) have found a relationship between K_s and ambient NO_3^- concentration. Furthermore, intraspecific differences have been observed (Carpenter & Guillard, 1971), although it is still unknown whether the differences in kinetic parameters observed between geographic strains are a result of acclimation (a physiological response to environmental conditions) or adaptation (a result of genetic mutations and Darwinian selection) (Maestrini & Bonin, 1981).

Nutrient uptake parameters can be related to different nutrient uptake strategies. The half-saturation constant provides an indication of whether a species is better adapted to taking up nutrients at low concentrations (low K_s, high affinity for nutrients) or whether it requires high concentrations (high K_s, low affinity). Low K_s species are termed "affinity strategists" whereas species which display high ν_{max} are more likely to be "growth strategists" (Sommer, 1989). However, the inadequacy of this parameter as an index of affinity (or uptake efficiency) has been pointed out by Healey (1980) and Aksnes & Egge (1991) and the ratio $\alpha = \nu_{max}/K_s$, the initial slope of the Michaelis-Menten curve, has been proposed as a more reliable indicator of substrate affinity (Healey, 1980).

Covariation in K_s and ν_{max} is well documented (Healey, 1980; Aksnes & Egge, 1991; Collos et al., 2005) and forms the basis of a simple model of competitive interactions (Figure 1.7). In this figure, (1) and (2) can be considered as 2 competing species

(McCarthy, 1981) or the same species before and after adaptation to increased nutrient concentrations (Doyle, 1975). In the former case, it is possible to predict that Species 1 will outcompete Species 2 at concentrations below the intersection of the 2 curves and, conversely, Species 2 will outcompete Species 1 at higher concentrations. The competitive interaction depicted in Figure 1.7 has been observed in the field although its predictive power is questionable (Collos et al., 1997). This is the "either or" situation described by Doyle (1975), whereby species can be genetically adapted to either high (i.e. Species 2) or low (i.e. Species 1) concentrations, but not both. Doyle (1975) postulated that there were no grounds for this type of adaptation to occur exclusively and that there should be species with genes coding for both a high ν_{max} and low K_s.

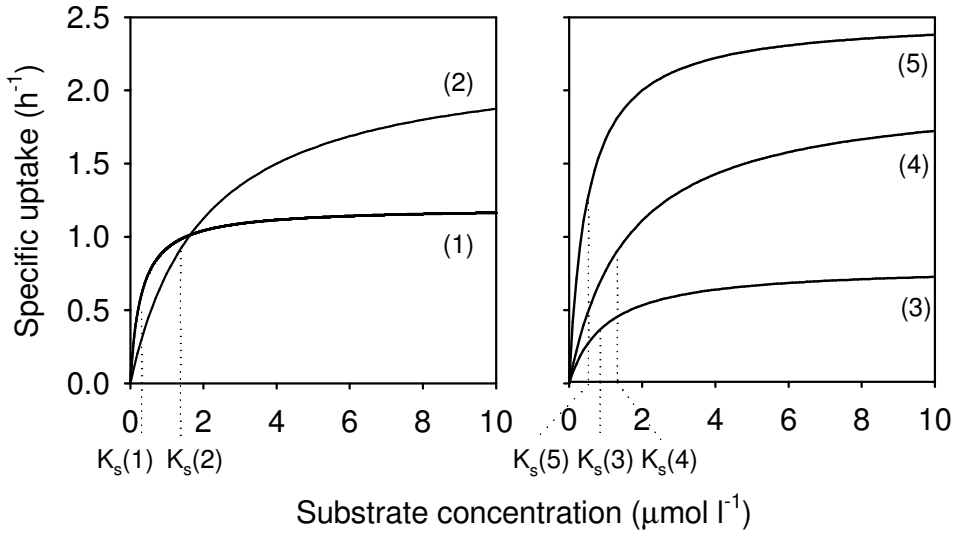

Figure 1.7 (a) Michaelis-Menten curves illustrating competition between a low nutrient-adapted species (1, low K_s, low ν_{max}) and a high nutrient-adapted species (2, high K_s, high ν_{max}). This is also the "either or" adaptation of a species to changing nutrient regime. (b) Form of adaptation to changing nutrient regime which is advantageous in all cases (adapted from Droop 1975). Increased nutrient concentrations result in both cases in an increased ν_{max} [from (3) to (4) or (3) to (5)], but can either involve an increase [(3) to (4)] or decrease [(3) to (5)] in K_s.

1.4.5. Factors influencing K_s and ν_{max}

The use of nutrient uptake kinetics in determining species-specific adaptations to their nutrient environment can be complicated by other factors influencing variability in K_s and ν_{max}. When comparing the uptake kinetics of different species it is difficult to determine whether the differences observed are a result of acclimation to the species' growth environment or due to genetic differences which have resulted in natural

selection for that particular cell line (in a clonal culture) or that group of cell lines (in a natural population).

It has recently been shown that K_s is linearly related to the highest NO_3^- concentration used to measure uptake kinetics and that ambient NO_3^- concentrations have a greater influence on K_s than interspecific differences, for a range of published studies carried out both in the field and with cultures (Collos et al., 2005). These authors showed that uptake can appear to be saturated at the highest experimental concentrations, but that a further increase in uptake will occur at higher concentrations, and that underestimation of K_s can occur if the concentration range is too narrow. Higher preconditioning NO_3^- or NH_4^+ concentrations (hence growth rate) have also been shown to increase cell-specific ν_{max} (by increasing the number of uptake sites per cell) although they do not influence K_s (Caperon & Meyer, 1972).

Temperature is also known to influence nitrogen uptake, whereby absolute uptake rates of NO_3^- are negatively correlated with temperature and those of NH_4^+ and urea are positively correlated (Lomas & Glibert, 1999). Aksnes & Egge (1991) hypothesised that both ν_{max} and K_s should increase with temperature, since both parameters are negatively correlated with handling time, which like all biochemical processes should be aided by increased temperature, within the limits of enzyme sensitivity. Experimental studies, however, have shown conflicting results: ν_{max} for NH_4^+ may increase with temperature (Lomas et al., 1996) although ν_{max} for urea is temperature-independent. Similar results were obtained by Fan et al. (2003) who found a positive correlation between temperature and α for NH_4^+ and amino acids but no temperature dependency of α for urea, but also a negative correlation between temperature and α for NO_3^-.

Nutrient uptake kinetics parameters can also change substantially during nitrogen starvation (Harrison, 1976). An increase in ν_{max} with starvation has been reported for batch cultures (Harrison, 1976), which contradicts the theory of adaptation to ambient concentrations (MacIsaac & Dugdale, 1969). Collos et al (1980) showed that the effect of nitrogen starvation on ν_{max} was dependent upon cellular nitrogen status prior to the experiment as well as on the duration of starvation and the nitrogen source under study. For NO_3, absolute maximum uptake (ρ_{max}) decreased during starvation of both previously nitrogen-limited and nitrogen-replete cells. However, the decrease in ρ_{max} was less drastic in previously replete cells because they could increase their specific maximum uptake (ν_{max}) by decreasing their cellular nitrogen quota. For NH_4^+, on the other hand, ν_{max} increased in both cases. Furthermore, a preliminary increase in ν_{max} was

observed within the first 6 h of starvation in both cases, indicating that contradictory results can be obtained depending on the length of the experiment.

Aksnes & Egge (1991) devised a model relating ν_{max} to the number of uptake sites and handling time and relating K_s to the area of each uptake site, handling time and the mass transfer coefficient (or relative velocity between nutrient and uptake sites). They hypothesised that ν_{max} was proportional to the square of cell radius and K_s was proportional to cell radius, relationships that were confirmed by Litchman et al. (2007) in a review of existing data on ν_{max}, K_s and cell size.

Finally, increasing uptake with substrate concentration can not always be described by the Michaelis-Menten equation, since non-saturating kinetics have been reported (Lomas & Glibert, 1999; Collos et al., 2005) as well as biphasic kinetics (Serra et al., 1978; Collos et al., 1992). The former consists of a continual linear increase with substrate concentration, whereas the latter shows a further increase in uptake after an initial saturation plateau. Both are usually observed when a wide range of substrate concentrations is used (up to 100 μmol N l^{-1}). The use of such high concentrations may be of ecological relevance under conditions of increasing eutrophication.

1.5. Nitrogen and HABs

In an effort to characterise the nitrogen nutrition of HAB species, comparisons of dinoflagellates and diatoms may be appropriate, since most HAB species are dinoflagellates (Smayda, 1997). This type of comparison has been carried out with published K_s values for a range of species both in culture and in the field by Smayda (1997) and also by Collos et al. (2005). Both studies concluded that dinoflagellates displayed higher K_s values than diatoms, suggesting that dinoflagellates should be more successful in nutrient-enriched waters, consistent with the "red tide sequence" in Margalef's Mandala (Margalef et al., 1979). However, the use of K_s as an index of affinity is flawed and comparisons of α may have been more useful. Lomas & Glibert (2000) also found lower K_s values for NO_3 in 3 diatom species relative to 3 flagellate species (only one of these being a dinoflagellate), but also higher ν_{max} and NR/NiR activities. Cell size is also known to influence ν_{max} and K_s (see previous section), therefore any comparison made between diatoms and dinoflagellates should take into account differences in cell size. Although Lomas & Glibert (2000) mentioned that their diatom and flagellate species spanned overlapping size ranges, the number of species used in their study was rather limited. A review by Litchman et al. (2007), using 5 dinoflagellate species and 6 diatom species, showed higher ν_{max} and K_s in dinoflagellates than in diatoms when ν_{max} was expressed on a per cell basis, although ν_{max} was higher for diatoms when ν_{max} was expressed on a carbon basis.

Notwithstanding the limitations of these studies, their conclusions, together with the occurrence of HABs in both oligotrophic and eutrophic environments, complicate the classical association between dinoflagellates and low nutrient conditions. Given the apparent disadvantage of dinoflagellates under nutrient-depleted conditions, but their often striking success in such environments, they must have evolved other adaptive strategies to offset this disadvantage. Smayda (1997) suggested four major adaptations: nutrient retrieval migrations, mixotrophy, secretion of allelochemicals (to minimise inter-specific competition) and allelopathy (to offset predation). In addition to these, the utilisation of recycled sources of nutrients may be significant in situations where new nutrients are depleted.

1.5.1. Preferential uptake of ammonium and urea

Ammonium is generally thought to be preferred over NO_3^- and to inhibit its uptake (see section 1.4.2), however little is known about the role of urea. In an attempt to determine whether diatoms and dinoflagellates exhibited different nutritional preferences, Dortch (1990) reviewed published literature values of ν_{max} and K_s for NO_3^- and NH_4^+ and found that both groups assimilated NH_4^+ preferentially but grew better on NO_3^-. The only exceptions were in upwelling areas, where NO_3^- was preferred.

HABs are often supported by recycled nitrogen sources, for example *Gymnodinium aureolum* blooms in the western English Channel (Le Corre & L' Helguen, 1993), mixed HAB assemblages (*Dinophysis acuta*, *Gymnodinium catenatum*, *Ceratium fusus* and *C. furca*) in the Ría de Vigo, north-west Spain (Rios et al., 1995) and blooms of *Alexandrium catenella* in Thau Lagoon, on the south coast of France (Collos et al., 2007). In the latter study, the authors hypothesised that blooms could be triggered by elevated urea concentrations, although this was complicated by the covariation between NH_4^+ and urea. *A. catenella* displayed a preference for NH_4^+ and urea over NO_3^-, as demonstrated by differences in ν_{max}, both in cultures and in the field (Collos et al., 2004). Similar results were obtained for blooms of *Lingulodinium polyedrum* and *Akashiwo sanguinea* off California (Kudela & Cochlan, 2000), *Prorocentrum minimum* in Chesapeake Bay and a mixed bloom (*Heterocapsa rotundata*, *H. triquetra* and *P. minimum*) in the Neuse Estuary, on the east coast of the United States (US) (Fan et al., 2003). Lomas et al. (1996) also measured a high affinity for urea (and speculated on a high affinity for NH_4^+) during blooms of the "brown tide" pelagophyte *Aureococcus anophagefferens* off the north-east coast of the US. On the other hand, a poor ability to utilise urea relative to NO_3^- and NH_4^+ (as shown by lower ν_{max}) has been reported for blooms of the dinoflagellate *Cochlodinium* sp. (Kudela et al., 2008a) and the fish-killing raphidophyte *Heterosigma akashiwo* (Herndon & Cochlan, 2007).

Blooms of the toxic diatom *Pseudo-nitzschia* on the US west coast have been attributed to either elevated NO_3^- (Horner et al., 2000; Marchetti et al., 2004) or NH_4^+ concentrations (Trainer et al., 2007). Field populations of *P. australis* from California were found to grow equally well on NO_3^-, NH_4^+ or urea, however *P. australis* cultures exhibited lower growth rates supported by urea relative to NO_3^- and NH_4^+ (Howard et al., 2007). Cochlan et al. (2008) found that the same species exhibited a preference for NO_3^- relative to NH_4^+ and glutamine, as shown by higher ν_{max} and lower K_s.

1.5.2. Nitrogen-toxicity interactions

Although there is evidence of genetic variability in cell toxicity (Cembella & Taylor, 1985), given the high intra-specific variability between strains isolated from different locations (Bates et al., 1978; Cembella & Taylor, 1985; Yoshida et al., 2001) or between natural samples and cultures (Kodama et al., 1982; Lundholm et al., 1994; Rhodes et al., 1996), it appears that toxin production may be a function of environmental conditions as well as a hereditary trait. Several studies have concluded that toxin profile (i.e. the proportion of each toxin produced) was a genetic trait (Cembella & Taylor, 1985; Boyer et al., 1987; Oshima et al., 1993; Anderson et al., 1994; Flynn et al., 1994), but later experiments reported changes in toxin profile with culture age (Boczar et al., 1988) and with salinity (Hwang & Lu, 2000).

As toxin production can be inversely related to growth rate, factors controlling growth, such as temperature, light, salinity and nutrients, could indirectly control toxin production (Proctor et al., 1975; Cembella, 1998). However, various authors have since contradicted this theory (White, 1978; Kodama, 1990; Etheridge & Roesler, 2005) and argue that variations in toxicity may be directly controlled by light and temperature and are not a consequence of altered growth rates (Hamasaki et al., 2001; Etheridge & Roesler, 2005; Lim et al., 2006).

PSP toxins are nitrogen-rich compounds, hence phosphorus limitation has been shown to increase toxin production in *Alexandrium tamarense* (Boyer et al., 1987) and in *A. minutum* (Flynn et al., 1994; Bechemin et al., 1999; Maestrini et al., 2000; Lippemeier et al., 2003). Maximum toxin synthesis in *A. minutum* was found to occur after nitrogen re-supply to deprived cells, however short-term phosphorus stress did not enhance toxin synthesis (Flynn et al., 1994) and they later found that toxin synthesis and content declined during nitrogen or phosphorus deprivation (Flynn et al., 1995). Lippemeier et al. (2003) also found a significant negative correlation between fluorescence-based photochemical efficiency (an indicator of nutrient limitation) and cell toxin content. Furthermore, high NH_4^+ concentrations have been associated with toxicity in *A. minutum* (Flynn et al., 1994) and in *A. tamarense* (Hamasaki et al., 2001). The utilisation of organic forms of nitrogen has also been found to stimulate toxin production. Uptake of urea, glycine, leucine and aspartic acid appear to enhance brevetoxin production in *Gymnodinium breve* (Shimizu & Wrensford, 1993; Shimizu et al., 1995). While *A. fundyense* is capable of taking up dissolved free amino acids, there

is no evidence for a link between amino acid uptake and toxicity in this species (John & Flynn, 1999). These authors found that toxicity was only enhanced by unnaturally high concentrations of arginine. Furthermore, Flynn et al. (1995) showed that toxicity varied with intracellular free arginine (the precursor for PSP toxin synthesis), which itself was increased by phosphorus deprivation.

Silicate and phosphate limitation have been shown to stimulate domoic acid (DA) production in *Pseudo-nitzschia* sp. in laboratory studies and in some field studies (Bates et al., 1998). High DA concentrations during *Pseudo-nitzschia* sp. blooms have been observed at low NO_3^- concentrations during post-upwelling conditions, suggesting that recycled nutrients supported growth and DA production (Walz et al., 1994). Bates et al. (1993) demonstrated that NH_4^+ prevented the growth of *P. multiseries* and enhanced DA production. Field and culture studies on *P. australis* showed that growth on urea as the sole nitrogen source enhanced cell toxicity without significantly affecting growth rate or biomass (Howard et al., 2007).

1.6. Aims & Objectives

This thesis aims to investigate the role of nitrogen nutrition in the initiation and maintenance of HABs in upwelling systems. The two systems chosen for this study were the Benguela and Iberian upwelling systems, where repeated studies were carried out to obtain information on temporal variation in nitrogen cycling and its control on HAB occurrence. Studies were carried out on an annual basis in the Benguela, but on a seasonal basis in the Iberian system. The aim was to compare the nitrogen nutrition of specific HAB species, when (quasi-) monospecific blooms occurred, or to adopt the "dinoflagellate-diatom" approach in determining ecological traits of HAB and non-HAB groups.

A species' ability to compete for particular nitrogen sources and concentrations will determine its success under certain conditions. Therefore, if adaptations can be determined for different species, this would enhance our ability to forecast blooms of particular species and their impacts. Upwelling systems are highly dynamic and a wide range of physical and nutrient regimes are encountered over short time-scales. Comparison between the different major upwelling systems is important to further our understanding of the ecological and oceanographic mechanisms underlying HAB population dynamics in these systems and to improve our predictive capability. This work fits into the general context of the SCOR/IOC programme for international cooperative research on HABs, GEOHAB (GEOHAB, 2001).

To investigate the relative importance of upwelling and other factors in the success of a certain species, the nitrogen nutrition of *Alexandrium minutum* strains isolated from the two upwelling systems and also from a UK estuary were compared.

The specific objectives of the study were to:

- Determine the relative roles of new versus regenerated nutrients in the initiation of HABs in upwelling systems, by adopting a comparative approach.
- Identify nitrogen nutrition strategies of HAB species in different regions and in cultures isolated from different geographical locations.
- Determine whether such nitrogen nutrition strategies are specific to upwelling systems.

2 Materials & Methods

2.1. Sampling

2.1.1. Lambert's Bay

Three field studies were carried out off Lambert's Bay, in the southern Benguela, as part of a Marine & Coastal Management (MCM) HAB research programme. They took place from 7 to 23 March 2006, 19 March to 11 April 2007 and 4 to 25 March 2008. Sampling was carried out daily on-board MCM research vessels *RV Ecklonia* (2006/07) or *RV Catenella* (2008) at the same station, 3.5 km off Lamberts' Bay (32°05.020 S, 18°16.010 E), over the shallow shelf region (approximately 50 m depth) (Figure 2.1). The station was marked by a permanent mooring comprising a 30 m Apprise Technologies thermistor chain, a Turner Designs SCUFA fluorometer and a 300 kHz RDI Workhorse Acoustic Doppler Current Profiler (ADCP).

Daily profiles of temperature, salinity, dissolved oxygen and chlorophyll fluorescence were taken using a Seabird Electronics Seacat CTD coupled with a Wetstar fluorometer. Dissolved oxygen (hereafter DO) and chlorophyll-a (hereafter chl-a) measurements from the CTD were calibrated against discrete measurements. Samples for analysis of DO, chl-a, NO_3^-, NO_2^-, NH_4^+, urea, phosphate (PO_4^{3-}) and silicic acid ($Si(OH)_2$, hereafter Si), measurements were taken on dates and at depths shown in Table 2.1. Samples for ^{15}N incubations were taken at the "surface" (0.5 m) and at 5 or 10 m, as shown in Table 2.1). Phytoplankton counts were performed on surface samples only in 2006/07 but on samples from both incubation depths in 2008. Water was collected using 5-l Niskin bottles (fired manually using a messenger) and transported ashore in dark 10-l buckets within 1 h of collection.

Measurements of photophysiological parameters were obtained in 2007/08 from regular deployments of a Chelsea Instruments Fastracka™ Fast Repetition Rate fluorometer (FRRf).

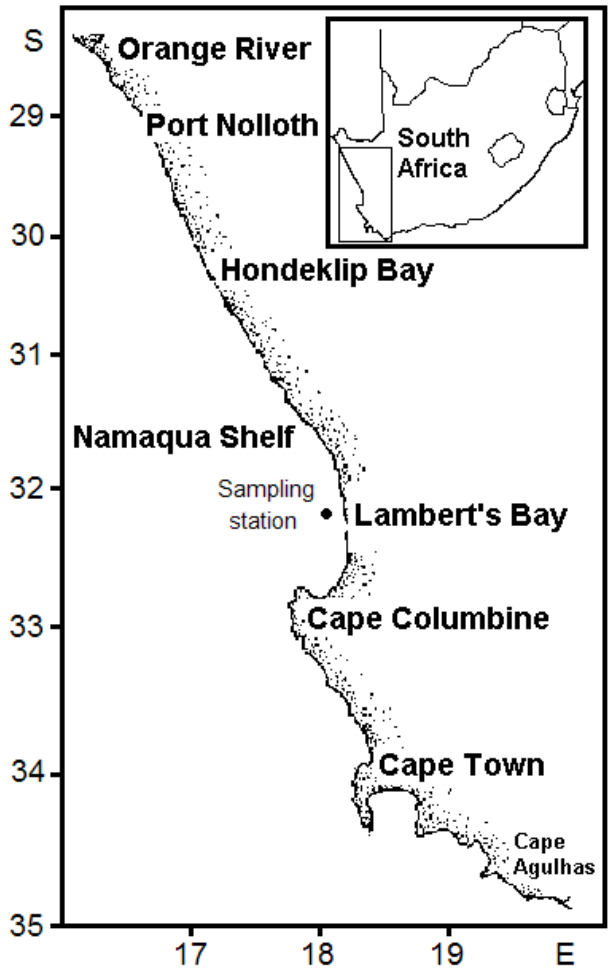

Figure 2.1. Map of the west coast of South Africa, showing the sampling station at Lambert's Bay.

Year	Date	Station	Sampling depth				Other activities
			DO	chl-a, PO_4^{3-}, Si	NO_3^-, NO_2^-, NH_4^+, urea	^{15}N	
2006	07-Mar	n/a		0.5, 5, 10, 15, 20	n/a	n/a	
	08-Mar	1		"	0.5, 5	0.5, 5	
	09-Mar	2		"	0.5, 5	0.5, 5	
	10-Mar	3		"	0.5, 10	0.5, 10	
	11-Mar	4		"	0.5, 10	0.5, 10	
	12-Mar	5		"	0.5, 5	0.5, 5	
	13-Mar	6		"	0.5, 5	0.5, 5	
	14-Mar	n/a		"	n/a	n/a	Offshore transect (2-14)
	15-Mar	7		"	0.5, 5	0.5, 5	
	16-Mar	8		"	0.5, 5	0.5, 5	Nutrient kinetics 1
	17-Mar	9		"	0.5, 5	0.5, 5	
	18-Mar	n/a		"	n/a	n/a	Pump station
	19-Mar	10		"	0.5, 5	0.5, 5	
	20-Mar	11		"	0.5, 5	0.5, 5	
	21-Mar	12		"	0.5, 5	0.5, 5	
	22-Mar	13		"	0.5, 5	0.5, 5	
	23-Mar	n/a		"	n/a	n/a	
2007	20-Mar	n/a		"	0.5, 5, 10, 15, 20	n/a	
	21-Mar	1		"	"	0.5, 5	Nutrient kinetics 2
	22-Mar	2		"	"	0.5, 5	
	23-Mar	3		"	"	0.5, 5	
	24-Mar	4	0.5, 45	"	"	0.5, 5	
	25-Mar	5	0.5, 45	"	"	0.5, 5	
	26-Mar	6		"	"	0.5, 5	
	27-Mar	n/a		"	"	n/a	
	28-Mar	7	0.5, 45	"	"	0.5, 5	Start long term inc
	29-Mar	8		"	"	0.5, 5	
	30-Mar	9		"	"	0.5, 5	
	31-Mar	n/a		"	"	n/a	
	01-Apr	10		"	"	0.5, 5	
	02-Apr	n/a	0.5, 43	"	"	n/a	
	03-Apr	n/a		"	"	n/a	Offshore transect (2-6)
	04-Apr	11		"	"	0.5, 5	End long term inc
	05-Apr	12		"	"	0.5, 5	
	06-Apr	13		"	"	0.5, 5	
	07-Apr	14	0.5, 42	"	"	0.5, 5	
	08-Apr	15		"	"	0.5, 5	Nutrient kinetics 3
	09-Apr	16		"	"	0.5, 5	
	10-Apr	17		"	"	0.5, 5	
	11-Apr	n/a		"	"	n/a	
2008	04-Mar	n/a		"	"	n/a	
	05-Mar	1		"	"	0.5, 5	
	06-Mar	2		"	"	0.5, 5	
	07-Mar	3	0.5, 45	"	"	0.5, 5	
	08-Mar	n/a		"	"	n/a	Offshore transect (3-11)
	09-Mar	4		"	"	0.5, 5	
	10-Mar	5		"	"	0.5, 5	
	11-Mar	6	0.5, 42	"	"	0.5, 5	
	12-Mar	7		"	"	0.5, 5	
	13-Mar	8	0.5, 34	"	"	0.5, 5	
	14-Mar	9		"	"	0.5, 5	
	15-Mar	10	0.5, 48	"	"	0.5, 5	
	16-Mar	11		"	"	0.5, 5	
	17-Mar	n/a		"	"	n/a	Offshore transect (3-11)
	18-Mar	12	0.5, 45	"	"	0.5, 5	
	19-Mar	13		"	"	0.5, 10	
	20-Mar	14		"	"	0.5, 5	
	21-Mar	15		"	"	0.5, 5	Nutrient kinetics 4
	22-Mar	16		"	"	0.5, 5	
	23-Mar	n/a		"	"	n/a	Offshore transect (3-11)
	24-Mar	17	0.5, 48	"	"	0.5, 5	
	25-Mar	18		"	"	0.5, 5	Nutrient kinetics 5

Table 2.1. Stations sampled off Lambert's Bay in March 2006, March/ April 2007 and March 2008, showing sampling depths for various parameters and additional activities carried out. Stations sampled on each transect are given in brackets.

2.1.2. Ría de Vigo

As part of the Spanish programme CRIA (Circulación en la RIA), led by Dr Des Barton of the Instituto de Investigaciónes Marinas (IIM) in Vigo, similar measurement to the South African programme were made in the Ría de Vigo. CRIA consisted of two parts, CRIA I targeting the downwelling, "HAB season" (26 to 30 September 2006) and CRIA II targeting the upwelling, "diatom" season (25 to 28 June 2007).

Sampling was carried out on-board the IIM research vessel *RV Mytilus*. Spatial surveys of temperature, salinity, chl-a fluorescence and turbidity were carried out using a lightweight towed undulating vehicle, MiniBAT FC60 (Ocean Scientific International Ltd.) fitted with an Applied Microsystems Ltd. (AML) Micro CTD, a Wet Labs WetStar fluorometer and a Campbell Scientific OBS 3 turbidity sensor. Continuous measurements of temperature, salinity and chl-a fluorescence were also made on surface water collected underway (2.5 m depth). Temperature, salinity, DO and chl-a fluorescence profiles were carried out at various stations along the ría (Table 2.2, Figure 2.2) using a Seabird Electronics 911+ CTD system coupled with a Seatech fluorometer and Seabird 18 oxygen sensor mounted on a sampling rosette fitted with 10-l Niskin bottles. Samples were collected from 3-6 depths in Milli-Q rinsed 5- or 10-l carboys for routine chl-a and nutrient analyses. These were stored in the dark until transported ashore (within <5 h). At some stations water was only collected from the underway supply (2.5 m). Water for ^{15}N incubations and associated NO_3^-, NH_4^+ and urea analyses and phytoplankton counts was collected from ~3 m in both years and occasionally from the chl-a maximum (10-12 m) in 2007 (Table 2.2).

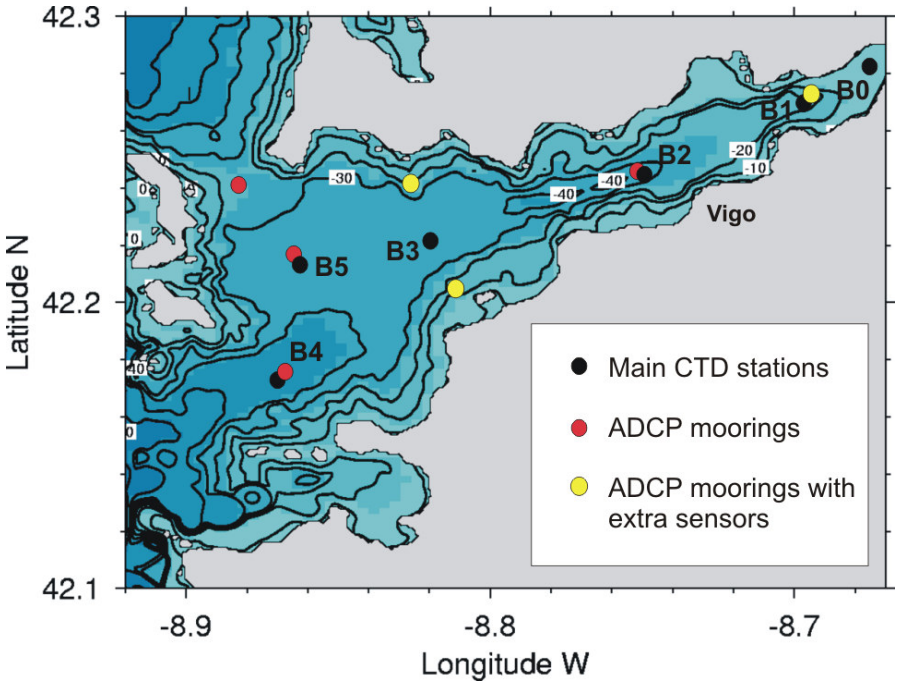

Figure 2.2. Map of the Ría de Vigo showing repeat CTD sampling stations (B0-B5) and ADCP moorings along the ría.

Date	Station	Latitude	Longitude	Tidal range	Time (GMT) GMT	Tide	Sampling depths (m) ^{15}N, nutrients, phyto	Sampling depths (m) chl-a, DO, nutrients
26/09/2006	B5	42.209	-8.861	2.4	08:59	low/ebb	2	2, 11, 20, 25, 29, 36
	B3	42.226	-8.818		11:42	low/flood	3	3, 10, 21, 31, 34
	B2	42.242	-8.759		13:15	flood	3	3, 9, 21, 31, 37
27/09/2006	B5	42.206	-8.863	2.2	06:00	high/ebb	3	3, 11, 21, 31, 37
	B5	42.209	-8.864		09:09	ebb	n/a	3, 10, 20, 30, 35
	B5	42.209	-8.864		12:00	flood	n/a	3, 11, 20, 31, 33
28/09/2006	B3	42.224	-8.818	2.0	06:08	high/ebb	3	3, 11, 21, 31, 36
	B3	42.225	-8.818		08:58	ebb	3	3, 11, 21, 31, 35
	B3	42.224	-8.817		12:16	low/ebb	n/a	2, 11, 21, 30, 34
29/09/2006	B2	42.243	-8.758	1.7	06:43	high/ebb	2	2, 10, 20, 27, 33
	B2	42.241	-8.760		09:25	ebb	3	3, 10, 20, 31, 39
	B2	42.242	-8.759			low/ebb	n/a	2, 11, 21, 31, 35
25/06/2007	B1	42.270	-8.700	1.3	08:02	flood	n/a	3, 10, 14, 19
	B2	42.242	-8.758		09:18	flood	3, 10	3, 10, 18, 31, 39
	B3	42.226	-8.818		11:13	high	3	3, 11, 20, 27, 37
	B4	42.177	-8.870		14:34	ebb	n/a	3, 10, 20, 31, 43
	B5	42.210	-8.860		16:08	low/ ebb		3, 11, 16, 21, 32
26/06/2007	B5	42.191	-8.858	1.6	08:14	low/ flood	UW	n/a
	B0	42.279	-8.675		10:10	high/ flood	UW	n/a
27/06/2007	B3	42.226	-8.819	1.7	07:15	low/ flood	n/a	3, 11, 16, 20, 34
	B3	42.226	-8.818		09:41	flood	3, 9	3, 9, 15, 21, 35
	B3	42.227	-8.818		12:46	high		3, 11, 16, 20, 36
28/06/2007	B0	42.283	-8.671	2.0	06:12	low/ ebb	n/a	3, 12, 21
	B1	42.270	-8.699		07:38	low/ flood	n/a	3, 12, 17
	B2	42.243	-8.758		08:45	low/ flood	3, 13	3, 13, 20, 25, 35
	B3	42.226	-8.819		11:35	flood	3*	3, 11, 15, 27, 36
	B4	42.179	-8.869		13:13	high/ flood	n/a	3, 11, 22, 31, 45
	B5	42.209	-8.861		14:32	high/ ebb	n/a	3, 12, 18, 25, 35

Table 2.2. Sampling stations during CRIA I and II. Stations were ordered from B0 at the head to B4 and B5 at the mouth of the ría. Times indicate the start of each CTD cast. UW = underway water supply, when no CTD cast was carried out. * indicates nutrient uptake kinetics experiment.

2.1.3. Fal Estuary

Field studies were undertaken in the Fal Estuary between 4 and 16 July 2006 and between 4 and 12 July 2007. The work took place simultaneously with the University of Southampton 3rd year undergraduate field course, which provided logistical support as well as background data for the estuary as a whole. In addition, a 3rd year undergraduate research project was carried out by Ms. Joanne Souter in 2007 investigating the distribution of *Alexandrium minutum* in the estuary.

Sampling was carried out between 0830 and 1400 GMT every day (except 6, 10, 12 and 13 July 2006 and 8 July 2007) on-board the University of Southampton vessel *RV Bill Conway* in the main estuary whereas a RIB (2 in 2006) was used to sample the shallower upper reaches (Figure 2.3). A number of stations were sampled repeatedly (Table 2.3, Figure 2.3) and these will form the focus of this study. Sampling took place on the ebb tide on 4-5 and 11-16 July 2006 and on 4-7 July 2007, but on the flood tide on 7-9 July 2006 and 10-12 July 2007. Sampling from the RIB was always carried out from the head towards the mouth of the estuary in 2007, therefore it followed the tide on 4-7 July and was against it on 10-12 July. In 2006, the sampling stations were covered by 2 RIBs therefore the stations were not sampled sequentially from head to mouth of the estuary.

On *RV Bill Conway* temperature, salinity and chl-a fluorescence profiles were carried out daily by groups of students at various stations along the estuary using a Falmouth Scientific Inc. CTD and fluorometer mounted on a rosette sampler fitted with 3-l General Oceanics Niskin bottles. They also collected samples for DO, chl-a, NO_3^-, PO_4 and Si throughout the estuary at the surface and at 1-2 additional depths where water depth was sufficient.

On the RIB, samples were taken from the surface only in 2006, but from 1-2 depths using a Niskin bottle in 2007. Temperature, salinity and DO profiles were carried out using a YSI 650 in 2006 and on 4, 6, 9 and 11 July 2007, whereas a YSI Inc. 6600 V2 handheld Multiparameter Water Quality Sonde (including a fluorescence probe) was used on 3, 5, 7, 10 and 12 July 2007. The difference between the two instruments' temperature and salinity readings was <1 % therefore no correction was applied.

Nutrient uptake incubations were performed on samples collected in 5-l carboys from the surface and occasionally the subsurface chl-a maximum, from either vessel or

occasionally in 2006 from a pontoon (Table 2.3). This water was also used for NO_3^-, NH_4^+, urea and chl-a analyses and phytoplankton cell counts.

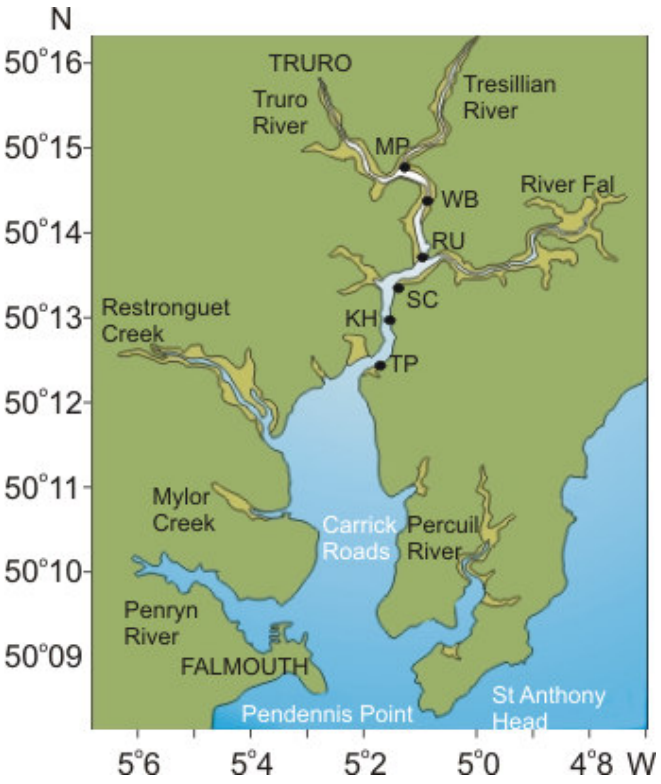

Figure 2.3. Map of the Fal estuary showing sampling stations; MP = Malpas; WB = Woodbury; RU = Ruan; SC = Smuggler's Cottage; KH = King Harry Reach; TP = Turnaware Point.

	Tidal range (m)	Malpas (MP)	Woodbury (WB)	Ruan (RU)	Smuggler's Cottage (SC)	King Harry Reach (KH)	Turnaware Point (TP)
Latitude (°N)		50.245-50.247	50.240-50.242	50.228-50.229	50.220-50.224	50.215-50.218	50.207-50.211
Longitude (°W)		5.022-5.023	5.014-5.015	5.016	5.022-5.027	5.027-5.028	5.028-5.030
a. 2006 RIB							
04/07	2.35			13:04 (+2.2)		13:34 (+2.7)	13:40 (+2.8)
05/07	2.25					13:44 (+1.9)	13:45 (+1.9)
07/07	2.60	12:03 (-1.9)	12:28 (-1.5)	13:00 (-0.9)	13:13 (-0.7)		13:24 (-0.5)
08/07	2.90	09:13 (-5.7)	10:18 (-4.6)	10:30 (-4.4)	10:49 (-4.1)		11:45 (-3.2)
09/07	3.30	09:07 (+5.7)	09:39 (-5.9)	10:13 (-5.6)	10:38 (-5.2)	11:00 (-4.9)	11:24 (-4.5)
11/07	4.10	?	?		10:32 (+5.4)	10:16 (+5.1)	10:00 (+4.8)
14/07	4.50	09:42 (+2.1)	10:07 (+2.5)		10:35 (+3.0)		11:19 (+3.7)
15/07	4.45	09:28 (+1.1)				10:51 (+4.5)	
16/07	4.20	08:58 (-0.2)	09:35 (+0.5)	09:55 (+0.8)	10:17 (+1.2)	10:40 (+1.5)	10:39 (+1.5)
b. 2006 Bill Conway							
04/07	2.35				10:01 (-0.8)	10:52 (+0.0)	11:14 (+0.4)
05/07	2.25				08:23 (-3.4)		10:11 (-1.6)
07/07	2.60				09:21 (-4.6)	10:03 (-3.9)	10:44 (-3.2)
08/07	2.90				09:27 (-5.5)	10:29 (-4.5)	10:49 (-4.1)
09/07	3.30					09:46 (-6.1)	10:50 (-5.4)
11/07	4.10				12:07 (-5.3)	12:28 (-5.0)	12:49 (-4.6)
12-07	4.20				12:43 (-5.5)	13:14 (-5.0)	13:33 (-4.7)
14/07	4.50				12:38 (+5.0)	12:15 (+4.6)	11:54 (+4.3)
15/07	4.45				12:17 (+3.9)		11:38 (+3.2)
16/07	4.20						
c. 2007 RIB							
04/07	3.85	09:10 (+1.4)	10:14 (+2.5)	10:44 (+3.0)	11:28 (+3.7)	12:20 (+4.6)	
05/07	3.80	09:13 (+0.8)*	09:58 (+1.5)	10:26 (+2.0)	11:08 (+2.7)		11:36 (+3.2)
06/07	3.65	09:23 (+0.2)	10:40 (+1.5)	11:40 (+2.5)	12:40 (+3.5)		13:34 (+4.4)
07/07	3.35	12:09 (+2.2)				12:49 (+2.9)	13:37 (+3.7)
10/07	2.85	09:12 (-3.9)*	09:52 (-3.2)	10:30 (-2.6)	11:14 (-1.9)	12:10 (-0.9)	12:46 (-0.3)
11/07	2.95	09:13 (-5.0)	09:59 (-4.3)	10:56 (-3.3)	12:01 (-2.3)		12:50 (-1.4)
12/07	3.25	09:17 (-6.0)	09:44 (-5.6)	10:16 (-5.1)		10:57 (-4.4)	11:26 (-3.9)
d. 2007 Bill Conway							
04/07	3.85				12:33 (+4.8)		11:53 (+4.2)
05/07	3.80				12:58 (+4.5)*		
06/07	3.65				13:20 (+4.2)		
07/07	3.35				13:10 (+3.2)*		
10/07	2.85			09:21 (-3.8)*			10:38 (-2.5)
11/07	2.95				09:52 (-4.4)*		
12/07	3.25			11:06 (-4.2)			11:57 (-3.4)

Table 2.3. (a) Sampling dates and times for the main stations sampled in the Fal Estuary in (a, b) 2006 and (c, d) 2007 using a RIB (a, c) or the research vessel *RV Bill Conway* (b, d). Figures in brackets represent time (hours) relative to high tide. * Indicates where nutrient uptake incubations were performed in 2007, however in 2006 samples for nutrient uptake were collected on separate occasions.

	Malpas (MP)	Woodbury (WB)	Ruan (RU)	Smuggler's Cottage (SC)	King Harry Reach (KH)	Turnaware Point (TP)
Latitude (°N)	50.245-50.247	50.240-50.242	50.228-50.229	50.220-50.224	50.215-50.218	50.207-50.211
Longitude (°W)	5.022-5.023	5.014-5.015	5.016	5.022-5.027	5.027-5.028	5.028-5.030
a. 2006 RIB						
04/07			0.2		0.2	0.2
05/07					0.2	0.2
07/07	0.2	0.2	0.2	0.2		0.2
08/07	0.2	0.2	0.2	0.2		0.2
09/07	0.2	0.2	0.2	0.2	0.2	0.2
11/07	0.2	0.2		0.2	0.2	0.2
14/07	0.2	0.2		0.2		0.2
15/07	0.2				0.2	
16/07	0.2	0.2	0.2	0.2	0.2	0.2
b. 2006 Bill Conway						
04/07				2, 13	2, 13	2, 14
05/07				0.5, 4, 14		0.5, 5, 17
07/07				0.5, 6, 12	5, 12	0.5, 14
08/07				0.5, 4, 11	0.5, 11	0.5, 15
09/07				0.5, 10, 14		0.5, 4, 12
11/07				2, 6, 12	2, 3, 10	2, 3, 12
14/07				2, 5, 12	2, 6, 12	0.5, 5, 15
15/07				0.5, 5, 11		0.5, 7, 15
16/07						
c. 2007 RIB						
04/07	0.2	0.2	0.2	0.2	0.2	
05/07	0.2	0.2	0.2	0.2		0.2
06/07	0.2, 1, 2.5	1, 3, 5.5	1, 5, 9		1, 5, 7	1, 2.5, 5
07/07	0.2				0.2, 10	0.2, 4
10/07	0.2	1, 5	1, 7	1, 12	1, 10	1, 6
11/07	1	1, 5	1, 7	1, 10		1, 8
12/07	1	1	1		1	1
d. 2007 Bill Conway						
04/07				0.5, 5, 10		0.5, 5, 10
05/07				0.5, 5, 10		
06/07				0.5, 2		
07/07				0.5, 8, 15		
10/07			0.5, 4, 8.5			0.5, 3, 16
11/07				0.5, 3, 10		
12/07			0.5, 7			0.5, 3, 14

Table 2.4. Sampling depths for the main stations sampled in the Fal Estuary in (a, b) 2006 and (c, d) 2007 using (a, c) a RIB or (b,d) the research vessel *RV Bill Conway*.

	Lambert's Bay			CRIA I		CRIA II		Fal 2006		Fal 2007	
	2006	2007	2008	Inc stns	General	Inc stns	General	Inc stns	General	Inc stns	General
NO_3	✓	✓	✓	XAAS	XAAS	✓	XAAS	✓	UG	✓	UG
PO_4	HW/TAP	TAP	TAP	XAAS	XAAS	✓	XAAS	✓	UG	✓	UG
Si	HW/TAP	TAP	TAP	XAAS	XAAS	✓	XAAS	×	UG	✓	UG
NH_4	✓	✓	✓	XAAS	XAAS	✓	XAAS	✓	×	✓	×
NO_2	✓	✓	✓	XAAS	XAAS	×	XAAS	×	×	×	×
Urea	✓	✓	✓	✓	×	✓	×	✓	×	✓	×
DO	TAP	TAP	TAP	×	CGC	CGC	CGC	×	UG	×	UG
chl-a	DC	DC	GCP	×	FGF	FGF	FGF	✓	UG	✓	UG
Phyto counts	DC	DC	GCP	✓	FGF	✓	FGF	✓	UG/FG*	✓	JS/FG*
ρN	✓	✓	✓	✓	n/a	✓	n/a	✓	n/a	✓	n/a
FRRf	×	✓	✓	×	×	×	×	×	×	×	×

Table 2.5. Personnel responsible for collecting the various data used in this thesis. Ticks indicate data produced by the author. Crosses indicate absence of data. HW = Howard Waldron (University of Cape Town); TAP = Trevor A. Probyn, DC = Desiree Calder and GCP = Grant C. Pitcher (Marine & Coastal Management); XAAS = Xavier Antón Álvarez-Salgado, CGC = Carmen Gonzáles Castro; FGF = Francisco Gómez Figueiras (Instituto de Investigaciones Marinas). UG = University of Southampton 3rd year undergraduates. * Phytoplankton samples collected by students (2006) or Joanne Souter (JS) (2007) but analysed by Fernando Gomez (FG).

2.2. Ancillary data

2.2.1. Meteorology

Wind speeds and directions in Lambert's Bay were obtained from the Nortier weather station situated 8.5 km from the sampling station (32.04 °S, 18.33 W), on a hill at 97 m altitude where it is exposed to maritime wind conditions. The data were supplied by the South African Weather Service (charlotte.mcbride@weathersa.co.za) upon request.

Wind data in the Ría de Vigo were obtained from the MeteoGalícia weather station (http://www.meteogalicia.es) on Islas Cíes for September, although in June the data were obtained from the Seawatch buoy off Cabo Silleiro that is maintained by Puertos del Estado (http://www.puertos.es/es/oceanografia_y_meteorologia/banco_de_datos/viento. html). Monthly rainfall data were obtained from the Islas Cíes MeteoGalícia station for the period October 2005 to July 2007. Daily solar radiation data were obtained from the Vigo campus MeteoGalícia station for September 2006 and June 2007.

Monthly rainfall, minimum and maximum temperatures and monthly duration of sunshine for the Fal Estuary were obtained from the UK Met Office meteorological station at St. Mawgan, situated at 103 m above mean sea level (http://www.metoffice.gov.uk/climate/uk/stationdata/).

2.2.2. Dissolved oxygen

In all studies DO concentrations obtained from the CTD electrode (or from the YSI sensor in the Fal) were calibrated against discrete sample measurements using the Winkler titration method as modified by Carpenter (1965). In Lambert's Bay, measurements were made in triplicate and in the Fal Estuary they were made in duplicate on a few occasions. CTD DO values were in ml l^{-1} in Lambert's Bay (except in 2007 when an arbitrary unit was given) and in the Ría de Vigo, whereas the YSI DO values were given as % saturation. Measured concentrations were also in different units in the 3 studies: ml l^{-1} in Lambert's Bay, μmol kg^{-1} in the Ría de Vigo and μmol l^{-1} in the Fal, therefore all measurements were converted to μmol l^{-1} for calibration, using the ideal gas law which gives a molar volume of 22.414 l at standard temperature and

pressure. CTD/YSI DO values and discrete measured concentrations were significantly correlated in all studies (Figure 2.4). In Lambert's Bay, a different CTD was used in 2007 that reported DO in a different unit, hence the difference in the slope of the calibration curve in this year. Also, different calibrations were obtained for March and April 2007. For these reasons, the DO data for this year should be interpreted with caution. Also, different calibrations were obtained for the two YSI probes in the Fal Estuary. The YSI 650 was not considered to provide reliable DO measurements, hence the data was not used.

Saturated DO concentration (DO_{sat}, ml l^{-1}) was calculated from temperature and salinity using the equation of Weiss (1970):

$$\ln (DO_{sat}) = Al + A2 * 100/T + A3 * \ln (T/100) + A4 * T/100 + S [B1 + B2 * T/100 + B3 (T/100)^2] \quad (2.1)$$

where Al = -173.4292

A2 = 249.6339

A3 = 143.3483

A4 = -21.8492

Bl = -0.033096

B2 = 0.014259

B3 = -0.001700

and T = temperature in Kelvin (= °C + 273.15)

S = salinity in g kg^{-1} (ppt)

These values were then converted to µmol l^{-1} following the equation:

$$DO_{sat(\mu mol)} = DO_{sat(ml)} / 22.414 * 1000 \quad (2.2)$$

Saturation percentages were calculated from the equation:

$$\%Sat = DO_{cal} / DO_{sat} \times 100 \quad (2.3)$$

where DO_{cal} is calibrated DO concentration (µmol l^{-1}) measured by the CTD.

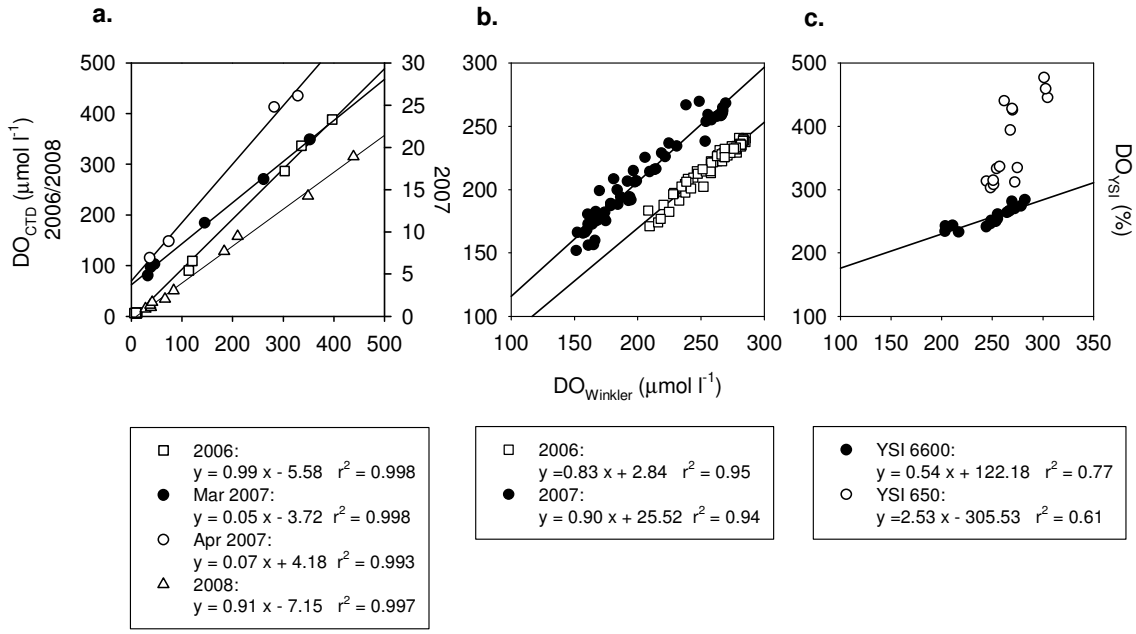

Figure 2.4. Calibration curves for DO in (a) Lambert's Bay, (b) the Ría de Vigo and (c) the Fal Estuary. In the Fal Estuary, calibrations are for the 2 YSI probes.

2.2.3. Nutrients

In Lambert's Bay, all nutrients were determined manually after filtration through Whatman GF/F filters within 2 h of collection. Measurements were made on a single water sample in triplicate for NH_4^+ and urea and in duplicate for NO_2^-, Si and PO_4^{3-}, but no replication was used for NO_3^- due to the time consuming nature of manual analysis. Nitrate concentrations were determined colourimetrically after reduction to NO_2^- on a cadmium column (see Appendix 1) and corrected for ambient NO_2^- (Nydahl, 1976). Silicic acid, PO_4^{3-}, NH_4^+, NO_2^- and urea were measured following the methods of Grasshoff et al. (1999) scaled to 5 ml sample volumes (see Appendix 1). Analytical precisions (calculated for each set of measurements from standard deviations of 3 replicate standard measurements (2 for NO_2^-), i.e. a measure of repeatability) were 0.12-0.24 µmol N l^{-1} for NO_3^- (coefficient of variation 0-3.5 %); 0.01-0.05 µmol N l^{-1} for NO_2^- (0-5.8 %); 0.04-0.10 µmol N l^{-1} for NH_4^+ (0-6.5 %) and 0.08-0.09 µmol N l^{-1} for urea (0-11.4 %).

In the Ría de Vigo the nutrient samples collected by IIM (NO_3^-, NO_2^-, NH_4^+, PO_4^{3-}, Si) were analysed within ~6 h in both years using an Alpkem autoanalyser following the method of Hansen & Grasshoff (1983) as modified by Mouriño & Fraga (1985), to a precision of 0.05 µmol l^{-1} for all nutrients. The additional measurements made in

association with the incubations were performed on fresh samples in 2006, but samples for NO_3^-, PO_4^{3-}, Si and NH_4^+ were frozen and analysed at NOCS in 2007. Nitrate, PO_4^{3-} and Si were analysed on a Skalar autoanalyser in 2007, following the methods of Armstrong et al. (1967), Murphy & Riley (1962) and Grasshoff et al. (1999), respectively. The ranges of precisions for various standard concentrations were 0-0.05 μmol l^{-1} (0.1-0.5 %), 0-0.04 μmol l^{-1} (0-1.7 %) and 0.03-0.18 μmol l^{-1} (0.2-1.2 %) for NO_3^-, PO_4^{3-} and Si, respectively. Frozen samples from 2006 were also analysed using these methods, for comparison with the measurements performed on fresh samples. Ammonium was measured using the fluorometric (o-Phthaldialdehyde, OPA) method of Holmes et al. (1999) (Appendix 1). After reagent addition, samples were incubated overnight in the dark and fluorescence was determined on a Turner Designs TD700 fluorometer (excitation wavelength 350 nm, emission wavelength 410-600 nm). Precision was 0-0.02 μmol l^{-1} (0.3-6.8 %) depending on standard concentration. Urea was determined manually on fresh samples following the diacetylmonoxime thiosemicarbazide method of Mulvenna & Savidge (1992) adapted to room temperature using reaction times of 72-96 h (Goeyens et al., 1998) in 2006 (Appendix 1), but following the method of Grasshoff et al. (1999) in 2007. Precisions were 0.01-0.05 μmol N l^{-1} (1-16.5 %) in 2006 and 0-0.04 μmol N l^{-1} (0-15.9 %) in 2007, depending on standard concentration.

In the Fal, routine nutrient measurements were carried out by the students who filtered two freshly collected 50 ml samples through 25-mm GF/F filters in syringe filter units then stored them in rinsed brown glass (NO_3^-, PO_4^{3-}) or polyethylene (Si) bottles. These were kept in a cool box and transported ashore where they were stored overnight in a refrigerator prior to analysis the following day. Phosphate and Si were analysed manually following the spectrophotometric method of Parsons et al. (1984) and NO_3^- + NO_2^- was analysed following the flow injection method of Johnson & Petty (1983). Additional nutrient analyses were performed in association with the nutrient uptake incubations. Filtrate obtained prior to the $^{15}NH_4^+$ incubation was decanted into three rinsed 20 ml Diluvials and kept cool until transported ashore.

In 2006, samples for NO_3^- + NO_2^-, PO_4^{3-} analyses were frozen and analysed at NOCS with a Burkard Scientific autoanalyser, following the methods of Hydes & Wright (1999) with precisions of 0.4-2.4 μmol l^{-1} (4.1-12.2 %) and 0.06-0.09 μmol l^{-1} (4.4-15.7

%), respectively. Samples for urea were frozen and analysed following the method of Goeyens et al. (1998) with precisions of 0.01-0.02 μmol l^{-1} (1.4-5.3 %).

In 2007, samples for $NO_3^- + NO_2^-$, PO_4^{3-} and Si were frozen and analysed at NOCS with a Skalar autoanalyser following the methods of Armstrong et al. (1967), Murphy & Riley (1962) and Grasshoff et al. (1999), respectively. Precisions were 0.28-0.69 μmol l^{-1} (1.4-13.7 %) for NO_3^-, 0.02-0.05 μmol l^{-1} (0.8-10.7 %) for PO_4^{3-} and 0.13-0.27 μmol l^{-1} (1.3-9.1 %) for Si. Urea was measured following the method of Grasshoff et al. (1999) with precisions of 0.02-0.08 μmol N l^{-1} (4.9-23.6 %). For this, samples were incubated on hot plates for 2.5 h. Ammonium analyses in both years were performed manually on fresh samples following the same methods as in CRIA II, with precisions of 0-0.04 μmol N l^{-1} (1.6-10.7 %) in 2006 and 0-0.03 (0.5-17.4 %) in 2007.

2.2.4. Chl-a

In Lambert's Bay, 100 ml samples were collected for chl-a and filtered onto 25-mm Whatman GF/F filters. Duplicate samples were filtered in association with nutrient uptake incubations. Filters were then placed in 10-ml centrifuge tubes and pigments extracted in 9 ml of 90 % acetone for at least 24 hours at -20 °C in the dark (Parsons et al., 1984). These samples were then centrifuged for 10 min to separate cellular debris from the solution. Fluorescence was determined using a Turner Designs 10-AU fluorometer calibrated with commercial chl-a (Sigma). Readings were taken before and after acidification with 2 drops of 10 % HCl to correct for phaeopigments. Extracted chl-a concentrations were significantly correlated with CTD fluorescence measurements in all years (Figure 2.5a).

In the Ría de Vigo, 100-250 ml were filtered in the laboratory onto 25-mm GF/F filters and filters were stored frozen at -20 °C. Chl-a was later extracted in 90 % acetone at 4 °C in the dark for 24 h. Chl-a concentrations were determined following the Welschmeyer method (Welschmeyer, 1994). Calibration curves are shown in Figure 2.5b.

In the Fal Estuary, 50 ml were filtered on-board onto 25-mm GF/F filters using a syringe and filters transferred directly into centrifuge tubes containing 7 ml 90 % acetone and stored in a refrigerator overnight. Chl-a concentrations were determined

following the Welschmeyer method (Welschmeyer 1994). CTD calibration curves are shown in Figure 2.5c. The fluorometer excitation wavelength was 436 nm and the emission wavelength 690 nm.

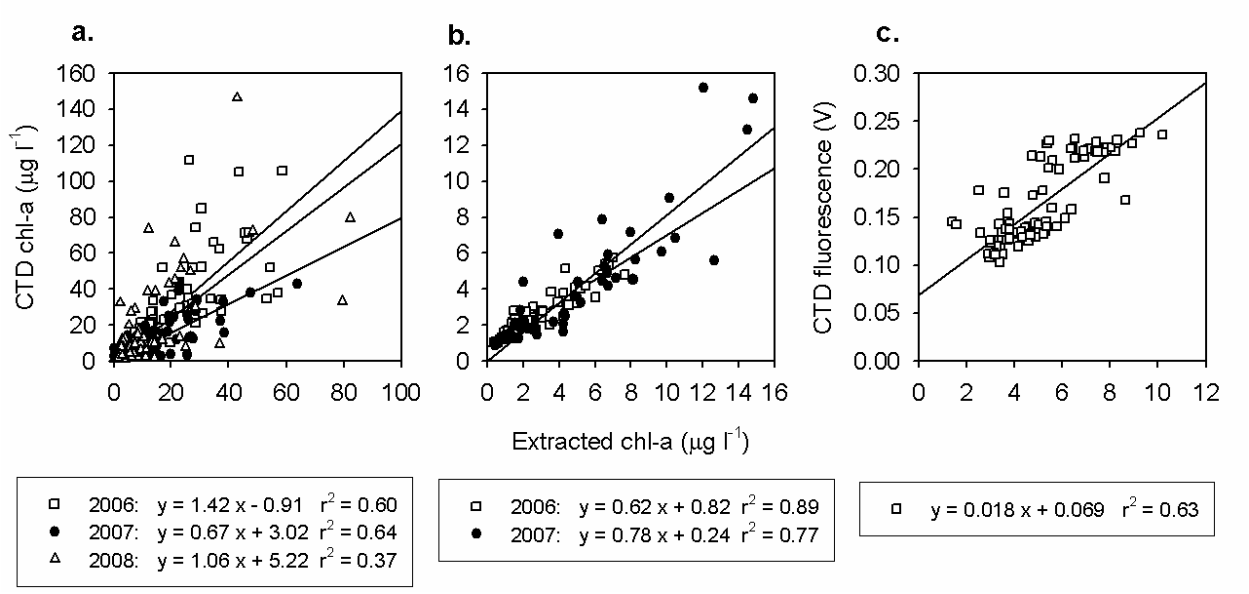

Figure 2.5. CTD calibration curves for chl-a in (a) Lambert's Bay, (b) the Ría de Vigo and (c) the Fal Estuary.

2.2.5. Phytoplankton counts

In Lambert's Bay, phytoplankton samples (100 ml) were preserved with buffered formalin (2.5 % final concentration) and stored in 100-ml clear plastic bottles. Subsamples of 10 ml were settled overnight and counted in 2-ml slides using inverted microscopy (Utermöhl, 1958). Identification was to species level where possible. Three species of *Pseudo-nitzschia* were enumerated in 2007, when *Pseudo-nitzschia* spp. was very abundant, including *P. australis* and 2 unidentified species. For the nutrient uptake kinetics experiments carried out on 16 March 2006, 21 March 2007, 8 April 2007, 21 and 25 March 2008, biomass estimates were made to determine the dominance of *Pseudo-nitzschia* (Expt 1), *Alexandrium catenella* (Expt 2) and *Dinophysis acuminata* (Expts 3-5). These were derived from cell volumes calculated from cell measurements and stereometric shapes (Hillebrand et al., 1999) followed by biovolume to carbon conversions (Menden-Deuer & Lessard, 2000). Due to the low number of species in these experiments and their consistent cell sizes, these estimates were considered to be robust, however the conversion to carbon biomass was not warranted for the routine cell counts as it may have introduced further inaccuracies.

For the Ría de Vigo and Fal Estuary, samples were preserved in association with the nitrogen uptake incubations and counted at NOCS. However, for a general analysis of spatial and temporal variation in phytoplankton community structure, the data provided by IIM for all stations and depths sampled in the Ría de Vigo were used. For the Fal, a selection of samples collected by students, Joanne Souter and those associated with the uptake incubations were re-counted in February 2009 by Dr Fernando Gómez at Laboratoire Arago in Banyuls-sur-Mer. The same methods were used in all cases.

In the Ría de Vigo and the Fal Estuary, water samples were preserved with Lugol's Iodine (1 % final concentration) and stored in 100-ml brown glass bottles for <7 months before counting. For each sample, a 10 ml volume was settled overnight and counted under a Leica inverted microscope (Utermöhl, 1958). Transects across the graticule diameter (between 1 and 4 depending on species number) were counted under 200 x magnification, then the whole chamber was scanned under 100 x magnification for larger, rarer cells (e.g. *Rhizosolenia* spp., *Ceratium* spp., *Dinophysis* spp., *Protoperidinium* spp...).

Cell concentrations were calculated from the equation:

$$Cell_{conc} = Cell_{count} * A_{chamber} / A_{count} * 1000 / V \quad (2.4)$$

where $Cell_{conc}$ is cell concentration in the sample (cells l^{-1}), $Cell_{count}$ is number of cells counted (sum of all transects), $A_{chamber}$ is the area of the sedimentation chamber (= 572.56 mm^2), A_{count} is the total area counted (sum of all transects, one transect being 27 mm^2 under 200 x magnification) and V is the volume settled.

Multivariate analyses were performed on the count data using the package Plymouth Routines In Multivariate Ecological Research (PRIMER, version 5). Between station similarities were calculated using the Bray-Curtis similarity index based on standardised cell concentrations after square root transformation. Data for all species were used, regardless of species contribution. The similarity matrices obtained were then used to perform cluster analyses. SIMilarity PERcentages (SIMPER) analysis was performed on standardised count data after square root transformation, to determine species' contribution to similarity within the clusters identified at similarity levels ranging from 40 to 60 %. The Shannon Diversity Index (Shannon, 1948) was calculated using PRIMER from:

$$H' = -\sum_{i=1}^{s} p_i \ln p_i \quad (2.5)$$

where S is the number of species and p_i is the proportion of each species i relative to total phytoplankton abundance.

2.2.6. FRRf

A Chelsea Instruments Fastracka™ FRRf fitted with PAR and depth sensors was deployed in the Benguela to a depth of 20 m in 2007 and 30 m in 2008 to measure variable fluorescence. Both light and dark measurements were made in sequences of 100 saturation flashlets followed by 20 decay flashlets. 8 repeat measurements were averaged in 2007 but in 2008 this was changed to 4 to increase the depth resolution. As a result, measurements were made approximately every 1.5 m in 2007 and every 0.7 m in 2008. Initial fluorescence (F_0), maximum fluorescence (F_m), variable fluorescence ($F_v/F_m = (F_m - F_0)/ F_m$), functional absorption cross-section of photosystem II (σ_{PSII}), and photosynthetic turnover (τ) were calculated using the software FRS (Chelsea Instruments Ltd., version 1.8).

2.3. Nitrogen uptake

2.3.1. Incubations

2.3.1.1. Standard uptake measurements

In Lambert's Bay, water from each depth (Table 2.1) was decanted into two 1-l Nalgene polycarbonate bottles and one 2-l Nalgene bottle. The 1-l samples were inoculated with stock solutions of $K^{15}NO_3$ and urea [$CO(^{15}NH_2)_2$] and the 2-l sample with $^{15}NH_4Cl$. All stock solutions had a concentration of 1µmol N ml^{-1} and ^{15}N purities were 99.6, 99.1 and 99.7 % for $K^{15}NO_3$, $CO(^{15}NH_2)_2$ and $^{15}NH_4Cl$, respectively. The volume of ^{15}N spike in each case was adjusted to achieve a final concentration of approximately 10 % of the ambient nutrient concentration (based on the previous day's concentration for NH_4^+ and urea and on the NO_3^- vs temperature relationship for NO_3^-). However, due to the extremely variable nutrient concentrations and to the fact that nutrients were measured after the spike addition, this was not always achievable and aqueous enrichments ranged from 1 to 93 % (average for all 3 years 19.5 ± 15.9) (Table 2.6). Immediately after spiking the NH_4^+ sample, exactly 1 l was transferred to a separate 1-l polycarbonate bottle for incubation, while the remaining 1 l was filtered through a 47-mm Whatman precombusted GF/F filter to measure time zero aqueous ^{15}N enrichment (R_0) in the filtrate. Subsamples were also taken from the filtrate for later analyses of ambient NO_3^-, NH_4^+ and urea. The measured NH_4^+ concentration was subsequently corrected for the $^{15}NH_4Cl$ spike addition.

Spiked samples were incubated in perspex incubation tubes for 3 h at simulated *in situ* temperatures (10-15 ºC) and irradiances. Fifty percent shading was achieved with grey neutral density filters (Lee) for the subsurface samples, whereas the surface samples were incubated in a clear tube. Water was re-circulated through the incubators via chiller units set at the respective *in situ* temperatures for the 2 incubation depths. The temperature maintained by each chiller was generally within 1 ºC of *in situ* temperature although on a few hot days it exceeded it by up to 2 ºC. Incubations were terminated by filtration onto 47-mm precombusted GF/F filters, which were then rinsed with artificial seawater and dried at 75 ºC overnight. 15N uptake by the <0.8 µm fraction was assumed to be negligible therefore no sequential filtrations were performed to measure the loss of particulate ^{15}N through the GF/F filters. For ^{15}N analyses, between 10 and 15 small (5

mm diameter) discs were punched out of each filter, depending on the amount of material present, and pelletted into tin capsules (Pellican Scientific, 5 x 9 mm).

In the Ría de Vigo, similar procedures were carried out, using 0.5-l Nalgene cylindrical polycarbonate incubation bottles and volumes of 0.5 l (1 l was spiked with $^{15}NH_4Cl$ then 0.5 l was decanted into a 0.5-l bottle for incubation). Samples were incubated in a grey plastic box placed on-deck, through which surface water flowed. For subsurface samples, 50 % shading was provided by a nylon mesh. Incubations lasted for 1h30-2h in 2006 and 2h30-3h in 2007. Filtration of $^{15}NO_3^-$ and ^{15}N-urea spiked samples was onto 25-mm Whatman GF/F filters using a Pall Gelman polyurethane 3-port in-line filter funnel manifold. Waste filtrate was evacuated via a drain plug and collected in a 1-l Büchner flask. Filtration of $^{15}NH_4^+$ spiked samples was carried out with a different system that allowed clean collection of the filtrate for later isotopic dilution analyses. Water was filtered through precombusted 47-mm Whatman GF/F filters using a polyphenylsulfone 47-mm magnetic filter funnel and collected in an acid-washed 500-ml borosilicate Büchner flask (rinsed with Milli-Q in-between samples).

In the Fal, the same incubation volumes, bottles and filtration systems were used as in the Ría de Vigo. In 2006, samples were incubated *in situ*, suspended from a pontoon just below the surface and on occasion at 2 m depth (Table 2.3). In 2007, incubations were carried out in an on-deck incubator as in the Ría de Vigo. Incubations lasted 3h45-5h15 in 2006 and 1h20 to 2h10 in 2007, due to different logistical constraints in the 2 years.

	Nutrient	Nutrient concs µmol N l^{-1}	Spike concs µmol N l^{-1}	Enrichment (%) Range	Mean (se)
LB2006	NH_4^+	0.1-1.7	0.1	6-48	24.3 (2.1)
	NO_3^-	0.1-29.8	0.1-2.4	4-93	23.5 (6.0)
	Urea	0.2-3.1	0.1-0.2	4-41	18.6 (1.9)
LB2007	NH_4^+	0.1-4.4	0.1	2-65	22.2 (2.6)
	NO_3^-	0.1-23.8	0.1-2.0	1-70	27.0 (3.5)
	Urea	0.1-3.7	0.1	4-32	15.0 (1.7)
LB2008	NH_4^+	0.2-5.0	0.1-0.4	2-31	14.8 (2.0)
	NO_3^-	0.1-29.3	0.05-2.2	1-66	15.4 (3.7)
	Urea	0.3-2.6	0.1-0.2	4-27	14.7 (1.5)
CRIA I	NH_4^+	0.6-4.6	0.1	3-17	8.5 (2.0)
	NO_3^-	0.8-2.5	0.1	4-9	5.3 (0.6)
	Urea	0.1-1.1	0.1	8-42	22.0 (4.0)
CRIA II	NH_4^+	0.1-2.5	0.01-0.1	0.3-26	16.1 (3.9)
	NO_3^-	0.1-6.8	0.1-1.0	1-95	60.5 (10.9)
	Urea	0.1-0.6	0.01-0.1	3-51	26.6 (5.8)
Fal 06	NH_4^+	0.1-0.9	0.1	10-45	35.7 (5.8)
	NO_3^-	0.2-18	2	10-90	26.1 (6.4)
	Urea	0.3-0.8	0.1	11-22	17.8 (0.8)
Fal 07	NH_4^+	0.2-2.3	0.1	4-52	18.8 (5.4)
	NO_3^-	2.2-41.3	2	4-47	11.9 (4.4)
	Urea	0.1-0.7	0.1	12-60	25.2 (4.9)

Table 2.6. Ambient concentrations of NH_4^+, NO_3^- and urea, concentrations of ^{15}N after spike addition and aqueous enrichment (range and mean ± standard deviation) obtained in the 7 field studies.

2.3.1.2. Nitrogen uptake kinetics

In Lambert's Bay, one experiment was performed in 2006, two in 2007 and two in 2008 (Table 2.7). The choice of dates and depths was guided by phytoplankton community structure. Prior to the experiments, net samples were examined briefly under a dissecting microscope to determine whether a particular species was dominant. Furthermore, experiments were generally carried out when ambient NO_3^-, NH_4^+ and urea concentrations were low, although this was not the case for NO_3^- in experiments 2 and 4 and for urea in experiments 1 and 5. In the case of urea, uptake rates were measured successfully at saturating concentrations, therefore ν_{max} was estimated from the mean of ν measured at the 4 or 5 highest concentrations. However, there were not enough measurements in the range of sub-saturating concentrations, therefore K_s could not be determined. For NO_3^-, neither K_s nor ν_{max} could be estimated in experiment 2, however a lower limit estimate of ν_{max} was derived from $\nu(NO_3^-)$ at the ambient NO_3^- concentration

of 16.9 μmol l^{-1}. In experiment 4, high NO_3^- additions (up to 88 μmol l^{-1}) were carried out and Michaelis-Menten kinetics were observed.

Water from a clean 10-l sampling bucket (from 5 m in 2006 and 2008, from 0 m in 2007) was decanted into eighteen 250-ml sterile polystyrene screw-capped culture flasks. Six 250-ml sample were spiked with different volumes of 10 % enriched 1 mmol N l^{-1} NO_3^- solution, another 6 with NH_4^+ solution and the remaining 6 with urea solution to obtain final concentrations between 0.4 and 25 μmol N l^{-1} for NO_3^- and between 0.2 and 15 μmol N l^{-1} for NH_4^+ and urea. In 2008, this method was modified slightly because the use of a 10 % enriched solution led to very low enrichments (<3 %) at the lowest nitrogen additions, when ambient concentrations were substantial. Instead, the lowest addition consisted of a pure ^{15}N spike (0.01 ml). Subsamples were taken for NH_4^+, urea (2 x 5 ml) and NO_3^- (1 x 15 ml) analyses. Samples were incubated for 2 h in a plastic box maintained at ambient seawater temperatures by water flow through the chiller unit. Incubations were terminated by filtration onto 25-mm precombusted GF/F filters. Samples were analysed in the same way as the standard uptake samples. In 2008 (experiment 4) samples were pre-filtered through a 200-μm mesh to remove the large number of small jellyfish that were present in the water at this time.

In the Ría de Vigo, nutrient uptake kinetics were measured on one occasion in 2007 (Table 2.2), on a water sample dominated by a mixed diatom community (*Skeletonema costatum*, *Leptocylindrus* spp., *Nitzschia* cf. *americana*, *Chaetoceros socialis*). The experiment was carried out in 75-ml Sterilin Iwaki culture flasks, in the same incubator as the standard uptake incubations. Final nutrient concentrations were between 0.3 and 30 μmol N l^{-1} and the incubation lasted 2h30.

In the Fal, 2 experiments were carried out in 2006 on samples collected from King Harry Pontoon, co-dominated by a mixture of diatoms and *Alexandrium* spp. (Table 2.3), using 500-ml polycarbonate bottles filled with 200 ml water. Incubations were carried out *in situ*, just below the surface, with final concentrations in the range 0.3-21 μmol N l^{-1} for NH_4^+ and urea and 3.7-32 μmol N l^{-1} for NO_3^- and incubation lengths of 3.5 to 4.25 h.

Exp. #	Date	Depth	Dominant species	Cell conc.	PON	Ambient conc.		
						NH_4^+	NO_3^-	Urea
Lambert's Bay								
1	16/03/2006	5	*Pseudo-nitzschia* (80 %)	7,980	13.7	0.18	0.09	1.68[c]
2	21/03/2007	0	*A. catenella* (77 %)	304	34.8	0.16	16.89[a]	0.27
3	08/04/2007	0	*D. acuminata* (91 %)	31	7.2	0.42	0.47	0.23
4	21/03/2008	5	*D. acuminata* (50 %)	5384	27.5	0.53	14.25[b]	0.57
5	25/03/2008	5	*D. acuminata* (33 %)	108	8.8	0.30	0.10	0.79[c]
Ria de Vigo								
1	28/06/2007	0	Mixed diatoms	n/a	n/a	0.33	0.52	0.17
Fal Estuary								
1	10/07/2006	0	Mixed diatoms + *Alexandrium*	n/a	n/a	0.44	2.72	-
2	13/07/2006	0	Mixed diatoms + *Alexandrium*	n/a	n/a	0.20	5.34	-

Table 2.7. Date, depth and ambient NO_3^-, NH_4^+ and urea concentrations (µmol N l^{-1}) for each nitrogen uptake kinetics experiment carried out in the 3 systems. Dominant species' concentrations (x 10^3 cells l^{-1}) and total PON concentrations (µmol N l^{-1}) are given for monospecific blooms.
[a] ambient concentration hindered the determination of both K_s and ν_{max};
[b] high NO_3 additions were carried out to obtain ν_{max} and K_s;
[c] ambient concentration hindered the determination of K_s, but ν_{max} was estimated from the mean of ν at 4 or 5 highest concentrations.

The choice of incubation length was important, as it can significantly bias the resulting kinetics. Nutrient uptake kinetics rely on the assumption that substrate concentration is constant over time, an assumption that is violated by non-steady state conditions, therefore the equation is only valid for describing instantaneous rates, which is extremely difficult even using incubation lengths <5 min (Goldman & Glibert, 1982b; Lomas et al., 1996). Not only is the use of such short incubation lengths experimentally impractical, it would also seriously bias the results if uptake rates were not constant over time, as is often the case (Collos, 1983; Harrison et al., 1989; Lomas et al., 1996; Collos et al., 1997). Transient high uptake, or "surge" uptake may occur in the first few minutes of the incubation, such as has been observed in response to nutrient addition in both nitrogen-starved cultures (Conway et al., 1976; Goldman & Glibert, 1982a) and nitrogen-sufficient natural assemblages (Lomas et al., 1996). In this case, ν_{max} will be overestimated if a short incubation time is used. Conversely, if there is a progressive increase in nitrogen uptake observed after a time lag, ν_{max} will be underestimated by a short incubation length.

Conversely the incubation length should be kept short enough that substrate depletion does not occur at the lowest concentrations during the course of the incubation, as this would result in first order, rather than Michaelis-Menten kinetics, at the lowest concentrations (Fisher et al., 1981) and an overestimation of K_s (McCarthy, 1981). The time-dependency of K_s is poorly documented but has been observed in a few studies (Goldman & Glibert, 1982b; Wheeler et al., 1982).

Furthermore, longer incubation times could lead to significant dilution of the ^{15}N-labelled NH_4^+ pool by regenerated ^{14}N and thus underestimation of uptake rates at the lowest concentrations and overestimation of K_s (Fisher et al., 1981). This problem can, however, be overcome by correcting $\nu(NH_4^+)$ for this isotope dilution, as described below (Glibert et al., 1982b), or simply by keeping incubation lengths under 6 h. Similar incubation lengths have been used in uptake kinetics experiments by Collos et al. (1997) with ambient NO_3^- concentrations of 0.21-4.0 µmol l^{-1} and NH_4^+ concentrations of 0.14-2.98 µmol l^{-1}.

2.3.2. Correction for isotope dilution

Aqueous enrichment was measured at the beginning and end of all incubations to correct for the increase in $^{14}NH_4^+$ relative to $^{15}NH_4^+$ caused by NH_4^+ regeneration during the course of the incubation. In Lambert's Bay, 900 ml (400 ml in Ría de Vigo and Fal) of the NH_4 uptake filtrate from the beginning (T_0) and end (T_t) of each incubation were transferred to acid-washed 1-l glass Schott Duran bottles. The 900 ml volume was chosen to leave sufficient head space for the sample to expand while freezing and also to facilitate the subsequent ammonium diffusion and recovery process. The head space provided a suitable surface to volume ratio to optimise the diffusion rate as well as creating sufficient space beneath the cap to suspend a GF/F filter while avoiding contamination from the sample. Furthermore, this allowed for some of the surplus filtrate to be retained for nutrient analyses (NO_3, NO_2, urea and NH_4^+ at T_0, NH_4^+ only at T_t).

To recover sufficient NH_4^+ for analysis by stable isotope mass spectrometry (i.e. >50 µg N and <3 At% enrichment), 10 µmol NH_4Cl solution was added to each sample as a "carrier" (i.e. 0.9 ml of a 10 mmol l^{-1} solution, but 0.4 ml in the Ría de Vigo and Fal). At Lambert's Bay in 2008, 0.9 ml of a 14.7 g l^{-1} $HgCl_2$ solution was also added to prevent further biological activity and ensure that bacterial activity would not recommence upon thawing. Aqueous samples from Lambert's Bay were immediately frozen at -20°C, whereas in the Ría de Vigo and Fal they were initially stored in a refrigerator on-board then transferred to a freezer in the laboratory at the end of the day.

These samples were returned frozen to the laboratory (MCM in Cape Town, IIM in Vigo, NOCS for Fal samples and CRIA I samples) and prepared for the recovery of NH_4^+ onto GF/F filters by diffusion. Magnesium oxide (MgO) was added to the thawed

samples to increase the pH to >9 and thus liberate NH_4^+ as gaseous NH_3 (Brooks et al., 1989). A pre-combusted halved 25-mm GF/F filter was wetted with 20 µl of a 6.25 M potassium hydrogen sulphate ($KHSO_4$) solution to obtain a trapping capacity of 175 µg N (Stark & Hart, 1996). The concentration of $KHSO_4$ was adjusted from their method to suit a larger filter size while maintaining the same trapping capacity. A filter was suspended from the inside of each bottle cap to recover the diffused NH_3 following the method of Probyn (1987) modified for the use of $KHSO_4$ instead of H_2SO_4. Bottles with suspended filters were left for 2-3 weeks then filters were removed and dried overnight at 75 °C and pelletted in the same way as the standard uptake filters. The isotopic composition of the ammonium trapped on the filters was measured by stable isotope ratio mass spectrometry to provide a measure of aqueous enrichment at the start (R_0) and at the end of the experiment (R_t).

2.3.3. Mass spectrometry

The isotopic composition of all samples was determined on a GV Instruments IsoPrime™ stable isotope ratio mass spectrometer (SIRMS) interfaced with a EuroVector Euro EA elemental analyser. The system was based on the Europa Tracermass developed by Preston & Owens (1983). Control of the instrument and data output in 2006/2007 was by the software package MassLynx™ (Waters Corp.), although IonVantage (GV Instruments) was used in 2008.

2.3.3.1. Principle

Samples first pass through the CHN elemental analyser where the Dumas combustion method is employed (Figure 2.6). Samples are placed in an autosampler carousel that sequentially drops them into a combustion furnace (1040 °C) where flash combustion takes place after injection of O_2 (10-20 ml). Here, the major elements in the sample (C, H, N) are oxidised to CO_2, H_2O, N_2O and N_2 gases, respectively. These gases are carried by a helium carrier flow (flow rate 100 ml min^{-1}) into the reduction furnace (650 °C), where N_2O is reduced to N_2 in the presence of a copper catalyst and excess O_2 is removed by copper oxidation. The remaining gases pass through a water trap (anhydrous magnesium perchlorate). If C is not being analysed, CO_2 is also removed by a trap ("Pelisorb", Pelican Scientific). The gases then pass through a gas chromatograph

(GC) column (55 °C), which temporally separates interfering gases such as CO (same mass as $^{14}N_2$).

The N_2 gas is then introduced into a triple collector mass spectrometer where it is ionised by an electron impact ionisation source (accelerating voltage 3400 V). The resulting ions pass through a flight tube then a fixed magnet separates them on the basis of their mass to charge ratio (m/z). Ions of mass 28 ($^{14}N^{14}N$), 29 ($^{14}N^{15}N$) and 30 ($^{15}N^{15}N$) are detected by the triple collector, composed of Faraday cups, which become charged when hit by ions. The ion flux is converted to a proportional electrical current corresponding to masses 28, 29 and 30. A reference gas of known isotopic composition is measured once before each sample and used to correct for any instrument drift. A constant vacuum is maintained by a Turbomolecular pump which clears the instrument of waste gases. Delta values (δ, the excess of ^{15}N in the sample relative to the reference gas) are then calculated by the software from the expression:

$$\delta = (R_{sam} - R_{ref})/ R_{ref} * 1000 \quad (2.6)$$

where δ is in ‰ and R_{sam} and R_{ref} are the sample and reference ratios of minor (mass 29) to major beam (mass 28). At low enrichments (<5 %) the contribution of mass 30 is insignificant therefore it is not taken into account for the calculation of δ. This raw δ is then corrected for the relative enrichment of the reference gas relative to air. Isotopic abundance (At%) is calculated from Equation 2.7, which can also be expressed as:

$$\delta = (At\%_{sam} - At\%_{nat})/ (At\%_{nat}) * 1000$$

Rearranging this equation gives:

$$At\%_{sam} = \delta * At\%_{nat} / 1000 + At\%_{nat} \quad (2.7)$$

where $At\%_{nat}$ is the natural isotopic abundance of ^{15}N (0.3663 %).

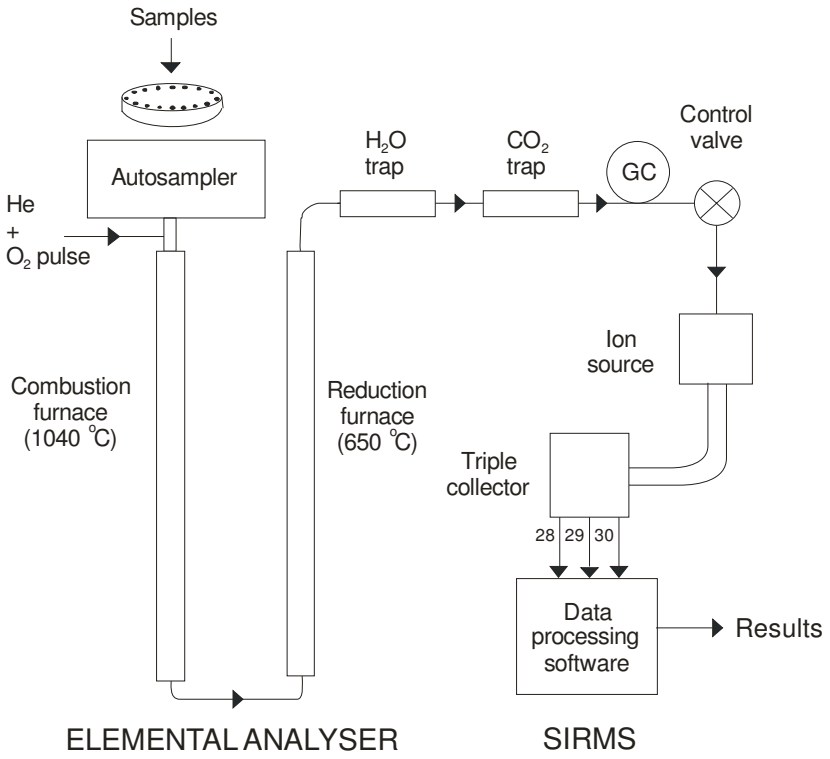

Figure 2.6. Schematic diagram of the elemental analyser interfaced with a stable isotope ratio mass spectrometer.

2.3.3.2. Instrument settings

The sensitivity of the instrument was adjusted to suit the sample size and expected enrichment, by altering the trap current (Table 2.8). The reference N_2 gas pressure was adjusted accordingly (from 15 to 30 psi).

Internal precision cannot be calculated for a continuous flow SIRMS since each sample is only measured once, as opposed to a dual inlet system which repeatedly measures both the sample and the reference gas.

Method precision was calculated from the standard deviation of repeated measurements of a urea standard (GV Instruments). Six standards were analysed for each batch of 30 samples. Precision was 0.0001 to 0.001 At% (CV between 0.02 and 0.30 %) for the 5 different sets of analyses performed between May 2006 and July 2008 (n = 15 to n = 47). Certified enriched ammonium sulphate standards (Aldrich) were also analysed to assess the accuracy of the instrument. The instrument drift was 0.002-0.009 At% at enrichments between 0.5 and 1 At%. Urea standards (N content 49.44 %) were also used to generate calibration curves for particulate nitrogen (PN) concentrations.

Trap	Mean sensitivity $\mu g\ nA^{-1}$	Sample range μg
100	23.81 (± 0.78)	100-300
200	9.04 (± 0.83)	50-150
250	5.99 (± 0.45)	30-90
300	4.41 (± 0.31)	25-75
400	4.19	20-70
500	2.89 (± 0.06)	15-50
600	2.72 (± 0.16)	5-35

Table 2.8. Various trap settings used for sample analysis and corresponding sensitivities, as determined from calibration curves of major beam height (nA) versus nitrogen content of weighed urea standards (µg). Approximate ranges of samples for which each trap setting was suitable are also shown.

2.3.3.3. Calculations

Standard nitrogen uptake

Nitrogen uptake (ρ in µmol N l^{-1} h^{-1}) was calculated from the equation of Dugdale & Wilkerson (1986):

$$\rho = r * PN/ (R * t) \quad (2.8)$$

where PN is particulate nitrogen (µmol N l^{-1})

t is incubation length (h)

r is At% excess of the particulate fraction (= $At\%_{sam}$ - $At\%_{nat}$)

R is At% enrichment of the aqueous medium:

$$R = (S * At\%_{nat}/ 100 + s * p)/ (S + s) * 100 - At\%_{nat} \quad (2.9)$$

where S is substrate concentration (µmol N l^{-1}), s is ^{15}N concentration after spike addition (µmol N l^{-1}) and p is ^{15}N spike purity.

For $\rho(NH_4^+)$, R can change quite appreciably during the course of the incubation due to microzooplankton excretion and/or bacterial regeneration. To take this into account, R was calculated at the start (R_0) and at the end (R_t) of each incubation. The amount of $^{15}NH_4^+$ present at T_0 and T_t can be expressed in 2 ways:

$$^{15}NH_4^+ = V * S_x * R_x + At\%_{nat} * C \quad (2.10a)$$

or

$$^{15}NH_4^+ = r_x (V * S_x + C) \quad (2.10b)$$

where V is sample volume (l), S_x is substrate concentration at t_x (µmol l^{-1}), C is the amount of NH_4^+ added as "carrier" (µmol) and r_x is the measured enrichment at t_x (At%). These can be combined to calculate R_0 and R_t:

$$R_x = [r_x (V * S_x + C) – At\%_{nat} * C]/ (V * S_x) \quad (2.11)$$

Measured R_0 values (R_{0meas}) were significantly correlated with theoretical values (R_{0calc}) calculated from the initial spike addition following Equation 2.9 (Figure 2.7). However, the regression coefficients were 0.9-2.4, which led to under- or overestimation of NH_4^+ uptake. To correct for this, it was assumed that R_t was affected in the same way as R_0 and the regression coefficient was used to adjust R_t.

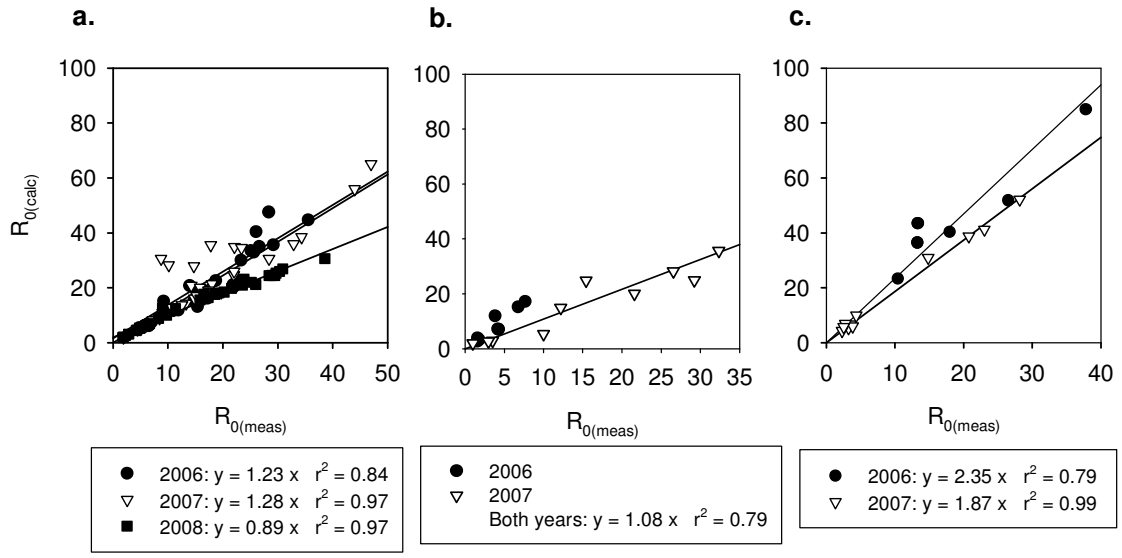

Figure 2.7. Linear correlations in (a) the Benguela, (b) the Ria de Vigo and (c) the Fal, between calculated R_0 and measured R_0 used to correct the measured R_t values in the final calculation of R_G. A single regression line was drawn for both years in the Ria de Vigo since the range of values in 2006 was more restricted than in 2007 and the slope may have been overestimated by excluding the 2007 values.

Using these corrected values, the average R over the time course of the incubation was then calculated based on the assumption that R decreases exponentially over time, following the equation of Glibert et al. (1982b):

$$R_G = R_0 / \ln(R_0/R_t) * (1-R_t/R_0) \quad (2.12)$$

This corrected value of aqueous enrichment (R_G) was then substituted for R in the calculation of uptake (Equation 2.8).

Ammonium regeneration rates

Ammonium recycling was calculated from the Blackburn-Caperon model (Blackburn, 1979; Caperon et al., 1979) since the NH_4^+ concentration always changed during the incubation:

$$r_{B\text{-}C} = [\ln(R_t/R_0)] / \ln(S_t/S_0) * (S_0 - S_t) \quad (2.13)$$

Nitrogen uptake kinetics

The kinetics parameters K_s (half-saturation constant) and ν_{max} (maximum PN-specific uptake rate) were obtained by fitting uptake (ν) versus concentration (S) data to the Michaelis-Menten equation using a computerised, iterative non-linear least squares regression (Jandel Scientific SigmaPlot).

$$\nu = \nu_{max} S/ (K_s + S) \quad (2.14)$$

where ν is PN specific uptake rate (h^{-1}), ν_{max} is maximum specific uptake rate (h^{-1}), S is substrate concentration (µmol N l^{-1}) and K_s is half-saturation constant (µmol N l^{-1}). The initial slope of the curve α, used as an indicator of nutrient affinity at concentrations < K_s, was calculated from $\alpha = \nu_{max}/ K_s$ (Healey, 1980).

The use of PN-specific rather than absolute uptake rates enables direct comparison with growth rates, however it implies that the presence of detrital nitrogen may lead to a dilution of the ^{15}N enrichment of the living particulate matter and thus an underestimation of ν and hence ν_{max}.

Cell-specific uptake rates (µmol N $cell^{-1}$ h^{-1}) are also used, although these are most suited to culture studies or monospecific blooms, where all the nitrogen uptake can be attributed to one species. In natural populations where other species are present, one must assume that all of the nitrogen is being taken up by the dominant species. The resulting $\nu_{max(cell)}$ will of course be an estimate, however its calculation is useful for

comparison with literature values and also to determine the effects of cell size. It was calculated for the Lambert's Bay experiments 1, 2 and 3 only, following the equation:

$$\nu_{max(cell)} = \nu_{max} * PN/ n \quad (2.15)$$

where PN is estimated nitrogen biomass (μmol N l^{-1}) of the dominant species (= Total PN * % dominance) and n is cell concentration of the dominant species (cells l^{-1}).

Ammonium inhibition kinetics parameters were determined by fitting the $\nu(NO_3^-)$ versus NH_4^+ concentration data to a modified Michaelis-Menten equation (Varela & Harrison, 1999) using the same regression technique as for the uptake kinetics:

$$\nu = \nu_{max} - (\nu_{max} * I_{max} * S)/ (K_i + S) \quad (2.16)$$

2.4. Statistics

Where comparisons were made between groups of data (e.g. between years), Student's t-tests were applied, provided that variances within each group were not significantly different (as determined by a two-tailed F-test). If this condition was not met, the non-parametric Mann-Whitney U-test was employed.

For matched pairs of samples (e.g. to compare simultaneous surface and subsurface measurements or measurements of different parameters made on the same water sample), the parametric paired t-test or the non-parametric Wilcoxon's signed ranks test were chosen, following the same criteria. The level of confidence used to determine significance was 95 % ($p < 0.05$).

3 Nitrogen nutrition of phytoplankton assemblages dominated by different HAB species in Lambert's Bay in March 2006, 2007 and 2008.

3.1. Introduction

3.1.1. General features of the Southern Benguela

3.1.1.1. Physical features

The Benguela upwelling system is one of the four major eastern-boundary upwelling systems in the world, alongside the California, Humboldt and Canary current systems. It is part of the anticyclonic South Atlantic Gyre, flowing northwards along the west coast of southern Africa. Although disputed, the boundaries of the Benguela can be considered as Cape Agulhas (34 ºS) to the south and Walvis Ridge (15 ºS) to the North (Shannon, 1985 and references therein). The Benguela is unique among upwelling systems in that it is bounded by warm currents at both extremities; by the Angola current to the North (from which it is separated by the Angola/Benguela front) and by the Agulhas current to the South (Shannon, 1985a). To the South, rings or filaments of warm Indian Ocean water shed periodically by the Agulhas Retroflection can penetrate the Benguela current (Figure 3.1).

Upwelling/relaxation cycles are forced locally by the wind stress field of southern Africa, whereby southeasterly Trade winds drive Ekman transport of the surface layer away from the shore, causing upwelling of cold, nutrient-rich deep water to the surface. Upwelled water originates from South Atlantic Central Water (i.e. from the thermocline), which displays a linear temperature-salinity plot, with temperatures between 6 and 16 ºC and salinities between 34.5 and 35.5 (Shannon, 1985a).

Offshore, the water column remains stratified while inshore the water column becomes well mixed, and an upwelling front may develop where the thermocline outcrops, separating warm offshore water from colder inshore water. Upwelled water is displaced offshore, and may sink again at the front. As in the other upwelling systems,

slow poleward undercurrents (Nelson & Hutchings, 1983) and faster subsurface equatorward jets are observed.

The Benguela is divided into two quasi-independent subsystems separated by the Lüderitz upwelling cell (27 ºS, Figure 3.1): the Northern (~ Namibian coast) and Southern Benguela (~ South African coast). The sampling station used in this study is situated in the latter, therefore this chapter will focus on the Southern Benguela. Wind fields in this region are related to displacements of the South Atlantic high pressure system (to the North in winter), changes in the seasonal pressure field over the adjacent subcontinent (from a well-developed low in summer to a weak high in winter) and to eastward moving cyclones produced by perturbations in the subtropical jet stream (Nelson & Hutchings, 1983). As a result, upwelling in the Southern Benguela is highly seasonal, occurring mainly during the spring and summer (September to March) (Andrews & Hutchings, 1980), while winter is characterised by quiescent, westerly winds. Seasonal variability is therefore higher in the Benguela than in the other upwelling systems, although interannual variability is less pronounced. Short-term variability in synoptic wind patterns during the upwelling season also drives upwelling/relaxation cycles at the time scale of 3-10 days, whereby relaxation events are associated with the eastward passage of cyclones (Nelson & Hutchings, 1983). The autumn and winter are characterised by periodic offshore, dry and warm “Berg” winds that are caused by the formation of a large high pressure cell over the subcontinent. These winds can carry substantial quantities of sand and dust up to 150 km offshore (Shannon & Anderson, 1982). Coastal trapped waves can also influence upwelling and shelf currents, for example by periodically creating an inshore poleward countercurrent during upwelling relaxation events (Shannon, 1985a).

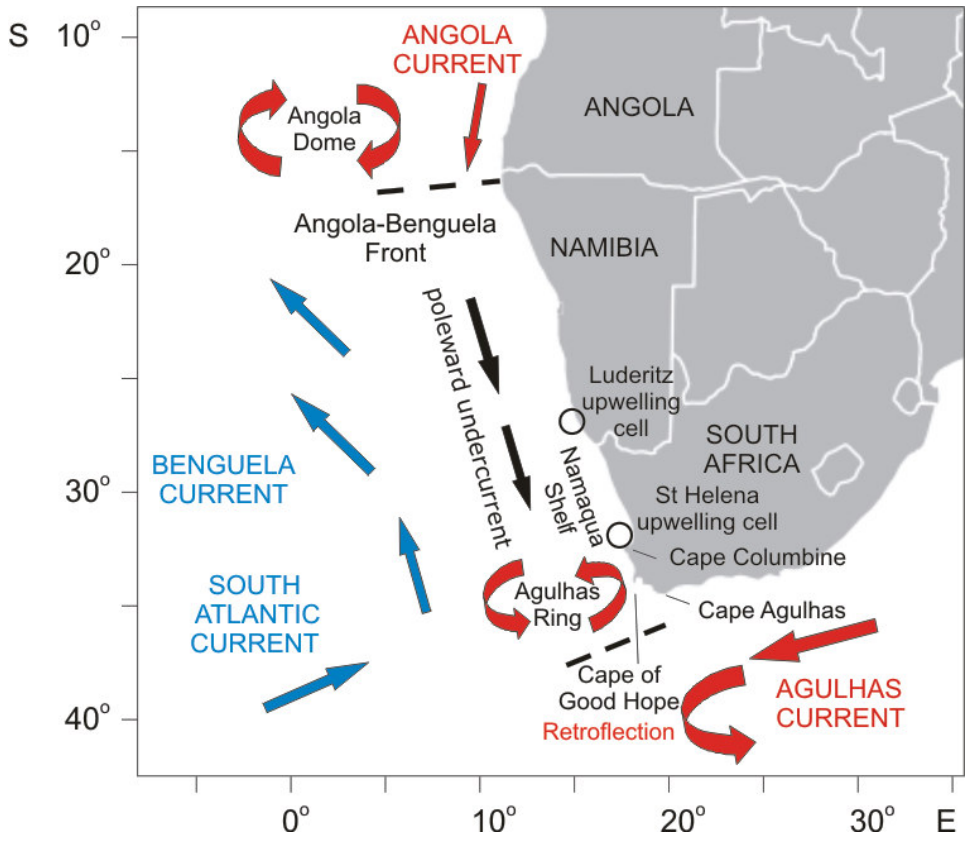

Figure 3.1. Map of Southern Africa showing general circulation patterns of the Benguela and adjacent currents. Adapted from Shannon (2001).

Upwelling is also influenced locally by the coastal topography and orientation of the coastline, and tends to be stronger where the shelf is narrower (e.g. the Namaqua upwelling centre) and in the vicinity of promontories and capes, (e.g. Cape Columbine and Cape Agulhas) (Nelson & Hutchings, 1983). To the North of Cape Columbine, between 33 and 32 ºS, the shelf broadens, with the outer shelf break running in a northwesterly direction and the shallow isobaths curving eastwards and northwards around the Columbine Peninsula. These broad shelf regions, such as the Namaqua Shelf, tend to favour stratification. This spatial variability in upwelling is shown in Figure 3.2, with upwelling occurring in the vicinity of headlandsand and upwelling filaments extending into the warmer offshore waters. Phytoplankton blooms can be fairly widespread, as shown in the examples of satellite images of surface chl-a for the three years of sampling (Figure 3.3).

Freshwater inputs are relatively low, since most of the west coast of South Africa is arid and characterised by few rivers. Most of the freshwater input is from the Olifants and Berg rivers, which is highest in winter with mean annual runoffs of 708 x 10^6 and 528 x 10^6 m^3, respectively (Shannon, 1985a).

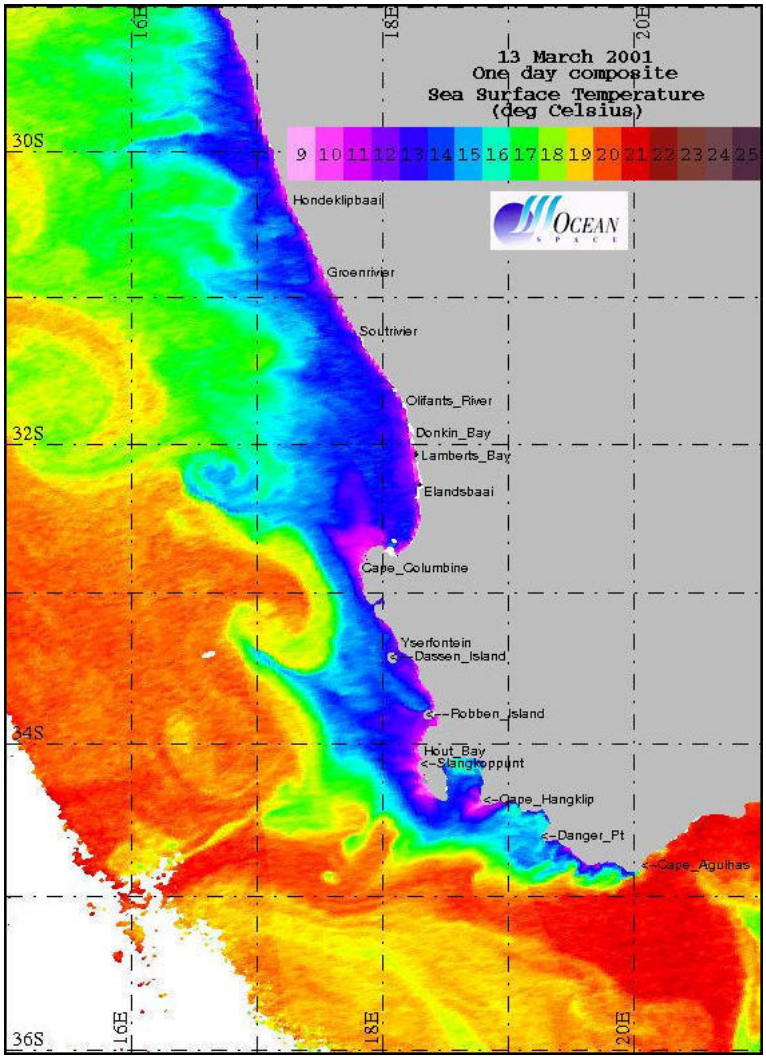

Figure 3.2. Sea-viewing Wide Field-of-view Sensor (SeaWiFS) satellite image of sea surface temperature showing upwelling off Cape Columbine, the Cape Peninsula and Cape Hangklip.

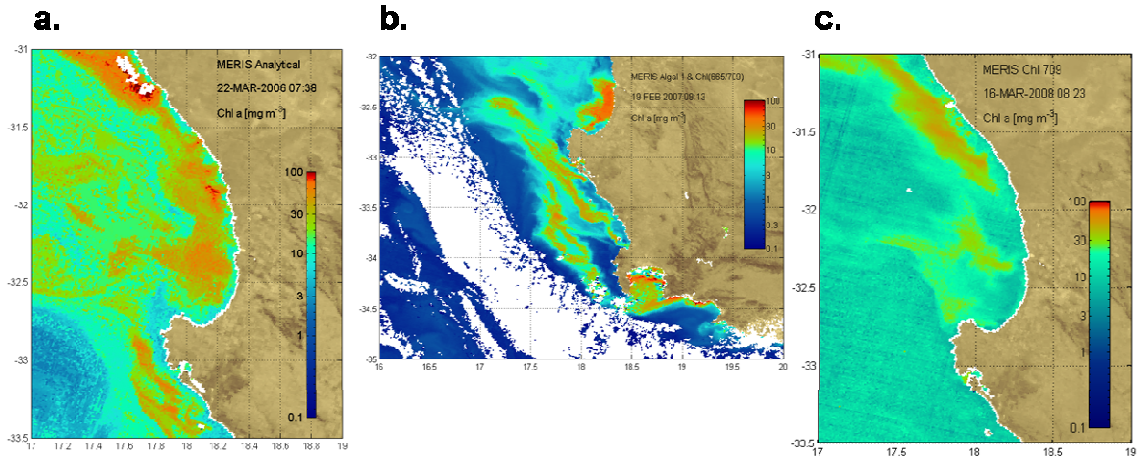

Figure 3.3. Medium Resolution Imaging Spectrometer (MERIS) satellite chl-a images from (a) 22 March 2006; (b) 19 February 2007 and (c) 16 March 2008. Courtesy of Stewart Bernard.

3.1.1.2. Chemical features

Upwelled water in the Benguela is fairly well oxygenated, with saturations of ~80-85 % (Shannon 1966). During upwelling relaxation, which favours phytoplankton growth, surface DO saturations can be as high as 180 % [Shannon (1985b) and references therein]. Remineralisation of organic matter in the vicinity of the Angola Dome and poleward advection of low oxygen water (LOW) at similar depths result in an oxygen minimum layer at 200-400 m. As a result, LOW is found at depth in the Northern Benguela and anoxic water has been reported near Walvis Bay, with associated high hydrogen sulphide concentrations (Pieterse & van der Post, 1967) and so-called hydrogen sulphide "eruptions" (Weeks et al., 2004). LOW in the Southern Benguela is generated locally in bottom waters (e.g. in St Helena Bay) in response to wind-driven physical and biogeochemical processes, such as high phytoplankton growth and subsequent decay under stratified conditions (Monteiro & van der Plas, 2006). Oxygen-deficient conditions are favourable for denitrification, which is known to occur in the Northern Benguela (Calvert & Price, 1971; Tyrrell & Lucas, 2002), but also in the St Helena Bay region (Bailey & Chapman, 1985). This usually occurs during periods of intense stratification, and may result in a NO_2^- or NH_4^+ maximum near the bottom, although this does not appear to be the case in St Helena Bay (Shannon, 1985b).

Typical nutrient distributions follow those of other upwelling systems, with high concentrations inshore during active upwelling and depletion by phytoplankton growth in the surface layer during quiescent periods, while nutrient regeneration occurs below the thermocline as the phytoplankton bloom decays. The gyral system in St Helena Bay favours retention and settling of organic matter, therefore nutrient regeneration rates are high (Shannon, 1985b). Nutrient concentrations in source SACW are typically in the range 10-18 μmol l^{-1} for NO_3^-, 0.8-1.5 μmol l^{-1} for PO_4^{3-} and 6-15 μmol l^{-1} for Si (Jones, 1971) and higher concentrations may be attained during its passage over shelf sediments where nutrient recycling takes place. Furthermore, phosphorus has been found to be released from organic matter prior to the simultaneous release of both nitrogen and phosphorus at a constant ratio (Grill & Richards, 1964). Bailey & Chapman (1985) have reported N:P ratios between 16 and 25 for the St Helena Bay region, with a PO_4^{3-} excess between 0.6 and 1.2 μmol l^{-1} at zero NO_3^-, and Si:N ratios between ~0.8 and 2.0. Lower N:P ratios of ~9 and a PO_4^{3-} excess of 0.11 were reported by Tyrrell & Lucas (2002) for shelf waters between 20 and 32 °S, which they attributed to denitrification and nutrient

trapping on the shelf. These combine to increase PO_4^{3-} concentrations but decrease NO_3^- concentrations relative to source waters. However, more recent findings suggest that they should rather be attributed to anaerobic ammonium oxidation ("Annamox") (Kuypers et al., 2005). Andrews & Hutchings (1980) reported N:P ratios between 10 and 20 at DO concentrations <4 ml l^{-1} and N:Si ratios decreasing from ~1.5 to 0.5 as DO concentration approached zero. They attributed the latter to the reduction of NO_3^- to NH_4^+ or to elemental nitrogen (which were not included in the ratio calculation). At DO concentrations between 4 and 7 ml l^{-1}, nitrogen uptake by phytoplankton resulted in the rapid decline of N:P and N:Si ratios to values <1.

Nitrogen uptake rates were found to be higher on the shelf relative to inshore and oceanic stations, with ρ(N) between ~0.3 and 0.5 μmol N l^{-1} h^{-1} for the former and ≤ 0.1 μmol N l^{-1} h^{-1} for the latter (Probyn, 1985). A synopsis of NO_3^- uptake measurements made in the Benguela between 1983 and 1991 showed rates ranging from <0.1 to 0.55 μmol N l^{-1} h^{-1} and revealed maximum potential uptake rates between 0.56 and 1.11 μmol N l^{-1} h^{-1}, depending on the acceleration term used in the calculation (Probyn, 1992). Hence, the system was fairly close to realisation of its maximum potential new production. f-ratios show substantial variation in the Benguela, from <0.1 to >0.9 (average 0.39), and display a hyperbolic relationship with ρ(NO_3^-) (Probyn, 1992). Furthermore, the f-ratio increases linearly with concentration at concentrations <2 μmol N l^{-1}, but then declines at higher concentrations, perhaps indicating a more rapid "shift-up" in ρ(NH_4^+) than in ρ(NO_3^-) following upwelling (Probyn, 1992). Probyn (1985) also found that picoplankton (<2 μm) ρ(N) was highest in the oceanic waters and was dominated by ρ(NH_4^+), whereas ρ(N) for the microplankton fraction (>20 μm) was dominated by ρ(NO_3^-), therefore the relative abundances of the various size classes can be responsible for variations in the f-ratio. Furthermore, the phytoplankton community as a whole expressed a preference for NH_4^+ over NO_3^- and urea, as shown by higher v_{max} and α (Probyn, 1985).

3.1.2. HABs in the Southern Benguela

3.1.2.1. HAB species and their impacts

Although primary production in upwelling systems is typically thought to be dominated by diatoms, the Benguela and other upwelling regions are also subjected to HABs (Kudela et al., 2005). Within the Southern Benguela, they tend to occur in late austral summer (February to April), although HABs have been reported as early as November (Pitcher et al., 2007). HABs were first suspected to be responsible for fluctuating fish stocks at the beginning of the 20th century (Gilchrist, 1914), and mass mortalities of fish, shellfish, seabirds and marine mammals have been reported since the mid-20th century (Copenhagen, 1953; Brongersma-Sanders, 1957). A harmful algae monitoring programme has been established since 1989, that involves daily sampling at Gordon's Bay (near Cape Town) and Eland's Bay on the west coast of South Africa (Pitcher & Calder, 2000).

HAB species reported by the monitoring programme between 1989 and 1997 include species from a range of phytoplankton groups, with 22 of the 34 species belonging to the class Dinophyceae, 2 to the Bacillariophyceae and the remaining 10 divided between various classes of flagellates (Pelagophyceae, Haptophyceae, Euglenophyceae) and one ciliate. The list includes both toxic species and high biomass producers, such as the dinoflagellates *Ceratium furca, C. lineatum, C. dens* and *Prorocentrum micans* (Pitcher & Calder, 2000). The photosynthetic ciliate *Mesodinium rubrum* has also been reported to form extensive blooms, causing anoxic events that have led to rock lobster mortalities (Horstman, 1981). In March 1994, a bloom of *C. furca* and *P. micans* in St. Helena Bay caused oxygen depletion to <0.5 ml l^{-1} and bacterial production of hydrogen sulphide, resulting in concentrations >50 µmol l^{-1} when the bloom decayed, killing 60 tonnes of rock lobster and 1,500 tonnes of fish (Matthews & Pitcher, 1996). A bloom of *Gonyaulax polygramma* occurred in 1962 in False Bay (Cape Town), causing 100 tonnes of dead fish and invertebrates to wash up on the beaches (Grindley & Taylor, 1962). The only other reported bloom of *G. polygramma* occurred in 2007, lasting for 2 months, and was associated with some marine fauna mortalities (Pitcher et al., 2008). Blooms of the brown tide pelagophyte *Aureococcus anophagefferens* were reported in 1997 in Saldanha Bay and associated with growth arrest in oysters and mussels (Probyn et al., 2001).

PSP was first attributed to *Alexandrium catenella* (Sapeika, 1948) and severe PSP outbreaks and even human fatalities have been reported (Sapeika, 1958; Popkiss et al., 1979; Muller et al., 1998; Pitcher & Cockcroft, 1998), with the highest incidences occurring north of St. Helena Bay (Pitcher & Calder, 2000). More recently, a bloom of *Alexandrium minutum* was reported in Cape Town harbour (Pitcher et al., 2007), suggesting that this species could also pose a threat to human health in the future. Furthermore, *A. catenella* blooms can cause direct poisoning of sardines (Pitcher & Calder, 2000) and even mussels (Horstman, 1981), as well as accumulating through the food chain to seabirds, seals and whales (Horstman, 1981; Pitcher & Calder, 2000).

DSP was first reported in 1991 on the west coast and attributed to *Dinophysis acuminata* (Pitcher et al., 1993b), although *D. fortii*, *D. tripos*, *D. hastata* and *D. rotundata* are now also known to occur on both the south and west coasts (Pitcher & Calder, 2000). *Dinophysis* spp. are present intermittently throughout the upwelling season, but tend to peak towards the latter part of it. Although they are generally a relatively minor component of the phytoplankton community, they are able to contaminate shellfish at cell concentrations as low as 2,000 cells l^{-1} and as a result the harvestable toxin limit is often exceeded in shellfish (Pitcher & Calder, 2000).

Pseudo-nitzschia australis and other, unidentified *Pseudo-nitzschia* spp. blooms also occur in the Southern Benguela (Pitcher & Calder, 2000; Fawcett et al., 2007), however no cases of ASP have been reported despite high concentrations of domoic acid found in association with the species (Fawcett et al., 2007).

Ichthyotoxic species include a dinoflagellate initially identified as *Gymnodinium mikimotoi* (= *Karenia mikimotoi*), although more recently 2 new *Karenia* species, *K. cristata* sp. Nov. and *K. bicuneiformis* sp. Nov., were discovered on the South African coast (Botes et al., 2004). The ichthyotoxic raphidophyte *Heterosigma akashiwo* also occurs on both the south and west coasts. Blooms of the former were associated with extensive mortalities of abalone (30 tonnes) in False Bay in 1989 (Horstman et al., 1991), whereas the latter has not been associated with faunal mortalities thus far. A bloom of *K. mikimotoi* in False Bay in 1995-96 was also associated with the presence of NSP-like toxins in mussels and respiratory disorders and skin irritations in bathers (Pitcher & Matthews, 1996).

3.1.2.2. Mechanisms of HAB formation

HABs around the South African coast are closely associated with the upwelling system, as they are generally restricted to the west of Cape Agulhas (Pitcher & Calder, 2000). They are particularly frequent north of Cape Columbine, where the broad Southern Namaqua shelf favours stratification. This area is also characterised by high residence times and retentive, near-surface circulation patterns (Holden, 1985). Blooms tend to occur towards the end of the upwelling season (March to April), when reduced wind stress and increased thermal stratification create favourable conditions for dinoflagellates (Pitcher et al., 1993a; Pitcher & Weeks, 2006). During the latter part of the upwelling season, synoptic wind patterns are responsible for short-term upwelling/relaxation cycles, which in turn influence community succession and hence the presence of HABs (Pitcher & Boyd, 1996; Pitcher et al., 1998).

The association of HABs with upwelling relaxation in the Benguela is consistent with Margalef's Mandala (Margalef, 1978), whereby the seasonal shift from diatoms in spring to dinoflagellates in summer occurs along a gradient of decreasing turbulence and nutrient availability. However, in the subsequent revision of the Mandala, the "red tide sequence" occurred under low turbulence/high nutrient conditions, a situation perceived as an "anomaly" (Margalef et al., 1979). This model is therefore not applicable to upwelling systems, where most of the nutrient input is from upwelling, and is perhaps more suited to coastal lagoons and embayments that are affected by high nutrient inputs from the adjacent land.

The physical mechanisms of HAB formation in the Benguela are now relatively well understood. Blooms are thought to originate in the region of the thermocline in stratified offshore waters and appear as surface blooms in the vicinity of the upwelling front, where the thermocline outcrops. Wind relaxation or reversal then leads to onshore advection and accumulation of the bloom (Pitcher et al., 1998). These blooms can then be transported poleward by an inshore counter-current, resulting in a latitudinal variation in the timing of HABs (Probyn et al., 2000).

In the Benguela and other upwelling systems, diatoms tend to dominate following a pulse of upwelling (or in the vicinity of an upwelling centre), whereas dinoflagellates increase in abundance during wind relaxation (or downstream of the upwelling centre), as new nutrients become depleted. In these situations, regenerated nitrogen becomes an important source for phytoplankton growth (Hutchings et al., 1995), therefore the ability

to utilise recycled forms of nitrogen more efficiently than diatoms would give HAB species a competitive advantage. This is the case at the end of the upwelling season in the Iberian upwelling system, with mixed red tide populations that are sustained by NH_4^+ uptake (Rios et al., 1995).

Time-series data indicate a high degree of interannual variability in the dominance of particular HAB species. This variability makes it very difficult to predict HABs at the species level (which is particularly important in terms of toxic outbreaks), since HABs may be stochastic events, i.e. a result of a species being present in the right place at the right time (Pitcher & Weeks, 2006). Furthermore, HAB species known to bloom in the Benguela belong to most of the functional groups identified by Smayda & Reynolds (2001), indicating that the Benguela comprises a wide range of habitat types, including fronts, coastal currents and upwelling/relaxation events, and that prediction even at the level of life forms is very challenging (Pitcher & Nelson, 2006).

3.1.3. Aims and objectives

The aim of this study was to test the hypothesis that "the success of HAB species in the Southern Benguela at the end of the upwelling season is attributable to their ability to utilise alternative sources of nitrogen or to their high affinity for NO_3 under low NO_3 conditions".

The hypothesis was tested during 3-week field surveys in March 2006, March/April 2007 and March 2008 off Lambert's Bay on the west coast of South Africa, with the specific objectives:

- to characterise short-term and interannual variations in hydrographic and nutrient conditions at the end of the upwelling season,
- to characterise short-term and interannual variations in phytoplankton community structure and the occurrence of HAB species,
- to link these with variations in nitrogen uptake rates (NO_3, NH_4 and urea) and nitrogen uptake kinetics and identify possible nitrogen nutrition strategies of HAB species.

3.2. Results

3.2.1. Wind

In 2006, winds were south-easterly prior to the survey, then south-westerly during most of the sampling period, with the exception of 18-19 March when wind direction switched to north-easterly (Figure 3.4a,b). Eastward components ranged from -3.5 to 3.3 m s^{-1} and northward components from -2.1 to 4.8 m s^{-1}.

In 2007, eastward components were very weak (≤1.3 m s^{-1}), with the exception of 19 March (-3.4 m s^{-1}), therefore winds alternated between southerly (16-18, 24-27 March) and northerly (19-23 March, 28 March-4 April), switching on a daily basis between 5 and 11 April (Figure 3.4c, d). Northward components ranged from -2.5 to 3.0 m s^{-1}.

In 2008, wind direction was predominantly south-westerly, with maximum eastward and northward components of 2.9 and 4.2 m s^{-1}, respectively (Figure 3.4e,f). Wind direction changed only for brief periods, including 5 March (south-easterly), 9 March (north-westerly), 16-17 March (north-easterly), 19 and 24 March (north-westerly). On these occasions, negative eastward and northward components reached -2.3 and -1.2 m s^{-1}, respectively.

3.2.2. Hydrography

3.2.2.1. Temperature

Temperatures in all years fluctuated as cold upwelling pulses alternated with periods of surface warming and stratification. In 2006, the sampling period was characterised on 3 occasions by surface warming (to 14-15 ºC), with a thermocline apparent at 5-10 m depth (Figure 3.5a) and these periods generally corresponded to northerly or weak southerly winds. In between these periods, upwelling pulses introduced colder (11-12 ºC) water to the surface and the water column was well mixed. These upwelling events were sometimes concurrent with stronger southerly winds (e.g. 21 Mach 2006, 26 March 2007, 14-15 March 2008, Table 3.1), although this was not always the case and the time-lag between changes in wind direction and temperature were not always equivalent (e.g. 21, 29 March 2007, 18-22 March 2008, Table 3.1).

In 2007, recently upwelled water (~11°C) was present at the surface at the start of the survey. During the period of northerly winds that ensued (until 23 March), surface temperatures warmed to 13.8 °C before wind reversal caused another pulse of upwelling to decrease surface temperatures to 11.0 °C (Figure 3.5b). Northerly winds then prevailed for most of the remaining period and the water column became strongly stratified with surface temperatures increasing from 11.8 to 16.8 °C over ~8 days and remaining between 16 and 17 °C thereafter. The warm surface layer was deeper than in 2006, with the thermocline observed at ~15-20 m.

In 2008, a period of stratification was observed between 7 and 12 March, with a shallow thermocline at ~5 m and surface temperatures reaching 17 °C (Figure 3.5c). A 4-day period of upwelling was then observed, after which a thermocline began to develop (17 March) and surface temperatures warmed to 13 °C by 21 March and to 15 °C by 25 March.

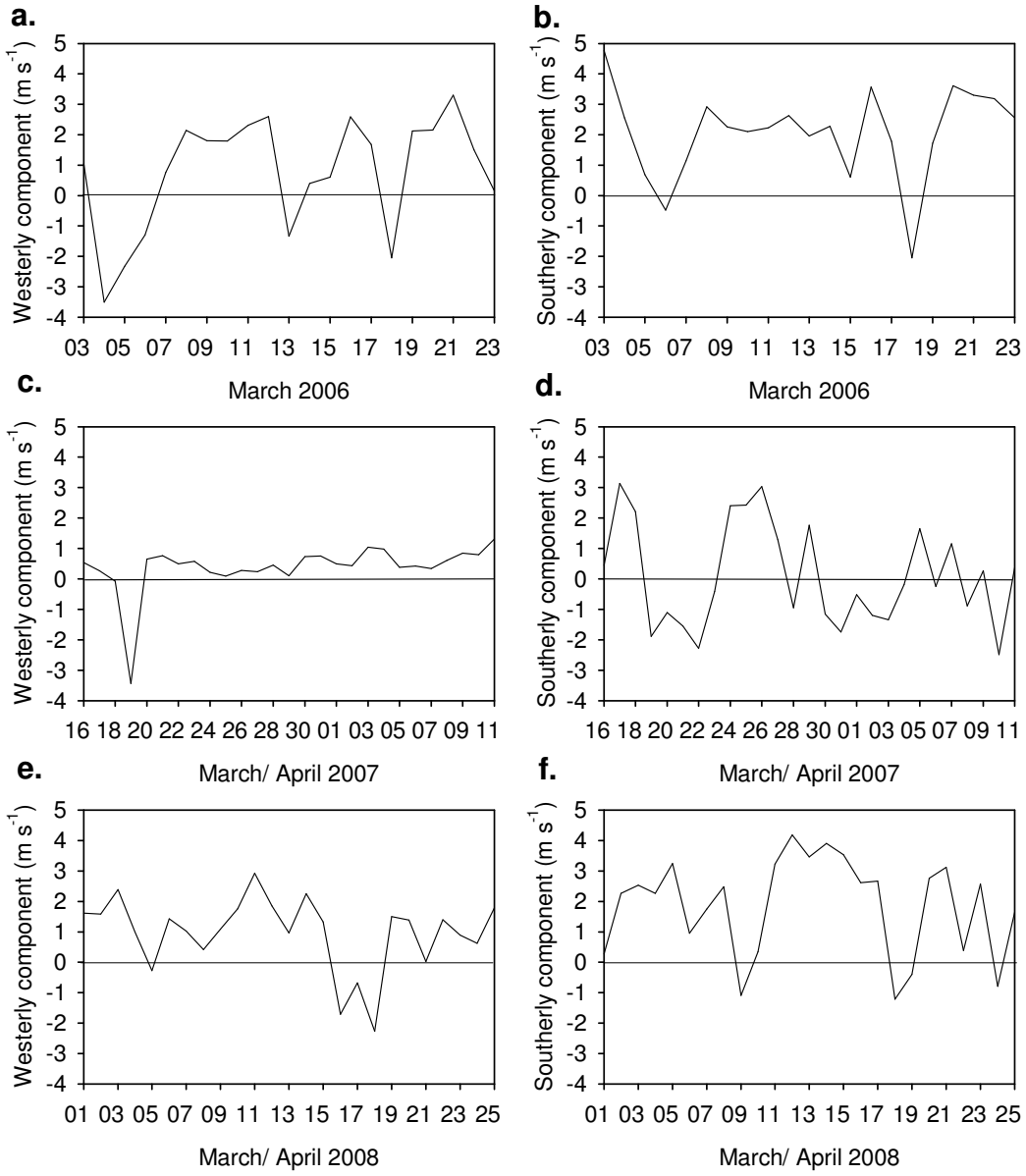

Figure 3.4. Daily westerly and southerly wind components in (a, b) 2006, (c, d) 2007 and (e, f) 2008.

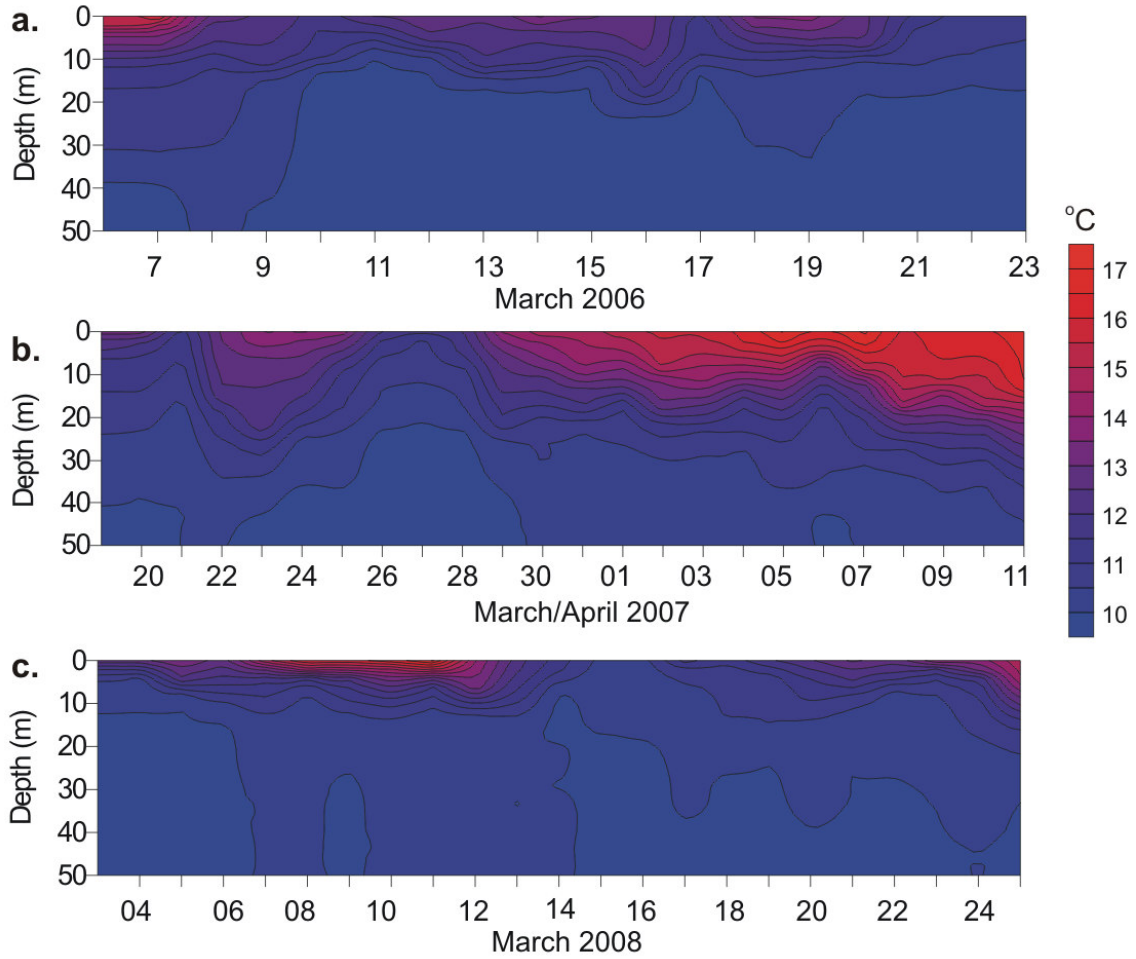

Figure 3.5. Temperature contour plots obtained from daily CTD casts in (a) 2006, (b) 2007 and (c) 2008.

Year	Date	Southerly wind component (m s^{-1})	Surface temp (°C)	Phyto cluster	$\rho(NO_3^-)$	*f*-ratio
2006	08-Mar	2.92	12.97	VII	0.160	0.81
	09-Mar	2.26	12.39	VII	0.329	0.83
	10-Mar	2.10	11.84	VII	0.109	0.84
	11-Mar	2.23	12.54	VII	0.403	0.83
	12-Mar	2.62	12.87	VII	0.091	0.83
	13-Mar	1.96	12.68	VII	0.111	0.86
	15-Mar	0.61	13.11	VII	0.016	0.95
	16-Mar	3.57	12.74	VII	0.030	0.78
	17-Mar	1.78	11.38	VII	0.337	0.84
	19-Mar	2.93	13.82	VII	0.017	0.82
	20-Mar	4.46	12.66	VII	0.314	0.73
	21-Mar	4.45	11.35	VII	0.206	0.71
	22-Mar	3.78	10.78	VII	0.296	0.73
2007	21-Mar	-1.54	11.17	II	0.609	0.87
	22-Mar	-2.29	13.08	VI	0.250	0.60
	23-Mar	-0.41	13.80	VI	0.045	0.28
	24-Mar	2.40	13.14	VI	0.054	0.20
	25-Mar	2.43	13.39	VI	0.086	0.22
	26-Mar	3.04	11.69	VI	0.013	0.21
	28-Mar	-0.95	11.80	II	0.008	0.24
	29-Mar	1.77	13.44	VI	0.103	0.27
	30-Mar	-1.16	14.17	VI	0.030	0.10
	01-Apr	-0.52	15.45	VII	0.028	0.10
	04-Apr	-0.19	16.03	I	0.008	0.06
	05-Apr	1.65	16.79	I	0.007	0.06
	06-Apr	-0.24	15.93	VII	0.040	0.29
	07-Apr	1.16	17.15	VII	0.023	0.12
	08-Apr	-0.89	15.77	I	0.009	0.08
	09-Apr	0.27	16.40	I	0.013	0.08
	10-Apr	-2.49	16.41	I	0.013	0.11
2008	05-Mar	3.25	13.52	VII	0.160	0.48
	06-Mar	0.95	12.84	VII	0.150	0.60
	07-Mar	1.75	14.85	VII	0.137	0.45
	09-Mar	-1.09	15.82	VII	0.002	0.02
	10-Mar	0.35	16.24	n/a	0.001	0.02
	11-Mar	3.23	17.08	n/a	0.001	0.01
	12-Mar	4.19	14.02	VII	0.024	0.22
	13-Mar	3.46	12.21	III	0.007	0.14
	14-Mar	3.91	11.23	III	0.003	0.17
	15-Mar	3.53	10.33	n/a	0.002	0.25
	16-Mar	2.62	10.30	III	0.003	0.24
	18-Mar	-1.21	11.15	IV	0.100	0.67
	19-Mar	-0.40	11.91	IV	0.093	0.59
	20-Mar	2.76	12.47	IV	0.141	0.68
	21-Mar	3.12	13.10	IV	0.177	0.65
	22-Mar	0.38	12.66	IV	0.183	0.55
	24-Mar	-0.79	13.70	V	0.004	0.04
	25-Mar	1.65	14.89	n/a	0.004	0.04

Table 3.1. Time-series of temperature, southerly wind component, phytoplankton cluster, ρ(NO3-) and f-ratio in all 3 years.

3.2.2.2. Salinity

In 2006, salinity was relatively isohaline throughout the water column, with maximum vertical differences of <0.2 (Figure 3.6a). Salinity was generally lowest at the bottom (34.53 to 34.75) and highest in the upper mixed layer (top 10-20 m), sometimes displaying a subsurface maximum. Maxima were generally 34.75-34.8, although on 19 March it was only 34.53. On 19, 22 and 23 March, salinity increased with depth, displaying a maximum at the bottom.

In 2007, a subsurface maximum was observed between 10 and 20 m from 20 to 31 March (Figure 3.6b), reaching higher values than in 2006 (34.89 to 35.54). Minimum concentrations were measured at the surface and at the bottom, ranging from 34.43 to 34.69 and vertical differences ranged from 0.19 to 0.88. From 1 to 11 April, salinities were lower and relatively isohaline, with vertical differences ranging from 0.05 to 0.20.

In 2008, much larger variations in salinity were observed, particularly on 5-8, 10-14, 20, 22 and 24-25 March, when highest salinities (~34.75-35.26) were measured in the top 20-30 m. On these occasions, a halocline was generally observed, below which salinities remained fairly constant (~34.8). On 4, 9, 15-19, 21 and 23 March, the water column was more or less isohaline, with vertical differences ranging from 0.02 to 0.14 (Figure 3.6c).

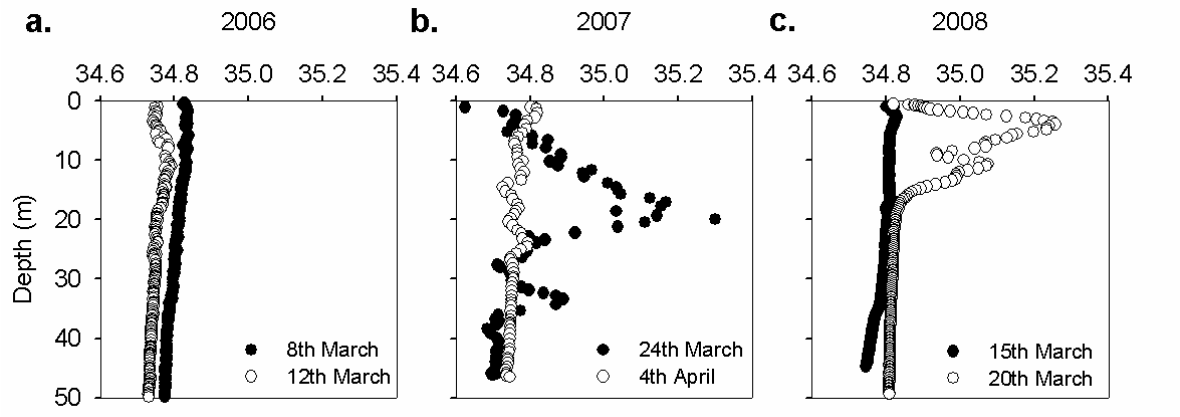

Figure 3.6. Examples of typical salinity profiles obtained from CTD casts in (a) 2006, (b) 2007 and (c) 2008.

3.2.3. Dissolved oxygen

DO saturations were highest (>100 %, 6-9 ml l^{-1}) in the warm, surface layer during periods of stratification, whereas concentrations in bottom waters were often <40 % and <1 ml l^{-1}. During the upwelling periods, low DO water was brought up to the surface, and DO saturation was < 100 % throughout the water column.

In 2006, DO_{Sat} decreased gradually with depth between 7 and 11 March, but a sharp gradient was observed at ~10 m thereafter, associated with the thermocline (Figure 3.7a). Below the thermocline, saturations were very low (≤ 20 %). At the end of the survey (21-23 March), when strong upwelling occurred, DO saturation was <40 % throughout the water column.

In 2007, higher saturations were observed (up to 160 % at the surface and up to 50 % at the bottom), consistent with the higher temperatures measured relative to 2006. Supersaturated waters were observed down to ~20 m, due to the deeper thermocline in this year (Figure 3.7b).

In 2008, even higher saturations (up to 180 %) were measured at the surface, although these declined rapidly with depth, due to the presence of a very shallow thermocline (5 m) (Figure 3.7c). Bottom DO saturation was similar to 2006 (≤ 20 %). DO saturations were significantly correlated with temperature in all years (Table 3.2).

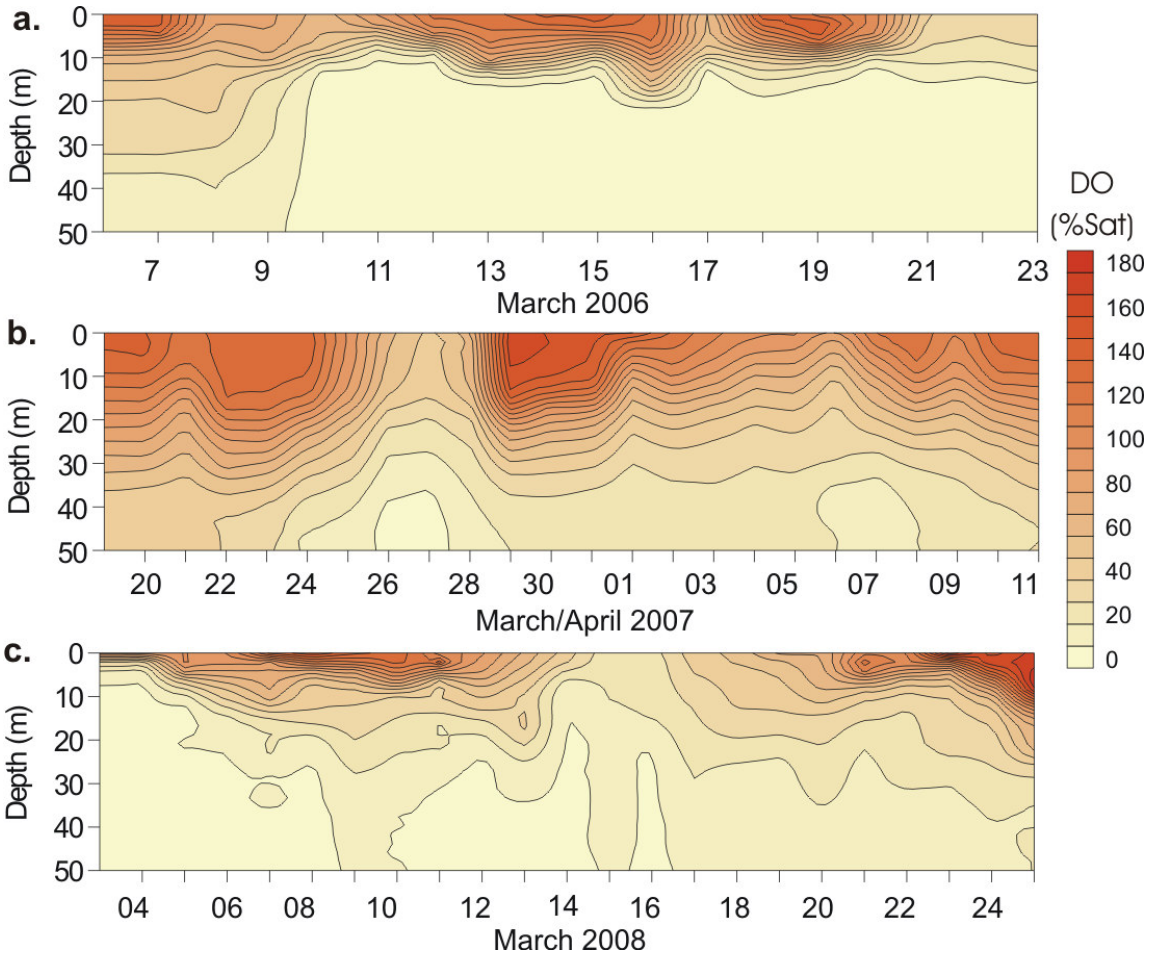

Figure 3.7. Contour plots of dissolved oxygen saturations obtained from daily CTD casts in (a) 2006, (b) 2007 and (c) 2008.

3.2.4. Nutrients

Nitrate concentrations increased with depth, with a particularly steep gradient during the stratified periods when nutrients were depleted in the surface. During the upwelling periods, higher concentrations were reached at the surface and the water column was more homogeneous (Figure 3.8). Surface concentrations ranged from ~0.05 µmol l^{-1} in all years, to 25.1, 23.2 and 29.3 µmol l^{-1} in 2006, 2007 and 2008, respectively. A very long period (13 days) of NO_3^- depletion was observed in 2007, whereas in the other years nutrients were replenished approximately every 4 days. As a result, NO_3^- concentrations measured at all 5 depths were significantly lower in 2007 relative to the other years (Student's t-test, $p < 0.001$).

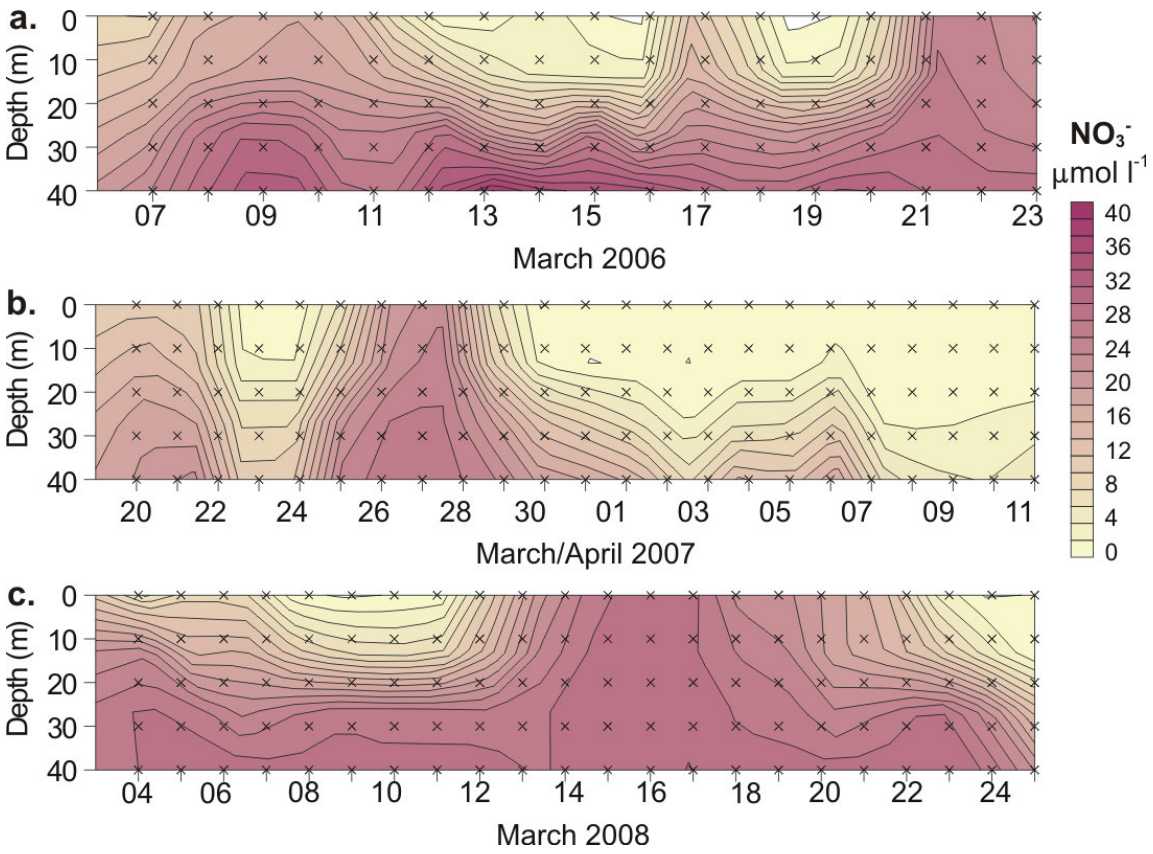

Figure 3.8. Contour plots of NO_3^- concentrations measured daily at 5 depths in (a) 2006, (b) 2007 and (c) 2008. Symbols indicate data points. N.B: samples taken only down to 20 m depth.

Nitrate concentrations displayed a significant negative linear correlation with temperature in 2006, when the temperature range was ~9 to 14 °C. In 2007 and 2008 the temperature range was ~10-17 °C and NO_3^- was generally depleted at 14 °C, resulting in an overall exponential decrease with temperature (Figure 3.9). In 2008, some samples exhibited a departure from this relationship between 11 and 13 °C, when unusually low concentrations were measured.

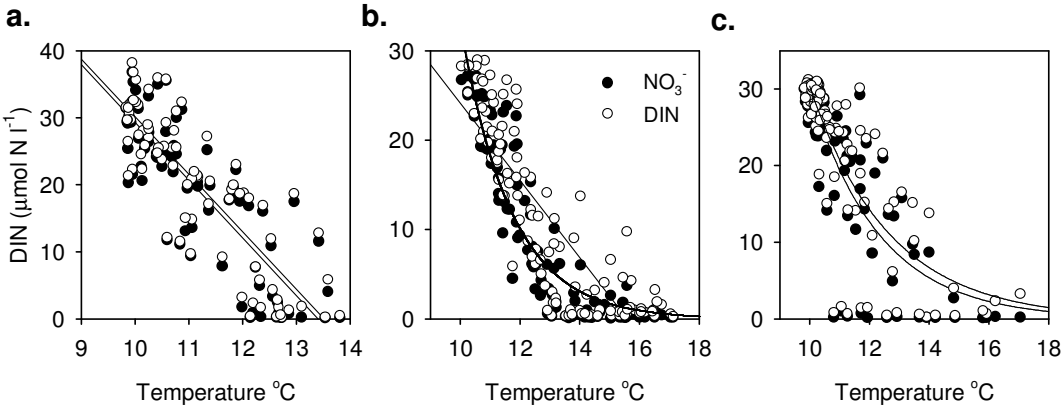

Figure 3.9. Relationships between NO_3^- and temperature and between total DIN and temperature in (a) 2006, (b) 2007 and (c) 2008. Parameters derived from linear regressions are shown in Table 3.1.

Variable	Relationship	a	b	r	n	Year
DIN vs temp	linear	-8.57**	115.8**	0.85	84	2006
	linear	-4.31**	67.2**	0.86	115	2007
	exponential	1326*	-0.38**	0.83	110	2008
NO_3^- vs temp	linear	-8.6**	115.3**	0.85	84	2006
	exponential	12368**	-0.59**	0.94	115	2007
	exponential	2177*	-0.42**	0.85	110	2008
PO_4^{3-} vs temp	linear	-0.66**	9.38**	0.87	84	2006
	exponential	126.7**	-0.38**	0.91	115	2007
	exponential	48.3**	-0.29**	0.81	110	2008
Si vs temp	linear	-13.43**	175.8**	0.81	84	2006
	exponential	28075	-0.67**	0.85	115	2007
	exponential	2673	-0.43**	0.71	104	2008
DO vs temp	linear	37.03**	-362.4**	0.97	2757	2006
	linear	16.17**	-124.3**	0.74	1798	2007
	linear	27.40**	-256.9**	0.91	3840	2008
DIN vs PO_4^{3-}	linear	11.82**	-3.31*	0.89	84	2006
	linear	12.20**	-3.21**	0.97	115	2007
	linear	11.94**	-2.25*	0.93	110	2008
NO_3^- vs PO_4^{3-}	linear	11.79**	-4.13**	0.89	84	2006
	linear	11.41**	-4.09**	0.97	115	2007
	linear	12.07**	-3.56**	0.92	110	2008
DIN vs Si	linear	0.53**	6.51**	0.87	84	2006
	linear	0.89**	2.72**	0.87	115	2007
	linear	0.56**	7.50**	0.83	104	2008
NO_3^- vs Si	linear	0.53**	5.63**	0.87	84	2006
	linear	0.85**	1.25*	0.89	115	2007
	linear	0.58**	5.96**	0.84	104	2008

Table 3.2. Parameters derived from regression analysis of nutrients versus temperature, DO (% saturation, obtained from CTD) versus temperature and between nutrients in all years. Linear relationships are described by the equation y = a * x + b and exponential relationships by the equation $y = a * e^{-bx}$. Significance of parameters and shown by * p < 0.05 or ** p < 0.01. r is the correlation coefficient (p < 0.01 in all cases) and n is number of measurements.

Phosphate concentrations followed the same patterns as NO_3^-, with lowest concentrations at the surface and maximum concentrations at depth (Figure 3.10). Surface concentrations ranged from ~0.2 to 3.0 µmol l^{-1} in all years, whereas deep concentrations ranged from 1.7 to 3.2 µmol l^{-1} in 2006, from 0.7 to 2.6 µmol l^{-1} in 2007 and from 2.0 to 3.2 µmol l^{-1} in 2008. PO_4^{3-} concentrations were also significantly lower in 2007 relative to 2006 and 2008 (Student's t-test, $p < 0.001$).

Phosphate was significantly correlated with temperature in all years (Table 3.2, Figure 3.11a). As with NO_3^-, the relationship was linear in 2006, but exponential in 2007 and 2008. Phosphate also displayed a significant linear correlation with both NO_3^- and total DIN (Table 3.2, Figure 3.11b). The regression coefficients indicated NO_3^-:PO_4^{3-} ratios of 11.8-12.2 and slightly lower DIN:PO_4^{3-} ratios of 11.4-12.1 in all years. However, individually calculated NO_3^-:PO_4^{3-} ratios ranged from <1 to 14.7 (all years, all depths), generally being lowest at the surface and increasing with depth (data not shown). Ratios dropped to <1 when NO_3^- and PO_4^{3-} became depleted and increased again when nutrient concentrations increased following pulses of upwelling.

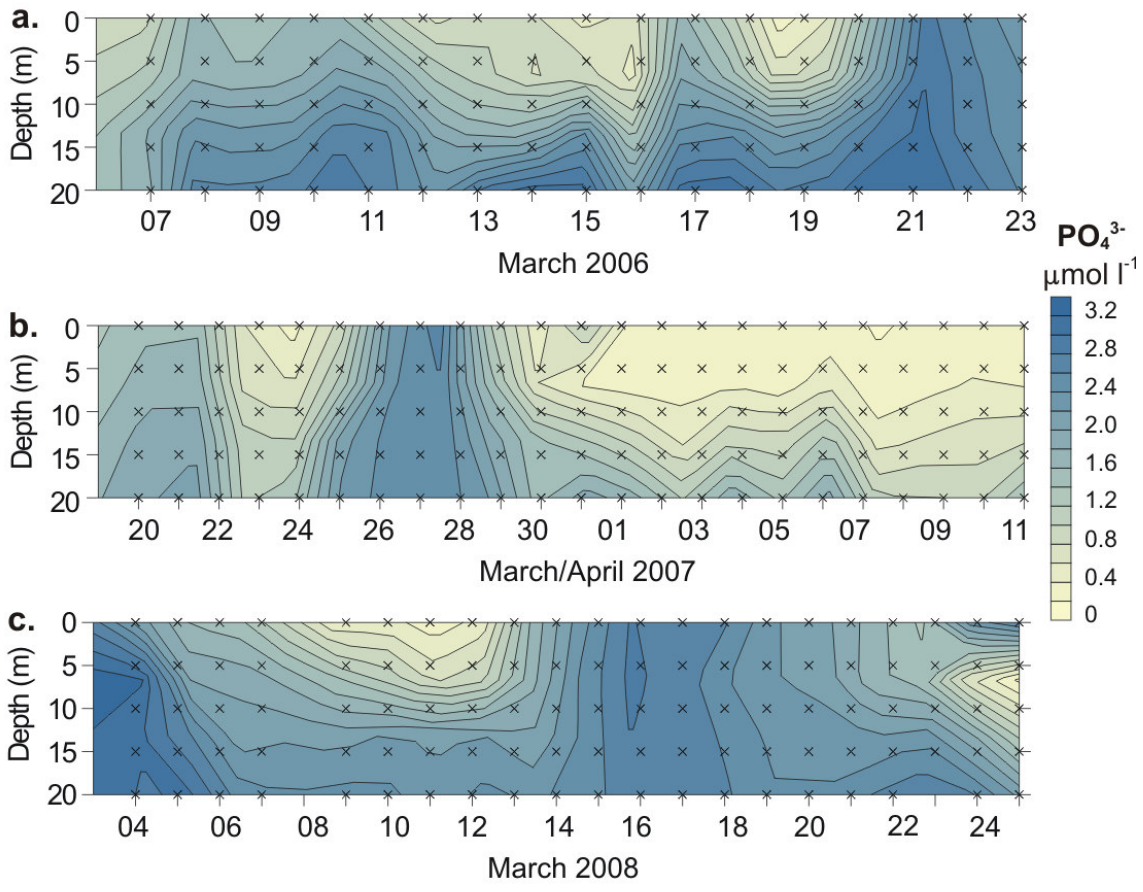

Figure 3.10. Contour plots of PO_4^{3-} concentrations measured daily at 5 depths in (a) 2006, (b) 2007 and (c) 2008. Symbols indicate data points. N.B: samples taken only down to 20 m depth.

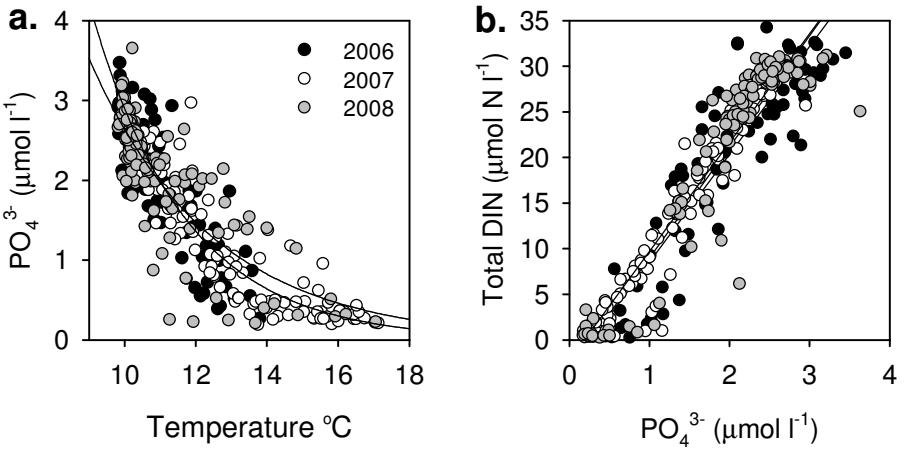

Figure 3.11. Relationships between (a) PO_4^{3-} and temperature and (b) total DIN and PO_4^{3-} in all 3 years.

Si followed the same distribution as NO_3^- and PO_4^{3-}, although Si concentrations reached higher maxima relative to NO_3^- (Figure 3.12) Minimum surface concentrations were ≤ 0.5 µmol l^{-1} in all years, whereas maximum surface concentrations were lower in 2007 (30.6 µmol l^{-1}) relative to the other years (49.0 and 45.7 µmol l^{-1} in 2006 and 2008, respectively). Si concentrations were significantly lower in 2007 relative to 2006 and 2008 (Mann-Whitney U-test, $p < 0.05$).

Si concentrations displayed a significant linear correlation with temperature in 2006 and significant exponential relationships with temperature in 2007 and 2008 (Table 3.2, Figure 3.13a). They were also significantly correlated with NO_3^- and total DIN, with similar NO_3^-:Si and DIN:Si ratios in 2006 and 2008 (0.53-0.58), but significantly higher ratios (Student's t-test, $p < 0.05$) in 2007 (0.85-0.89) (Table 3.2, Figure 3.13b).

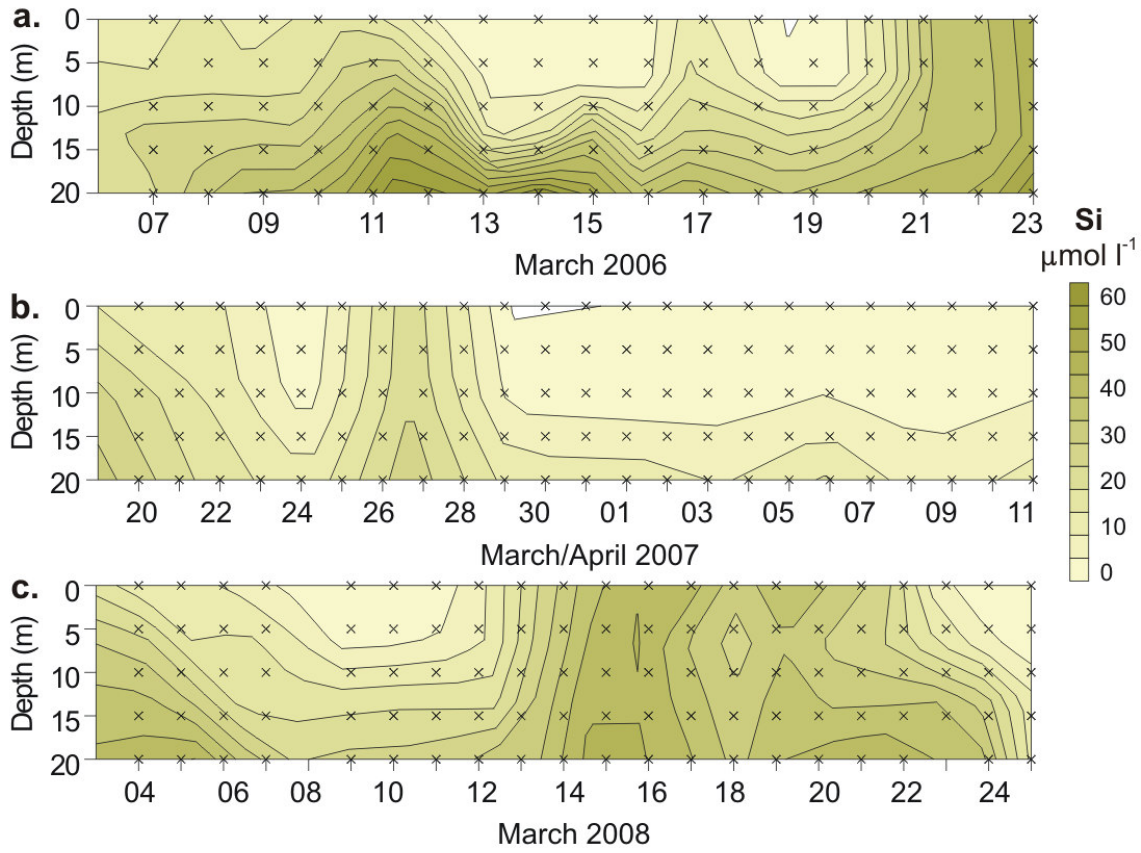

Figure 3.12. Contours of Si concentrations measured daily at 5 depths in (a) 2006, (b) 2007 and (c) 2008. Symbols indicate data points. N.B: samples taken only down to 20 m depth.

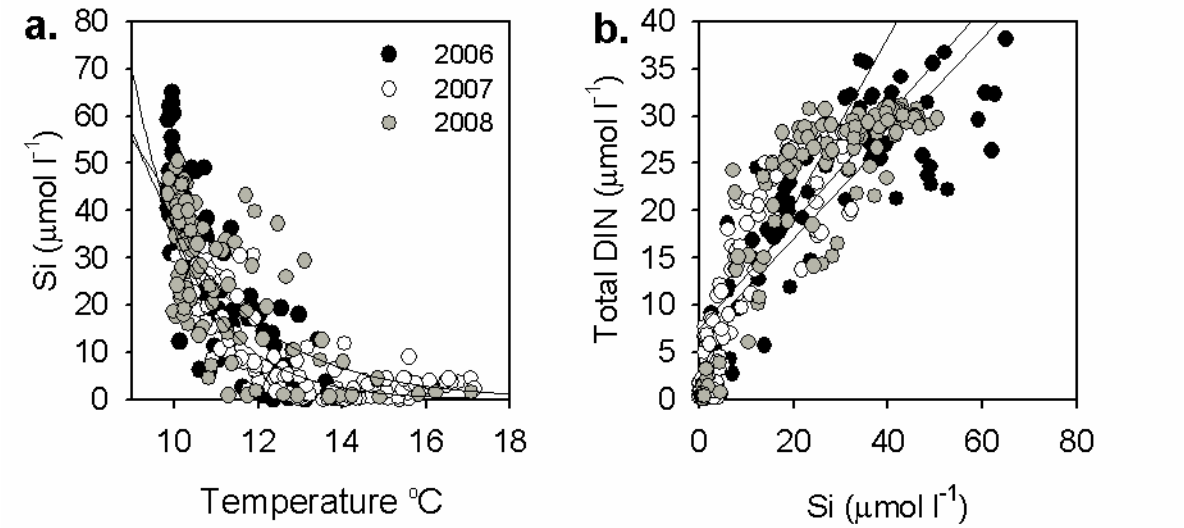

Figure 3.13. Relationships between (a) Si and temperature and (b) total DIN and Si in all 3 years.

The vertical distribution of NH_4^+ varied considerably with time (Figure 3.14), sometimes displaying a homogeneous distribution (e.g. 15-18 March 2006, 20-22 March 2007, 18-20 March 2008), sometimes a decrease with depth (21-22 March 2006, 26-28 March 2007, 11-15 March 2008) and sometimes an increase with depth (3-11 March 2007).

In 2006, NH_4^+ concentrations ranged from 0.08 to 1.49 µmol N l^{-1} at the surface and from 0.13 to 1.74 µmol N l^{-1} at the subsurface incubation depth (hereafter "subsurface") (Figure 3.14a,d). In 2007, concentrations ranged from 0.07 to 4.16 µmol N l^{-1} at the surface and from 0.05 to 4.41 µmol N l^{-1} in the subsurface (Figure 3.14b,e). In 2008, they ranged from 0.07 to 4.75 µmol N l^{-1} at the surface and from 0.22 to 5.02 µmol N l^{-1} in the subsurface (Figure 3.14c,f).

Concentrations were significantly higher in the subsurface relative to the surface in 2006 (paired t-test, $n = 14$, $p < 0.05$), however the difference was not significant in 2007 or in 2008. Furthermore, NH_4^+ concentrations at all depths were significantly higher in 2007 relative to the other 2 years (Mann-Whitney U-test, $p < 0.05$).

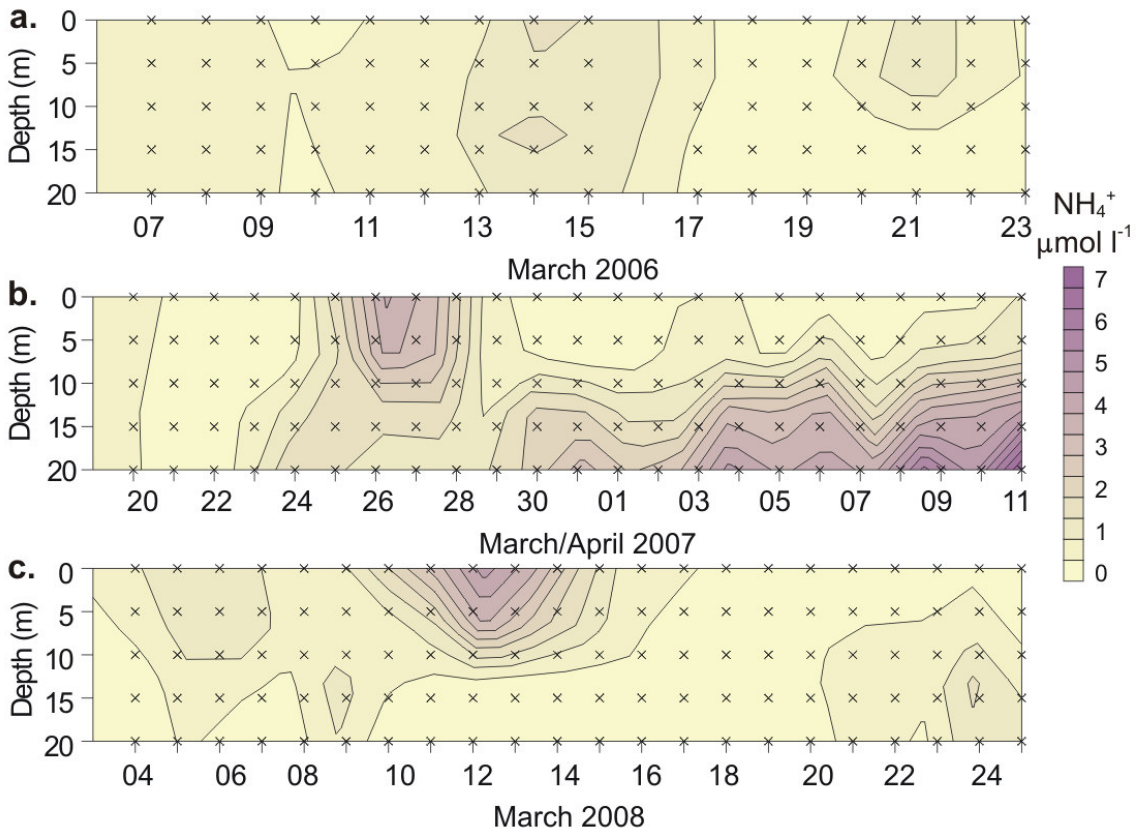

Figure 3.14. Contour plots of NH_4^+ concentrations measured daily at 5 depths in (a) 2006, (b) 2007 and (c) 2008.

In 2006, urea concentrations ranged from 0.17 to 0.95 μmol N l^{-1} (mean 0.42 ± 0.06) at the surface and from 0.54 to 3.11 μmol N l^{-1} in the subsurface (mean 1.46 ± 0.20) (Figure 3.13a,d). In 2007, they ranged from 0.15 to 1.29 μmol N l^{-1} (mean 0.53 ± 0.07) at the surface and from 0.44 to 3.65 μmol N l^{-1} (mean 1.34 ± 0.18) in the subsurface (Figure 3.13b,e). In 2008, concentrations ranged from 0.24 to 2.60 μmol N l^{-1} (mean 0.84 ± 0.12) at the surface and from 0.24 to 1.51 μmol N l^{-1} (mean 0.77 ± 0.07) in the subsurface (Figure 3.13c,f).

Concentrations in both 2006 and 2007 were significantly higher at the subsurface depth than at the surface (paired t-test, $p < 0.01$, n = 13 in 2006, n = 17 in 2007), although they were not significantly different in 2008 (Mann-Whitney U-test, $p > 0.05$). There were no significant differences in urea between years.

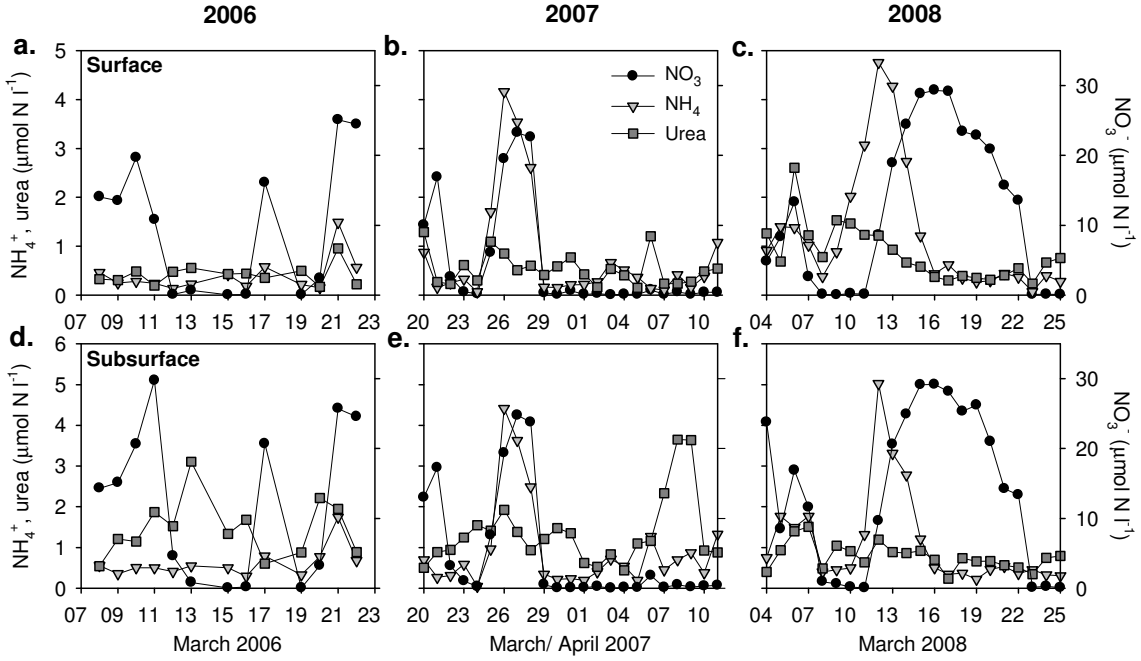

Figure 3.15. Concentrations of NO_3^-, NH_4^+ and urea at the surface in (a) 2006, (b) 2007 and (c) 2008 and in the subsurface in (d) 2006, (e) 2007 and (f) 2008.

3.2.5. Chl-a

In all years, high chl-a concentrations developed during periods of stratification, generally following wind reversal, and usually displayed a maximum at 5-10 m depth, although occasionally the maximum was at the surface (e.g. 24 March 2007, 4-5 March 2008) (Figure 3.16). Surface concentrations ranged from 9.4 to 57.1 µg l^{-1} (mean 19.4 ± 3.2 µg l^{-1}) in 2006, from 0.3 to 28.8 µg l^{-1} (mean 9.7 ± 2.1 µg l^{-1}) in 2007 and from 0.3 to 82.3 µg l^{-1} (mean 9.5 ± 3.6 µg l^{-1}) in 2008. In 2006, stratification did not persist for longer than 4 days and chl-a concentrations were always >8 µg l^{-1}, whereas in 2007 and 2008 concentrations dropped occasionally to <1 µg l^{-1}. In April 2007, the persistence of warm, stratified conditions led to a decline in chl-a, which remained <5 µg l^{-1} for the last 10 days of the survey. Overall, chl-a concentrations were significantly higher in 2006 relative to both 2007 and 2008 (Student's t-test, $p<0.001$).

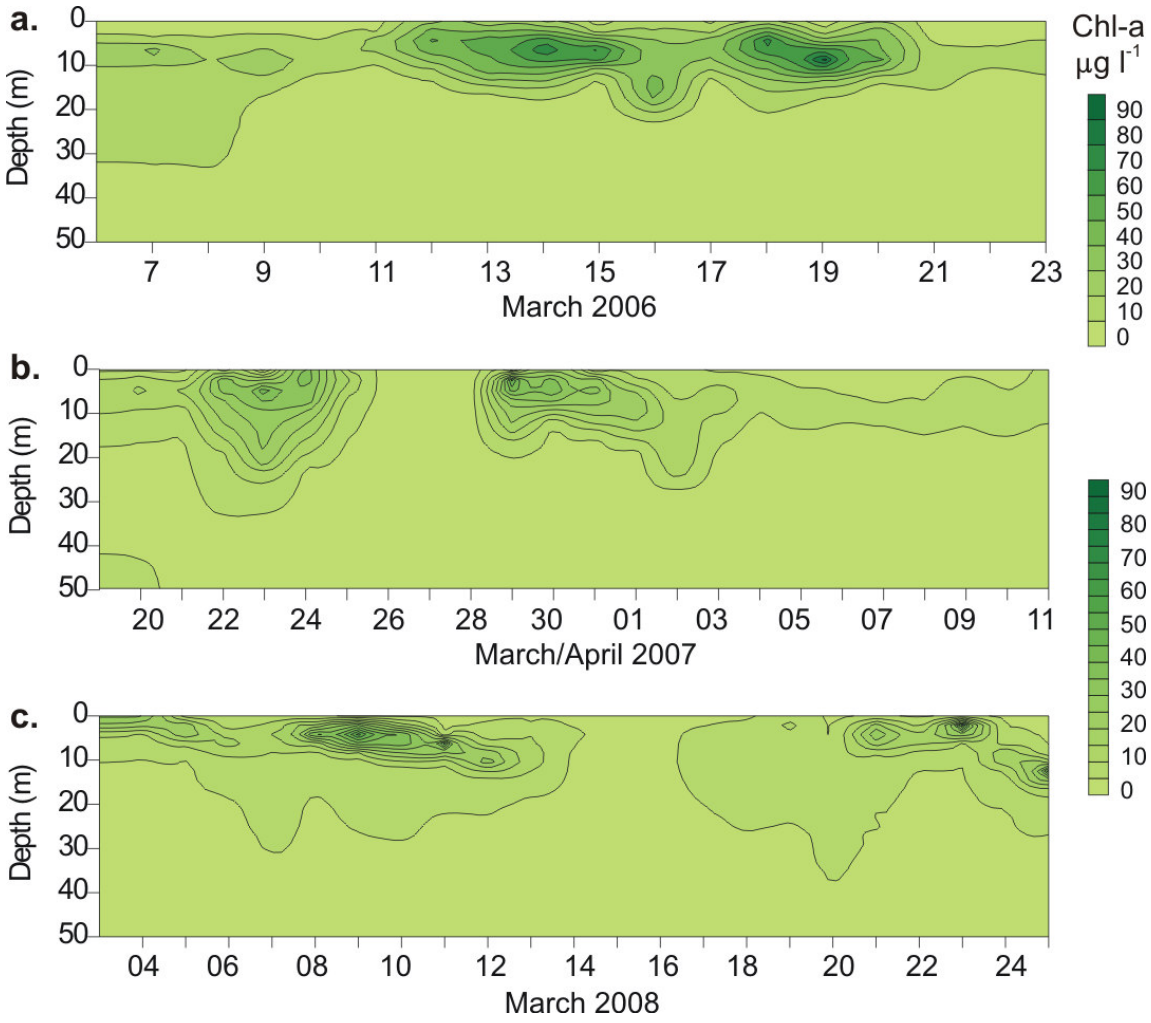

Figure 3.16. Contour plots of chl-a concentrations obtained from calibrated daily CTD casts in (a) 2006, (b) 2007 and (c) 2008. N.B: different scale bars apply for (a) and (b,c).

3.2.6. Phytoplankton community structure

3.2.6.1. Cell concentrations

In 2006, diatoms were always dominant, representing 96-100% total phytoplankton cells (Figure 3.17a). The dominant diatom species were *Pseudo-nitzschia* spp. (up to 85 % and 13.1 x 10^6 cells l^{-1}) and *Chaetoceros* spp. (up to 41 % and 4.8 x 10^6 cells l^{-1}) (Figure 3.17d). Dinoflagellates never exceeded 4 % total cell concentration (3.7 x 10^5 cells l^{-1}) and were composed mainly of *Prorocentrum* spp. (*P. micans* & *P. triestinum*) and *Scrippsiella trochoidea* (Figure 3.17g).

In 2007, dinoflagellates dominated the community on several occasions (65 % on 21 March, 100 % on 4-5 and 8-10 April), while diatoms dominated during other periods (71-100 %, 20, 22-25 March, 29 March-3 April & 6-7 April) (Figure 3.17b). When diatoms were dominant the main species present were *Skeletonema costatum* (28-85 %, up to 20.0 x 10^6 cells l^{-1}), *Chaetoceros* spp. (8-93 %, up to 9.3 x 10^6 cells l^{-1}) and *Pseudo-nitzschia* spp. (2-30 %, up to 1.2 x 10^6 cells l^{-1}) (Figure 3.17e). The PSP-producing dinoflagellate *Alexandrium catenella* dominated at the start of the survey (48 % cell concentration, 77 % carbon biomass on 21 March), with cell concentrations reaching 4.5 x 10^5 cells l^{-1}. On 4-5 and 9-10 April two *Gymnodinium* species dominated, representing together 92-100 % total cell numbers (1.1 x 10^6 cells l^{-1}), while on 8 April the community was co-dominated by the DSP producer *Dinophysis acuminata* (44%, 3.1 x 10^4 cells l^{-1}) and a small (<12 µm) *Gymnodinium* species (54 %, 3.7 x 10^4 cells l^{-1}) (Figure 3.17h), although in terms of biomass *D. acuminata* was 91% dominant.

In 2008, diatoms were most often numerically dominant, although dinoflagellates were dominant on several occasions, representing up to 95 % of total cell numbers (Figure 3.17c). The main diatom species were *Chaetoceros* spp. (mainly between 4 and 9 March, representing 42 to 83 % of total cell numbers, with up to 6.9 x 10^6 cells l^{-1}), *Pseudo-nitzschia* spp. (up to 67 % and 2.3 x 10^6 cells l^{-1}) and *Minidiscus trioculatus* (33 to 94 % betwen 18 and 22 March, representing up to 4.9 x 10^6 cells l^{-1}) (Figure 3.17f). The main dinoflagellate species were *Dinophysis acuminata* (up to 1.8 x 10^5 cells l^{-1}, but generally a small proportion of the phytoplankton community) and *Gyrodinium zeta* (particularly at the start of the survey, with 8.2 x 10^6 cells l^{-1}, representing 50 % of the cell numbers) (Figure 3.17i).

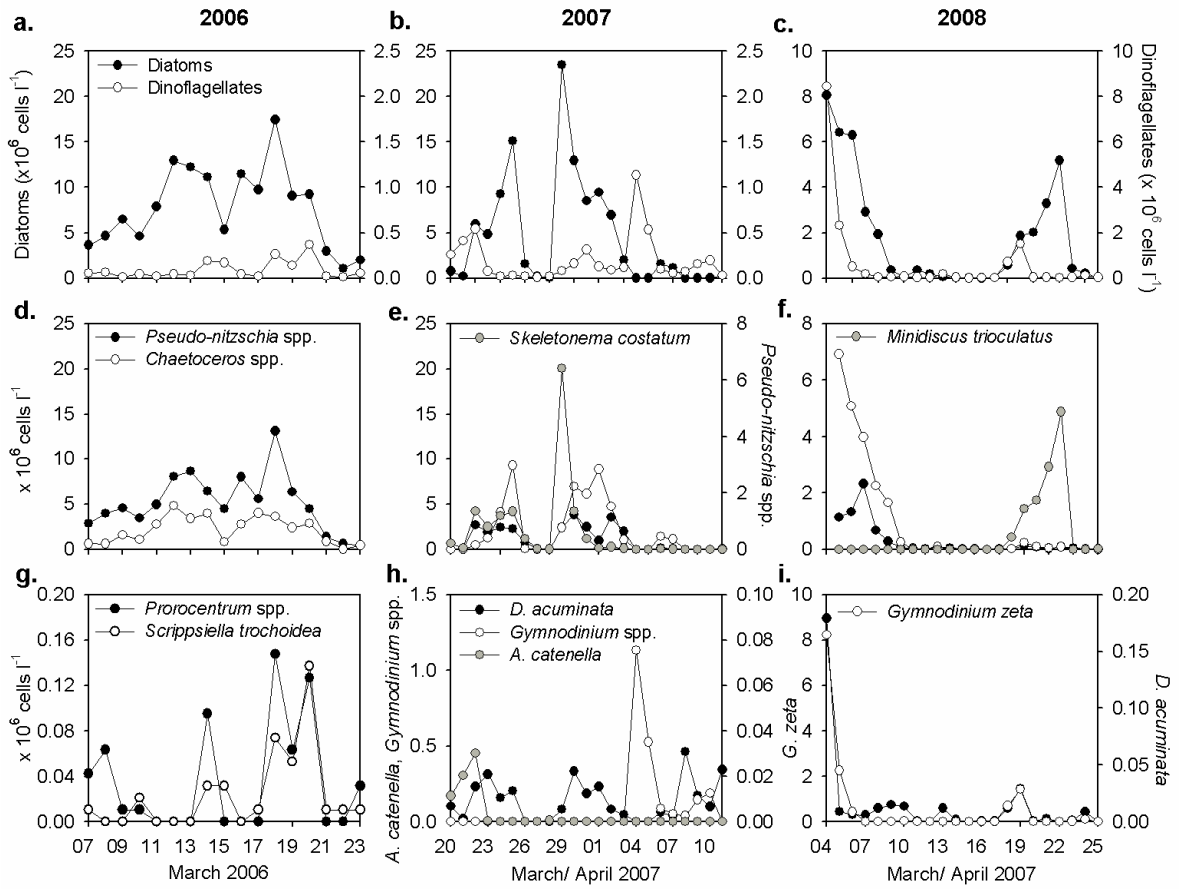

Figure 3.17. Total cell concentrations of diatoms and dinoflagellates in (a) 2006, (b) 2007 and (c) 2008 and concentrations of the most abundant species of diatoms in (d) 2006, (e) 2007 and (f) 2008 and of dinoflagellates in (g) 2006, (h) 2007 and (i) 2008. Black symbols represent *Pseudo-nitzschia* spp. and open circles represent *Chaetoceros* spp. in d, e and f; black symbols represent *Dinophysis acuminata* in h and i.

3.2.6.2. Cluster analysis

To assess whether there were similarities between phytoplankton communities in all years, cluster analyses were performed on the 2006, 2007 and 2008 data combined. The stations were divided into 7 clusters at the 50 % similarity level (stations that clustered separately were omitted) (Figure 3.18). The phytoplankton species responsible for between-station similarities within these clusters are shown in Table 3.3. All the 2006 stations were grouped together into Cluster VII, whereas 2007 stations were divided into Clusters I, II, VI and VII and 2008 stations into Clusters III, IV, V and VII.

The occurrence of each Cluster is shown in Table 3.1 together with southerly wind component and surface temperature. Cluster I was the only one entirely dominated by dinoflagellates (*Gymnodinium* spp. and *Dinophysis acuminata*), whereas Clusters IV, VI and VII were dominated by diatoms and Clusters II, III and V were mixtures of diatoms and dinoflagellates. Cluster I displayed the lowest Shannon diversity index (H') and very low chl-a and occurred in warm, nutrient-depleted waters characterised by low DIN:P and DIN:Si ratios. Cluster II was characterised by the presence of *A. catenella* and *Skeletonema costatum* and had the highest average chl-a biomass and H' value. Cluster III was co-dominated by *Scrippsiella trochoidea*, *Pseudo-nitzschia* spp. and *Gyrodinium* spp. and displayed very low chl-a, although a high H', occurring in cold, nutrient-replete waters with high DIN:P and DIN:Si ratios. Cluster IV consisted of stations immediately following those of Cluster III, occurring under similar conditions, with slightly warmer temperatures and lower nutrients, and was dominated by *Minidiscus trioculatus*. Cluster V was co-dominated by *Coscinodiscus* spp. and *Gyrodinium zeta* and was associated with low nutrients and nutrient ratios and moderately high chl-a. Clusters VI and VII were co-dominated by *Chaetoceros* spp. and *Pseudo-nitzschia* spp. (with *Skeletonema costatum* also present in Cluster VI) and occurred under a wide range of temperature and nutrient conditions.

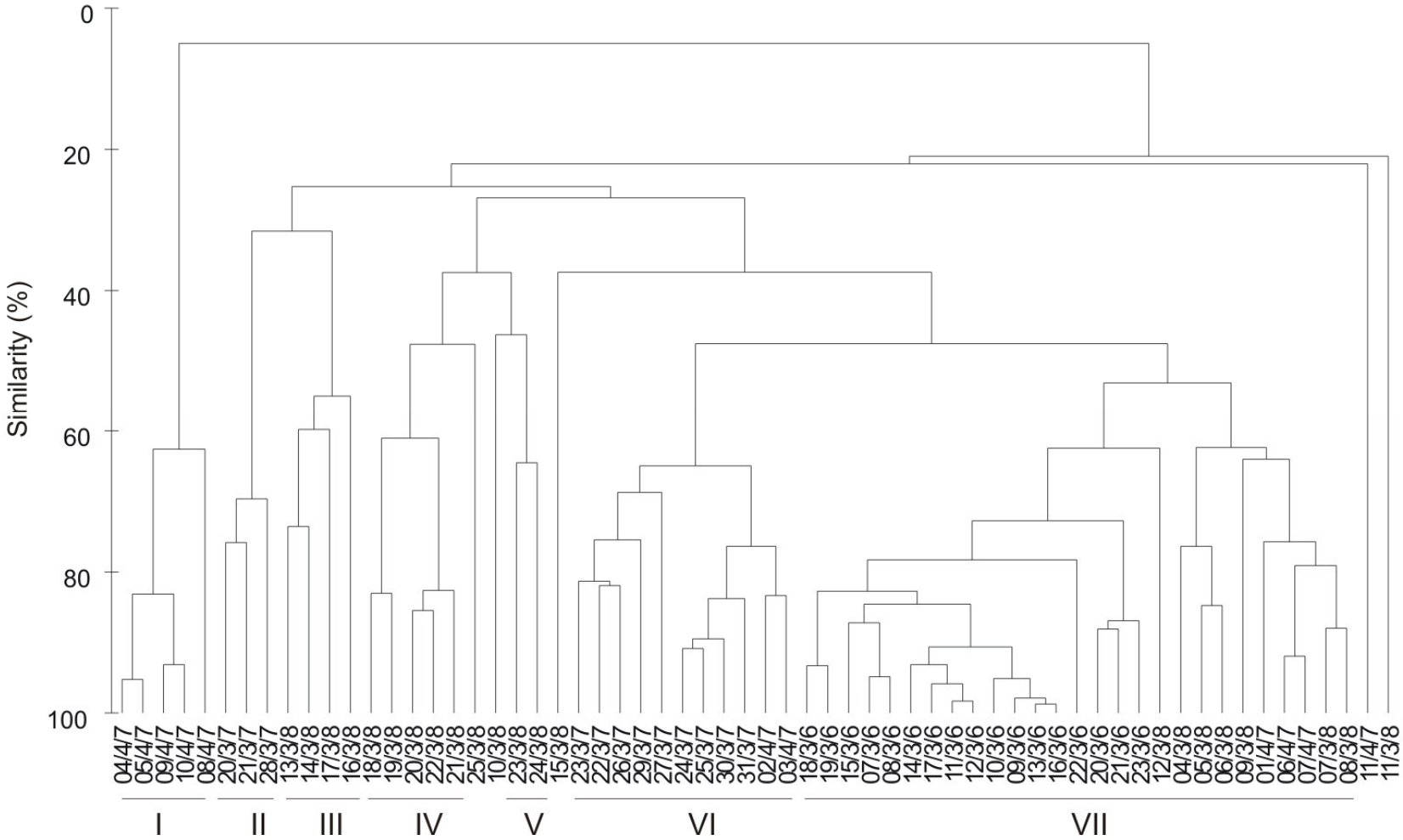

Figure 3.18. Dendrogram derived from calculations of Bray-Curtis similarity indices between stations in all years combined, using the statistical package PRIMER. Clusters formed at the 50 % similarity level are labelled (I-VII) as in the text.

Cluster	Dates	Species	% contribution to similarity	% diatoms	chl-a	H'	Temp	NO_3	PO_4	Si	DIN:P	DIN:Si
I	4,5, 8-10 Apr 07	*Gymnodinium* spp.	93.1	0.0 (0.0)	1.5 (0.4)	0.3 (0.1)	16.4 (0.2)	0.2 (0.1)	0.3 (0.0)	3.5 (0.3)	2.6 (0.6)	0.2 (0.0)
		D. acuminata	6.2									
II	20,21,28 Mar 07	*S. costatum*	31.6	60.0 (12.4)	13.3 (7.2)	1.5 (0.2)	12.1 (0.6)	16.5 (3.6)	2.1 (0.5)	22.3 (5.8)	8.5 (0.4)	0.8 (0.1)
		A. catenella	21.3									
		Thalassiosira spp.	16.2									
		S. trochoidea	11.5									
III	13,14,16,17 Mar 08	*Scrippsiella trochoidea*	39.0	35.7 (16.4)	1.3 (0.5)	1.2 (0.3)	11.4 (0.4)	25.5 (2.5)	2.5 (0.2)	35.5 (5.9)	11.4 (0.2)	0.9 (0.1)
		Pseudo-nitzschia spp.	16.7									
		Gyrodinium spp.	14.4									
		Coscinodiscus	9.7									
		D. acuminata	9.2									
IV	18-22 Mar 08	*M. trioculatus*	52.5	79.2 (13.7)	10.0 (1.3)	0.8 (0.2)	12.3 (0.4)	19.3 (2.2)	1.8 (0.2)	32.8 (2.8)	11.0 (0.2)	0.6 (0.0)
		Coscinodiscus spp.	11.0									
		Chaetoceros spp.	9.4									
		Pseudo-nitzschia spp.	9.3									
V	23,24 Mar 08	*Coscinodiscus* spp.	39.1	78.6 (14.1)	9.1 (2.1)	1.3 (0.3)	13.8 (0.1)	0.1 (0.0)	0.3 (0.1)	0.7 (0.1)	1.5 (1.1)	0.6 (0.3)
		G. zeta	14.5									
		Pseudo-nitzschia spp.	11.3									
		Chaetoceros spp.	10.2									
		Leptocylindrus	7.7									
VI	22-27, 29-31 Mar,	*S. costatum*	29.2	97.4 (0.8)	14.3 (3.1)	1.1 (0.1)	13.8 (0.4)	4.9 (2.5)	0.9 (0.2)	4.6 (2.6)	4.1 (1.3)	1.8 (0.3)
	2-3 Apr 07	*Chaetoceros* spp.	28.6									
		Pseudo-nitzschia spp.	18.5									
		Bacteriastrum spp.	11.0									
VII	7-23 Mar 06, 1,6,7 Apr 07	*Pseudo-nitzschia* spp.	47.7	94.4 (2.1)	17.6 (3.4)	0.7 (0.1)	13.5 (0.3)	7.5 (1.6)	1.2 (0.1)	11.2 (2.5)	5.1 (0.8)	1.2 (0.3)
	4-9,12 Mar 08	*Chaetoceros* spp.	47.0									

Table 3.3. Main species contributions to total similarity (up to 80 % cumulative percentage, with a minimum of 2 species shown) within clusters defined at the 50 % similarity level using the statistical package PRIMER and mean (standard error) % diatoms, chl-a, Shannon diversity index (H'), temperature, NO_3, PO_4 and Si concentrations and DIN:P and DIN:Si ratios for each cluster.

3.2.7. Nitrogen uptake and regeneration

3.2.7.1. Standard uptake

Rates of nitrogen uptake generally followed the upwelling/downwelling cycles, whereby absolute nitrogen uptake ρ(N) was dominated by $\rho(NO_3^-)$ during active upwelling (e.g. 8-13, 17, 20-22 March 2006, 21 March 2007, 18-20 March 2008, Table 3.1), and by $\rho(NH_4^+)$ and ρ(urea) during stratified, NO_3^--depleted periods (e.g. 15-16, 19 March 2006, 30 March-10 April 2007, 9-12 March 2008, Table 3.1). However, this was not always the case (e.g. 26 March 2007, 14-16 March 2008, Table 3.1).

In 2006, $\rho(NO_3^-)$ at the surface (0.02-0.40 μmol N l^{-1} h^{-1}) was not significantly different from the subsurface (0.01-0.55 μmol N l^{-1} h^{-1}). Ammonium and urea uptake were also not significantly different between surface and subsurface, with $\rho(NH_4^+)$ ranging from 0.04 to 0.15 μmol N l^{-1} h^{-1} at the surface and from 0.03 to 0.21 μmol N l^{-1} h^{-1} in the subsurface and ρ(urea) from 0.01 to 0.06 μmol N l^{-1} h^{-1} at the surface and from 0.01 to 0.11 μmol N l^{-1} h^{-1} in the subsurface (Figure 3.19a,d). Overall, $\rho(NO_3^-)$ was significantly higher than $\rho(NH_4^+)$, which was significantly higher than ρ(urea) at both depths (Wilcoxon's test, $p < 0.05$).

In 2007, $\rho(NO_3^-)$ was particularly high for the *Alexandrium catenella*-dominated assemblage on 21 March (0.61 μmol N l^{-1} h^{-1} at 0 m, 0.53 μmol N l^{-1} h^{-1} at 5 m) but was generally low for the rest of the survey, with similar values at both depths (0.01-0.25 μmol N l^{-1} h^{-1} at 0 m, <0.01 to 0.29 μmol N l^{-1} h^{-1} at 5 m) (Figure 3.19b,e). Ammonium uptake was relatively high, ranging from 0.02 to 0.19 μmol N l^{-1} h^{-1} at 0 m and from 0.02 to 0.25 μmol N l^{-1} h^{-1} at 5 m. Urea uptake displayed the lowest rates, ranging from <0.01 to 0.08 μmol N l^{-1} h^{-1} at 0 m and from <0.01 to 0.10 μmol N l^{-1} h^{-1} at 5 m, where it was significantly higher (Wilcoxon's test, $p < 0.05$). Overall, $\rho(NH_4^+)$ was significantly higher than both $\rho(NO_3^-)$ and ρ(urea) at both depths (Wilcoxon's test, $p < 0.05$).

In 2008, $\rho(NO_3^-)$ was relatively low at the surface, ranging from <0.01 to 0.18 μmol N l^{-1} h^{-1}, but higher in the subsurface, ranging from <0.01 to 0.57 μmol N l^{-1} h^{-1} (Figure 3.19c,f). Ammonium uptake ranged from <0.01 to 0.14 μmol N l^{-1} h^{-1} at the surface and from 0.01 to 0.20 μmol N l^{-1} h^{-1} in the subsurface. Both $\rho(NO_3^-)$ and $\rho(NH_4^+)$ were significantly higher in the subsurface relative to the surface (Wilcoxon's test, $p < 0.01$). Urea uptake was significantly lower than both $\rho(NO_3^-)$ and $\rho(NH_4^+)$ at both depths (Wilcoxon's test, $p < 0.05$), ranging from <0.01 to 0.06 μmol N l^{-1} h^{-1} at the surface and

from <0.01 to 0.14 µmol N l^{-1} h^{-1} in the subsurface, where it was significantly higher (Wilcoxon's test, $p < 0.05$). Nitrate uptake was significantly lower than in 2006 (Student's t-test, $p < 0.01$), but higher than in 2007 (Mann-Whitney U-test, $p < 0.05$), whereas $\rho(NH_4^+)$ was significantly lower than in 2007 (Student's t-test, $p < 0.01$).

The alternating dominance of new (NO_3^-) and regenerated nitrogen (NH_4^+ and urea) uptake during the upwelling/relaxation cycles was reflected in the highly variable *f*-ratios of 0.11-0.85 at the surface and 0.10-0.81 in the subsurface in 2006 (Figure 3.19g), 0.06-0.87 at 0 m and 0.03-0.79 at 5 m in 2007 (Figure 3.19h) and 0.01-0.68 at the surface and 0.03-0.76 in the subsurface in 2008 (Figure 3.19i). Overall, *f*-ratios were significantly higher in 2006 than in 2007 and 2008 (Student's t-test, $p < 0.01$).

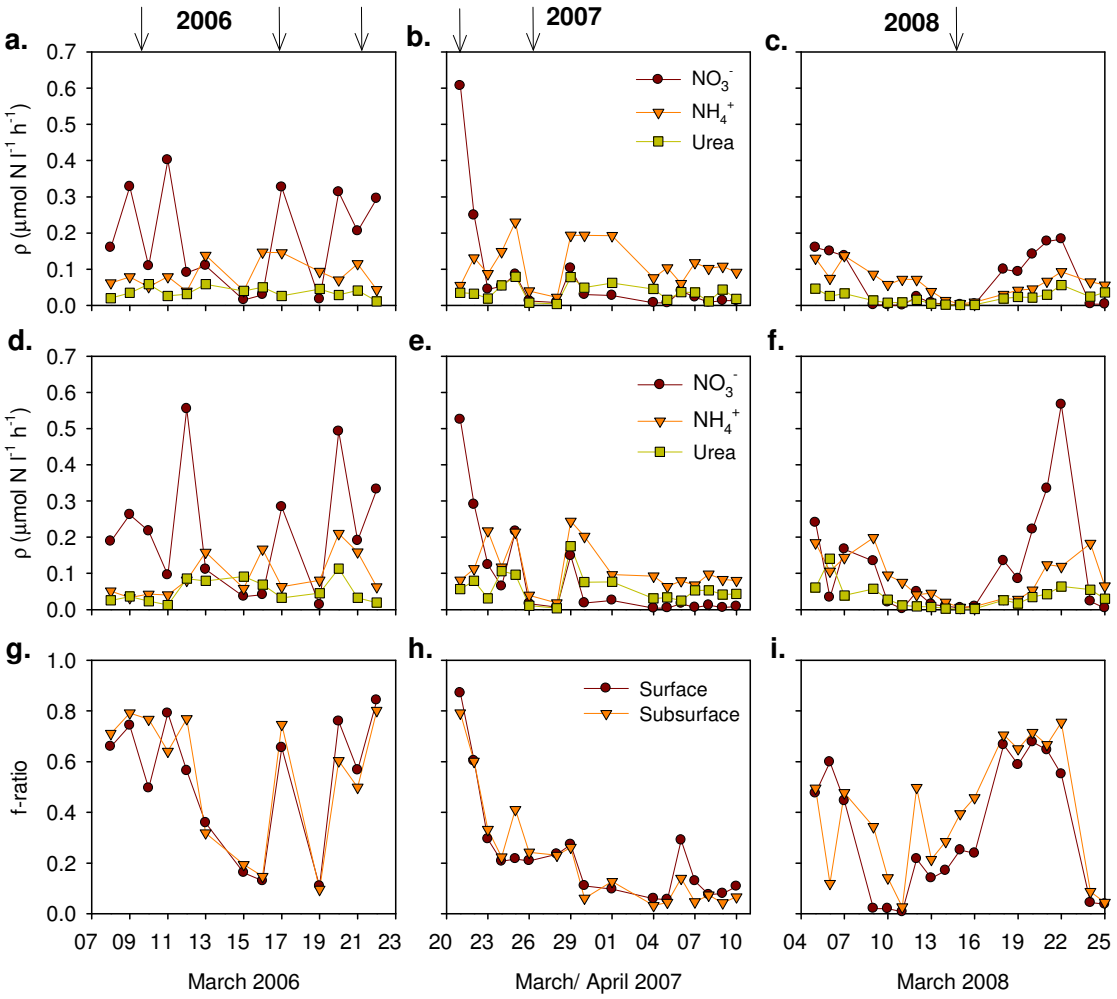

Figure 3.19. Surface uptake rates of NO_3^-, NH_4^+ and urea in (a) 2006, (b) 2007 and (c) 2008; subsurface uptake rates in (d) 2006, (e) 2007 and (f) 2008; *f*-ratios at both depths in (g) 2006, (h) 2007 and (i) 2008. Arrows indicate upwelling events.

Both $\rho(NO_3^-)$ and the *f*-ratio displayed significant linear correlations with wind (previous day northward component) at both depths in 2006 ($r^2 = 0.54$, $n = 26$, $p < 0.01$).

These relationships were not observed in 2007 or 2008 due to variable time lags between changes in wind direction and in nitrogen uptake. However, the correlation was significant for all 3 years combined, after removal of 21-22 March 2007, which represented the unusual combination of high *f*-ratios and northerly winds (Figure 3.20).

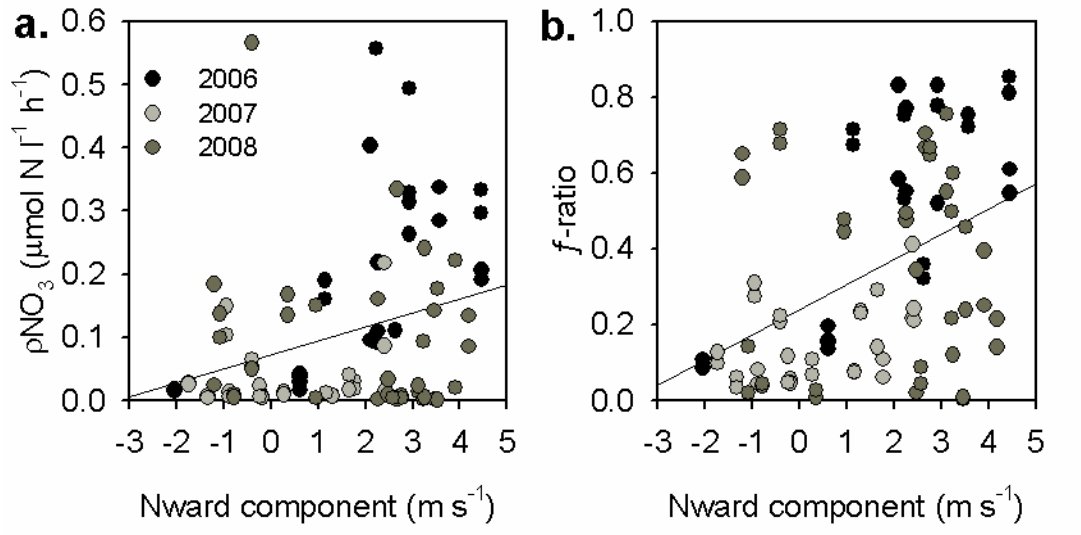

Figure 3.20. (a) $\rho(NO_3^-)$ and (b) *f*-ratio at both incubation depths versus northward wind component in 2006, 2007 and 2008. Significant linear correlations ($p < 0.01$) were found for all data combined (but not for 2007 or 2008 alone). Equations are: $y = 0.022 x + 0.072$ ($r^2 = 0.09$) in (a) and $y = 0.07 x + 0.24$ ($r^2 = 0.20$) in (b).

Nitrate uptake was highest in Clusters II, IV and VII, whereas $\rho(NH_4^+)$ was highest in Clusters I and VI (Table 3.4). Highest *f*-ratios were measured in Clusters II, IV and VII, whereas the lowest ratios (<0.1) were measured in Clusters I and V (Table 3.4).

Cluster	Dates	Species	$\rho(NO_3^-)$	$\rho(NH_4^+)$	*f*-ratio
I	4,5, 8-10 Apr 07	*Gymnodinium*, *D. acuminata*	0.01 (0.0)	0.10 (0.01)	0.08 (0.01)
II	20,21,28 Mar 07	*S. costatum, A. catenella, Thalassiosira, S. trochoidea*	0.31 (0.25)	0.04 (0.01)	0.55 (0.26)
III	13,14,16,17 Mar 08	*S. trochoidea, Pseudo-nitzschia, Gyrodinium, Coscinodiscus, D. acuminata*	0.00 (0.00)	0.02 (0.01)	0.18 (0.02)
IV	18-22 Mar 08	*M. trioculatus, Coscinodiscus Chaetoceros, Pseudo-nitzschia*	0.14 (0.02)	0.06 (0.01)	0.63 (0.03)
V	23,24 Mar 08	*Coscinodiscus* spp., *G. zeta Pseudo-nitzschia, Chaetoceros, Leptocylindrus*	0.00	0.07	0.04
VI	22-27, 29-31 Mar, 2-3 Apr 07	*S. costatum, Chaetoceros Pseudo-nitzschia, Bacteriastrum*	0.08 (0.02)	0.15 (0.02)	0.27 (0.05)
VII	7-23 Mar 06, 1,6,7 Apr 07 4-9,12 Mar 08	*Pseudo-nitzschia, Chaetoceros*	0.14 (0.02)	0.09 (0.01)	0.43 (0.05)

Table 3.4. Mean (standard error) $\rho(NO_3^-)$, $\rho(NH_4^+)$ (μmol N l^{-1} h^{-1}) and *f*-ratios for each cluster as defined in Table 3.2.

3.2.7.2. Ammonium regeneration

Regeneration rates r(NH_4^+) were highly variable, but displayed no significant differences between the surface and subsurface. Rates ranged from 0.03 to 0.33 µmol N l^{-1} h^{-1} at both depths in 2006, from 0.01 to 0.47 µmol N l^{-1} h^{-1} in 2007 and from 0.02 to 0.33 µmol N l^{-1} h^{-1} in 2008. Although r(NH_4^+) was on average higher in 2007 (0.18 ± 0.02 µmol N l^{-1} h^{-1}) relative to the other years (0.13 ± 0.02 µmol N l^{-1} h^{-1} in 2006 and 0.12 ± 0.01 µmol N l^{-1} h^{-1} in 2008), these differences were not statistically significant.

Ammonium uptake and regeneration rates were significantly correlated in all 3 years (n = 22 in 2006, n = 33 in 2007, n = 35 in 2008, $p < 0.01$), with regression coefficients of 0.39, 0.48 and 0.60 in 2006, 2007 and 2008, respectively (Figure 3.21).

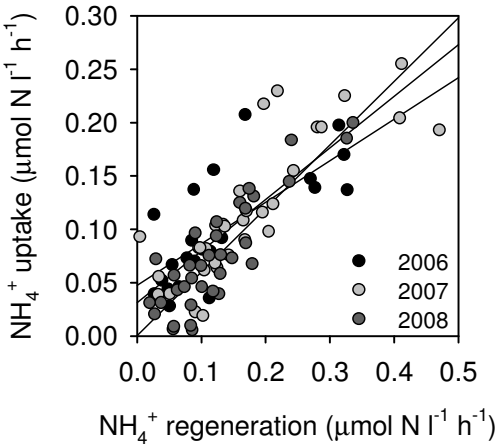

Figure 3.21. Correlations between ρ(NH_4^+) and r(NH_4^+) in all years ($p < 0.01$). Equations are: 2006: $y = 0.39 x + 0.05$ ($r^2 = 0.54$); 2007: $y = 0.48 x + 0.03$ ($r^2 = 0.69$); 2008: $y = 0.60 x + 0.001$ ($r^2 = 0.76$).

3.2.7.3. Nitrogen uptake kinetics

The *Pseudo-nitzschia*-dominated assemblage displayed a preference for NH_4^+ over NO_3^- and for NO_3^- over urea in terms of its maximum PN-specific uptake rate (ν_{max}), with ν_{max} (NH_4^+): ν_{max}(NO_3^-) and ν_{max}(urea): ν_{max}(NO_3^-) ratios of 1.2 and 0.3, respectively. The half-saturation constant (K_s) could not be determined for urea, but it was similar for NO_3^- and NH_4^+, resulting in similar α values (Table 3.5a).

The *Alexandrium catenella*-dominated assemblage displayed a preference for NO_3^- over both forms of recycled nitrogen, with a ν_{max}(NH_4^+): ν_{max}(NO_3^-) ratio less than 0.9, and a ν_{max}(urea):ν_{max}(NO_3^-) ratio less than 0.2. Exact ratios could not be determined because ν_{max} was a lower limit estimate.

Dinophysis acuminata was only truly dominant (91 % of total phytoplankton carbon biomass) in 2007, whereas in 2008 it only represented 50 % total biomass in Experiment 4, co-occurring with *Coscinodiscus* spp. and *Polykrikos schwartzii*, and 33 % in Experiment 5, co-occurring with *Gyrodinium* spp., *Protoperidinium excentricum* and *P. schwartzii*. However, the communities in Experiments 3 and 5 displayed very similar nitrogen uptake kinetics, with little differences observed in ν_{max} and α between years, the greatest discrepancy being 41 % (ν_{max} for urea, higher in 2007). Both assemblages showed a very strong preference for NH_4^+ relative to NO_3^- at both saturating and limiting concentrations, with ν_{max}(NH_4^+): ν_{max}(NO_3^-) ratios of 4.0 and 4.2 and α(NH_4^+): α(NO_3^-) ratios of 4.7 and 5.5. They also exhibited a preference for urea over NO_3^-, with ν_{max}(urea):ν_{max}(NO_3^-) ratios of 1.8 and 1.3 and an α(urea): α(NO_3^-) ratio of 2.6 in 2007 (not determined in 2008). The community in Experiment 4, however, displayed 7-fold higher ν_{max}(NO_3^-), but 2-fold lower ν_{max}(NH_4^+) and 1.5 to 2-fold lower ν_{max}(urea) relative to Experiments 3 and 5. In contrast to the others, this community displayed a strong preference for NO_3^- over NH_4^+ in terms of ν_{max}, with a ν_{max}(NH_4^+):ν_{max}(NO_3^-) ratio of 0.3, although the α(NH_4^+):α(NO_3^-) ratio of 4.0 indicated that at limiting concentrations NH_4^+ was preferred. Since the experiment was conducted at high NO_3^- concentrations, the comparison of ν_{max} is more relevant. The absence of measurements below 15 μmol l^{-1} could, for example, mask biphasic kinetics with a first saturation plateau at lower concentrations.

An inhibition kinetics experiment carried out on the phytoplankton assemblage in Experiment 5 revealed a maximum inhibition constant (I_{max}) of 0.68 and a half-inhibition constant (K_i) of 4.21 μmol N l^{-1} (Figure 3.22f).

All communities displayed similar ν_{max} for NH_4^+ (increasing 29 % between the lowest and highest values) and to a lesser extent for urea (increasing 2-fold), whereas ν_{max} for NO_3^- was more variable, increasing 7-fold between the lowest (Experiments 3 and 5) and the highest values (Experiment 4). *Pseudo-nitzschia* displayed the highest affinity (α) for NO_3^-, 3- to 4- fold higher than the other species, whereas *D. acuminata* (Experiments 3 and 5) displayed the highest affinity for NH_4^+ (2 to 3-fold higher) and urea (1.5- to 2-fold higher).

However, due to differences in cell size between the dinoflagellate species and *Pseudo-nitzschia*, estimates of cell-specific ν_{max} ($\nu_{max(cell)}$) displayed different patterns. These could only be calculated for Experiments 1-3, since the phytoplankton communities in Experiments 4 and 5 were mixed assemblages. Cellular ν_{max} was 1-2 orders of magnitude lower for *Pseudo-nitzschia* (cell volume $V_{cell} \approx 5 \times 10^2\ \mu m^3$) relative to the dinoflagellates ($V_{cell} \approx 1.4 \times 10^4\ \mu m^3$). A similar pattern was observed for α, with lowest values measured in *Pseudo-nitzschia* and highest in *D. acuminata* (Table 3.6).

There was no apparent relationship between K_s and V_{cell} for these species (data not shown). Whereas K_s values measured for *Pseudo-nitzschia* (NH_4^+ and NO_3^-) and for *A. catenella* (NH_4^+) were close to the values predicted by the V_{cell}-K_s relationship derived by Litchman et al. (2007), K_s for *D. acuminata* (all nitrogen sources) and *A. catenella* (for urea) were only 24-37 % of the predicted values (Table 3.6).

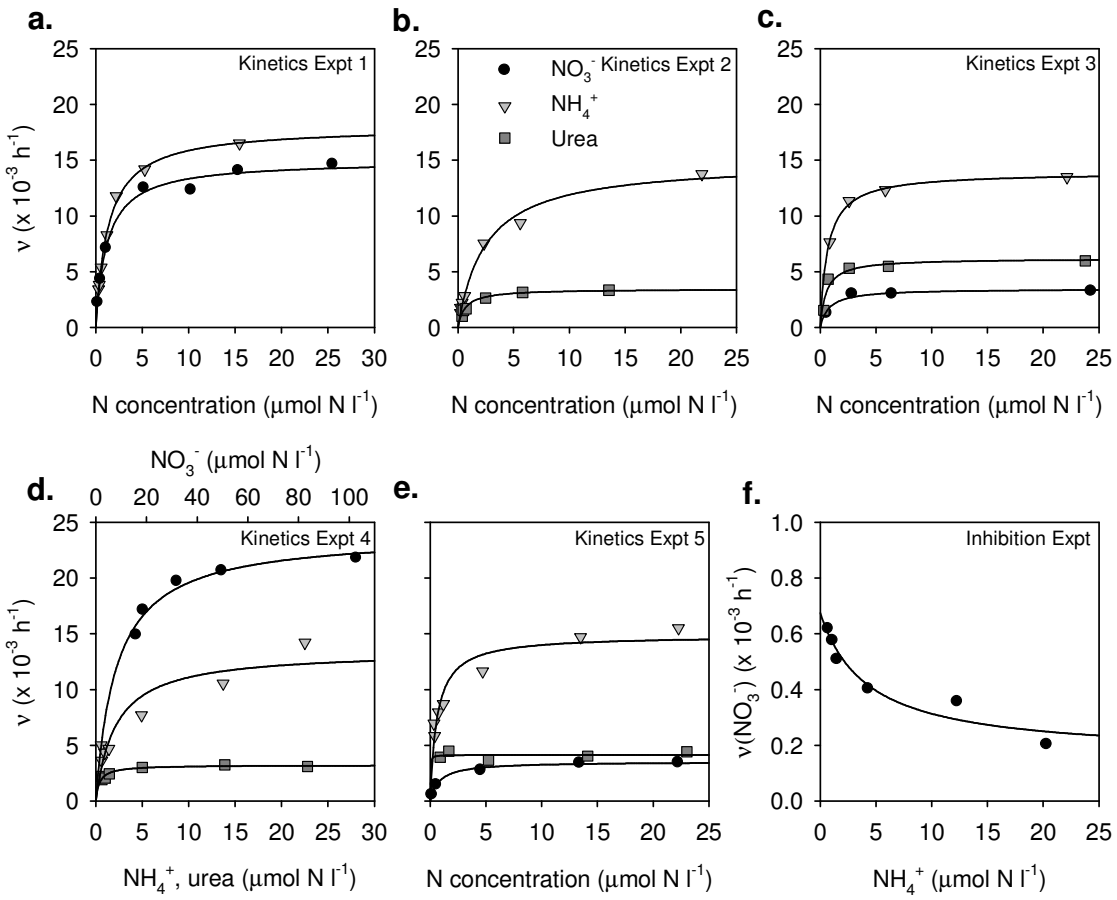

Figure 3.22. PN-specific nitrogen uptake versus nitrogen concentration fitted to the Michaelis-Menten equation $v = v_{max}*S/ (K_s + S)$ using iterative non-linear least squares regression (SigmaPlot, Jandel Scientific) for samples dominated by (a) *Pseudo-nitzschia* spp., (b) *Alexandrium catenella*, (c,d,e) *Dinophysis acuminata*; (f) $v(NO_3^-)$ versus NH_4^+ concentration obtained from an NH_4^+ inhibition kinetics experiment run in parallel with experiment (e), fitted to the modified Michaelis-Menten equation $v = v_{max} - v_{max}*I_{max}*S/ (K_i + S)$

Dominant species	ν_{max}			K_s			α			$\frac{\nu_{max}(NH_4^+)}{\nu_{max}(NO_3^-)}$	$\frac{\alpha(NH_4^+)}{\alpha(NO_3^-)}$	$\frac{\nu_{max}(urea)}{\nu_{max}(NO_3^-)}$	$\frac{\alpha(urea)}{\alpha(NO_3^-)}$
	NO_3^-	NH_4^+	Urea	NO_3^-	NH_4^+	Urea	NO_3^-	NH_4^+	Urea				
Pseudo-nitzschia	15.0 (0.4)*	18.0 (0.3)*	4.9 (0.3)[b]	1.21 (0.15)*	1.34 (0.07)*	nd	12.4	13.4	nd	1.20	1.08	0.33	nd
A. catenella	>17.5[a]	14.9 (0.8)*	3.5 (0.2)*	nd	2.52 (0.36)*	0.65 (0.12)*	nd	5.9	5.4	< 0.85	nd	<0.20	nd
D. acuminata	3.5 (0.2)*	13.9 (0.2)*	6.2 (0.6)*	0.79 (0.26)	0.67 (0.06)*	0.53 (0.22)	4.4	20.7	11.7	3.97	4.68	1.77	2.64
D. acuminata (mixed)	24.0 (0.9)*	6.2 (0.6)*	3.2 (0.1)*	8.24 (1.46)*	0.53 (0.22)	0.41 (0.08)*	2.9	11.7	7.8	0.26	4.02	0.13	2.68
D. acuminata (mixed)	3.5 (0.1)*	14.6 (0.9)*	4.4 (0.3)[b]	0.82 (0.13)*	0.62 (0.14)*	nd	4.3	23.5	nd	4.17	5.52	1.26	nd

Table 3.5. Maximum PN-specific uptakes ν_{max} (x 10^{-3} h^{-1}) and half-saturation constants K_s (µmol N l^{-1}) with standard errors given in brackets. α is the ratio ν_{max}/K_s (x 10^{-3} h^{-1} (µmol N l^{-1})$^{-1}$). Ratios of ν_{max} and α between different nitrogen sources are given as indicators of nutrient preferences.
[a] ν (NO_3^-) measured at an ambient NO_3^- concentration of 16.9 µmol l^{-1} is given as a lower limit estimate of ν_{max}.
[b] ν_{max} was derived from the mean of ν(urea) at 4 or 5 saturating concentrations.
*** $p < 0.05$.**

Exp. #	Dominant species	V_{cell} (µm^3)	$\nu_{max(cell)}$			$K_{s(pred)}$	$K_{s(meas)}:K_{s(pred)}$			$\alpha_{(cell)}$		
			NO_3^-	NH_4^+	Urea		NO_3^-	NH_4^+	Urea	NO_3^-	NH_4^+	Urea
1	*Pseudo-nitzschia*	518	0.02	0.03	0.01	0.92	1.32	1.46	nd	0.02	0.02	nd
2	*A. catenella*	13739	nd	1.30	0.31	2.23	nd	1.13	0.29	nd	1.15	1.06
3	*D. acuminata*	14009	0.74	2.90	1.30	2.24	0.35	0.30	0.24	2.10	9.69	5.49

Table 3.6. Cell volume (V_{cell}) of the dominant phytoplankton species, cell-specific $\nu_{max(cell)}$ (pmol N $cell^{-1}$ h^{-1}) and $\alpha_{(cell)}$ (pmol N $cell^{-1}$ h^{-1} (µmol N l^{-1})$^{-1}$; K_s predicted from the relationship between K_s and V_{cell} derived by Litchman et al. (2007) and ratio of measured K_s to predicted K_s.

3.2.8. FRRf

Photochemical efficiency of photosystem II (PSII), F_v/F_m, was generally lowest at the surface (Figure 3.23), ranging from 0.1 to 0.3 in both 2007 and 2008 (mean 0.17 ± 0.02 and 0.20 ± 0.02, respectively). Values increased with depth, reaching a maximum of 0.4 to 0.6 between 5 and 10 m (means 0.44 ± 0.02 and 0.43 ± 0.02 at 10 m in 2007 and 2008, respectively), then remaining constant or decreasing slightly with depth.

The functional absorption cross-section of PSII (σ_{PSII}) followed a similar pattern, with surface values between 158 and 737 m^2 (µmol quanta)$^{-1}$ in 2007 (mean 461 ± 36) and between 60 and 452 m^2 (µmol quanta)$^{-1}$ (mean 281 ± 25) in 2008. Values increased to a maximum between 5 and 10 m, with mean values at 10 m of 625 ± 42 m^2 (µmol quanta)$^{-1}$ in 2007 and 423 ± 25 m^2 (µmol quanta)$^{-1}$ in 2008.

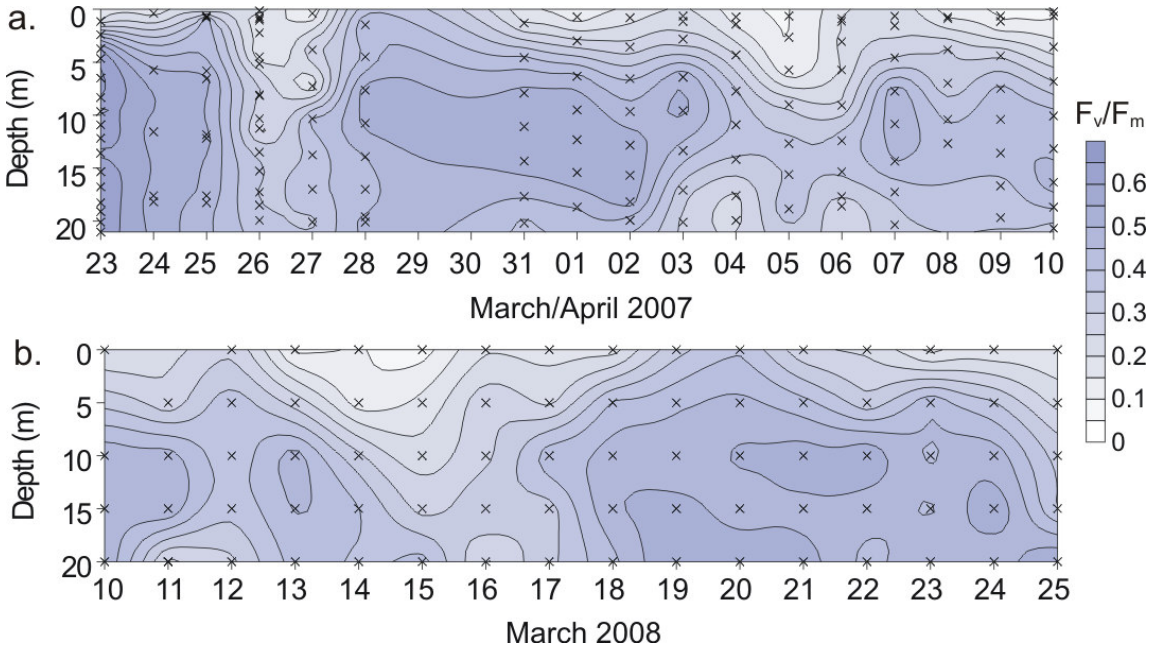

Figure 3.23. Contour plots of F_v/F_m obtained from FRRf casts in (a) 2007 and (b) 2008.

There was a significant positive correlation between F_v/F_m and σ_{PSII} in both years (r^2 = 0.22, n = 146, $p < 0.01$ in 2007 and r^2 = 0.28, n = 135, $p < 0.01$ in 2008, Figure 3.24a). There was also a significant positive correlation between the *f*-ratio and F_v/F_m in both years (r^2 = 0.25, n = 26, $p < 0.01$ in 2007 and r^2 = 0.37, n = 26, $p < 0.01$ in 2008, Figure 3.24b). However, the *f*-ratio displayed no correlation with σ_{PSII} despite the correlation between F_v/F_m and σ_{PSII}.

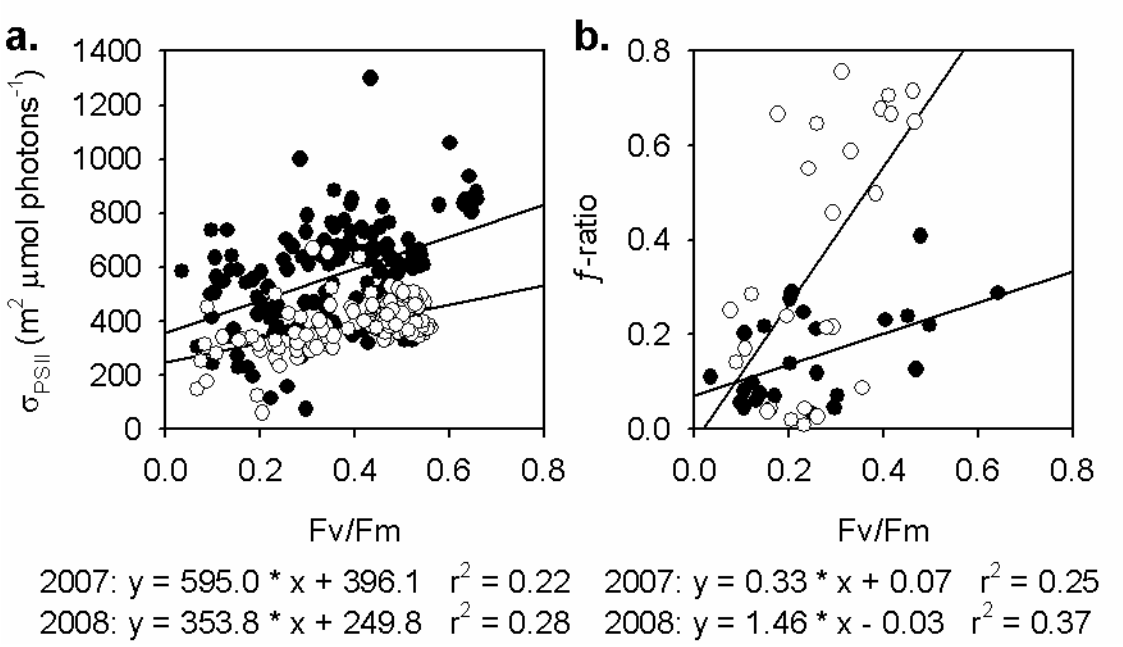

Figure 3.24. Correlations between (a) σ_{PSII} and F_v/F_m in 2007 (n = 146, $p < 0.01$) and in 2008 (n = 135, $p < 0.01$), and (b) between the *f*-ratio and F_v/F_m in 2007 and 2008 (n = 26, $p < 0.01$).

3.3. Discussion

3.3.1. Hydrography

The observed alternations between cold and warm surface temperatures in the Southern Benguela were consistent with the pulsed upwelling that characterises the seasonal transition between active upwelling in summer and quiescence in winter. The temperatures and salinities measured (~11-17 °C and 34.4-35.5) were within the range characteristic of South Atlantic Central Water (SACW) (Shannon, 1985a). A wide range of temperatures was measured at the surface, whereas the salinity range was narrower (34.4-34.8), hence there was no correlation between temperature and salinity. Therefore, all surface water was upwelled SACW, the coldest having recently upwelled and the warmest having warmed since upwelling, but conserving its original salinity.

Oxygen concentrations in bottom waters were lower than in source SACW, as is often the case in the Benguela region (Shannon, 1985b). Concentrations <1 ml l^{-1} were measured below the thermocline at temperatures <10.5 °C, even as shallow as 10 m. Previous studies that found similar results concluded that bacterial decomposition of sinking organic matter was responsible for this oxygen depletion (Jones, 1971; Shannon, 1985b). Low oxygen water in the Southern Benguela is thought to be formed locally, rather than advected from the Northern Benguela, as shown by the different thermohaline properties of these water masses (Shannon, 1985b; Monteiro & van der Plas, 2006). The temperatures and salinities measured in oxygen-depleted waters in this study were similar to the mean published by Shannon et al. (1985) for the region between 30 and 35 °S (9.5 °C and 34.7), confirming that oxygen depletion was a result of local biological processes.

Following upwelling, low DO water was brought to the surface, where concentrations dropped as low as 1.3 ml l^{-1} (at 10.3 °C). Although surface DO concentrations are known to drop following upwelling in the Southern Benguela, previous studies only reported a drop to 5 ml l^{-1} (Shannon, 1966). Concentrations increased to values as high as 9 ml l^{-1} concurrently with surface warming, stratification and increased phytoplankton biomass, because of photosynthesis. An increase from 1.6 to 10.9 ml l^{-1} was observed over a 7 day period, from 17-25 March 2008, even greater than that reported by Pieterse & van der Post (1967) for Walvis Bay. Therefore, it

appears that fluctuations in surface DO concentrations were particularly pronounced during the present study, with extremely low concentrations during upwelling, increasing rapidly to very high concentrations during stratification.

3.3.2. Nutrient remineralisation

In 1934, Alfred Redfield noted that the nutrient (N, P) composition of seawater was identical to that of plankton (Redfield, 1934) and this was attributed to the stoichiometric uptake and subsequent remineralisation of nutrients by phytoplankton (Sverdrup et al., 1942). However, it has since been noted that the N:P requirements of phytoplankton vary between species and with growth stage (Arrigo, 2005). Departures from the so-called "Redfield ratio" of ~16 can be attributed to a number of biogeochemical processes such as different remineralisation rates (Harrison, 1980), denitrification (Tyrrell & Law, 1997), anaerobic ammonium oxidation or "Anammox" (Arrigo, 2005) and "nutrient trapping" (Alvarez Salgado et al., 1997; Tyrrell & Lucas, 2002).

In the current study, the regression coefficient derived from the linear correlation between DIN and PO_4^{3-} was ~12 mol DIN (mol PO_4^{3-})$^{-1}$ in all years. This is higher than the value of 9 published by Tyrrell & Lucas (2002) for the Benguela, but lower than that of 14 obtained from the global dataset compiled by Tyrrell & Law (1997). A PO_4^{3-} excess of 0.26 to 0.28 was observed at zero DIN, indicating that PO_4^{3-} was non-limiting at low NO_3^- concentrations, consistent with previous studies in the Benguela (Dittmar & Birkicht, 2001; Tyrrell & Lucas, 2002). In contrast to these results, measurements of NO_3^- and PO_4^{3-} in the Iberian upwelling system compiled for the period 1977-1998 yielded an N:P ratio greater than the Redfield ratio (17.9 mol NO_3^- (mol PO_4^{3-})$^{-1}$) and a very low PO_4^{3-} excess at zero NO_3^- (0.02 µmol l^{-1}) (Álvarez–Salgado et al., 2002) although lower N:P ratios (<10) were found in spring and summer in the surface waters of the Ría de Ferrol (Bode et al., 2005).

In this study, newly upwelled water generally had an N:P ratio of 10-12 and subsequent nutrient uptake caused further departure from Redfield (down to values <0.1), consistent with a study by Andrews & Hutchings (1980) that revealed a decline in N:P ratios with increasing DO concentration as a result of phytoplankton uptake. This, however does not indicate that nutrient uptake did not follow Redfield stoichiometry, it is simply due to the fact that the initial ratio was <16 (Tyrrell & Lucas, 2002). All low

N:P values in this dataset were associated with low PO_4^{3-} concentrations (<1.5 μmol l^{-1}), i.e. there were no "LNP points", defined by Tyrrell & Law (1997) as data points where N:P < 3 and PO_4 > 1.5 μmol l^{-1}, and used as evidence of denitrification. High nitrogen deficits ($\Delta N = 16 * [PO_4^{3-}] - [NO_3^-]$), i.e. > 20 μmol l^{-1}, as measured by Tyrrell & Lucas (2002), were also used as an indicator of denitrification. The highest ΔN measured in the present study were 13.6 μmol l^{-1} (mean 3.7 ± 0.5 μmol l^{-1}) in 2006, 10.6 μmol l^{-1} (mean 3.0 ± 0.2 μmol l^{-1}) in 2007 and 19.5 μmol l^{-1} (mean 2.4 ± 0.4 μmol l^{-1}) in 2008, therefore it seems unlikely that the low N:P ratios in this study were due to denitrification [although more recent findings suggest this was more likely Annamox (Kuypers et al., 2005)]. The data used by Tyrrell and Lucas (2002) were collected in the Northern Benguela (20-32°S), where hypoxia is widespread due to the advection of low oxygen water (LOW) from the Angola Basin (Chapman & Shannon, 1985; Shannon, 1985a; Monteiro & van der Plas, 2006). In contrast, LOW in the Southern Benguela is generated locally (in St Helena Bay) in response to wind-driven physical (e.g. stratification) and biogeochemical processes (e.g. new production) (Monteiro & van der Plas, 2006). Thus, denitrification should be more widespread in the low oxygen waters of the Northern Benguela, but does not appear to be prominent in this study.

An alternative explanation for the low N:P ratios could be different rates of remineralisation for DIN and PO_4^{3-}. To investigate this, one can estimate the ratio of NO_3^- and PO_4^{3-} remineralisation rates from linear regression of the residuals of the correlations between NO_3^- and temperature (ΔNO_3^-) and between PO_4^{3-} and temperature (ΔPO_4^{3-}). Since temperature and nutrients are negatively correlated in upwelling regions, any departures from linearity can be attributed to biogeochemical processes such as nutrient recycling, therefore the correlation between ΔNO_3^- and ΔPO_4^{3-} should reveal whether the scatter around the regression line is due to a biogeochemical process that alters nutrient concentrations stoichiometrically, or if it is due to random distribution. ΔNO_3^- and ΔPO_4^{3-} were significantly correlated in all years (n = 84, 115 and 110 in 2006, 2007 and 2008, respectively, $p < 0.01$), with regression coefficients between 8.3 and 8.8 (i.e. lower than Redfield), indicating that PO_4^{3-} was remineralised preferentially to NO_3^-. Similarly, ΔSi and ΔNO_3^- were significantly correlated, with regression coefficients between 0.31 and 0.33, indicating that NO_3^- was remineralised more rapidly than Si.

3.3.3. Nitrogen uptake

Nitrogen uptake rates fluctuated widely during the upwelling/relaxation cycles, with the largest variations observed in $\rho(NO_3^-)$ (1-2 orders of magnitude). The relative contributions of new and regenerated nitrogen sources also varied, with f-ratios ranging from 0.04 to 0.89. Such variations in $\rho(NO_3^-)$ and the f-ratio have been previously reported in the Benguela from a number of studies, where $\rho(NO_3^-)$ ranged from ~0.01 to ~0.55 and f-ratios from ~0.02 to 0.87 (Probyn, 1992). The data compiled by Probyn (1992) was fitted to the model of Dugdale et al. (1990) used to describe the relationship between $\rho(NO_3^-)$ and $\nu(NO_3^-)$ in the California, Peru and Canary currents. The model is based on observations from drifter studies that followed a recently upwelled parcel of water (MacIsaac et al., 1985). According to this model, $\nu(NO_3^-)$ and $\rho(NO_3^-)$ are low immediately following upwelling due to the small population size and low initial $\nu(NO_3)$. As the population drifts away from the upwelling centre, a "shift-up" (or acceleration) in $\nu(NO_3^-)$ is observed once the phytoplankton community has acclimated to the increased irradiance, and the acceleration term depends on the initial NO_3^- concentration. If biomass accumulates, then $\rho(NO_3^-)$ increases exponentially with increasing $\nu(NO_3^-)$, otherwise a linear relationship is observed. The increased uptake rates eventually result in nutrient depletion, which occurs after ~72 h regardless of the initial NO_3^- concentration. This leads to a "shift-down" response in $\nu(NO_3^-)$ and phytoplankton sink out of the euphotic zone. This model has been used to calculate maximum potential new production in the California, Peru and Canary currents (Dugdale et al., 1990) and in the Benguela (Probyn, 1992). Maximum observed new production was close to the maximum potential in all systems except the California current. Maximum observed $\rho(NO_3^-)$ was 0.55 μmol N l^{-1} h^{-1} in the Benguela, while theoretical maxima ranged from 0.56 to 1.11 μmol N l^{-1} h^{-1} depending on the acceleration term (Probyn, 1992). In the present study, maximum surface $\rho(NO_3^-)$ was 0.40, 56 and 0.18 μmol N l^{-1} h^{-1} in 2006, 2007 and 2008, respectively. The "shift-up" model was originally applied to diatom populations that are typically favoured by upwelling. In 2006, the population was dominated by *Pseudo-nitzschia*, therefore the comparison is valid, however the maximum $\rho(NO_3^-)$ in 2007 was during an *Alexandrium catenella* bloom. The occurrence of high biomass dinoflagellate blooms in the Benguela is thought to be at least partly a result of physical accumulation (e.g. at the upwelling

front) (Pitcher et al., 1998), therefore the high $\rho(NO_3^-)$ could be a result of increased biomass through physical processes rather than cellular growth.

When NO_3^- depletion occurred, phytoplankton turned to regenerated nitrogen to support their nitrogen demands, with $\rho(NH_4^+)$ up to 11-fold higher than $\rho(NO_3^-)$ and reaching a maximum of 0.25 μmol N l^{-1} h^{-1}. This high $\rho(NH_4^+)$ was supported by high regeneration rates, whereby $r(NH_4^+)$ exceeded $\rho(NH_4^+)$ on average by a factor of 2. The resulting excess NH_4^+ may have accumulated in the surface layer and this would explain the very high NH_4 concentrations measured on some occasions (up to 5 μmol N l^{-1}). Accumulation of NH_4^+ during the decline of the diatom spring bloom were reported in the North Atlantic (Johnson et al., 2007). These authors demonstrated that at high temperatures and increased pH, this can lead to the emission of NH_3 to the atmosphere.

The implications of this NH_4^+ accumulation would be potential inhibition of $\rho(NO_3^-)$ by NH_4^+. Indeed, evidence for inhibition of $\rho(NO_3^-)$ by NH_4^+ was provided by extremely low $\rho(NO_3^-)$ at NH_4^+ concentrations >2 μmol N l^{-1} (Figure 3.25b). Further evidence was illustrated by the ammonium inhibition experiment conducted in 2008 that revealed an I_{max} of 0.68 and a K_i of 4.21 μmol N l^{-1}. Although I_{max} was relatively high (on a scale of 0 to 1), K_i was also high, indicating that inhibition was not very severe for that assemblage. For comparison, K_i values reported for the North-East Atlantic were between 0.04 and 0.23 μmol N l^{-1} (L' Helguen et al., 2008), while K_i measured in cultures of *Emiliania huxleyi* was reported to be 0.24 μmol N l^{-1} (Varela & Harrison, 1999). In the associated nitrogen uptake kinetics experiment, however, the ratio $\nu_{max}(NH_4^+)$: $\nu_{max}(NO_3^-)$ was 4.2, indicating that the phytoplankton community displayed a strong preference for NH_4^+ over NO_3^-, therefore preference rather than inhibition may have determined the relative rates of $\rho(NO_3^-)$ and $\rho(NH_4^+)$.

Interestingly, $\rho(NH_4^+)$ displayed a significant negative linear correlation with NO_3^- in all 3 years combined ($p < 0.01$, Figure 3.25), indicating possible competitive inhibition of $\rho(NH_4^+)$ by NO_3^-. Although inhibition of $\rho(NO_3^-)$ by NH_4^+ is more commonly reported, competitive inhibition between various nitrogen sources has been observed in cultures (Collos, 1989). This effect could be responsible for the decoupling between $\rho(NH_4^+)$ and $r(NH_4^+)$, as highest $r(NH_4^+)$: $\rho(NH_4^+)$ ratios were generally associated with NO_3^- concentrations >25 μmol N l^{-1}.

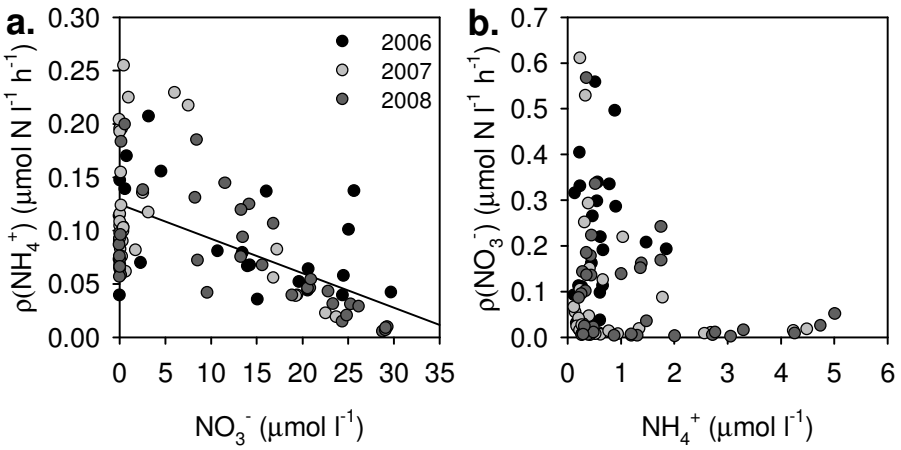

Figure 3.25. Relationships between (a) $\rho(NH_4^+)$ and NO_3^- concentration and (b) $\rho(NO_3^-)$ and NH_4^+ concentrations in all years. The equation of the regression line for all years combined in (a) is: $y = -3.23 x + 0.12$ ($r^2 = 0.32$, $n = 96$, $p < 0.01$).

The significant linear correlation between F_v/F_m and the *f*-ratio indicated that during periods of high $\rho(NO_3^-)$, i.e. during periods of upwelling, photochemical efficiency of photosystem II was enhanced. Although NH_4^+ is often preferred over NO_3^-, highest photochemical efficiency in this study was linked with a dependence on NO_3^- uptake. This is consistent with the finding that phytoplankton may express a preference for uptake of NH_4^+ but not for growth on NH_4^+ (Dortch, 1990). Furthermore, the linear correlations between wind direction, the *f*-ratio and F_v/F_m could be exploited to estimate new production on larger spatial and temporal scales.

3.3.4. HAB assemblages

Previous studied have shown that the occurrence of HABs along the west coast of South Africa is clearly linked to wind forcing and water column stability (Pitcher et al., 1998; Probyn et al., 2000; Pitcher & Nelson, 2006; Fawcett et al., 2007) and this is confirmed by the present study. In contrast, little is known about the nitrogen nutrition of HAB species during the upwelling/quiescence cycles.

The different assemblages identified by cluster analysis could be linked to a certain extent with nutrient regime. Clusters I (*Dinophysis acuminata*/ *Gymnodinium* spp.) and V (*Coscinodiscus* spp./ *Gyrodinium zeta*) were associated with warm, nutrient depleted waters, whereas Clusters II (*A. catenella*/ *Skeletonema costatum*), III (*Scrippsiella trochoidea*/ *Pseudo-nitzschia* spp.) and IV (*Minidiscus trioculatus*) were associated with recently upwelled water, i.e. lower temperatures and higher NO_3^- concentrations and DIN:P ratios. Clusters VI (*S. costatum*/ *Chaetoceros* spp.) and VII (*Pseudo-nitzschia* spp./ *Chaetoceros* spp.) were observed under a wide range of temperature and nutrient conditions, indicating that they were able to adapt to fluctuating conditions, in particular by utilising recycled nitrogen when NO_3^- became limiting.

Potentially harmful species were present in all of the clusters, with *Dinophysis acuminata* in Cluster I, *Alexandrium catenella* in Cluster II and *Pseudo-nitzschia* spp. in Clusters III to VII, representing 9 to 48 % total similarity. However, since *Pseudo-nitzschia* spp. are very small cells, their contribution in terms of biomass was probably insignificant in Clusters IV and V (9 to 11 %). These clusters were mixed assemblages, with low contributions from HAB species. They were present under very different conditions from one another and did not present radically different ecophysiological characteristics (such as nutrient uptake rates) to the clusters that were characterised by HAB species. This suggests that there was no clear distinction between environmental conditions that favoured HAB relative to "non-HAB" assemblages. A closer investigation of the HAB clusters, the prevailing environmental conditions under which they occurred and the nutrient acquisition strategies that allowed them to succeed under such conditions is therefore warranted to determine whether the occurrence of HABs is stochastic (i.e. a result of their being "in the right place at the right time") or if it is dictated by specific environmental conditions and therefore to a certain extent predictable.

3.3.4.1. *Alexandrium catenella*

The *A. catenella* bloom that peaked on 21 March 2007, was present before the start of our survey, therefore we do not know under which conditions it was initiated. However, it displayed a very high $\rho(NO_3^-)$ (0.61 µmol N l^{-1} h^{-1}) and *f*-ratio (0.87) and the concentration of *A. catenella* cells dropped rapidly when NO_3^- became depleted, indicating a high requirement for NO_3^-. Nitrate uptake by the *A. catenella* bloom was the highest measured in all 3 years, higher than the maximum measured rate in the Benguela for the period 1983-1991 (Probyn, 1992), and the maximum values measured in the Californian, Peruvian and North-West African upwelling systems (Dugdale et al., 1990) and one order of magnitude higher than in the Iberian upwelling system (Bode et al., 2005). Also, the second pulse of upwelling (25-26 March) reintroduced *A. catenella* cells, confirming the link between upwelling/high nutrients and the presence of *A. catenella*, although cell numbers were 2 orders of magnitude lower and thus ρNO_3^- was much lower.

Although it became more abundant over the next 3 days, it then disappeared from the community, possibly because of competitive exclusion by diatoms, but most likely due to alongshore (and to a lesser extent onshore) advection. *A. catenella* is known to form cysts in the Lambert's Bay area (Joyce & Pitcher, 2004) and it has been suggested that encystment occurs in response to nutrient starvation (Anderson et al., 1984), therefore the disappearance of *A. catenella* could possibly be attributed to encystment and sinking in response to nutrient depletion. Similarly, the reintroduction of *A. catenella* cells during the second pulse of upwelling may have resulted from excystment and vertical transport of the cells.

Studies of *Alexandrium catenella* blooms and cultures have yielded contradictory results with respect to their nitrogen requirements. For example, the optimal range of concentrations for *A. catenella* growth in culture was higher for NO_3^- (221-8830 µmol l^{-1}) relative to NH_4^+ (25-200 µmol l^{-1}) in a study by Siu et al. (1997). Furthermore, Matsuda et al. (1999) reported a high $K_s(NO_3^-)$ for growth (3.3-7.7 µmol l^{-1}). In the Mediterranean, blooms were associated with high NO_3^- and NH_4^+ concentrations on the north-east Spanish coast (Bravo et al., 2008), whereas NH_4^+ and urea were the main nitrogen sources fuelling a bloom in the Thau Lagoon on the French coast (Collos et al., 2007). A similar dichotomy exists for other *Alexandrium* species. For example, an *A.*

minutum bloom in Cape Town Harbour displayed extremely high $\rho(NH_4^+)$ (up to 1.1 μmol N l^{-1} h^{-1}) but very low $\rho(NO_3^-)$ (<0.05 μmol N l^{-1} h^{-1}) (Pitcher et al., 2007). In contrast, $\rho(NO_3^-)$ represented 85-91 % of total ρ(N) during the peak of an *A. minutum* bloom in the Penzé Estuary (NW France), whereas $\rho(NH_4^+)$ dominated ρ(N) before and after the bloom (Maguer et al. 2004). The authors estimated the N requirements of the 21-day bloom at 184 μmol l^{-1} NO_3^- and 25 μmol l^{-1} NH_4^+, based on ^{15}N uptake rates, cell concentrations and doubling rates, (Maguer et al., 2004).

Measurements of ρ(N) in the field provide limited information on nutritional preference, since in upwelling systems $\rho(NO_3^-)$ increases as a "shift-up" response to increased NO_3^- concentrations supplied by upwelling (Dugdale et al., 1990; Dugdale et al., 2006). This is demonstrated in the present study by the significant correlation between f-ratios and wind direction, used as an indicator of upwelling, hence NO_3^- concentration (Figure 3.25). Furthermore, the Relative Preference Index or RPI (McCarthy et al., 1977) is also biased by ambient concentrations, particularly in upwelling systems where NO_3^- can be much more abundant than NH_4^+ (Stolte & Riegman, 1996). The uptake kinetics parameters, however, can provide valuable information on the nutritional preferences of a given species (Dugdale, 1967; Dortch, 1990) and the potential outcome of interspecific competition for nutrients (Eppley et al., 1969), although they too can vary in response to nitrogen starvation (MacIsaac & Dugdale, 1969; Collos, 1980) and to elevated ambient nitrogen concentrations (Caperon & Meyer, 1972; Collos et al., 2005).

In this study, v_{max} was at least 17 % higher for NO_3^- than for NH_4^+ and 5-fold higher than for urea, whereas α for NH_4^+ and urea were low, indicating that *Alexandrium catenella* was a poor competitor for recycled nitrogen at the low concentrations ($<K_s$) measured during the bloom. In the Thau Lagoon, *A. catenella* displayed a preference for NH_4^+, as shown by higher v_{max} and α for NH_4^+ relative to NO_3^- (Collos et al., 2004). *A. catenella* in the Thau Lagoon displayed the second highest v_{max} of all the dinoflagellate species in Table 3.7 for all 3 nutrients, indicating that it was a very good competitor for high nitrogen concentrations. It was, however, a relatively poor competitor for all nitrogen sources at limiting concentrations (particularly urea), as shown by low α values. The lower v_{max} and K_s values for NH_4^+ and urea in the Benguela could be a result of natural selection for low nutrient-adapted cell lines (Doyle, 1975) in an environment where NH_4^+ and urea concentrations are often <1 μmol N l^{-1}, whereas they can be as high as 8 and 4 μmol N l^{-1}, respectively, in the Thau Lagoon (Collos et al., 2007).

Out of the five studies carried out on HAB dinoflagellates in upwelling systems presented in Table 3.7, *A. catenella* in the Benguela was the only one that expressed a preference for NO_3^- over NH_4^+, and its $\nu_{max}(NO_3^-)$ was higher than those of the other species. However, its $\nu_{max}(NH_4^+)$ was similar to that of *Akashiwo sanguinea*, which was the highest out of the five studies, although its α for NH_4^+ was at the low end of the spectrum, indicating that it was a better competitor for NH_4^+ at high concentrations. On the other hand, it displayed both a low ν_{max} and α for urea, indicating that it was a poor competitor for urea at both high and low concentrations. Higher ν_{max} for NH_4^+ and similar (if not lower) ν_{max} for NO_3^- and urea were measured in cultures of the raphidophyte *Heterosigma akashiwo* isolated from the California upwelling system (Herndon & Cochlan, 2007) (Table 3.7). The higher α measured for *H. akashiwo* indicated that it was also a better competitor for NH_4^+ at limiting concentrations, which is consistent with the hypothesis that small flagellates express a preference for NH_4^+ (Glibert et al., 1982a; Probyn, 1985). Overall, *A. catenella* in this study displayed characteristics typically attributed to diatoms.

Nitrate concentrations in the other studies were low, therefore the higher ν_{max} for NO_3^- in the Benguela could be explained by acclimation to a higher ambient concentration, which is mediated by an increase in the number of uptake sites on the cell surface (Caperon & Meyer, 1972). Temperature can also influence variability in the uptake kinetics of NH_4^+ and NO_3^-, whereby ν_{max} and α for NH_4^+ are positively correlated with temperature and α for NO_3^- is negatively correlated with temperature (Lomas et al., 1996; Fan et al., 2003). The lower temperature in the Benguela relative to the other studies (Table 3.7) could contribute to lowering ν_{max} and α for NH_4^+, however the large differences in α for urea were due to other factors since urea uptake is thought to be temperature-independent (Fan et al., 2003). In the latter case, interspecific differences were probably the most significant.

3.3.4.2. *Pseudo-nitzschia spp.*

Pseudo-nitzschia was particularly abundant in Cluster VII, representing 48 % total similarity, although it was also present in Clusters III and VI (17-18 %) and to a lesser extent in Clusters IV and V (9-11 %). Cluster VII comprised all the 2006 stations, when *Pseudo-nitzschia* was present in very high concentrations (>10^6 cells l^{-1} except on the last 2 days), but also some stations in 2007 and 2008 when concentrations were

generally lower (0.2 x 10^5 to 3 x 10^5 cells l^{-1} in 2007 and 0.1 x 10^6 to 2.3 x 10^6 cells l^{-1} in 2008).

Cluster VII occurred under a wide range of nutrient concentrations (0.02 to 25.1 μmol l^{-1} NO_3^-, 0.2 to 2.9 μmol l^{-1} PO_4^{3-} and 0.04 to 49.0 μmol l^{-1} Si). In 2006, highest cell concentrations were reached during periods of wind relaxation or reversal, during which NO_3^- became depleted in the surface layer. During these periods, *Pseudo-nitzschia* was able to maintain its population size (4.5-8.6 x 10^6 cells l^{-1}) and remain dominant despite the depletion of NO_3^- and Si and increase in dinoflagellate abundance. Larger cells require a greater amount of intracellular N to survive, as shown by the positive correlation between minimum cell-specific nitrogen quota and cell volume (Aksnes & Egge, 1991; Litchman et al., 2007). Therefore, *Pseudo-nitzschia* would require less nitrogen per cell due to its smaller cell size relative to dinoflagellates. The success of *Pseudo-nitzschia* in stratified environments due to its small cell size and efficient nutrient uptake has also been reported for the California current (Cochlan et al., 2006; Trainer et al., 2007). In addition, *Pseudo-nitzschia* displayed high $\rho(NH_4^+)$ in all years (0.039 to 0.192 μmol N l^{-1} h^{-1}, mean 0.094 ± 0.008 μmol N l^{-1} h^{-1}) that exceeded $\rho(NO_3^-)$ during the NO_3^--depleted periods, showing that *Pseudo-nitzschia* was able to turn to NH_4^+ when NO_3^- became limiting.

Although $\rho(NO_3^-)$ was as low as 0.002 μmol N l^{-1} h^{-1} during the NO_3^--depleted periods, when NO_3^- concentrations were high (>10 μmol l^{-1}) following upwelling pulses in 2006, *Pseudo-nitzschia* displayed high uptake rates of up to 0.40 μmol N l^{-1} h^{-1} at the surface, with maximum uptake ~30% higher than that measured in *Pseudo-nitzschia* spp. populations in the Juan de Fuca eddy (Washington coast, USA) (Marchetti et al., 2004). This flexibility, which allows *Pseudo-nitzschia* to take advantage of both high and low NO_3^- concentrations, would increase its competitive advantage under fluctuating conditions. This would also explain why *Pseudo-nitzschia* was present in a wide range of clusters and under varying conditions. However, *Pseudo-nitzschia* is not always abundant in upwelling regions, suggesting that its success is determined by factors other than nutrients and/or may depend on the duration of the upwelling/downwelling cycles.

The nutrient uptake kinetics experiment revealed a higher PN-specific ν_{max} for NH_4^+ relative to both dinoflagellate populations and for NO_3^- relative to *Dinophysis acuminata*. However, on a per-cell basis, ν_{max} was low relative to the dinoflagellate species, due to its smaller cell size (Table 3.6), consistent with the V_{cell}-ν_{max} relationship derived by Litchman et al. (2007). This trend of lower cell-specific but higher biomass-

specific ν_{max} seems to hold true for diatoms as a whole relative to dinoflagellates (Litchman et al., 2007). Higher biomass-specific ν_{max} may be due to an increased number of smaller uptake sites per unit cell surface area (Aksnes & Egge, 1991). Thus, when cell size effects are eliminated, *Pseudo-nitzschia* appears to be a "velocity" strategist (Sommer, 1984), as is generally the case for small, r-selected diatoms (Litchman et al., 2007).

Pseudo-nitzschia displayed a high α for both NO_3^- and NH_4^+ relative to the dinoflagellate species in Table 3.7, indicating that it had a high affinity for NO_3^- and NH_4^+. Thus, the combination of high ν_{max} and high α indicates that *Pseudo-nitzschia* was adapted to both high and low nutrient concentrations, which was apparent in its success during both upwelling and relaxation cycles.

However, ν_{max} and α for NO_3^- were lower in this study than in *Pseudo-nitzschia australis* cultures isolated from the Californian upwelling system (Cochlan et al., 2008) (Table 3.7). This can be explained by the nutrient history of the cultures, which were grown on 70 μmol l^{-1} NO_3^- as the sole nitrogen source. Such pre-conditioning effects were also observed by Fan et al. (2003). Although the medium was NO_3^--depleted prior to starting the experiments, the cells were not nitrogen-starved, therefore regulation of ν_{max} and α in response to nitrogen depletion had most likely not yet taken place. The same order of preference, as shown by comparison of ν_{max} values ($NH_4^+ > NO_3^- >$ urea) was observed in the present study as in culture experiments using *P. multiseries* (Radan, 2008) and *P. cuspidata* (Auro, 2007), showing a general trend in preference for NH_4^+, as is often observed in phytoplankton due to the lower energetic cost of NH_4^+ assimilation relative to NO_3^- (Dortch, 1990).

The Californian *P. australis* also had a higher ν_{max} for NH_4^+ than in this study, even though it was not preconditioned with NH_4^+. If *Pseudo-nitzschia* in the California system responds as well to high NH_4^+ concentrations as it does in culture, this would support the hypothesis that high anthropogenic NH_4^+ concentrations (>12 μmol l^{-1}) are responsible for blooms of *P. pseudodelicatissima* on the Washington coast (Trainer et al., 2007). *P. australis* cultures had a similar α to that in this study, indicating that the Californian strain was more competitive at high NH_4^+ but not at limiting NH_4^+ concentrations.

3.3.4.3. *Dinophysis acuminata*

Although *Gymnodinium* spp. were responsible for 93 % similarity within Cluster I, *D. acuminata* co-occurred with *Gymnodinium* spp. at 3 of those 5 stations, hence *Gymnodinium* spp. and *Dinophysis* can be assumed to be adapted to similar environmental conditions. *D. acuminata* was also responsible for 9 % similarity within Cluster III, although the contribution of *D. acuminata* to total cell numbers was very low (1-5 %).

Cluster I occurred in 2007 under highly stratified, NO_3^--depleted (0.1-0.5 μmol l^{-1}) conditions and was dependent on recycled nitrogen, with *f*-ratios of ~0.1. This community therefore conformed with the traditional concept of dinoflagellates being adapted to low nutrients and low turbulence (Margalef, 1978). Studies carried out in the Galician Rías, within the Iberian upwelling system, have also demonstrated that during the downwelling season (late summer/ autumn) communities dominated by *Dinophysis acuta* and *Gymnodinium catenatum* rely on NH_4^+ (Rios et al., 1995).

In both nitrogen uptake kinetics experiments that were dominated by *Dinophysis acuminata*, ν_{max} and α were 4-fold higher for NH_4^+ than for NO_3^- and 30 to 80 % higher for urea than for NO_3^-, therefore *D. acuminata* expressed a preference for recycled over new nitrogen. Furthermore, the NH_4^+ inhibition kinetics experiment demonstrated that NH_4^+ inhibited $\rho(NO_3^-)$, although the high K_i value showed that inhibition occurred at relatively high concentrations. All dinoflagellate species in Table 3.7 except *Alexandrium catenella* (this study) and *Gymnodinium catenatum* cultures (Yamamoto et al., 2004) displayed similar trends, with $\nu_{max}(NH_4^+)$: $\nu_{max}(NO_3^-)$ ratios ranging from 2.1 to 16.2 and ν_{max}(urea): $\nu_{max}(NO_3^-)$ ranging from 1.3 to 9.2. *D. acuminata* also had a higher affinity for NH_4^+ and urea relative to NO_3^-, with 5- and 3-fold higher α for NH_4^+ and urea, respectively (Table 3.7). With a few exceptions (*G. catenatum*, *A. catenella* and *Cochlodinium* spp.), dinoflagellates generally displayed a higher affinity for recycled nitrogen relative to NO_3^-. Thus, dinoflagellates were generally better competitors for recycled nitrogen at both saturating and limiting concentrations.

In 2007, *D. acuminata* displayed a lower $\nu_{max}(NO_3^-)$ than all other species in Table 3.7 except *Cochlodinium* spp. (Kudela et al., 2008b) and a mixed assemblage in the Central North Pacific Gyre (Sahlsten, 1987), indicating that *D. acuminata* was not able to compete for high concentrations of NO_3^-, hence its appearance in the phytoplankton community after a long period of NO_3^- depletion. Maximum uptake of NH_4^+ and urea

was towards the middle of the range for dinoflagellates, whereas α was higher for NH_4^+ than in all other species including most diatoms. This suggests that *D. acuminata* is an "affinity strategist" (Sommer, 1984), well adapted to growing at very low NH_4^+ and urea concentrations, although it was less competitive at low NO_3^-. The difference in α for NH_4^+ is also consistent with the higher temperature observed during the *D. acuminata* bloom, which would favour a higher α (Fan et al., 2003), although it is difficult to disentangle temperature effects from species-specific differences.

The half-saturation constants for *D. acuminata* were among the lowest of the range of experiments in Table 3.7, and lower for all 3 nutrients than the value predicted by the K_s-V_{cell} relationship derived by Litchman et al. (2007) (Table 3.6). This suggests the existence of an ecological trait that may give this species an advantage under nutrient-depleted conditions, which could offset the disadvantage of low growth rates typical of K-selected species. This seems to be the case for other dinoflagellate species, since the K_s-V_{cell} relationship is not significant for dinoflagellates alone (Litchman et al., 2007).

These results show that *D. acuminata* has a high affinity for all 3 nitrogen sources and a preference for recycled forms over NO_3^- which give it a competitive advantage under nutrient depleted conditions, e.g. during wind relaxation in upwelling systems. Although this was confirmed by the mixed *D. acuminata/* other dinoflagellates assemblage in Experiment 5, the mixed assemblage comprising *D. acuminata* and diatoms (*Minidiscus trioculatus* 88 % total cell numbers) in Experiment 4 revealed a very high $\nu_{max}(NO_3^-)$. However, this may have been predominantly attributable to a high $\nu_{max}(NO_3^-)$ for the diatom populations. Nonetheless, *D. acuminata* was very abundant at 5 m in 2008 at ambient NO_3^- concentrations as high as 26 μmol l^{-1}, and often co-occurred with *Coscinodiscus* spp. This suggests that *D. acuminata* was perhaps also able to acclimate to high NO_3^- concentrations, or that a range of different genotypes were present with varying nitrogen nutrition characteristics. Such differences in nutrient utilisation have been shown in between strains of *Pseudo-nitzschia caliantha* and *P. fraudulenta* isolated from the same water sample (Thessen et al., 2009).

Finally, mixotrophic behaviour (Jacobson & Anderson, 1994) and okadaic acid production (Carlsson et al., 1995), both of which are characteristic of *Dinophysis* spp., have been suggested as competitive strategies contributing to dinoflagellate species' success under nutrient-depleted conditions (Eppley et al., 1969; Smayda, 1997), and may have contributed to the success of *D. acuminata* at certain times during this study.

Species	Cell size x 10^3 µm^3	Location	ν_{max} NO_3^-	ν_{max} NH_4^+	ν_{max} Urea	K_s NO_3^-	K_s NH_4^+	K_s Urea	α NO_3^-	α NH_4^+	α Urea	$\nu_{max}(NH_4^+)$ / $\nu_{max}(NO_3^-)$	$\alpha(NH_4^+)$ / $\alpha(NO_3^-)$	ν_{max}(urea) / $\nu_{max}(NO_3^-)$	α(urea) / $\alpha(NO_3^-)$	Temp °C	Reference
Cultures																	
Dinoflagellates																	
Alexandrium catenella	14	Thau Lagoon	3-47	26	25	0.6-28.1	2	28.4	nd	13	0.9	nd	nd	nd	nd	20	a
Gymnodinium catenatum			207.1	107.5	nd	7.59	33.6	nd	27.3	3.2	nd	0.5	0.1	nd	nd		b
Diatoms																	
P. australis	1.4-4.6	California	105.3	80.0	nd	2.82	5.37	nd	37.3	14.9	nd	0.8	0.4	nd	nd	15.0	c
Raphidophyte																	
Heterosigma akashiwo	0.3-0.9	California	18.0	28.0	2.9	1.47	1.44	0.42	12.2	19.4	6.9	1.6	1.6	0.1	0.6	20.0	d
Blooms																	
Dinoflagellates																	
Akashiwo sanguinea	20-100	California	5.2	15.1	7.2	1.00	2.37	0.43	5.2	6.4	16.7	2.9	1.2	1.4	3.2	15.1	e
Alexandrium catenella	**14**	**Benguela**	**>17.5**	**14.9**	**3.5**	**nd**	**2.52**	**0.65**	**nd**	**5.9**	**5.4**	**<0.9**	**nd**	**<0.2**	**nd**	**11.2**	**f**
A. catenella	14	Thau Lagoon (S. France)	24.0	64.0	61.0	4.60	8.40	43.90	5.2	7.6	1.4	2.7	1.5	2.5	0.3	20.0	a
Cochlodinium spp.	10-50	California	0.9	>4.0	2.1*	1.00	nd	4.06*	0.9	0.3	0.8*	4.4	nd	2.3	0.9	15.0	g
Dinophysis acuminata	**14**	**Benguela**	**3.5**	**13.9**	**6.2**	**0.79**	**0.67**	**0.53**	**4.4**	**20.7**	**11.7**	**4.0**	**4.7**	**1.8**	**2.6**	**15.8**	**f**
Lingulodinium polyedrum	16.8-63	California	3.9	8.1	10.6	0.47	0.59	0.99	8.2	13.7	10.7	2.1	1.7	2.8	1.3	15.0	h
Prorocentrum minimum		Choptank Estuary (Chesapeake Bay)	53.8	868.6	492.6	7.12	5.09	16.84	7.6	170.6	29.3	16.2	22.6	9.2	3.9	15.7-23.0	i
Diatoms																	
Pseudo-nitzschia	**0.45**	**Benguela**	**15.0**	**18.0**	**4.9**	**1.21**	**1.34**	**nd**	**12.4**	**13.4**	**nd**	**1.2**	**1.1**	**0.3**	**nd**	**12.6**	**f**
Mixed assemblages																	
		Central North Pacific gyre	3.0	16.0	16.0	0.03	0.03	0.02	100.0	533.3	800.0	5.3	5.3	5.3	8.0		j
		Washington coast upwelling	5.8	6.8	4.6	0.05	0.71	0.78	116.0	9.6	5.9	1.2	0.1	0.8	0.1		k
		Western New Zealand	13.8	20.7	12	1.1	0.5	0.5	12.5	41.4	24.0	1.5	3.3	0.9	1.9		l
Mixed dinoflagellates		Neuse Estuary (N. Carolina)	4.0	52.9	5.77	0.54	2.38	0.37	0.6	10.4	0.3	13.3	18.6	1.4	0.6	11.2-13.2	i
		Benguela (Expt 5)	**3.5**	**14.6**	**4.4**	**0.82**	**0.62**	**nd**	**4.3**	**23.5**	**nd**	**4.2**	**5.5**	**1.3**	**nd**	**14.2**	**f**
Diatoms + dinoflagellates		**Benguela (Expt 4)**	**24.0**	**6.2**	**3.2**	**8.24**	**0.53**	**0.21**	**2.9**	**11.7**	**15.2**	**0.3**	**4.0**	**0.1**	**5.2**	**11.9**	**f**

Table 3.7. Summary of nitrogen uptake kinetics experiments performed on cultures, monospecific blooms, and mixed assemblages, adapted from Kudela et al. (2008b). a: Collos et al. (2004); b: Yamamoto et al. (2004); c: Cochlan et al. (2008); d: Herndon & Cochlan (2007); e: Kudela et al. (2008a); f: this thesis; g: Kudela et al. (2008b); h: Kudela & Cochlan (2000); i: Fan et al. (2003); j: Sahlsten (1987); k: Dortch & Postel (1989); l: Chang et al. (1995a). Data from this study are shaded in grey.

3.4. Conclusion

The results of this study revealed extremely high variability in hydrographic conditions, phytoplankton community structure and nitrogen uptake off Lambert's Bay, on the west coast of South Africa. This highly dynamic region is influenced by local wind patterns which drive upwelling/relaxation cycles on timescales of days. During active upwelling, deep water characterised by low temperatures and low DO concentrations and high nutrient concentrations is brought to the surface. During subsequent relaxation periods, this water warms and stratification promotes phytoplankton growth, which in turn depletes nutrients, reduces DIN:P and DIN:Si ratios and increases DO concentrations. Whereas some assemblages are favoured by active upwelling [e.g. Clusters II (*A. catenella*/ *Skeletonema costatum*), III (*Scrippsiella trochoidea*/ *Pseudo-nitzschia* spp.) and IV (*Minidiscus trioculatus*)], others [e.g. Clusters I (*Dinophysis acuminata*/ *Gymnodinium* spp.) and V (*Coscinodiscus* spp./ *Gyrodinium zeta*)] were associated with warm, nutrient depleted waters. Some diatom assemblages [Clusters VI (*S. costatum*/ *Chaetoceros* spp.) and VII (*Pseudo-nitzschia* spp./ *Chaetoceros* spp.)] were observed under a wide range of temperature and nutrient conditions, indicating that they were able to adapt to fluctuating conditions, in particular by utilising recycled nitrogen when NO_3^- became limiting.

Furthermore, specific nutritional characteristics were attributed to different HAB species that occurred during the 3 surveys. *Alexandrium catenella* bloomed at high NO_3^- concentrations and appeared to have a high requirement for NO_3^- since it disappeared when NO_3^- became depleted. It also displayed the highest surface $\rho(NO_3^-)$ and f-ratio measured in all 3 surveys. The higher v_{max} for NO_3^- relative to NH_4^+ and urea indicated a preference for NO_3^- over recycled nitrogen.

The toxic diatom *Pseudo-nitzschia* spp. was favoured by upwelling and was able to rapidly utilise the high nutrient concentrations supplied by upwelling. Biomass accumulation occurred during wind relaxation and *Pseudo-nitzschia* then switched to NH_4^+ as its main source of nitrogen as NO_3^- became depleted. The high v_{max} and α for both NO_3^- and NH_4^+ confirmed that *Pseudo-nitzschia* is poised to utilise either source of nitrogen at both saturating and limiting concentrations. Cellular v_{max}, however, was 2 orders of magnitude lower than for the dinoflagellate species, consistent with its smaller cell size.

Dinophysis acuminata bloomed during stratified periods, when NO_3^- concentrations were low, and displayed low *f*-ratios indicative of its reliance on recycled nitrogen. Its success under such conditions is attributable to a very high affinity for NH_4^+, as shown by its high α, which gave it a competitive advantage even though it did not display a high affinity for NO_3^-. Its low ν_{max} for NO_3^-, however, would explain why it was outcompeted by other species during periods of upwelling. But as it displayed a high ν_{max} for NH_4^+, it would also be favoured by high NH_4^+ concentrations. Although high NH_4^+ concentrations are not generally measured in this region, this finding could be used to model potential increases in DSP outbreaks in the context of increasing NH_4^+ loading in coastal waters.

4 Comparison of community structure and nitrogen uptake during the upwelling and downwelling seasons in the Iberian upwelling system

4.1. Introduction

4.1.1. The Iberian upwelling system

The eastern boundary of the North Atlantic subtropical gyre, comprising the Canary and Portugal currents, is another of the world's four major eastern boundary currents. It extends from 44 to 10 °N, from the north-west coast of Spain to the north-west coast of Africa. As in the Benguela, upwelling is driven by Trade Winds and offshore Ekman transport of the coastal equatorward surface current. The upwelling system is divided into two regions, the Iberian coast and the north-west African coast, with little continuity between them due to the influence of the Mediterranean outflow. This chapter will focus on the former, which will herein be referred to as the Iberian upwelling system.

Upwelling here is seasonal, occurring from approximately March to September when northerly winds prevail, whereas the rest of the year is characterised by southerly winds and downwelling (Fraga, 1981). The duration of the upwelling season and the intensity of upwelling show a pronounced decadal variability, which may be linked with variations in the North Atlantic Oscillation (NAO) (Guisande et al., 2004). The upwelling season is characterised by upwelling/relaxation cycles of 1-2 weeks (Blanton et al., 1987).

During upwelling, northerly winds prevail and circulation patterns comprise an equatorward coastal current, an equatorward jet over the continental slope and a poleward offshore counter-current as well as a poleward undercurrent (Estrada, 1995). Upwelled water extends offshore as filaments, particularly where the coastline is marked by capes and promontories. These filaments transport organic matter to the oligotrophic waters of the subtropical gyre and this export represents a significant fraction of new production during the upwelling season (Arístegui et al., 2004). Upwelled water originates from either subpolar (<12.2 °C, <35.66) or subtropical (>12.2 °C, >35.66) branches of Eastern North Atlantic Central Water (ENACW) (Ríos et al., 1992). The

less nutrient-rich water (0-6 µmol l^{-1} NO_3^-) of subtropical origin lies above the more nutrient-rich water (6-10 µmol l^{-1} NO_3^-) of subpolar origin, therefore the latter only enters the shelf during strong upwelling events.

During downwelling, southerly winds prevail and the whole water column is characterised by poleward flow. Poleward slope currents generate a downwelling front between oceanic and shelf waters, the position of which is determined by runoff and wind stress (Haynes & Barton, 1990).

4.1.2. The Rías Baixas

The Rías Baixas of Galicia are four large coastal indentations of more than 2.5 km^3, situated between 42 and 43 °N and comprising, from north to south, Rías de Muros, Arousa, Pontevedra and Vigo (Figure 4.1). Circulation in these rías is influenced by upwelling/relaxation cycles on the shelf. During upwelling the rías behave as an extension of the shelf, whereby positive circulation forces upwelled ENACW from the shelf into the rías along the bottom while surface water flows out of the rías (Figure 4.2). During downwelling, surface water flowing into the rías converges with water flowing out and forms a downwelling front, thus the outflow occurs at depth (Figueiras et al., 1994). Salinity in the rías ranges from 20.0 at the head to 35.7 at the mouth during coastal upwelling (Figueiras & Rios, 1993). During upwelling, the injection of nutrients into the rías stimulates phytoplankton growth and the resulting biomass is then exported out of the ría, where it may sink and become remineralised (Figure 4.2). The recycled nutrients may then be re-injected into the rías along with the upwelled nutrients (Álvarez-Salgado et al., 1993). This "secondary remineralisation" allows the rías to support very high rates of primary production, particularly towards the end of the upwelling season when remineralised nutrient concentrations are at a maximum (Álvarez-Salgado et al., 1997).

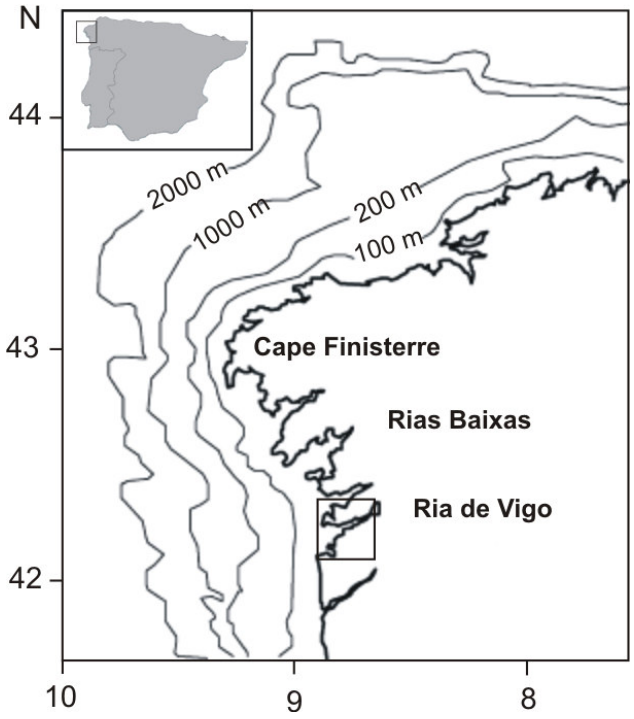

Figure 4.1. Map of the north-west Iberian Peninsula, showing the four Galician Rías Baixas. The Ría de Vigo is enlarged in Fig. 2.3 (Chapter 2).

The Ría de Vigo has a surface area of 176 km^2, a length of 32 km, a width of 1-10 km and a maximum depth of 40 m in the central channel. It is partially mixed, with a tidal velocity range of 10-30 cm s^{-1} and a mesotidal range of 2-4 m. The mouth of the ría is divided into two main channels by the Ciès Islands, a narrow northern channel of sill depth 25 m and a wider and deeper southern channel (45 m depth). It has a relatively small catchment area (~589 km^2) and runoff is generally low, with minimum rates in summer (5-10 m^3 s^{-1}) and maximum rates in winter (30-35 m^3 s^{-1}) (Nogueira et al., 1997). Sewage flux from Vigo is ~0.5 m^3 s^{-1} (Ríos, 1992), which represents an average PO_4^{3-} input of 130 µmol l^{-1} (Pérez et al., 1986).

Nitrate and NO_2^- concentrations in the bottom waters of the ría tend to peak in July-August at ~8 and 0.75 µmol l^{-1}, respectively, whereas corresponding surface concentrations tend to be depleted during this period. Deep NH_4^+ concentrations increase throughout summer, reaching a maximum in September-October (~4 µmol l^{-1}), whereas surface concentrations tend to remain low throughout the summer, peaking in October-November. The contribution of NH_4^+ to total DIN increases from 25 to 65 % between January and August concurrent with a decrease in the proportion of NO_3^- from 70 to 20 %, due to the more rapid recycling of NH_4^+ (Nogueira et al., 1997). N:P ratios are 15-17 (close to Redfield) in the upwelled ENACW but decrease rapidly as the water

enters the ría, where it is influenced by very high PO_4^{3-} inputs. N:P ratios are lowest in spring (~8) and summer (~3) (Nogueira et al., 1997).

As in most temperate ecosystems, two seasonal phytoplankton blooms are observed, one in spring (May) and another in autumn (September), with surface chl-a concentrations generally >8 µg l^{-1} in both cases. However, chl-a concentrations remain relatively high throughout the summer, due to the input of nutrients from upwelling (Nogueira et al., 1997). Gross annual primary production is highest in spring and summer (1-8 g C m^{-2} d^{-1}) and lowest in winter (0.2 g C m^{-2} d^{-1}), although a high degree of variability occurs with the upwelling/relaxation cycles (Arístegui et al., 2004).

New production estimates for shelf waters between 42 and 44 °N during the upwelling season are relatively low compared to primary production, resulting in a seasonally-averaged f-ratio of 0.35 (Álvarez-Salgado et al., 2002). This value is similar to the average published for the Benguela (Probyn, 1992), but lower than expected for a major upwelling system and reported for the California current [0.4-0.8, Dugdale et al. (2006)]. This has been attributed to low continental inputs, low nutrient concentrations in ENACW and low average coastal winds. Furthermore, during the upwelling/ relaxation cycles, a switch from net autotrophy to net heterotrophy occurs, resulting in a low average f-ratio (Arístegui et al., 2004).

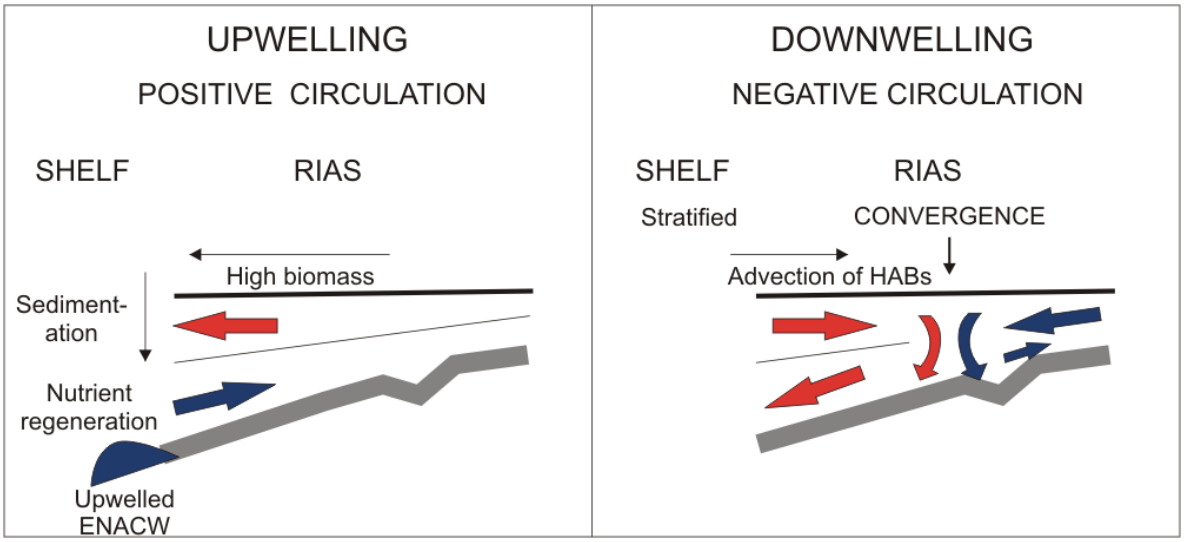

Figure 4.2. Schematic diagram of circulation in the Rías Baixas during upwelling and downwelling seasons. Modified from Crespo et al. (2006). Blue arrows represent cold water and red arrows represent warm water.

The Rías Baixas are used extensively for the cultivation of blue (or Mediterranean) mussels *Mytilus galloprovincialis*, which are grown on ropes suspended from mussel rafts (*bateas*). The rías are the largest producer of mussels worldwide, with a production

of 250,000 tonnes per year, representing 40 % of European production and 15 % of world production, with a first sale value of 80 million US dollars (Labarta et al., 2004). Although mussel cultivation is supported by high rates of primary production, it is also under threat by a number of toxic species that are known to bloom in the rías (Fraga, 1989). HABs have been monitored since 1976, initially by the Spanish Institute of Oceanography (IEO), then by the Marine Environment Quality Control Centre (CCCMMM) since 1992.

4.1.3. HABs in the Rías Baixas

Seasonal succession in phytoplankton assemblages involves a shift from small diatoms (*Skeletonema costatum* and *Thalassiosira pseudonana*), cryptophytes and other small flagellates in winter (when river runoff is high) to large centric diatoms in spring, pennate diatoms (e.g. *Nitzschia seriata*) and heterotrophic dinoflagellates during summer upwelling (e.g. *Protoperidinium* spp.) and autotrophic dinoflagellates during autumn downwelling. The abundance of diatoms is correlated to upwelling, particularly during the first half of the year, when heterotrophs are present in lower numbers (Figueiras & Rios, 1993). Similar successional patterns are observed on shorter time scales, during the upwelling/relaxation cycles that occur during summer, with a shift from diatoms to toxic dinoflagellates accompanying stabilisation of the water column following a strong upwelling event. The horizontal distribution of diatoms and dinoflagellates also reflects the intensity of upwelling or stratification along the rías, with diatoms dominating towards the interior, where upwelling is strongest, whereas dinoflagellates tend to occur in the outer, more stratified parts of the rías (Tilstone et al., 1994).

HABs are a regular occurrence in the Rías Baixas and along the Portuguese coast during the summer months (June to October) (Fraga, 1989; Jiménez et al., 1992; Moita, 1993; Figueiras et al., 1994) and have been reported since 1916 (Sobrino Buhigas, 1918). Shellfish poisoning outbreaks have been known to occur since 1976 (Estrada et al., 1984; Moita, 1993). These are caused by the DSP producers *Dinophysis acuminata* and *D. acuta* and the PSP producers *Gymnodinium catenatum* and *Alexandrium tamarense*. Total losses to the shellfish industry attributed to these toxic outbreaks have been estimated at 10-20 million euros per year on average between 1989 and 1998 (Scatasta et al., 2003).

While *D. acuminata* is generally present in low numbers throughout the upwelling season, *D. acuta* and *G. catenatum* tend to appear during downwelling events in late summer-early autumn (Fraga et al., 1988; Figueiras et al., 1994). *D. acuminata* and *D. acuta* also tend to be spatially segregated, with *D. acuminata* associated with lower salinity waters (Reguera et al., 1993b). Blooms of the yessotoxin producer *Lingulodinium polyedrum* and of the ichthyotoxic species *Heterosigma akashiwo* have also been reported (Sobrino Buhigas, 1918; Pazos et al., 1995a). *A. tamarense* and *G. catenatum* were not recorded in Galician waters prior to the 1970s and their apparent increase has been attributed to enhanced eutrophication of the rías as a result of increased sewage discharges, expansion of the mussel farms and increase in forest fires (Wyatt & Reguera, 1989). The duration of the upwelling season has also decreased by ~85 days over the last 40 years, causing an increase in the renewal time of the rías, from ~2.2 to ~5.1 s m^{-2} (Álvarez-Salgado et al., 2008). However, contradictory results were obtained in the same region using ship-based measurements (Guisande et al., 2004; McGregor et al., 2007) and in other upwelling systems including the Benguela (Gregg et al., 2005), consistent with the hypothesis that upwelling would intensify as a result of global climate change (Bakun, 1990). The prolonged renewal time is positively correlated with the number of days of mussel farm closures caused by toxic outbreaks. This is due to the success of HAB species such as *Dinophysis* spp. in low turbulence environments (Álvarez-Salgado et al., 2008).

Advection of established offshore populations has been suggested as the origin of HABs in the rías (Fraga et al., 1993; Pazos et al., 1995b; Sordo et al., 2000), although *in situ* development as a result of resuspension and germination of cysts within the rías has also been suggested (Fraga et al., 1990; Figueiras & Pazos, 1991a; Pazos et al., 1995b; Figueiras et al., 1998). HAB species such as *Gymnodinium catenatum* are found in the offshore upwelling assemblages, such as the Sines upwelling centre off the Portuguese coast (Estrada, 1995), which are then transported towards the Galician coast by surface poleward currents. These warm currents can be advected into the rías during upwelling relaxation (Fraga et al., 1993) and it has been suggested that HAB populations originating off the Portuguese coast may be advected into the Galician rías 450 km to the north (Estrada, 1995). A later study, however, failed to detect any *G. catenatum* cells in the poleward current waters and hypothesised that *G. catenatum* grew and accumulated at the downwelling front associated with the slope (Figueiras et al., 1998).

The reversal of circulation that leads to downwelling is thought to favour selection of motile species such as *G. catenatum*, which can maintain themselves in the surface layer (Fraga et al., 1988; Figueiras et al., 1994; Fermin et al., 1996). For example, *G. catenatum* cells are able to overcome downwelling velocities of 10 m day^{-1} (Figueiras et al., 1995). HABs can also develop during weak upwelling, when it is sufficient to raise the nutricline to ~10 m but not so intense that diatoms are favoured over HAB species (Figueiras & Rios, 1993). In this situation, dinoflagellates can undertake diel vertical migrations that allow them to exploit the high nutrient concentrations at the nutricline during the night and photosynthesise during the day in the surface layer. This involves synthesis of carbohydrates during the day, which can then supply the energy required for basal metabolism, migration, nutrient acquisition and synthesis of structural compounds, as shown by Figueiras & Fraga (1990).

During the upwelling season diatom growth is sustained by NO_3^-, as shown by the relationship between *f*-ratio and upwelling index (Rios et al., 1995). The concentration of regenerated NH_4^+ increases throughout the season, with autumn dinoflagellate populations relying on NH_4^+ as their main source of nitrogen.

4.1.4. Aims and objectives

The aim of this work was to determine how nitrogen nutrition of HABs during the downwelling season differs from that of diatom populations during the upwelling season and to identify particular nitrogen nutrition strategies in HAB species that may be specific (and common) to upwelling systems. Specific objectives were:

- to characterise the hydrographic and nutrient conditions during the downwelling (September 2006) and upwelling (June 2007) seasons,
- to compare phytoplankton community structure during both seasons and determine whether a HAB population was present during the downwelling season,
- to compare the uptake rates of NO_3^-, NH_4^+ and urea in both seasons and identify possible nitrogen nutrition strategies displayed by HABs, and to compare these with strategies identified in the Benguela.

4.2. Results

4.2.1. Meteorological conditions

4.2.1.1. Wind

In September 2006, winds were north-westerly for the first 10 days, alternating between north-westerly and south-westerly between 10 and 20 September, then south-westerly for the last 10 days. Westerly components were -1.4 to 4.5 m s^{-1} and southerly components were -3.8 to 11.0 m s^{-1} (Figure 4.3a, c).

Wind direction in June 2007 was more variable, spanning a wider range of westerly (-4.8 to 4.7 m s^{-1}) and southerly components (-10.5 to 11.4 m s^{-1}). Winds were north-easterly for the first week, then alternated between south-easterly and south-westerly for the following 2 weeks then were north-easterly again until the end of the month (Figure 4.3 b, d).

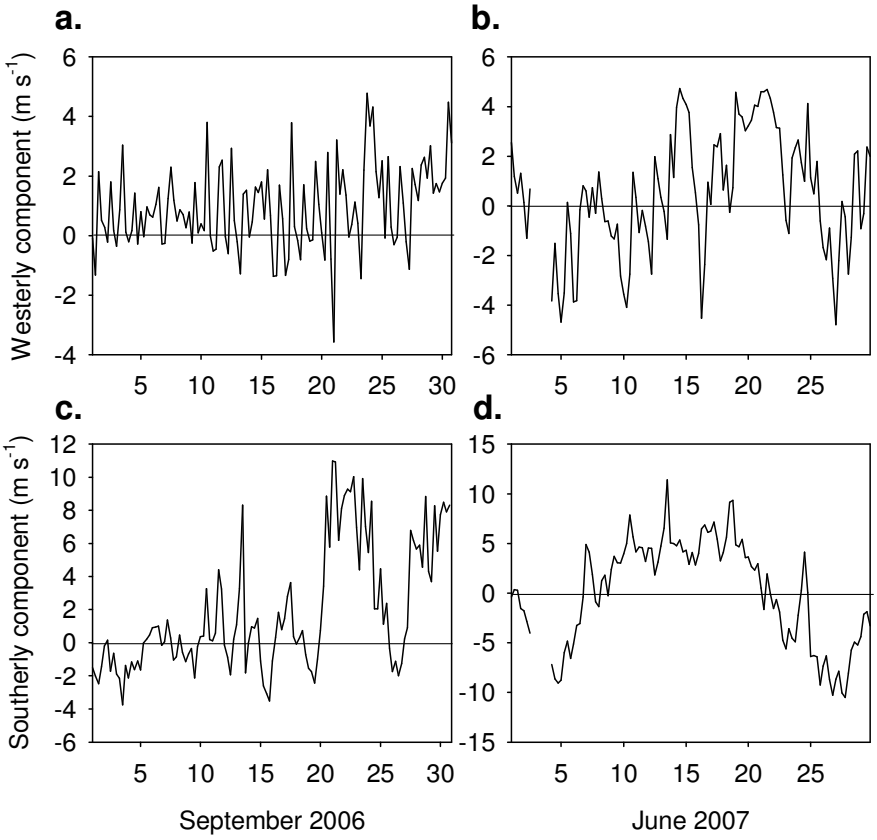

Figure 4.3. Westerly and southerly wind components in (a, c) September 2006 and (b, d) June 2007 measured at the meteorological station on Islas Ciès in September and by the meteorological buoy off Cape Silleiro in June.

4.2.1.2. Rainfall and solar radiation

Rainfall was generally low during the summer months (<35 mm), with the highest value occurring in August 2006 (Figure 4.4a). Highest rainfall was recorded in November 2006 (205 mm), followed by March 2006 (130 mm). Total rainfall between November and April was equivalent in both years (433 and 438 mm, respectively).

Incoming solar radiation was on average 48 % higher in June 2007 than in September 2006, with values ranging from 986 to 3183 x 10 kJ m^{-2} in June and from 618 to 2471 x 10 kJ m^{-2} in September (Figure 4.4b,c). Radiation was particularly high at the start of the September survey (1985 x 10 kJ m^{-2}), dropping to 875-1142 x 10 kJ m^{-2} for the rest of the survey. In June, radiation increased from the start (1918 x 10 kJ m^{-2}) to the end of the survey (3183 x 10 kJ m^{-2}).

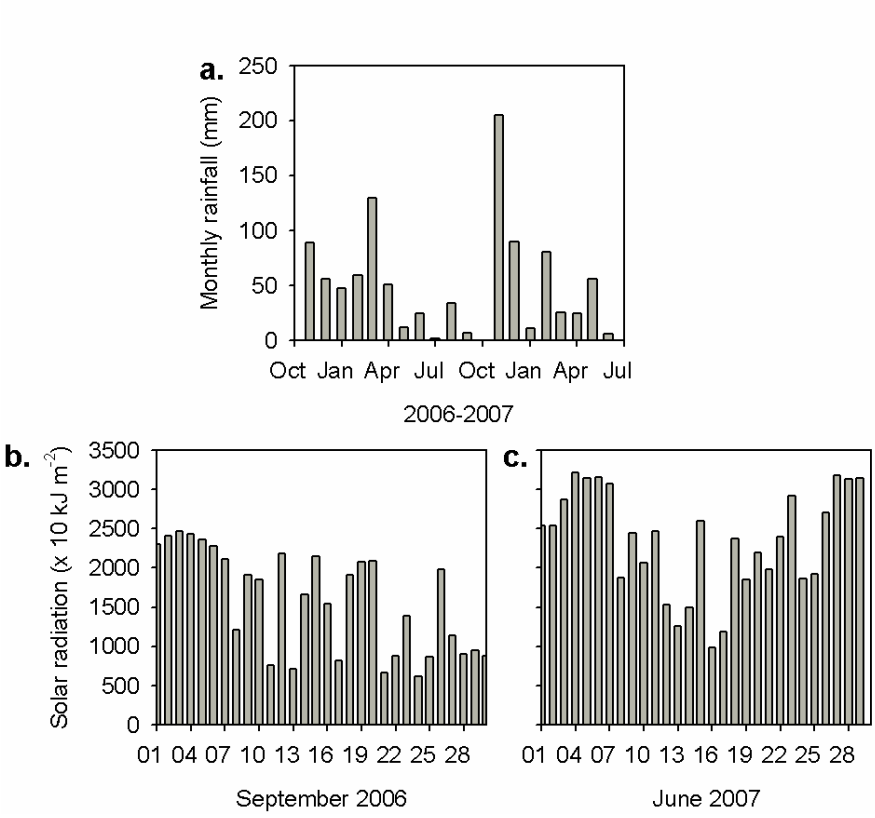

Figure 4.4. (a) Total monthly rainfall measured at the Islas Ciès meteorological station between November 2005 and June 2007 and daily solar radiation measured at Vigo campus meteorological station in (b) September 2006 and (c) June 2007.

4.2.2. Hydrography

4.2.2.1. Tides

At the start of the 2006 survey (26 September), the tidal state was close to spring, with a range of 2.8 m. By the end of the survey the tide was almost neap, the range having decreased to 1.1 m (Figure 4.5a, b). In June 2007, the tide was close to neap at the start of the survey, with a range of 1.3 m on 25 June, increasing to 2.0 m by 28 June (Figure 4.5c, d).

On 27, 28 and 29 September 2006 and 27 June 2007 repeat stations were carried out on different tidal states (high, low and intermediate). On 26 and 30 September 2006 and 25 and 28 June 2007, sampling was carried out at several stations along the estuary, with the ebbing tide on 30 Sept and 28 June, against the ebbing tide on 26 Sept and against the flooding tide on 25 June.

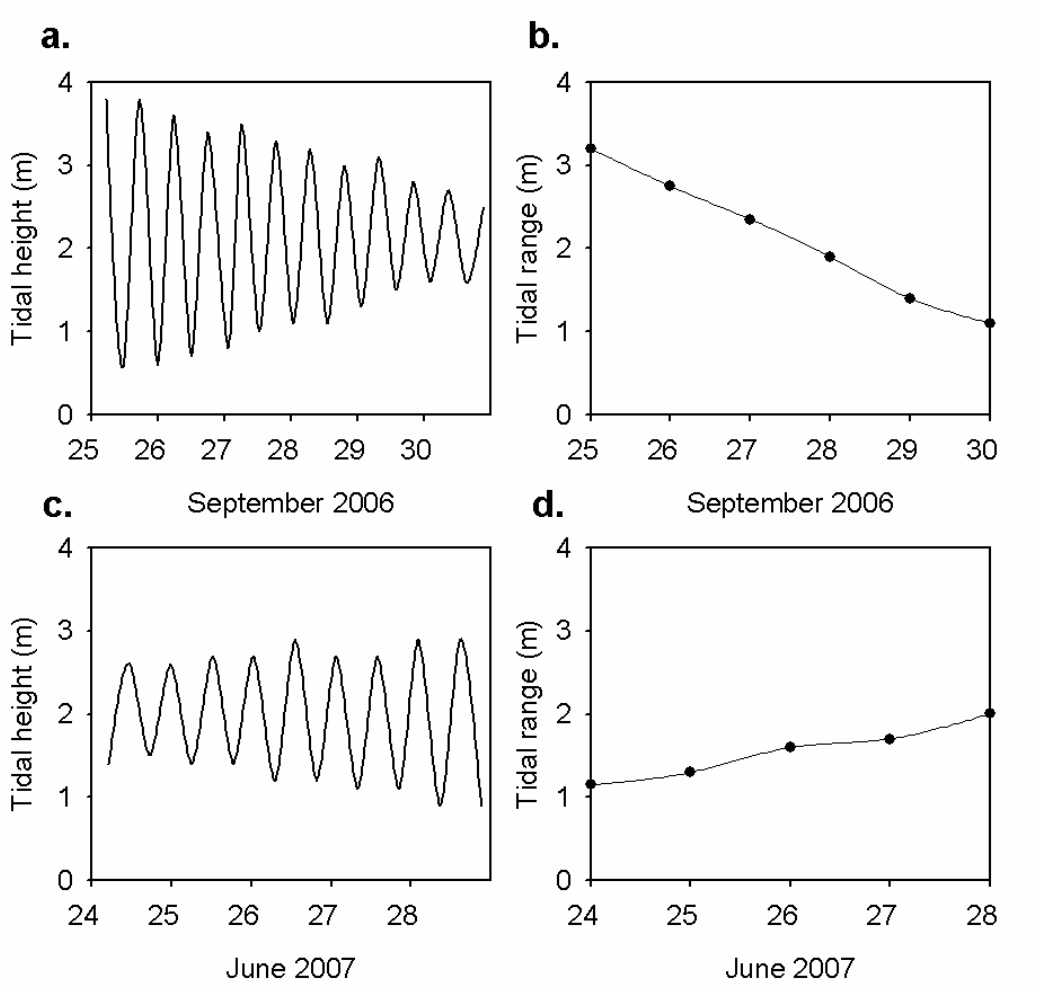

Figure 4.5. (a) Tidal heights and (b) tidal ranges between 25 and 30 September 2006; (c) tidal heights and (d) tidal ranges between 24 and 28 June 2007.

4.2.2.2. Temperature

At the start of the 2006 survey (26 Sept), the water column was stratified in the southern mouth of the ría, which was characterised by remnants of upwelled water below ~5 m (Figure 4.6). A downwelling front was apparent in the vicinity of station B2, where the 17.6 °C isotherm deepened from ~5 to ~15 m. By the end of the survey (30 Sept) the water column had warmed and was isothermal between B2 and B5, with temperatures of ~18 °C measured throughout the water column (Figure 4.6, Figure 4.8).

Surface temperature increased along the ría, from 17.3 °C at B5 and B2 to 18.2 °C at B2 (Figure 4.8). Surface temperature variations with tidal state were small, increasing by 0.36 °C at B3 and by 0.25 °C at B2, between high and low tide, although at B5 temperature was 0.16 °C lower at low tide than at high tide (Table 4.1).

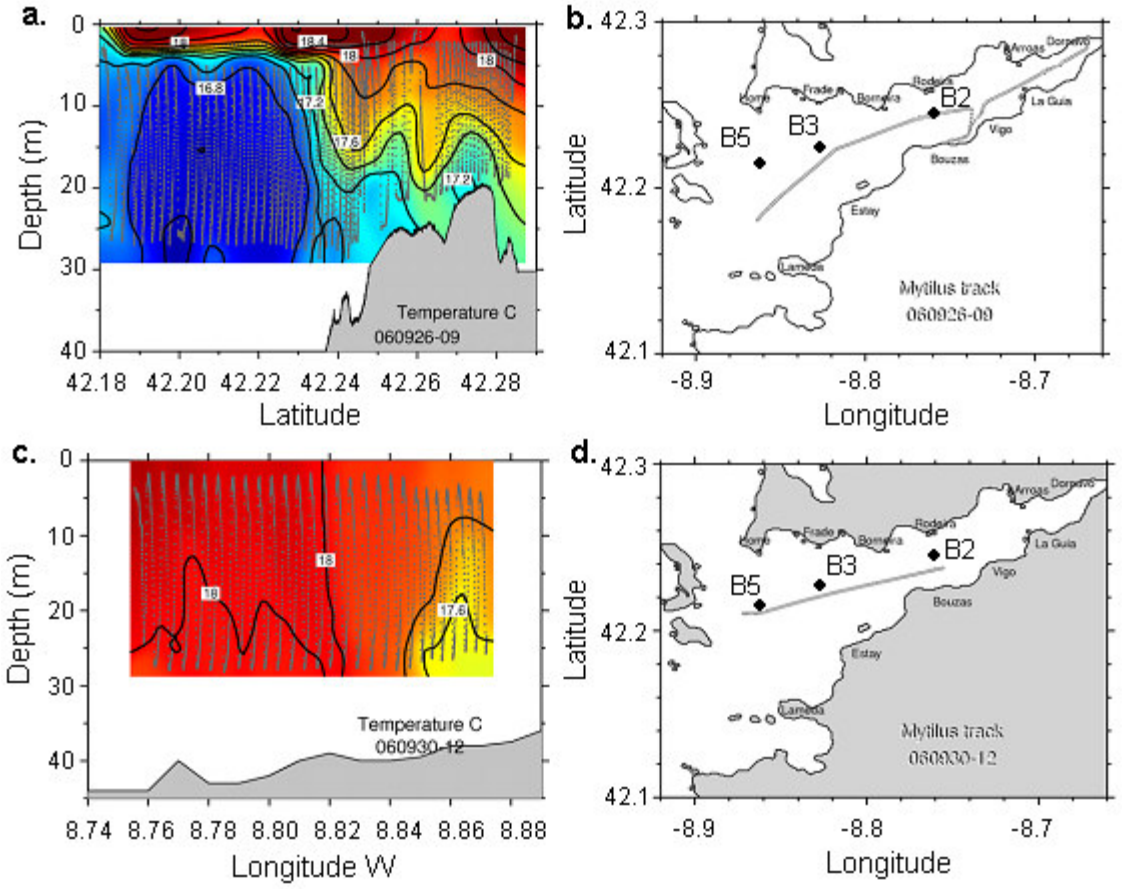

Figure 4.6. Temperature contour plots obtained from MiniBAT deployments along longitudinal transects of the ría on (a) 26 September and (c) 30 September 2006. The ship's tracks are shown in (b) for 26 September and (d) for 30 September. Courtesy E.D. Barton.

In 2007, the water column was stratified throughout the ría, displaying little horizontal variation in temperature. At the start of the survey (25 June), surface temperatures were ~19 °C, the thermocline was at 15-20 m depth and recently upwelled water (~13.5 °C) was present below 20 m. By 28 June the thermocline was uplifted to ~5-10 m and surface water had cooled to ~18 °C (Figure 4.7, Figure 4.8). Surface temperatures were significantly higher in 2007 than in 2006, whereas bottom temperatures were significantly lower (Mann-Whitney U-test, $p < 0.05$).

On 25 June, surface temperature increased from 18.9 at B5 to 19.6 °C at B3, but was slightly lower at B2 (19.3 °C). Higher temperatures were measured at the inner stations B0 and B1 (19.9-20.0 °C). On 28 June, surface temperature differences were small, varying from 17.5 to 18.0 °C between B0 and B5, with the lowest temperatures measured at B0. At B3, surface temperature dropped by 0.69 °C between high and low tide (Table 4.1).

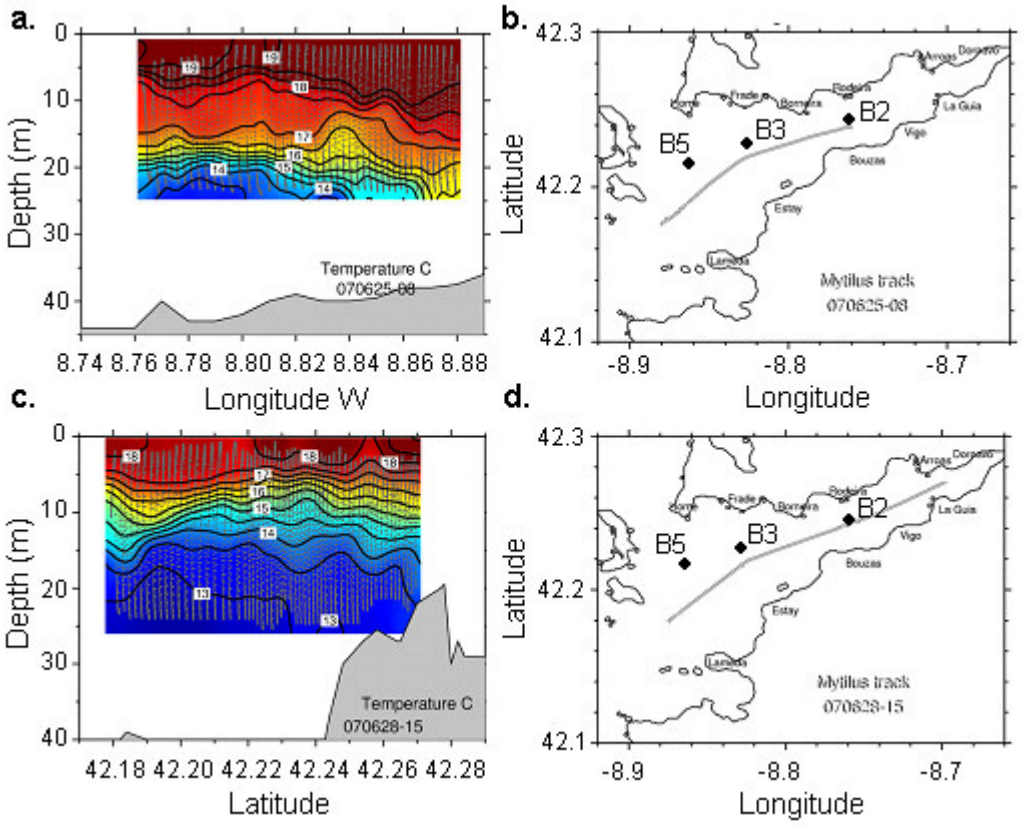

Figure 4.7. Temperature contour plots obtained from MiniBAT deployments along longitudinal transects of the ría on (a) 25 June and (c) 28 June 2007. The ship's tracks are shown in (b) for 25 June and (d) for 28 June. Courtesy E.D. Barton.

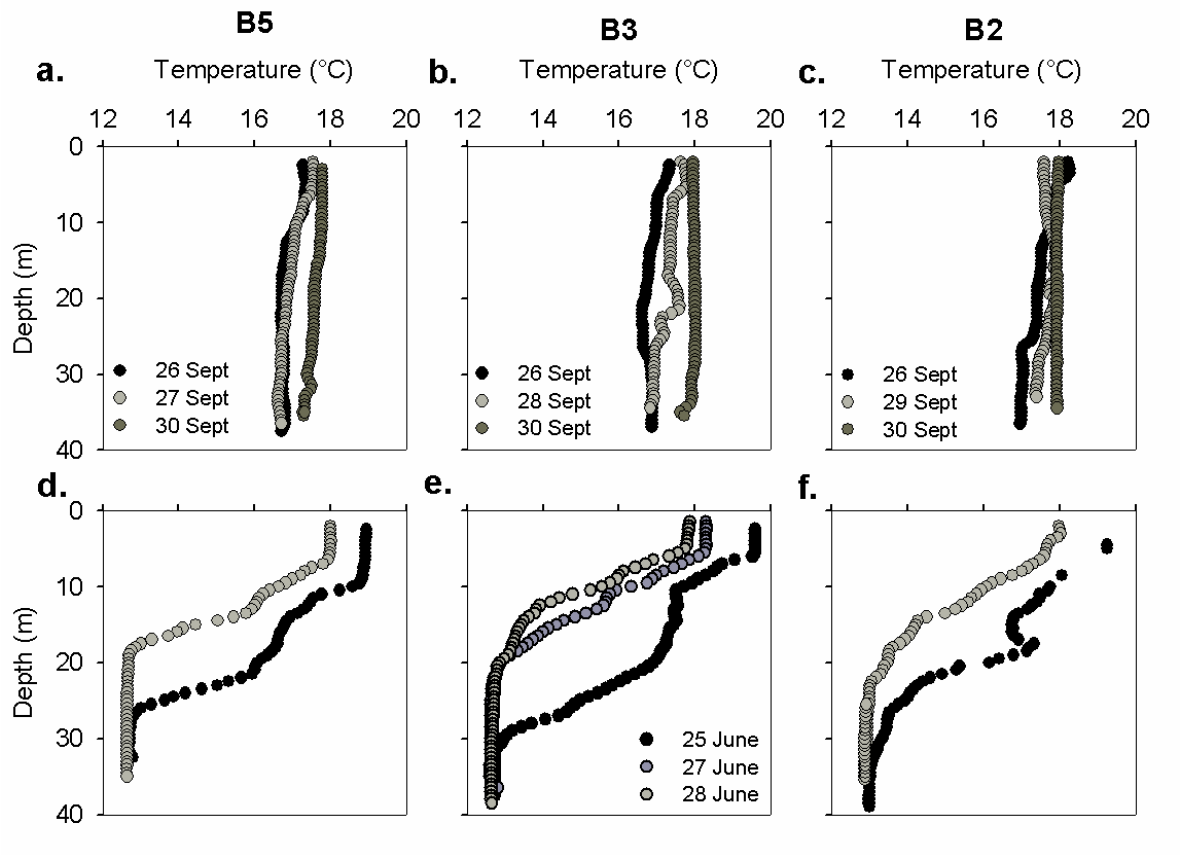

Figure 4.8. Temperature profiles obtained from CTD casts in (a, b, c) September 2006 and (d, e, f) June 2007 at stations (a, d) B5, (b, e) B3 and (c, f) B2. N.B: sampling dates were the same in (d,e,f).

Date	Station	Latitude	Longitude	Time	Hrs before/ after HT	Temp	Salinity	DO
27/09/2006	B5.1	42.206	-8.863	06:00	-0.2	17.66	35.28	113
	B5.2	42.209	-8.864	09:09	3.0	17.55	35.46	117
	B5.3	42.209	-8.864	12:00	5.8	17.50	35.43	118
28/09/2006	B3.1	42.224	-8.818	06:08	-0.7	17.36	35.28	115
	B3.2	42.225	-8.818	08:58	2.8	17.38	35.26	115
	B3.3	42.224	-8.817	12:16	5.5	17.72	35.18	115
29/09/2006	B2.1	42.243	-8.758	06:43	-0.8	17.59	35.15	111
	B2.2	42.241	-8.760	09:25	1.9	17.80	35.12	112
	B2.3	42.242	-8.759	12:11	4.6	17.84	35.15	114
27/06/2007	B3.1	42.226	-8.819	07:16	5.7	17.61	33.51	104
	B3.2	42.226	-8.818	09:41	-4.3	17.91	33.12	105
	B3.3	42.227	-8.818	12:44	-1.3	18.30	33.98	109

Table 4.1. Variations in surface temperature (°C), salinity and DO (% saturation) measured at fixed stations at different tidal states in September 2006 and June 2007.

4.2.2.3. Salinity

In September 2006, the water column was relatively homogeneous with respect to salinity. Salinity was high throughout the ría (>35) and decreased between 26 and 30 September. This was not a result of differences in tidal state, as sampling was generally closer to high tide on 30 September. At the downwelling front, salinity was vertically homogeneous, whereas throughout the rest of the ría salinity increased slightly with depth, particularly towards the head of the ría (Figure 4.9). At stations B5-B2 the salinity difference between surface and bottom was <0.3 on 26 Sept whereas on 30 Sept it was 0.3-0.6 (Figure 4.11). Surface salinity varied by <0.3 between B5 and B2 on both 26 and 30 September and variation with tidal state was low at all stations (0.03-0.15, Table 4.1).

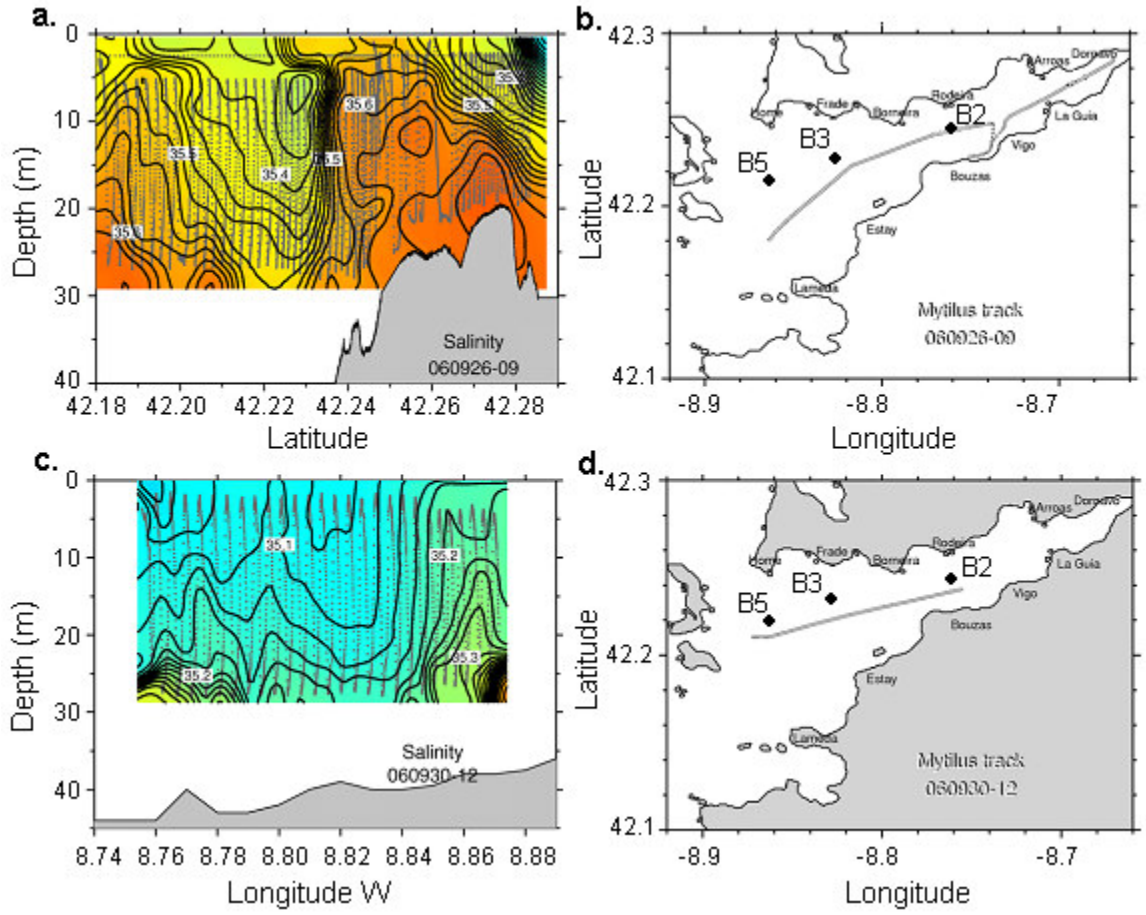

Figure 4.9. Salinity contour plots obtained from MiniBAT deployments along longitudinal transects of the ría on (a) 26 September and (c) 30 September 2006. The ship's tracks are shown in (b) for 26 Sept and (d) for 30 Sept. Courtesy E.D. Barton.

In June 2007, surface salinities were significantly lower than in September, whereas bottom salinities were significantly higher (Mann-Whitney U-test, $p < 0.05$). A halocline was clearly visible at 10-15 m, with salinities increasing by ~2 between surface and bottom (Figure 4.11). Salinities in the top 25 m increased by ~0.5 between 25 and 28 June, but did not vary below 25 m. Surface salinity showed greater horizontal variation than in September, decreasing by 0.7 between stations B5 and B2 and by a further 2.5 between B2 and B0 on 25 June. On 28 June the total variation between B5 and B0 was 1.5. Variation with tidal state was also more pronounced. At B3, surface salinity was 0.5 to 0.9 higher when sampled closest to high tide than at other sampling times (Table 4.1).

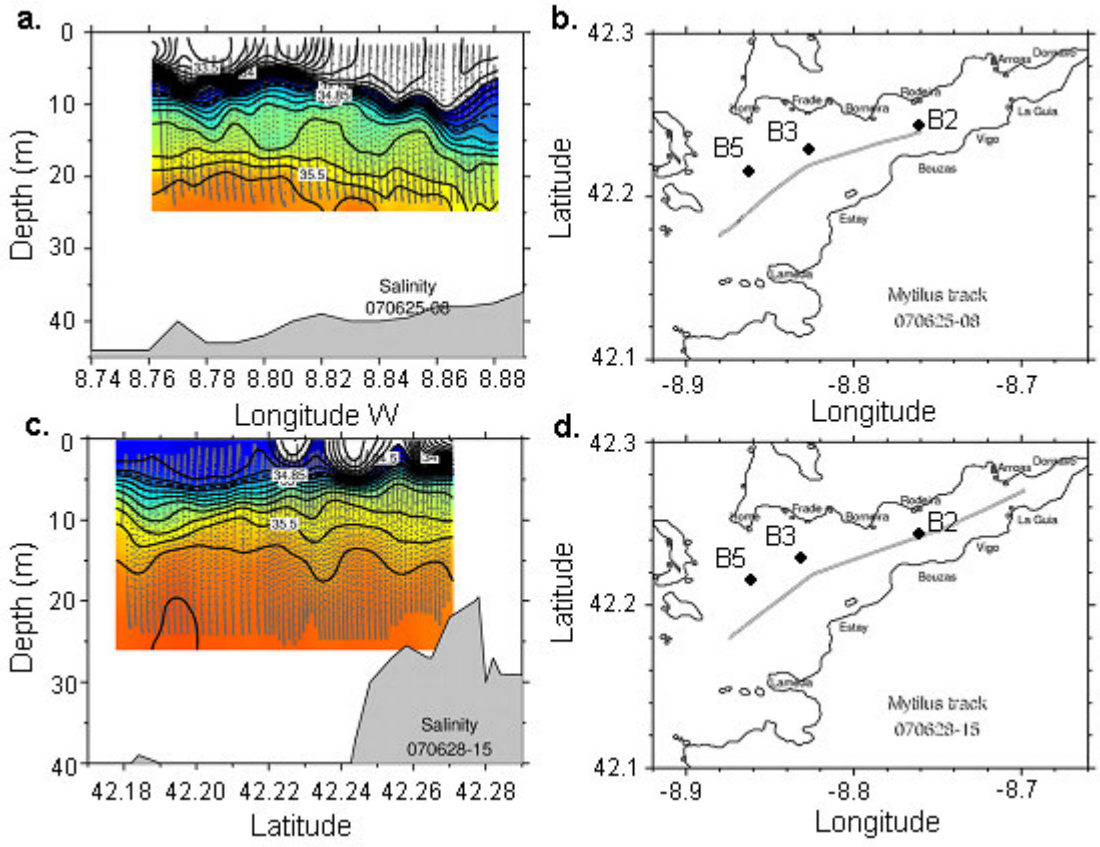

Figure 4.10. Salinity contour plots obtained from MiniBAT deployments along longitudinal transects of the ría on (a) 25 June and (c) 28 June 2007. The ship's tracks are shown in (b) for 25 June and (d) for 28 June. Courtesy E.D. Barton.

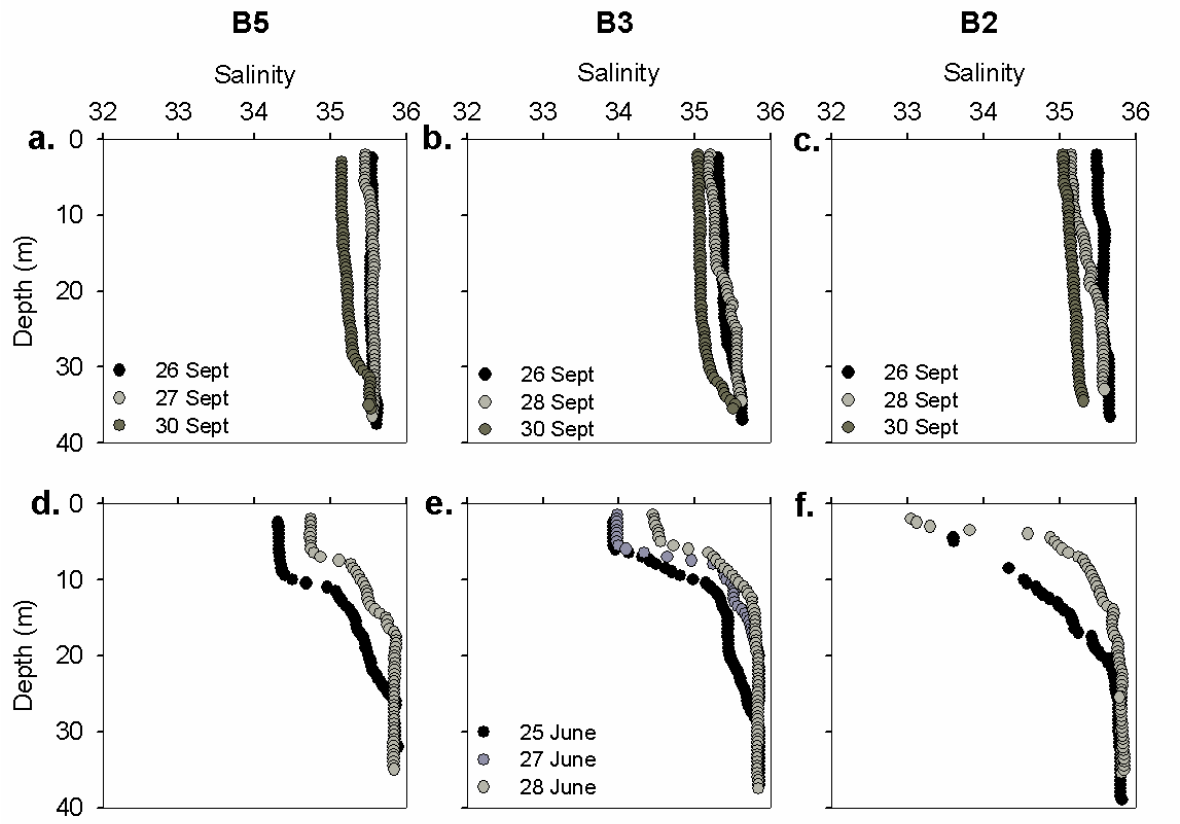

Figure 4.11. Salinity profiles obtained from CTD casts in (a, b, c) September 2006 and (d, e, f) June 2007 at stations (a, d) B5, (b, e) B3 and (c, f) B2. N.B: sampling dates were the same in d,e,f.

4.2.3. Dissolved oxygen

In September 2006, DO saturations were similar throughout the ría. Saturations were also relatively homogeneous throughout the water column, decreasing slightly with depth. At B5, saturations dropped from 115-120 % at the surface to 100-110 % at the bottom on 26 and 27 Sept, although on 30 Sept the drop was more significant, with saturations dropping below 100 % at ~30 m (Figure 4.12). At B3, saturations started to decrease at ~20 m depth on 26 and 28 Sept, whereas on 30 Sept it decreased only below ~30 m. At B2, greater temporal variation was observed, with saturations increasing by ~20 % throughout the water column between 26 and 30 Sept.

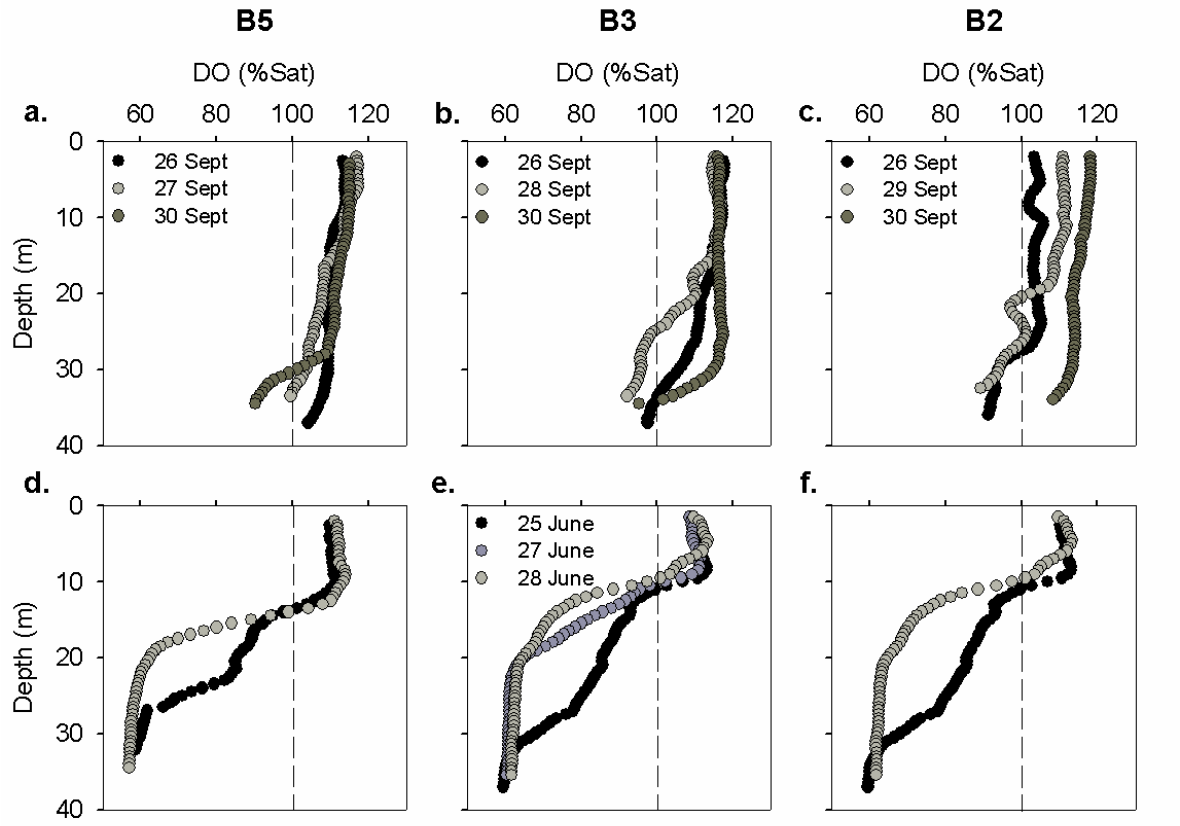

Figure 4.12. Profiles of DO saturation obtained from CTD casts in (a, b, c) September 2006 and (d, e, f) June 2007 at stations (a, d) B5, (b, e) B3 and (c, f) B2. Dashed lines indicate 100 % saturation. N.B: sampling dates were the same in (d,e,f).

In June 2007, both surface and bottom saturations were significantly lower than those in September (Student's t-test, $p < 0.01$ and Mann-Whitney U-test, $p < 0.05$). Saturations were high (mean 109 %) at the surface, but dropped rapidly below the pycnocline (mean 60 %), consistent with the predominance of photosynthesis over respiration in the euphotic zone and of respiration over photosynthesis in the deeper

waters. The decline in saturation occurred more rapidly and at shallower depths on 28 June than on 25 June, consistent with the shallowing of the pycnocline. Profiles were similar for all stations, except that the decline in DO saturation associated with the pycnocline occurred at a deeper depth at B5 than at B3 and B2 (Figure 4.12). DO concentrations were significantly correlated with temperature (DO = 11.98 T + 13.65, r^2 = 0.64, n = 67, $p < 0.01$) in June, but not in September.

4.2.4. Nutrients

In September 2006, NO_3^- concentrations were relatively homogeneous throughout the water column, displaying an increase with depth of <1 µmol l^{-1}. Horizontal variations were also slight, with surface concentrations varying by < 0.3 µmol l^{-1} (Figure 4.13 a,b,c). Concentrations decreased by up to 1.3 µmol l^{-1} between 26 Sept and 30 Sept, although an initial increase was observed on 28 Sept (B3) and 29 Sept (B2). This was not attributable to differences in tidal state, since similar concentrations were measured at various points of the tidal cycle both on 28 and 29 Sept (Table 4.2).

Ammonium concentrations were highest at B2, with concentrations ranging from 1.1 to 4.7 µmol l^{-1} at the surface, whereas at B5 and B3 they ranged from 0.8 to 2.1 µmol l^{-1}. Concentrations increased with depth, to between 1.7 and 4.5 µmol l^{-1} at B5 and B3 and between 4.1 and 5.2 µmol l^{-1} at B2 (Figure 4.13d,e,f). At B5, surface concentrations remained similar until 30 Sept, although deep concentrations increased from 1.7 to 5.3 µmol l^{-1}. At B3, concentrations increased throughout the water column between 26 and 28 Sept (by 0.4 to 1.4 µmol l^{-1}), although on 30 Sept concentrations were similar to 26 Sept, with the exception of the deepest concentration, which increased to 5.5 µmol l^{-1}. Ammonium concentrations were 34 and 44 % higher at high tide relative to low tide at B5 and B2, respectively (Table 4.2).

Phosphate and Si profiles were very similar to NH_4^+ profiles, displaying the same spatial and temporal variations. Surface PO_4^{3-} concentrations were 0.1-0.3 µmol l^{-1} at B5 and B3, increasing with depth, to between 0.3 and 0.8 µmol l^{-1} (Figure 4.13g,h). At B3, concentrations increased throughout the water column (by 0.10 to 0.22 µmol l^{-1}) between 26 Sept and 28 Sept, then dropped again to their initial values on 30 Sept, with the exception of the deepest, which increased (Figure 4.13h). Concentrations were higher at B2 than at the other stations on 26 Sept, although on 30 Sept they were similar in the top 10 m and lower at depth, relative to B5 and B2. Phosphate concentrations

were highest at high tide at B5, although little variation was observed with tidal state at B3 and B2 (Table 4.2).

Silicate concentrations at B5 were 2.1-3.0 µmol l^{-1} at the surface, increasing to 3.5-8.7 µmol l^{-1} at 30 m (Figure 4.13j,k). At B2, surface concentrations were higher than at B3 and B5 between 26 and 29 Sept (2.4-5.4 µmol l^{-1} at the surface and 6.8-10.1 µmol l^{-1} at the bottom), although on 30 Sept they dropped to 2.3-3.2 µmol l^{-1} (Figure 4.13l). Concentrations decreased with the tide at B5, although this was not observed at the other stations (Table 4.2).

Date	Station	Latitude	Longitude	Time	Hrs before/ after HT	NO_3^-	NH_4^+	Urea	PO_4^{3-}	Si	chl-a
27/09/2006	B5.1	42.206	-8.863	06:00	-0.2	1.44	1.29	-	0.25	2.98	1.03
	B5.2	42.209	-8.864	09:09	3.0	1.27	0.92	-	0.11	2.44	0.81
	B5.3	42.209	-8.864	12:00	5.8	1.13	0.96	-	0.15	2.17	0.68
28/09/2006	B3.1	42.224	-8.818	06:08	-0.7	2.43	1.93	0.37	0.23	2.72	3.30
	B3.2	42.225	-8.818	08:58	2.8	2.62	1.84	0.19	0.26	2.78	4.39
	B3.3	42.224	-8.817	12:16	5.5	2.58	2.08	-	0.28	2.97	4.47
29/09/2006	B2.1	42.243	-8.758	06:43	-0.8	2.35	4.70	-	0.42	3.64	3.42
	B2.2	42.241	-8.760	09:25	1.9	2.03	3.93	1.14	0.38	3.44	5.37
	B2.3	42.242	-8.759	12:11	4.6	2.14	3.27	0.65	0.39	3.57	6.42
27/06/2007	B3.1	42.226	-8.819	07:16	5.7	0.01	0.06	-	0.10	1.03	7.96
	B3.2	42.226	-8.818	09:41	-4.3	0.00	0.00	-	0.07	1.33	6.39
	B3.3	42.227	-8.818	12:44	-1.3	0.01	0.09	-	0.06	1.07	5.22

Table 4.2. Variations in surface NO_3^-, NH_4^+, PO_4^{3-}, Si (µmol l^{-1}) and chl-a (µg l^{-1}) measured at fixed stations on different tidal states in September 2006 and June 2007.

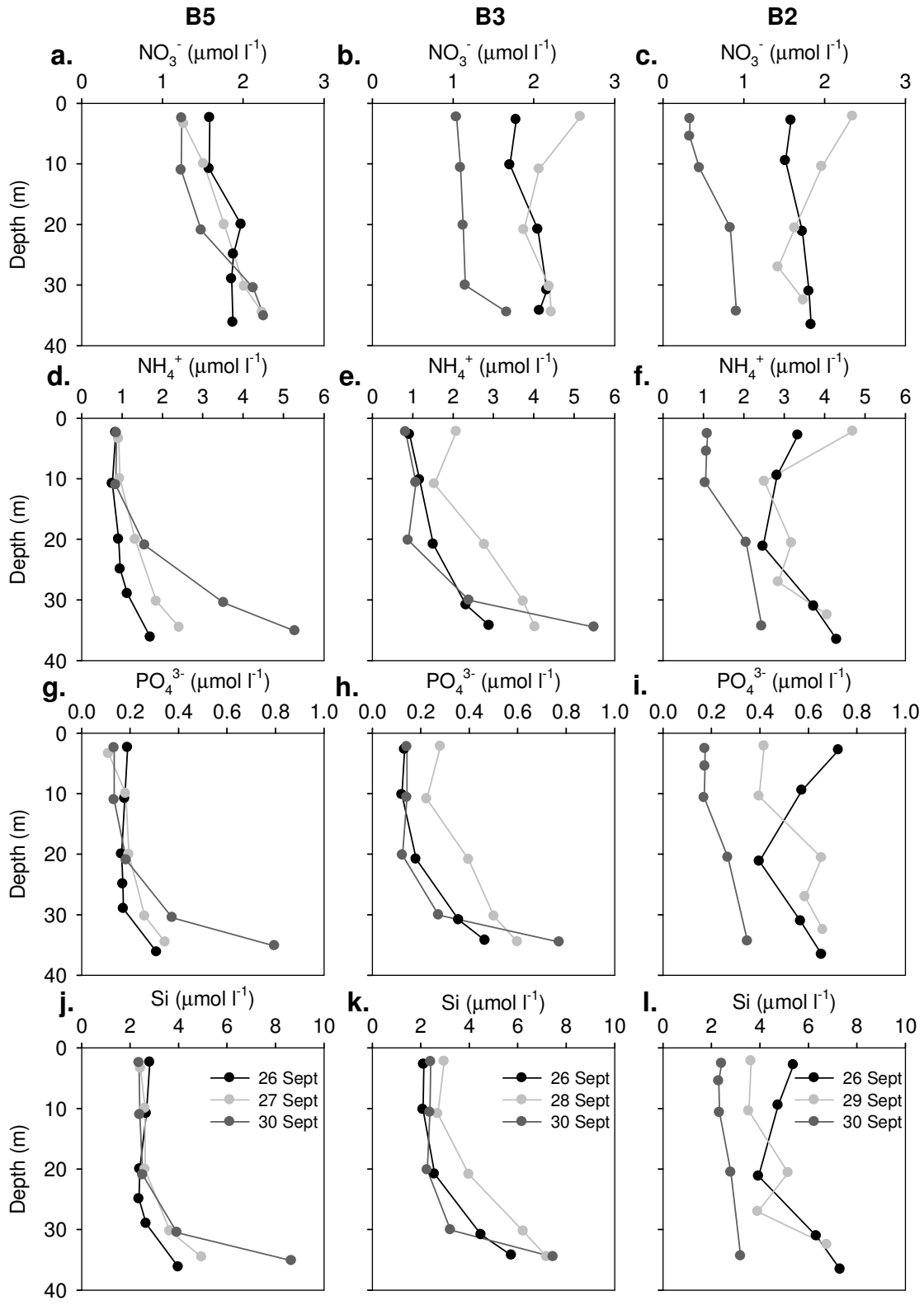

Figure 4.13. Profiles of (a, b, c) NO_3^-, (d, e, f) NH_4^+, (g, h, i) PO_4^{3-} and (j, k, l) Si at stations (a, d, g, j) B5, (b, e, h, k) B3 and (c, f, i, l) B2 on 3 sampling dates in September 2006, as shown in the legend.

In June 2007, NO_3^- concentrations were very low (<1.5 µmol l^{-1}) in the top 10-20 m at the start of the survey, increasing with depth to maximal concentrations of 9-11 µmol l^{-1} at 30-40 m depth (Figure 4.14a-c). Surface concentrations were significantly lower than in September, whereas bottom concentrations were significantly higher (Mann-Whitney U-test, $p < 0.05$). Profiles were similar throughout the ría on 25 June, although on 28 June higher concentrations were measured in the top 20 m at B2 (>5 µmol l^{-1}) relative to the other stations. Concentrations below ~10 m increased between 25 and 28 June, consistent with the raising of the pycnocline. Surface concentrations showed very little variation with tidal state (Table 4.2).

Ammonium was depleted throughout the ria at the surface (≤0.1 µmol l^{-1}), increasing to 3.0-3.6 µmol l^{-1} at the bottom (Figure 4.14d-f). On 28 June, NH_4^+ was still depleted in the surface at B3 and B5 but had increased at B2 (1.9 µmol l^{-1}). At B5, the concentration at 10 m also increased (1.9 µmol l^{-1}). At B3, NH_4^+ concentration increased to 3.1 and 2.0 µmol l^{-1} at 10 m on 25 and 27 June, respectively, but was depleted again in the top 10 m on 28 June. Both surface and bottom concentrations were significantly lower than in September (Mann-Whitney U-test, $p < 0.05$). Surface concentrations showed no consistent pattern in variation with tidal state (Table 4.2).

Phosphate displayed a similar distribution to NO_3^-, and was also significantly lower than in September at the surface (Student's t-test, $p < 0.05$), but significantly higher at the bottom (Mann-Whitney U-test, $p < 0.05$). Surface concentrations were < 0.1 µmol l^{-1} at all stations between 25 and 28 June, with the exception of B2 on 28 June where it increased to 0.40 µmol l^{-1} (Figure 4.14g-i). Bottom concentrations were 0.7-0.9 µmol l^{-1} at all stations. At B2, concentrations increased throughout the water column on 28 June. As with the other nutrients, no specific pattern in PO_4^{3-} concentrations was identified with respect to tidal state (Table 4.2).

Silicate distribution broadly followed that of PO_4^{3-}. Surface concentrations were ≤ 1.0 µmol l^{-1} at B5 and B3 on both 25 and 28 June, but higher at B2 (1.4 and 3.6 µmol l^{-1}, respectively) (Figure 4.14j-l). Surface concentrations were also significantly lower than in September (Student's t-test, $p < 0.001$), although bottom concentrations were not significantly different (Mann-Whitney U-test, $p > 0.05$).

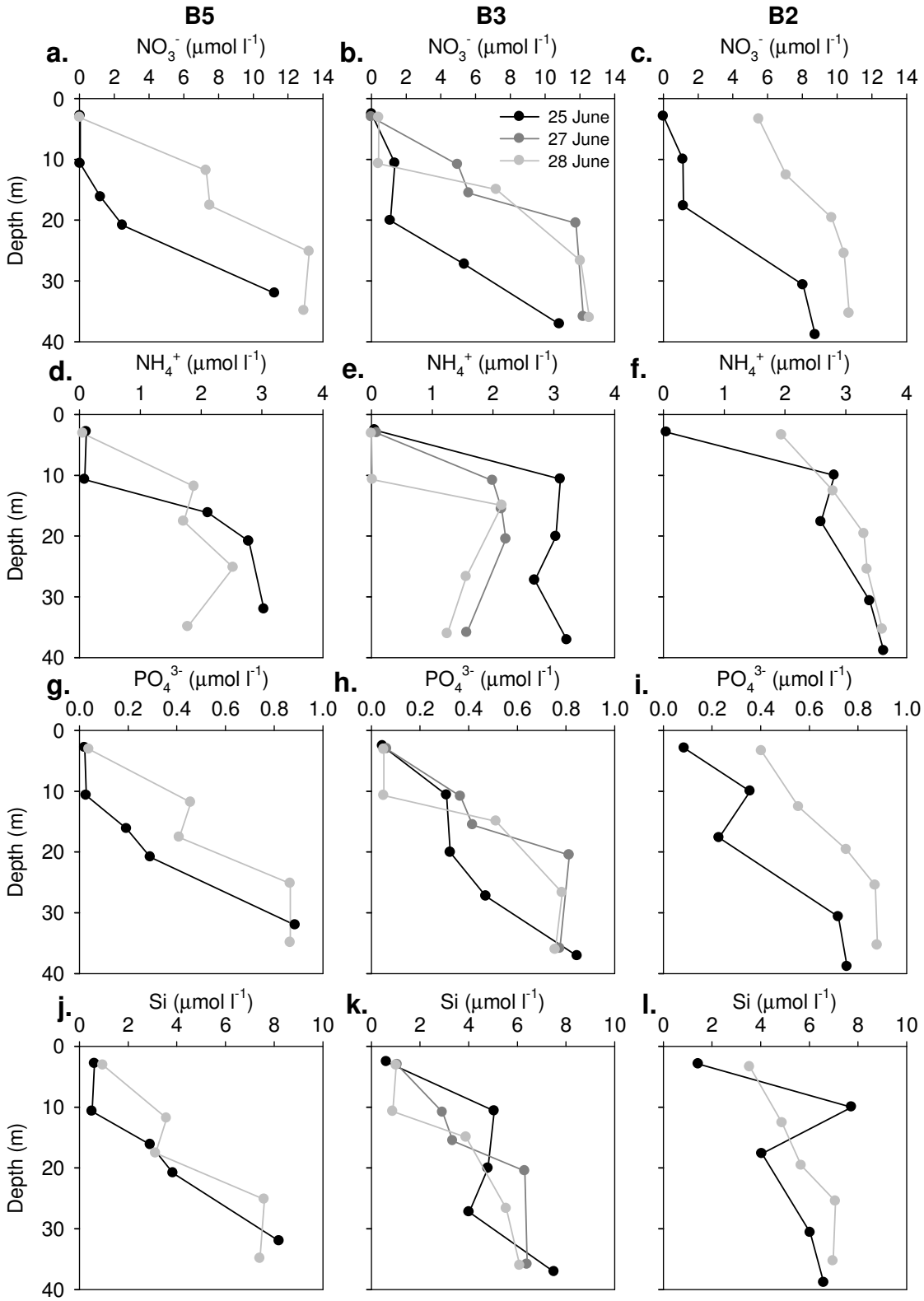

Figure 4.14. Profiles of (a, b, c) NO_3^-, (d, e, f) NH_4^+, (g, h, i) PO_4^{3-}, and (j, k, l) Si at stations (a, d, g, j) B5, (b, e, h, k) B3 and (c, f, i, l) B2 measured on 2 or 3 sampling dates in June 2007, as shown in the legend.

At B5, Si increased between 25 and 28 June at most depths below the surface, whereas at B3 they decreased at some depths and increased at others (Figure 4.14k). At B2, concentrations increased at all depths except at 10 m, where a maximum was observed on 28 June (Figure 4.14l). There did not appear to be any correlation between Si concentration and tidal state (Table 4.2).

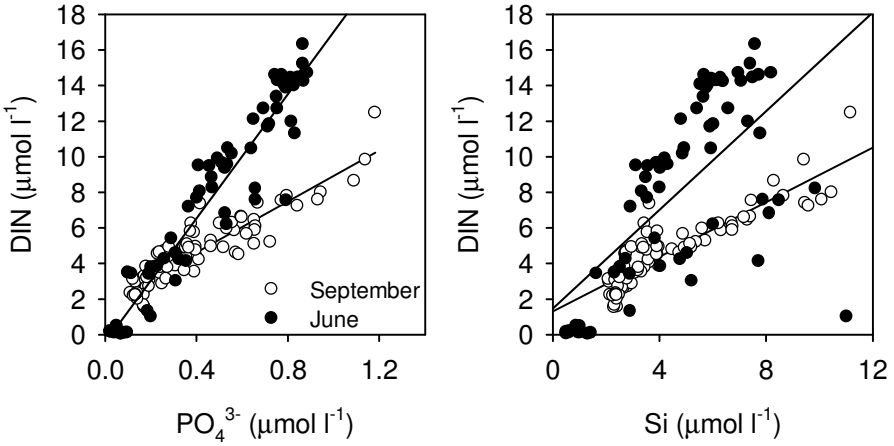

Figure 4.15. Linear regressions of (a) DIN versus PO_4^{3-} concentrations and (b) DIN versus Si concentrations measured at all stations and depths in September 2006 (open symbols) and June 2007 (closed symbols).

Nitrate was significantly correlated with PO_4^{3-} and Si in both September and June, although better correlations were obtained when using total DIN (= NO_3^- + NO_2^- + NH_4^+) (Figure 4.15,Table 4.3), since NH_4^+ was an important fraction of total DIN (51.6 ± 1.4 % in September and 35.9 ± 3.0 % in June), with average concentrations of 2.4 ± 0.2 µmol l^{-1} and 2.3 ± 0.2 µmol l^{-1}, respectively. The regression coefficient of the DIN vs PO_4^{3-} regression (or DIN:P ratio) was higher in June than in September, and was higher than for the NO_3^- vs PO_4^{3-} regression in both cases. The DIN:Si ratio was higher in June than in September and was higher than the NO_3^-:Si ratio in both cases (Table 4.3). In September, the DIN:P ratio was less than 50 % of the Redfield ratio of 16, whereas in June it was very similar to Redfield. The DIN:Si ratio in September was <1, indicating that N was limiting, whereas in June a ratio >1 indicated that Si was limiting for diatoms.

Nitrate was significantly correlated with temperature in June and September, whereas DIN and Si were significantly correlated with temperature only in June (Table 4.3). Phosphate was significantly correlated with temperature in June and September, with a lower level of significance for the latter.

Relationship	a	b	r	n	Month
DIN vs PO_4^{3-}	17.46	-0.44	0.96**	67	June
	7.17	1.75	0.91**	80	Sept
NO_3^- vs PO_4^{3-}	13.41	-0.96	0.85**	67	June
	0.79	1.44	0.36**	80	Sept
DIN vs Si	1.39	1.47	0.66**	67	June
	0.77	1.30	0.88**	80	Sept
NO_3^- vs Si	0.88	1.39	0.49**	67	June
	0.10	1.33	0.39**	80	Sept
DIN vs temp	-1.97	38.6	-0.89**	67	June
	0.57	-5.34	-0.15	80	Sept
NO_3^- vs temp	-1.78	32.9	-0.92**	67	June
	-0.40	8.73	-0.40**	80	Sept
PO_4^{3-} vs temp	-0.10	1.98	-0.79**	67	June
	0.13	-1.94	-0.31*	80	Sept
Si vs temp	-0.45	11.69	-0.42**	67	June
	0.81	-10.04	-0.20	80	Sept

Table 4.3. Results of linear regressions among nutrients and between nutrients and temperature. a = regression coefficient; b = y-axis intercept; r = correlation coefficient; n = number of observations. * $p < 0.05$; ** $p < 0.01$.

4.2.5. Chl-a

Chl-a concentrations were relatively low in September 2006, particularly at the start of the survey (<5 µg l^{-1}). At this time there was little horizontal variation between stations B5 and B2. By 30 September chl-a had increased and showed a horizontal gradient, with maximum concentrations of 5.8, 7.1 and 8.1 µg l^{-1} at B5, B3 and B2, respectively (Figure 4.16a-c). At the start of the survey, chl-a was relatively homogeneous throughout the water column, whereas on 30 Sept chl-a concentrations were highest in the top 15-25 m and decreased with depth.

In June 2007, a pronounced chl-a maximum was observed at ~10 m depth. Maximum concentrations were 10.5, 15.8 and 6.5 µg l^{-1} at B5, B3 and B2, respectively on 25 June. On 28 June they had increased at B5 and B2, to 25.8 and 25.1 µg l^{-1}, respectively, whereas at B3 concentrations remained the same. Surface concentrations were not significantly different from September, although concentrations at 10 m were significantly higher (Mann-Whitney U-test, $p < 0.05$).

The proportion of microplankton (chl-a > 20 µm) was significantly lower in September than in June, whereas the proportions of nanoplankton (chl-a >2 and <20 µm) and picoplankton (chl-a < 2 µm) were significantly higher (Mann-Whitney U-test for micro- and nanoplankton, Student's t-test for picoplankton, $p < 0.05$).

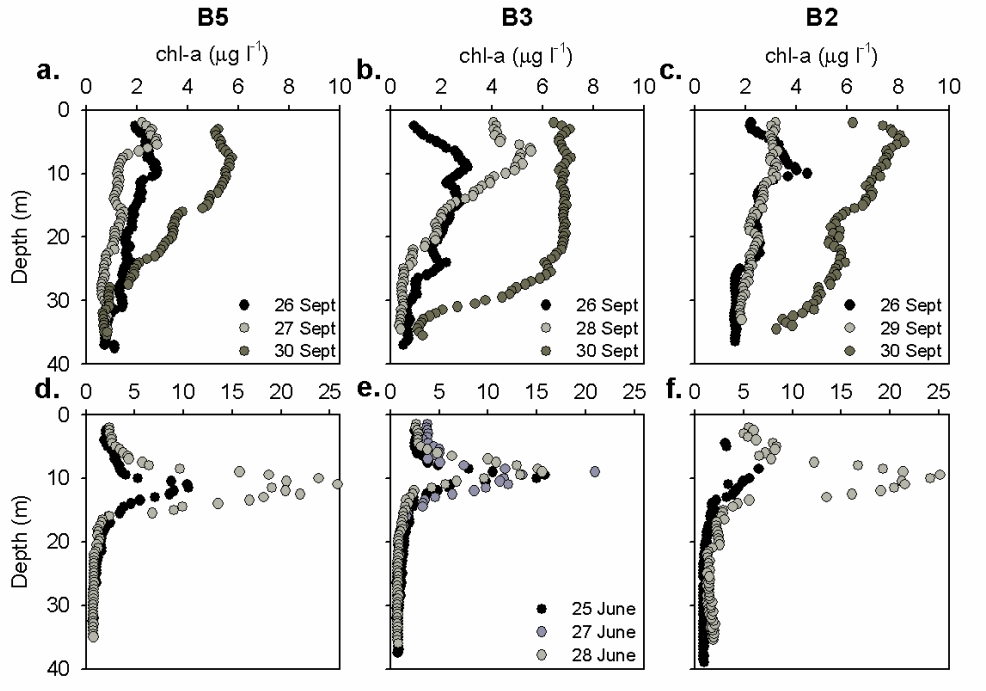

Figure 4.16. Chl-a profiles obtained from CTD fluorescence measurements in (a, b, c) September 2006 and (d, e, f) June 2007 at stations (a, d) B5, (b, e) B3 and (c, f) B2. Note the difference in scale between 2006 and 2007. N.B: sampling dates were the same in (d,e,f).

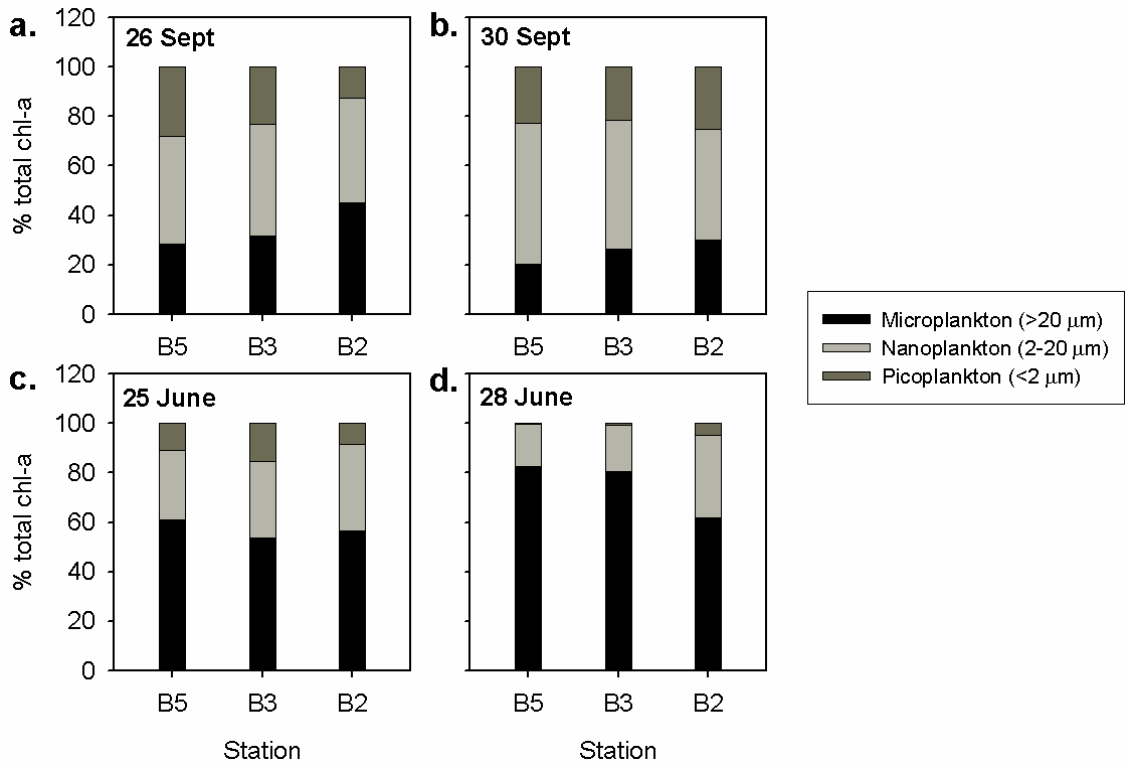

Figure 4.17. Depth-averaged proportions of total chl-a represented by microplankton, nanoplankton and picoplankton on (a) 26 September, (b) 30 September, (c) 25 June and (d) 28 June.

4.2.6. Phytoplankton community structure

4.2.6.1. General community structure

In September 2006, the phytoplankton community was numerically dominated by a mixture of dinoflagellates (up to 66 %) and small flagellates (up to 82 %), whereas the proportion of diatoms was <52 %. Maximum concentrations were 0.22 x 10^6 for diatoms, 0.35 x 10^6 for dinoflagellates and 0.70 x 10^6 cells l^{-1} for flagellates. In June 2007, the phytoplankton community was dominated by diatoms, which represented 65 to 99 % of total phytoplankton cells, with concentrations as high as 15 x 10^6 cells l^{-1}. Dinoflagellate concentrations only reached a maximum of 0.27 x 10^6 cells l^{-1}, representing up to 37 % of total phytoplankton cells, whereas flagellates reached 0.24 x 10^6 cells l^{-1} (35 % of total cell concentration). Highest cell concentrations were generally reached at the surface or at 10 m depth and increased from a maximum of 3.4 x 10^6 cells l^{-1} (B2 10 m) to a maximum of 14.9 x 10^6 cells l^{-1} (B2, 3 m) between 25 and 28 June (Figure 4.18).

Dinoflagellate concentrations were significantly correlated with microplankton chl-a (>20 μm) (data not shown) both in September ($r^2 = 0.26$, n = 46, $p < 0.01$) and in June ($r^2 = 0.53$, n = 37, $p < 0.01$). Diatoms displayed the same correlation, although with lower levels of significance ($r^2 = 0.09$ and 0.17, respectively, $p < 0.05$).

Cluster analysis performed on data from all stations and depths in September 2006 resulted in 4 clusters at the 55 % similarity level (Appendix 2, Table 4.4). Clusters I and II comprised shallow samples (3-10 m) from 26 to 29 September. Whereas B5 and B3 stations from different dates clustered together (Cluster II), B2 stations from 26 and 29 September were divided into Clusters I and II, respectively. Clusters III and IV comprised deeper samples (10 to 36 m) from 26-29 September and all samples from 30 September. Species' diversity was high in all clusters, as shown by the Shannon Diversity Index (H'), therefore the relative contribution of each species to total similarity was low (Table 4.4). Cryptophytes, the diatom *Nitzschia longissima* and a small *Gymnodinium* species were responsible for similarity within all clusters. Species that contributed to similarity within specific clusters included the dinoflagellates *Scrippsiella trochoidea* and *Prorocentrum gracile*, the diatom *Chaetoceros* spp., and the ichthyotoxic raphidophyte *Heterosigma akashiwo* for Cluster I; the dinoflagellates *Ceratium fusus* and *Protoperidinium divergens* for Cluster II; the diatom *Guinardia delicatula* and the flagellate *Solenicola setigera* for Cluster III and the dinoflagellate *Amphidinium* spp. for Cluster IV.

The shallower samples (Clusters I and II) both had significantly higher proportions of diatoms than the deeper samples and a significantly lower % dinoflagellates (with the exception of I vs III). Cluster III had the highest proportion of diatoms and Cluster IV had the highest proportion of dinoflagellates (Table 4.4). H' was also significantly lower for Cluster I than for Cluster II, which in turn was significantly lower than for Clusters III and IV (Student's t-test, $p < 0.01$), indicating that diversity was higher at depth. The clusters could also be linked to a certain extent with nutrient conditions, although not with temperature or salinity (Table 4.5). For example, Clusters I and III displayed significantly higher PO_4^{3-} and Si concentrations and lower DIN:P ratios relative to Cluster II (Student's t-test, $p < 0.01$). Cluster IV also had significantly lower PO_4 and Si concentrations (Student's t-test, $p < 0.001$) and higher DIN:P ratios (Mann-Whitney U-test, $p < 0.05$) relative to Cluster III. Cluster II had significantly lower Si:DIN ratios than Clusters III and IV (Student's t-test, $p < 0.01$). Interestingly, NO_3 concentrations did not seem to have any effect on community structure.

Cluster analysis performed on the data from June 2007 produced 4 clusters at the 50 % similarity level (Appendix 2, Table 4.6). Cluster I comprised samples from the inner- to mid-ría stations B0 to B3, from the shallower depths (3 to 10 m) on 25-27 June but from deeper depths (17-25 m) on 28 June. Cluster II comprised the shallow samples from the outer- to mid- ría stations (B5 to B3) on 25 June, but also deeper (13-18 m) samples from the inner station B2 on 28 June. Clusters III and IV generally comprised the deeper samples, ranging from 14 to 22 m, with the inner stations (B1 and B2) belonging to Cluster III and the outer and mid-ría stations (B5 to B3) belonging to Cluster IV. H' values were similar to September 2006, ranging from 1.5 to 2.6. The lowest value was measured in Cluster I, in which two diatom species, *Skeletonema costatum* and *Nitzschia* cf. *americana* contributed 50 % to total similarity within the cluster. Cluster II was significantly more diverse, with *Leptocylindrus* spp. and *Chaetoceros socialis* also contributing to similarity. Both of these clusters had significantly higher percentages of diatoms (>90 %) relative to Clusters III and IV. Clusters III and IV had significantly higher H', and they comprised cryptophytes and dinoflagellates as well as diatoms.

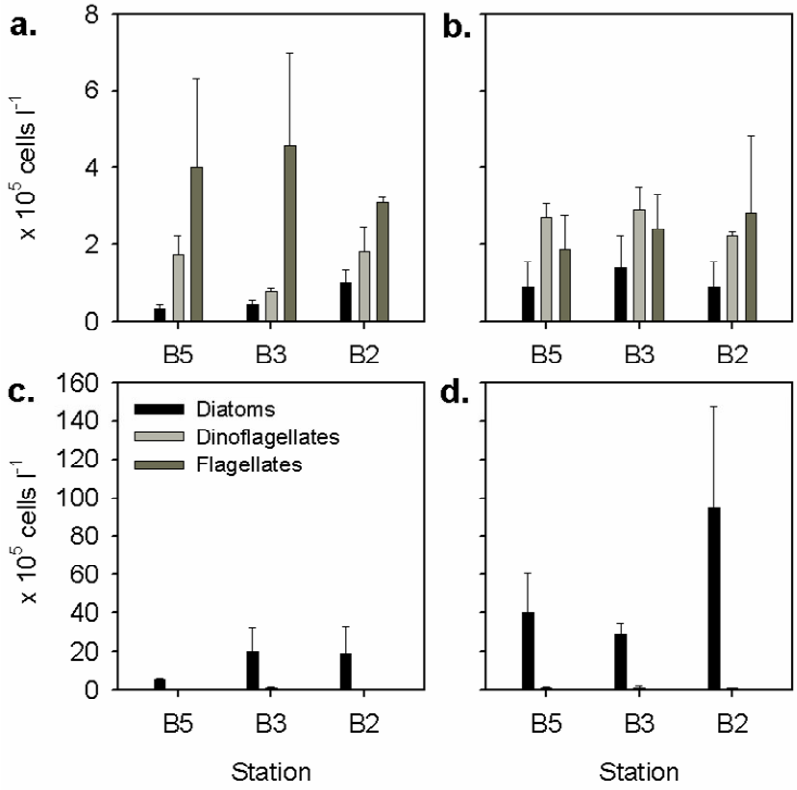

Figure 4.18. Means of cell concentrations at 3 and 10 m (with standard errors shown as error bars) of diatoms, dinoflagellates and flagellates at B5, B3 and B2 on (a) 26 September 2006, (b) 30 September 2006, (c) 25 June 2007 and (d) 28 June 2007.

Cluster	Samples in cluster	Species	% contribution to total similarity	H'	% diatoms	% dino-flagellates
I	26 B2 3-10 m	Cryptophyceae	10.8	2.2 ± 0.23	16.4 ± 9.1	33.3 ± 9.9
		Cachonina niei	7.2			
		Chaetoceros spp.	6.5			
		Nitzschia longissima	5.7			
		Small *Gymnodinium* sp.	5.6			
		Thalassiosira rotula	4.8			
		Heterosigma akashiwo	4.5			
		Scrippsiella trochoidea	4.5			
		Prorocentrum gracile	4.5			
II	26-27 B5 3 m	Cryptophyceae	16.1	1.3 ± 0.39	4.6 ± 2.9	25.8 ± 9.3
	26-28 B3 3-10 m	*Cachonina niei*	7.5			
	29 B2 3-10 m	*Ceratium fusus*	5.4			
		Nitzschia longissima	5.3			
		Small *Gymnodinium* sp.	4.9			
		Pseudo-nitzschia delicatissima	4.7			
		Protoperidinium divergens	4.7			
		Ceratium furca	4.4			
III	28 B3 30 m	Cryptophyceae	10.4	2.2 ± 0.09	35.8 ± 12.1	20.1 ± 8.9
	29 B2 20-39 m	Unidentified centric diatom	7.9			
	30 B5 35 m	*Nitzschia longissima*	7.5			
	30 B3 35 m	Small *Gymnodinium* sp.	5.6			
		Pseudo-nitzschia delicatissima	5.4			
		Guinardia delicatula	5.1			
		Solenicola setigera	4.0			
		Thalassiosira rotula	3.9			
		Medium pennate diatom	3.8			
IV	26-27 B5 10-36 m	Cryptophyceae	10.5	2.3 ± 0.24	16.1 ± 8.4	49.8 ± 13.5
	26 B3 20-35 m	Small *Gymnodinium* sp.	8.4			
	28 B3 20, 35 m	*Nitzschia longissima*	6.0			
	26 B2 20-34 m	*Cachonina niei*	5.3			
	30 B5 2-30 m	*Amphidinium* spp.	5.2			
	30 B3 2-30 m	*Pseudo-nitzschia delicatissima*	5.1			
	30 B2 2-34 m	Unidentified centric	5.0			
		Small fusiform naked dinoflagellate	4.6			

Table 4.4. SIMPER analysis of phytoplankton species' contributions to similarity within clusters identified at the 55 % similarity level and mean H', % diatoms and % dinoflagellates in each cluster in September 2006.

Month	Cluster	Temp. °C	Salinity	NO_3^-	NH_4^+	PO_4^{3-}	Si	DIN:P	Si:DIN
					µmol l^{-1}				
June	I	16.54 ± 0.69	34.27 ± 0.41	4.08 ± 1.10	2.94 ± 0.60	0.51 ± 0.08	5.07 ± 0.65	11.76 ± 1.75	3.37 ± 1.69
	II	16.82 ± 0.49	35.06 ± 0.15	2.88 ± 0.79	1.10 ± 030	0.22 ± 0.05	2.29 ± 0.41	14.27 ± 2.46	2.80 ± 0.88
	III	17.12 ± 0.09	35.29 ± 0.14	1.32 ± 0.17	4.24 ± 1.64	0.51 ± 0.28	6.28 ± 2.23	13.07 ± 3.60	1.09 ± 0.04
	IV	15.08 ± 0.81	35.59 ± 0.09	5.36 ± 1.87	2.03 ± 0.39	0.43 ± 0.10	4.20 ± 0.53	16.93 ± 0.82	0.68 ± 0.11
Sept	I	18.05 ± 0.22	35.5 ± 0.02	1.55 ± 0.03	3.08 ± 0.26	0.65 ± 0.08	5.07 ± 0.32	7.58 ± 0.59	1.04 ± 0.00
	II	17.42 ± 0.09	35.3 ± 0.13	1.91 ± 0.15	1.82 ± 0.39	0.22 ± 0.04	2.73 ± 0.18	18.74 ± 3.91	0.74 ± 0.07
	III	17.42 ± 0.13	35.5 ± 0.08	1.88 ± 0.13	4.48 ± 0.41	0.69 ± 0.06	7.31 ± 0.79	9.78 ± 0.39	1.09 ± 0.07
	IV	17.32 ± 0.10	35.4 ± 0.22	1.53 ± 0.11	1.86 ± 0.20	0.28 ± 0.03	3.53 ± 0.31	13.94 ± 0.62	1.01 ± 0.04

Table 4.5. Mean (± standard error) temperature, salinity, nutrients and nutrient ratios for each cluster as defined in Tables 4.4 and 4.6.

Cluster	Samples in cluster	Species	% contribution to total similarity	H'	% diatoms	% dino-flagellates
I	25,28 B1 3-10 m	*Skeletonema costatum*	30.5	1.5 ± 0.3	94.1 ± 6.5	3.4 ± 6.0
	25,28 B2 3 m	*Nitzschia* cf. *americana*	22.4			
	27 B3 3 m					
	28 B2 20-25 m					
	28 B1 17 m					
	28 B0 3 m					
II	25,28 B5 3-12 m	*Leptocylindrus danicus*	22.6	1.9 ± 0.3	95.6 ± 1.8	3.7 ± 1.6
	25,28 B4 3-11 m	*Leptocylindrus minimus*	8.8			
	25,28 B3 2-11 m	*Skeletonema costatum*	8.3			
	27 B3 9 m	*Nitzschia* cf. *americana*	6.5			
	28 B5 18 m	*Chaetoceros socialis*	6.1			
	28 B3 15 m					
	28 B2 13 m					
III	25 B2 18 m	Cryptophyceae	13.9	2.6 ± 0.5	61.8 ± 4.4	13.9 ± 10.6
	25 B1 14 m	*Nitzschia* cf. *americana*	8.8			
		Skeletonema costatum	8.8			
		Nitzschia longissima	8.2			
		Pseudo-nitzschia delicatissima	7.8			
		Small fusiform naked dino	7.3			
IV	25 B5-B3 16-20 m	*Leptocylindrus danicus*	12.6	2.6 ± 0.3	51.9 ± 16.8	34.3 ± 19.0
	27 B3 15-21 m	Cryptophyceae	10.0			
	28 B4 22 m	Small *Gymnodinium* sp.	8.3			
		Small fusiform naked dino	5.2			
		Rhizosolenia stolterfothii	5.1			
		Leptocylindrus minimus	4.9			
		Pseudo-nitzschia delicatissima	4.8			

Table 4.6. SIMPER analysis of phytoplankton species' contributions to similarity within clusters identified at the 55 % similarity level and mean H', % diatoms and % dinoflagellates in each cluster in June 2007.

4.2.6.2. HAB species

In 2006, *Dinophysis acuta* was present at all stations except at B2 on 26 September, and was generally restricted to the top 10 m, although on 30 September it was distributed throughout the water column, down to 20-30 m (Figure 4.19). Highest concentrations were observed at B2 towards the end of the survey (maximum 3.9 x 10^3 cells l^{-1} on 29 and 3.7 x 10^3 cells l^{-1} on 30 September). *Dinophysis caudata* was never abundant at the surface and was generally found at deeper depths relative to *D. acuta* (down to 36 m). It was relatively abundant at B5 at the start of the survey, displaying a maximum at 30 m (3.6 x 10^3 cells l^{-1}), then decreased in abundance throughout the rest of the survey (to <0.4 x 10^3 cells l^{-1} on 30 September). At B3 and B2, *D. caudata* abundance peaked on 28-29 September, reaching 2.8-4.5 x 10^3 cells l^{-1} (Figure 4.19).

Gymnodinium catenatum decreased in abundance at B5 and B3 during the survey, with maximum concentrations decreasing from 1.5 to 0.3 x 10^3 cells l^{-1} at B5 and from 20.2 to 0.8 x 10^3 cells l^{-1} at B3. At B2, no cells were observed on 26 September and the highest concentration was measured on 29 September (11.1 x 10^3 cells l^{-1}), dropping to 2.1 x 10^3 cells l^{-1} on 30 September. Because of their low numerical abundance, the toxic dinoflagellates did not influence the clustering of stations. However, concentrations of *D. acuta* and *G. catenatum* were significantly higher in Cluster II relative to Cluster III (Mann-Whitney U-test, $p < 0.05$).

Pseudo-nitzschia delicatissima was particularly abundant at B5, displaying a maximum (30.8 to 34.7 x 10^3 cells l^{-1}) at 10-20 m depth. At B3 and B2, *P. delicatissima* often displayed a surface maximum and was generally more abundant at B2 than at B3. Concentrations increased between 26 and 30 September, from maxima of 4.0 x 10^3 and 4.2 x 10^3 cells l^{-1} to maxima of 7.5 x 10^3 and 14.3 x 10^3 cells l^{-1} at B3 and B2, respectively. *P. delicatissima* was responsible for 4.7-5.4 % total similarity within Clusters II, III and IV. *P. delicatissima* concentrations were significantly higher in Clusters II and IV relative to Cluster III (Mann-Whitney U-test, $p < 0.05$). *P. seriata* was also more abundant at B5 relative to the other stations, although concentrations were generally low (< 1.0 x 10^3 cells l^{-1}).

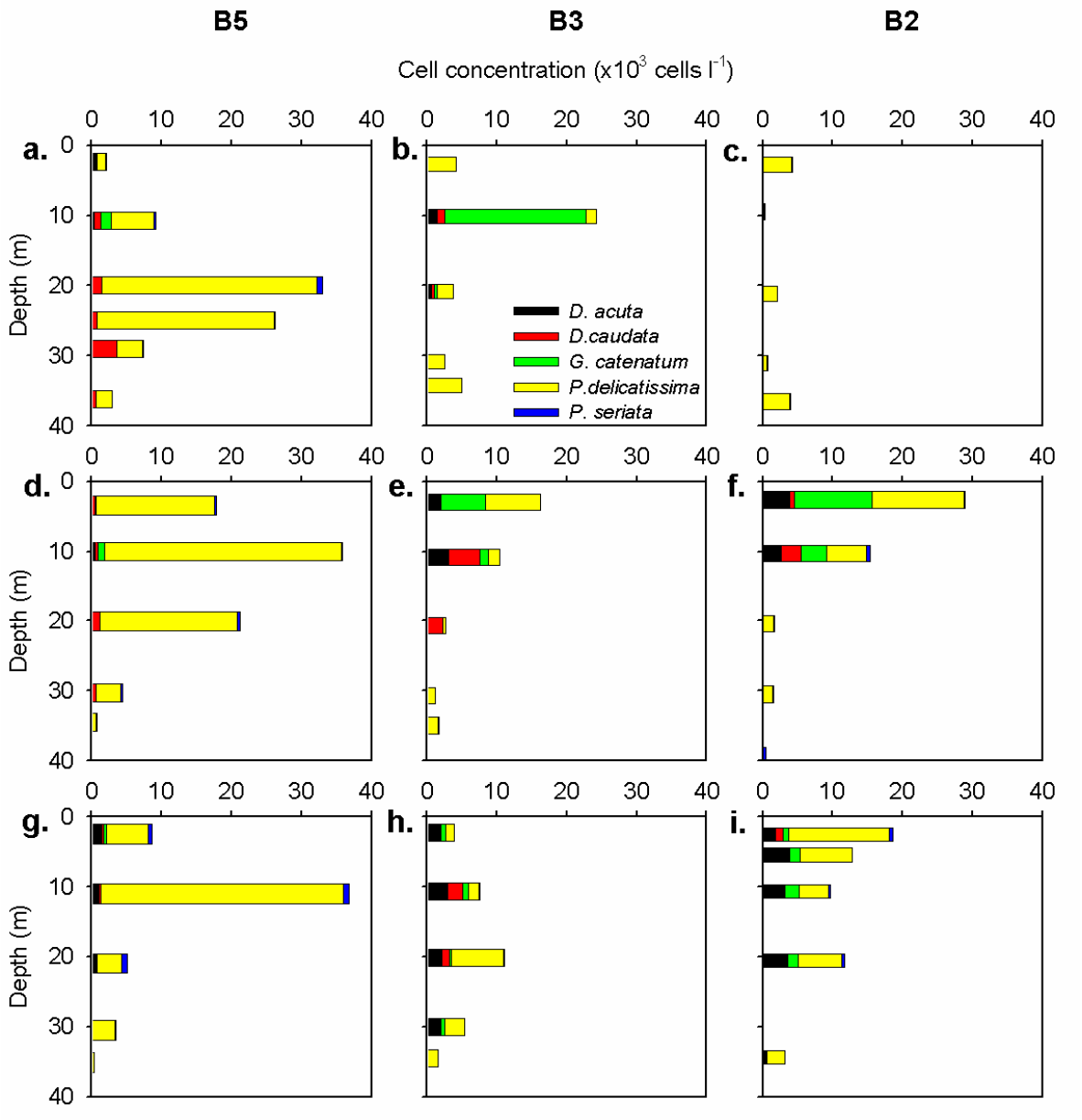

Figure 4.19. Cell concentrations of toxic species at (a,d,g) B5, (b,e,h) B3 and (c,f,i) B2 on (a,b,c) 26 September, (d) 27 September, (e) 28 September, (f) 29 September and (g,h,i) 30 September 2006.

In June 2007, the most abundant HAB species were *Pseudo-nitzschia delicatissima* and *P. seriata*, although *Dinophysis acuminata* was also present (Figure 4.20). *P. seriata* was the most abundant at B5 and B3 on 25 June, reaching concentrations of 50.5 x 10^3 and 237.6 x 10^3 cells l^{-1}, respectively, at 10 m. *P. delicatissima*, however, was more abundant at B2 (maximum 10.2 x 10^3 cells l^{-1}). *P. delicatissima* became more abundant on 28 June, reaching concentrations of 72.8 x 10^3, 12.1 x 10^3 and 52.8 x 10^3 cells l^{-1} at B5, B3 and B2, respectively. Meanwhile, *P. seriata* concentrations declined at B5 and B3, dropping to maxima of 16.0 and 56.6 x 10^3 cells l^{-1}, respectively, whereas at B2 they increased to a maximum of 25.2 x 10^3 cells l^{-1}.

Dinophysis acuminata was most abundant at 10 m at B3, where it reached 15 x 10^3 cells l^{-1} on 25 June, although it declined to 4 x 10^3 cells l^{-1} on 28 June. At B5 and B2, concentrations were <2.5 x 10^3 cells l^{-1} on both dates (Figure 4.20). Both *P. seriata* and *D. acuminata* concentrations were significantly higher for Cluster II than for all other clusters (Mann-Whitney U-test, $p < 0.05$).

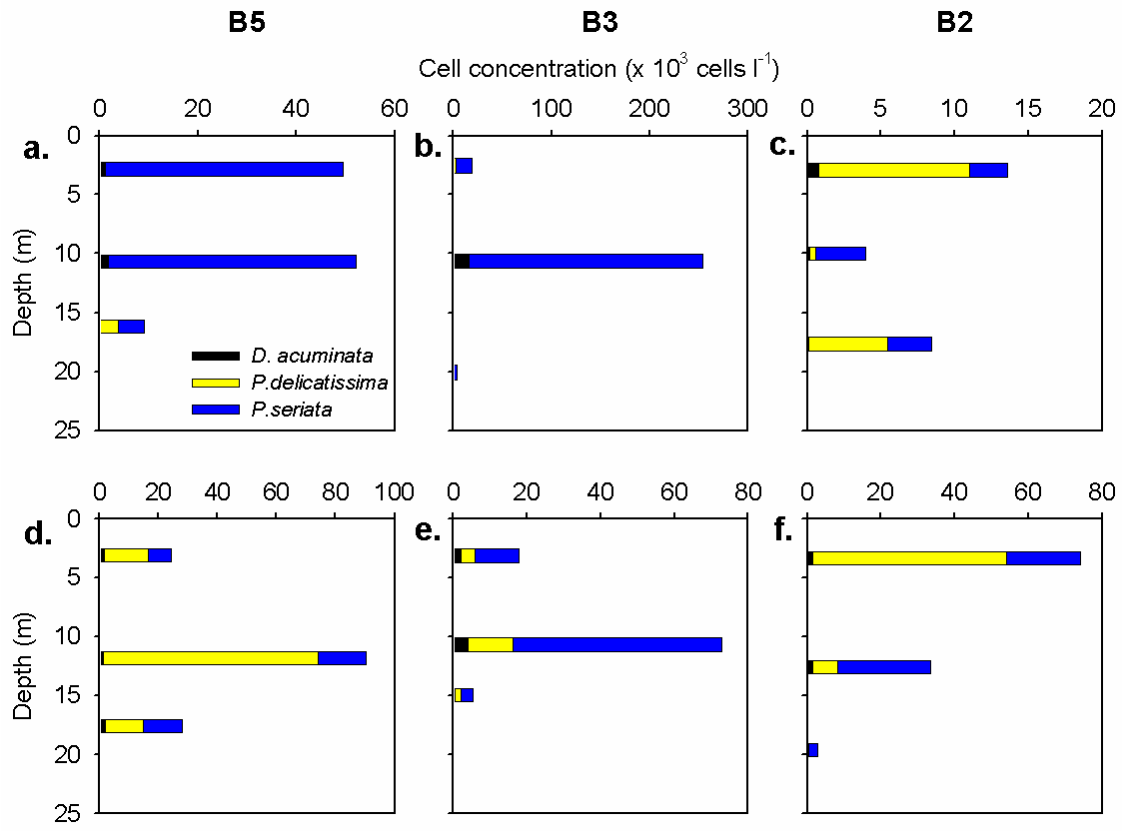

Figure 4.20. Cell concentrations of toxic species at (a,d) B5, (b,e) B3 and (c,f) B2 on (a,b,c) 25 June and (d,e,f) 28 June 2007.

4.2.7. Nitrogen uptake

4.2.7.1. Uptake and regeneration rates

In September 2006, nitrogen was taken up predominantly in the form of NH_4^+ [52 to 74 % total ρ(N)], followed by urea (15 to 32 %), whereas ρ(NO_3^-) contributed <20 % (Figure 4.21). Total ρ(N) showed little variation between stations and over time, except at B2 where it increased by 58 % between 26 and 29 September. Ammonium uptake ranged from 0.035 to 0.061 µmol N l^{-1} h^{-1}, ρ(urea) from 0.008 to 0.026 µmol N l^{-1} h^{-1} and ρ(NO_3^-) from 0.004 to 0.013 µmol N l^{-1} h^{-1}. f-ratios were very low, particularly at B2 (0.05 to 0.08), whereas they were 0.10 to 0.16 at B3 and B5 (Figure 4.22).

In June 2007, total ρ(N) was significantly higher (on average 4-fold) than in September 2006 (Student's t-test, $p < 0.0001$). This was due to significant increases in ρ(NH_4^+) (3-fold) ρ(NO_3^-) (7-fold) and ρ(urea) (6-fold) (Mann-Whitney U-test, $p < 0.05$). Highest total ρ(N) was measured at B3 and B2 (0.21-0.44 µmol N l^{-1} h^{-1}), whereas at B5 and B0 ρ(N) was 0.18-0.19 µmol N l^{-1} h^{-1}. Surface ρ(NH_4^+) ranged from 0.044 to 0.203 µmol N l^{-1} h^{-1}, ρ(NO_3^-) from 0.030 to 0.114 µmol N l^{-1} h^{-1} and ρ(urea) from 0.024 to 0.341 µmol N l^{-1} h^{-1}. Ammonium uptake was 30 % to 2-fold higher in the chl-a maximum relative to the surface, whereas ρ(urea) and ρ(NO_3^-) were higher at the surface (3- to 9-fold and 4-fold, respectively) (Figure 4.21h,i). The contribution of NH_4^+ to total ρ(N) varied between 10 and 74 % at the surface and between 75 and 80 % in the chl-a maximum. Urea was also an important source of nitrogen, particularly at the surface at B2 (41-78 %). f-ratios were significantly higher (on average 2-fold) than in September (Mann-Whitney U-test, $p < 0.05$), ranging from 0.08 to 0.48 (Figure 4.22).

Ammonium regeneration rates were highly variable, ranging from 0.063 to 0.457 µmol N l^{-1} h^{-1} in September and from 0.002 to 0.297 µmol N l^{-1} h^{-1} in June. Although r(NH_4^+) was on average higher in September (0.202 ± 0.071 µmol N l^{-1} h^{-1}) relative to June (0.133 ± 0.036 µmol N l^{-1} h^{-1}), this difference was not statistically significant (Student's t-test, $p > 0.05$).

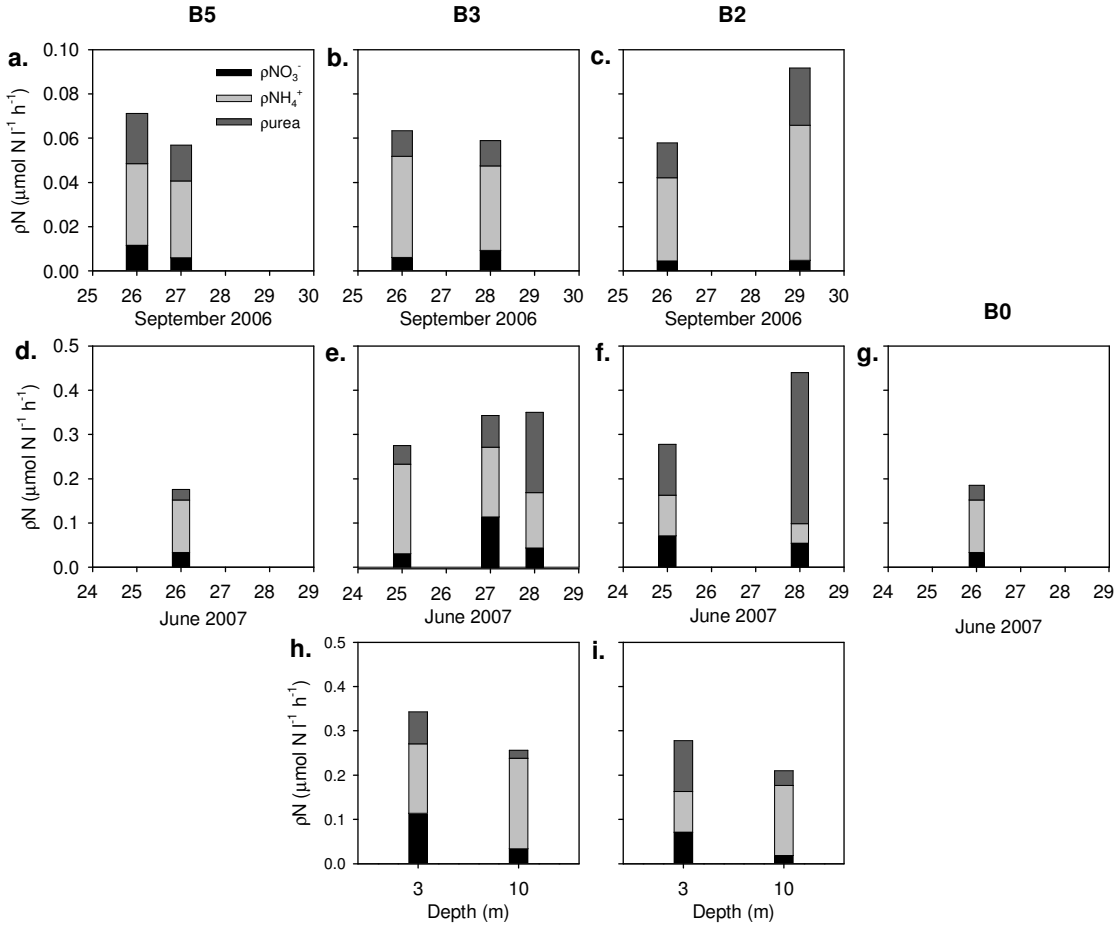

Figure 4.21. Surface nitrogen uptake rates at stations (a,d) B5, (b,e) B3, (c,f,) B2 and (g) B0 in (a-c) September 2006 and (d-g) June 2007. Data from B3 (28 Sept) and B2 (29 Sept) are means of 2 measurements made at different times of day (SE = 0.003, 0.001 and 0.004 for NO_3^-, $NH_4^+$and urea, respectively at B3 and 0.0003, 0.002 and 0.002 at B2). Uptake rates at 3 and 10m (h) at B3 on 27 June 2007 and (i) at B2 on 28 June 2007.

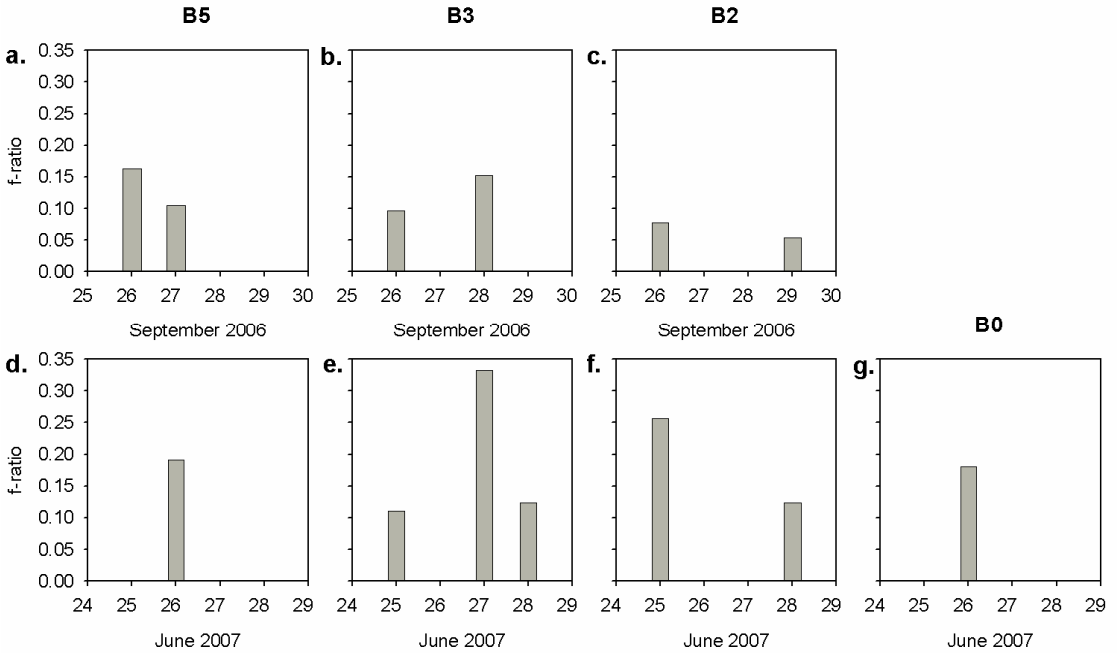

Figure 4.22. *f*-ratios measured at stations (a,d) B5, (b,e) B3, (c,f) B2 and (g) B0 in (a-c) September 2006 and (d-g) June 2007.

4.2.7.2. Nitrogen uptake kinetics

Maximum PN-specific uptake (ν_{max}) was 5-fold higher for NH_4^+ than for urea, which was 2.6-fold higher than for NO_3^- (Table 4.7). The α value was also higher for NH_4^+ relative to NO_3^-, but only by 41 %, and values were similar for NO_3^- and urea. The differences in α were less pronounced due to the positive correlation between K_s and ν_{max} ($r^2 = 0.999$, $n = 3$, $p < 0.05$).

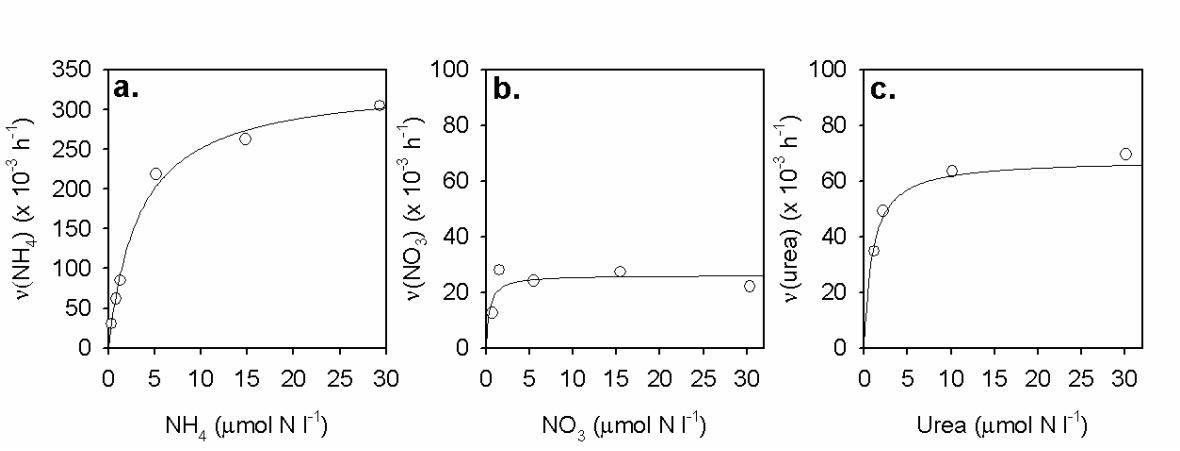

Figure 4.23. Nitrogen uptake versus ambient concentration fitted to the Michaelis-Menten equation for uptake kinetics using SigmaPlot (Jandel Scientific). Note the different scale in (a).

	Ambient N	ν_{max}	K_s	α	$\nu_{max}(NH_4)$ / $\nu_{max}(NO_3)$	ν_{max}(urea) / $\nu_{max}(NO_3)$	$\alpha(NH_4)$ / $\alpha(NO_3)$	α(urea) / $\alpha(NO_3)$
NO_3	0.52	26.2 ± 3.6**	0.37 ± 0.35	70.8	12.82	2.58	1.41	1.01
NH_4	0.33	335.9 ± 12.6**	3.36 ± 0.44**	100.0				
Urea	0.17	67.7 ± 3.1**	0.95 ± 0.24*	71.3				

Table 4.7. Nitrogen uptake kinetics parameters ν_{max} (x 10^{-3} h^{-1}), K_s (µmol N l^{-1}) and α (x 10^{-3} h^{-1} (µmol N l^{-1})$^{-1}$) and standard errors derived from Figure 4.23. Ambient nitrogen concentrations (µmol N l^{-1}) measured in the water sampled for the experiment are also shown (µmol N l^{-1}) * $p < 0.05$; ** $p < 0.01$.

4.3. Discussion

4.3.1. Hydrographic features during the upwelling and downwelling seasons

The hydrographic conditions that prevailed in September 2006 and June 2007 were typical of the downwelling and upwelling seasons, respectively. In September, southerly winds were predominant and the water column was relatively homogeneous with respect to temperature, salinity and DO saturation, as a consequence of downwelling (Figueiras et al., 1994). The downwelling front was observed in the vicinity of station B2, evidenced by vertical temperature and salinity isolines. The position of the downwelling front is known to vary as a result of the relative contributions of freshwater flow out of the ría and the inflow of shelf water into the ría (Álvarez-Salgado et al., 2000). Temperatures were high (>16.6 °C) throughout the water column, consistent with the advection of warm surface shelf water of subtropical origin into the ría (Figueiras et al., 1994; Figueiras et al., 2002).

In June, winds were predominantly southerly between 9 and 21 June, indicating that no water was upwelled during the 2 weeks prior to the survey. Winds switched to northerly (upwelling) during the 3 days preceding the survey, although with relatively weak components (< 4 m s^{-1}), therefore upwelling was not strong enough to mix the water column and so the water column remained stratified. A thermocline was observed between 10 and 20 m, showing positive estuarine circulation, with a warm, less saline surface layer flowing out of the ría (T = 18-20 °C, S = 33.1-34.9) and colder, more saline water (T = 13-15 °C, S = 35.4-35.9) flowing into the ría at depth. Surface salinities were significantly higher in September than in June, consistent with 2-fold higher rainfall occurring during the 3 months prior to the June survey. This indicates the potential importance of freshwater flow on the hydrographic conditions in spring/early summer, as also shown by Figueiras & Pazos (1991b) for 3 of the Rías Baixas.

Upwelled ENACW water is characterised by temperatures in the range 10.5-15 °C, that are significantly correlated with salinities in the range 35.5-36.0 (Álvarez-Salgado et al., 2002). The origin of ENACW (tropical $ENACW_t$ or polar $ENACW_p$) can be determined from its salinity, whereby $ENACW_p$ is characterised by S < 35.6 (Harvey, 1982) and $ENACW_t$ by S > 35.7 (Pollard & Pu, 1985). Bottom water temperatures in the ría during the June survey were 12.7-13.0 °C as far up as station B2, with salinities of ~35.8. This confirms that recently upwelled $ENACW_t$ had entered the ría during

upwelling and penetrated as far as B2. Upwelling is thought to occur after a ~ 3d time lag relative to wind conditions (Álvarez-Salgado et al., 2002), therefore the upwelled water present at the bottom of the ría at the start of the survey could be linked to relatively weak northerly winds between 21 and 23 June (with a brief period of southerly winds on 24 June), which would explain why it did not penetrate the euphotic layer. Bottom salinities at the inner stations B0 and B1 increased from ~35.2 to ~35.7 between 25 and 28 June, indicating that a pulse of upwelling had caused another surge of upwelled water into the ría, as shown by the uplifted isotherms and increased surface nutrient concentrations. This could be linked to intensified northerly winds from 25 June onwards. Nitrate, PO_4 and Si concentrations of 5.6, 0.32 and 1.6 μmol l^{-1} have been reported for $ENACW_t$, and "preformed" concentrations (i.e. concentrations in source waters at 100 % DO saturation) were estimated at 3.5, 0.19 and 0.3 μmol l^{-1} (Pérez et al., 1993). The NO_3^-, PO_4^{3-} and Si concentrations measured in upwelled water (~13 °C) in this study were 11.5 ± 0.35 μmol l^{-1}, 0.80 ± 0.02 μmol l^{-1} and 6.8 ± 0.25 μmol l^{-1}, respectively, indicating that nutrient concentrations in the upwelled water increased several-fold while it travelled along the continental shelf. Bode et al. (2005) also found higher nutrient concentrations than those characteristic of ENACW in the Ría de Ferrol (one of the Rías Altas, north of Cape Finisterre, which is thought to be the divide between $ENACW_t$ to the south and $ENACW_p$ to the north). They attributed these differences to remineralisation of organic matter, using Apparent Oxygen Utilisation (AOU) to support this hypothesis. AOU is calculated from the difference between the measured DO concentration and the equilibrium saturation concentration at the temperature and salinity of the sample. Negative values (equivalent to DO < 100 % saturation) indicate the utilisation of oxygen for the oxidation of NH_4^+ to NO_2^- and of NO_2^- to NO_3^-. In this study, DO saturation was on average 59.2 ± 1.2 % at the bottom of the ría and DO concentrations were lower than those published for $ENACW_p$ (Pérez et al., 1993), suggesting that remineralisation was responsible for the increased nutrient concentrations in the rías relative to source $ENACW_t$.

4.3.2. Nutrient characteristics during the upwelling and downwelling seasons

Nitrate, PO_4^{3-} and Si displayed significant negative correlations with temperature for both seasons combined (Table 4.8). For September alone, the correlation coefficient was much lower for NO_3^- and was insignificant for PO_4^{3-} and Si. This could be attributed to the fact that the ría was not affected by upwelling at that time of year, thus other processes altering nutrient concentrations were predominant. The relationship between nutrients and temperature is to be expected in upwelling systems, where nutrients are drawn down by phytoplankton concurrently with warming of upwelled water as it ages (Dugdale et al., 1989). DO was also significantly correlated with temperature, indicating that recently upwelled water had lower concentrations than the surface water in the ría, because DO is produced in the surface by photosynthesis, but is utilised at depth by heterotrophic and chemical remineralisation of organic matter.

Total DIN (= $NO_3^- + NO_2^- + NH_4^+$) was significantly correlated with PO_4^{3-} and Si in both seasons. Total DIN was used rather than NO_3^{3-} due to the high contribution of NH_4^+, and this yielded higher correlation coefficients than NO_3^- alone. Álvarez-Salgado et al. (2002) compiled data from upwelled ENACW water at various stations on the continental shelf (depth > 1000 m) sampled during a number of cruises between 1977 and 1998 and found a significant relationship between NO_3^{3-} and PO_4^{3-}, with a slope of 17.9. A stronger correlation may have been obtained by including $NO_2^- + NH_4^+$, although concentrations of these nitrogen forms are generally low in shelf waters (Álvarez-Salgado et al., 1997). Ammonium can be produced either from primary recycling in the euphotic zone, with a time-scale of hours to days (e.g. excretion), or from secondary recycling, also known as nutrient trapping, which occurs in deeper waters or at the sediment-water interface on a time-scale of days to weeks. The latter occurs as a result of organic matter export from the rías and subsequent sinking on the continental shelf. Within the rías, mussel excretion represents an input of 2-3 μmol NH_4^+ $(g\ mussel)^{-1}\ h^{-1}$ (Smaal & Prins, 1993), while sinking faecal matter supports high benthic (secondary) remineralisation rates (Baudinet et al., 1990). Ammonium regeneration rates measured in this study were high (mean 0.20 ± 0.07 and 0.13 ± 0.04 μmol N $l^{-1}\ h^{-1}$ in September and June, respectively), on average 5-fold higher than $\rho(NH_4^+)$ in September but similar to $\rho(NH_4^+)$ in June. This confirms the importance of pelagic primary recycling as a source of NH_4^+, which is sufficient to support uptake by phytoplankton in early summer. Furthermore, secondary recycling is high in the

organically rich sediments of the shelf adjacent to the Rías Baixas, due to the presence of large populations of benthic organisms (López-Jamar et al., 1992). The very low f-ratios measured in the present study (0.10 ± 0.01 in September and 0.22 ± 0.05 in June) also underline the importance of recycled nitrogen for phytoplankton growth.

The DIN:P ratio of 17.5 obtained for June from the regression of DIN vs PO_4^{3-} was similar to those reported for upwelled $ENACW_t$ (Pérez et al., 1993; Álvarez-Salgado et al., 2002). On the other hand, the DIN:P ratio derived from linear regression in September was only 7.2, indicating that phytoplankton growth at this time was nitrogen-limited. The lowest ratios were measured at the bottom of the ría (~35 m), where PO_4^{3-} concentrations were highest (>0.5 μmol l^{-1}), but DIN concentrations were relatively low because NO_3^- concentrations did not increase with depth. However, individual DIN:P ratios ranged from 7.2 to 25.3 and the mean of all calculated ratios was 13.5 ± 0.45, therefore the severity of nitrogen limitation was perhaps overestimated by linear regression. In June, DIN:P ratios in surface waters ranged from 0.5, when DIN was depleted, to 34.2 at higher DIN concentrations. The difference in the range of DIN:P ratios measured in September and in June can be attributed to the presence of high DIN concentrations in the upwelled water in June (10 to 18 μmol l^{-1}) at PO_4^{3-} concentrations of 0.6 to 0.9 μmol l^{-1}, whereas in September similar PO_4^{3-} concentrations corresponded to DIN concentrations <9 μmol l^{-1}.

NO_3^-: PO_4^{3-} ratios below Redfield (between 5.5 and 9.3) were also measured in the Ría de Ferrol, although the seasonal pattern was the opposite, whereby low ratios were measured in late spring-early summer and high ratios (18.3 ± 1.6) were measured in September (Bode et al., 2005). The N:P ratio of upwelled ENACW water is generally close to the Redfield ratio (Pérez et al., 1993), therefore higher ratios would be expected during the upwelling season. Indeed, in this study ratios ~16 were measured in June in the deep, cold, nutrient-rich (i.e. recently upwelled) waters. As upwelled water ages, N:P ratios decline as nutrient concentrations are altered by various biogeochemical processes. Whereas photosynthesis and nitrification follow Redfield stoichiometry, denitrification, nitrogen fixation and anaerobic ammonium oxidation (Anammox) can cause departures from this ratio. Large NO_3^- deficits (ΔN ~20 to 40 μmol l^{-1}) can be used as an indicator of denitrification (Tyrrell & Lucas, 2002). In this study, ΔN values ranged from < 1 to13 μmol l^{-1} and the highest values were found near the bottom of the ría. These relatively low values, together with the lack of "LNP" points (depleted NO_3^- and high PO_4^{3-}) suggest that denitrification was not significant in this study. Also,

denitrification must occur in anoxic waters and the Iberian shelf is generally well oxygenated (Álvarez-Salgado et al., 1997).

Different remineralisation rates for different nutrients will modify the nutrient ratios of the source water, therefore more rapid recycling of Si and PO_4^{3-} relative to NO_3^- will enhance the relative enrichment of these two nutrients and lower N:P and N:Si ratios. More rapid recycling of PO_4^{3-} relative to NO_3^- has been observed in the laboratory (Garber, 1984) and in the field (Harrison, 1980), including the Galician Rías (Prego, 1993) and this can prevent complete organic nitrogen oxidation if the residence time of organic matter in the lower water column is relatively short. On the shelf, the ratio of remineralised DIN to remineralised PO_4^{3-} was found to be lower than Redfield (12.2-15.0) in a study using a simple mixing model to estimate the relative contributions of nutrients from source waters and from remineralisation (Álvarez-Salgado et al., 1997), although in a later study using regression analysis of ΔNO_3^- versus ΔPO_4^{3-}, Álvarez-Salgado et al. (2002) found a remineralisation ratio close to Redfield (16.4) on the Iberian shelf. In the present study, ΔNO_3^- and ΔPO_4^{3-} were significantly correlated both in June and in September, with correlation coefficients of 5.1 and 1.3, respectively (Table 4.8), indicating that PO_4^{3-} was remineralised preferentially to NO_3^- relative to Redfield stoichiometry (Harrison, 1980). The ratios obtained in this study are several-fold lower than the values of 12.2-16.4 and 8.0-18.5, respectively, reported for the Iberian (Álvarez-Salgado et al., 1997, 2002) and NW African upwelling systems (Rowe et al., 1977; Treguer & Le Corre, 1979). This would suggest that the difference between the recycling rates of PO_4^{3-} and NO_3^- is even more pronounced within the rías than on the open shelf.

In the present study, Si:DIN ratios were lower in June (0.32) than in September (1.02) and were generally lowest at the bottom of the ría in September, whereas in June they were lowest in the surface. The ratio for June is within the range published for $ENACW_t$ (0.29-0.40) (Pérez et al., 1993; Álvarez-Salgado et al., 1997), indicating that in September recycling processes caused a departure from the nutrient ratios typical of upwelled water. The $\Delta Si:\Delta NO_3^-$ ratio was lower in June (0.36) relative to September (2.20), indicating that Si was remineralised more rapidly in September.

Relationship	a	b	r	n	Area	Season	Authors
DIN vs PO_4	17.46	-0.44	0.96**	67	Ría de Vigo	June	This study
	7.17	1.75	0.91**	80	Ría de Vigo	Sept	This study
	17.9	-0.34	0.97**	685	Iberian Shelf (>1000 m)	All year	Álvarez-Salgado et al. (2002)
Si vs DIN	0.32	2.21	0.66**	67	Ría de Vigo	June	This study
	1.02	-0.39	0.88**	80	Ría de Vigo	Sept	This study
DIN vs temp	-1.97	38.6	-0.89**	67	Ría de Vigo	June	This study
NO_3 vs temp	-1.78	32.9	-0.92**	67	Ría de Vigo	June	This study
	-0.40	8.73	-0.40**	80	Ría de Vigo	Sept	This study
	-3.43	50.6	-0.93**	692	Iberian Shelf (>1000 m)	All year	Álvarez-Salgado et al. (2002)
PO_4 vs temp	-0.10	1.98	-0.79**	67	Ría de Vigo	June	This study
	0.13	-1.94	0.31*	80	Ría de Vigo	Sept	This study
	-0.18	2.73	-0.92**	685	Iberian Shelf (>1000 m)	All year	Álvarez-Salgado et al. (2002)
Si vs temp	-0.45	11.69	-0.42**	67	Ría de Vigo	June	This study
	0.81	-10.04	0.20	80	Ría de Vigo	Sept	This study
DO vs temp	11.98	13.65	0.80**	67	Ría de Vigo	June	This study
	-2.9	305.9	0.07	80	Ría de Vigo	Sept	This study
ΔDIN vs ΔPO_4	12.41	0.00	0.91**	67	Ría de Vigo	June	This study
ΔNO_3 vs ΔPO_4	5.10	0.00	0.51**	67	Ría de Vigo	June	This study
	1.28	0.00	0.53**	80	Ría de Vigo	Sept	This study
	16.4	0.00	0.8**	685	Iberian Shelf (>1000 m)	All year	Álvarez-Salgado et al. (2002)
ΔSi vs ΔDIN	0.73	0.00	0.69**	67	Ría de Vigo	June	This study
ΔSi vs ΔNO_3	0.36	0.00	0.28*	67	Ría de Vigo	June	This study
	2.20	0.01	0.52**	80	Ría de Vigo	Sept	This study
	0.48	0.00	0.73*	609	Iberian Shelf (>1000 m)	All year	Álvarez-Salgado et al. (2002)
ΔDIN vs ΔDO	0.10	0.00	0.89**	67	Ría de Vigo	June	This study
ΔNO_3 vs ΔDO	-0.041	0.00	-0.49**	67	Ría de Vigo	June	This study
	5.00	-0.64	0.11	80	Ría de Vigo	Sept	This study
ΔPO_4 vs ΔDO	-0.007	0.00	-0.88**	67	Ría de Vigo	June	This study
	-2.44	-0.65	0.02	80	Ría de Vigo	Sept	This study

Table 4.8. Slope (a) and y axis intercept (b) derived from linear regression between various parameters in this study and in Álvarez-Salgado et al. (2002). * $p < 0.05$ and ** $p < 0.01$; n = number of observations.

4.3.3. Nitrogen uptake during the upwelling and downwelling seasons

Nitrogen uptake rates in this study were significantly higher during the upwelling season relative to the downwelling season, with a mean total ρ(N) of 0.30 ± 0.03 μmol N l^{-1} h^{-1} in the former and 0.07 ± 0.01 μmol N l^{-1} h^{-1} in the latter. The *f*-ratio was also significantly higher in June, although NH_4^+ remained the principal source of available nitrogen, therefore *f*-ratios were low in both seasons (0.12 ± 0.02 in September and 0.17 ± 0.03 in June). This is surprising, since one would expect the *f*-ratio to be >0.5 in June, when upwelling supplies high NO_3^- concentrations and NH_4^+ regeneration rates are low (Nogueira et al., 1997). This was the case in the Benguela study (Chapter 3), where a significant positive correlation was observed between northward wind component and the *f*-ratio. Published *f*-ratios for the California upwelling system are high, ranging from 0.4 to 0.8 (Dugdale et al., 2006). In the Benguela, they can range from <0.1 to ~1, with an average of 0.39 ± 0.03 (Probyn, 1992). In the Iberian system, the upwelling season-averaged *f*-ratio is 0.33, lower than in the California current but similar to the Benguela (Álvarez-Salgado et al., 2002).

Bode et al. (2005) measured higher $\rho(NO_3^-)$ relative to $\rho(NH_4^+)$ in the Ría de Ferrol in July, when NO_3^- concentrations were higher than NH_4^+ (although still <1 μmol N l^{-1}), but the opposite in September, when NH_4^+ concentrations were higher. In the present study, NH_4^+ appeared to be taken up preferentially to NO_3^- in both seasons. For example, $\rho(NH_4^+)$ was 3- to 7-fold higher than $\rho(NO_3^-)$ at stations B5 and B3 in September despite higher NO_3^- concentrations. This difference was even more pronounced (8- to 14-fold) at B2, where NH_4^+ was more abundant than NO_3^-. With one exception, $\rho(NO_3^-)$ was highest (0.02-0.12 μmol N $l^{-1}h^{-1}$) at NH_4^+ concentrations <0.5 μmol N l^{-1}, and remained <0.02 μmol N $l^{-1}h^{-1}$ at higher concentrations, suggesting that $\rho(NO_3^-)$ was inhibited by NH_4^+. Both preferential uptake of NH_4^+ relative to NO_3^- and inhibition of NO_3^- uptake by NH_4^+ have been widely reported [see review by Dortch (1990)]. These phenomena are linked to the lower energetic cost of NH_4^+ assimilation relative to NO_3^-, which must first be reduced intracellularly to NO_2^- then to NH_4^+ before the latter can be synthesised into amino acids and proteins. Nitrogen uptake kinetics parameters can indicate preference, whereby a higher v_{max} for NH_4^+ than for NO_3^- would suggest preference for NH_4^+ over NO_3^-. The presence of NH_4^+ in NO_3^- kinetics experiments, however, can potentially cause inhibition of NO_3^- uptake and bias the results (Dortch, 1990; Collos et al., 2004).

A nitrogen uptake kinetics experiment was carried out on a mixed diatom assemblage in June, with an ambient NH_4^+ concentration of 0.33 µmol N l^{-1}. This was below the range of concentrations generally thought to inhibit NO_3^- uptake (Syrett & Morris, 1963; Goering et al., 1970), therefore the ratio $\nu_{max}(NH_4^+)$: $\nu_{max}(NO_3^-)$ of 12.8 should indicate a genuine preference for NH_4^+, rather than inhibition. According to Dortch (1990), the $K_s(NH_4^+)$: $K_s(NO_3^-)$ of 9.1 should indicate a preference for NO_3^-, however the inadequacy of K_s as a measure of nutrient affinity under certain conditions has been established (Healey, 1980; Aksnes & Egge, 1991) therefore the ratio of $\alpha(NH_4^+)$: $\alpha(NO_3^-)$ is perhaps more appropriate. In this study, the α ratio was 1.4, confirming that NH_4^+ was preferred, although the preference was more strongly expressed at saturating concentrations (higher ν_{max}) relative to limiting concentrations (higher α).

The observed covariation in K_s and ν_{max} between species is well documented (Healey, 1980; Aksnes & Egge, 1991; Collos et al., 2005) and suggests that phytoplankton can adapt either to high nutrients (by increasing ν_{max}) or to low nutrients (by reducing K_s), but not both together. In this case, the phytoplankton community was adapted to high NH_4^+ concentrations at the expense of a poor adaptation to high NO_3^- concentrations. It must be noted here that such experiments carried out on a mixed assemblage produce species-averaged values of K_s and ν_{max}, which makes their interpretation more difficult. The ratios $\nu_{max}(NH_4^+)$: $\nu_{max}(NO_3^-)$ and $K_s(NH_4^+)$: $K_s(NO_3^-)$ were several-fold higher than those measured in the Benguela (Chapter 3), which were 1.2 and 1.1 for *Pseudo-nitzschia* spp. and 4.0 and 0.8 for *Dinophysis acuminata* (Table 3.4). Although $\nu_{max}(NH_4^+)$: $\nu_{max}(NO_3^-) > 1$ was observed in 13 out of the 16 other studies where the ratio could be calculated (Table 3.7), comparably high ratios were only measured in the Neuse and Choptank Estuaries on the US east coast. Furthermore, the Choptank Estuary measurement of $\nu_{max}(NH_4^+)$ was the only one higher than that measured in the Ría de Vigo. The experiment also revealed a preference for urea over NO_3^-, with a ν_{max}(urea): $\nu_{max}(NO_3^-)$ ratio of 2.6, although the α ratio of 1.0 revealed no preference at limiting concentrations. Higher ν_{max} for urea than for NO_3^- was observed at 8 of the 13 other experiments, with ratios ranging from 1.4 to 9.2, although these ratios were generally lower than for NH_4^+.

The low ν_{max} and K_s measured for NO_3^- indicate that large increases in NO_3^- concentration would not have increased $\nu(NO_3^-)$ by more than 2-fold, since at the ambient NO_3^- concentration of 0.53 µmol N l^{-1}, $\nu(NO_3^-)$ was 50 % of ν_{max}. A urea addition of 30 µmol N l^{-1} would have increased ν(urea) by a mere 32 %, but on the other

hand, $\rho(NH_4^+)$ would have increased 7-fold with an NH_4^+ addition of 5 μmol N l^{-1}, therefore NH_4^+, and not NO_3^- or urea appeared to be limiting phytoplankton growth.

Nitrate uptake rates in June were on average 10-fold lower than those measured in the California (Dugdale et al., 2006) and Benguela upwelling systems (Probyn, 1992) and 7-fold lower than the maximum values measured in the Cap Blanc upwelling region (Dugdale et al., 1990). They were, however, one order of magnitude higher than those measured in the Ría de Ferrol in both June and September [A. Bode, pers. comm., revision of data originally published in Bode et al. (2005)]. It must be noted that in the Ría de Ferrol 24 h incubations were carried out, therefore including dark uptake, which this study did not. This could contribute significantly to the difference in uptake rates.

PN-specific rates were particularly high in June (0.026 ± 0.004) relative to September (0.005 ± 0.001) and to the values obtained in the Benguela (0.006 ± 0.0004). However, due to the relatively low biomass, this did not lead to higher ρ(N), which was of the same order of magnitude as in the Benguela. According to Dugdale et al. (1990), $\nu(NO_3^-)$ is a function of ambient NO_3^- and if biomass accumulation occurs as a result of the "shift-up" in $\nu(NO_3^-)$, then $\rho(NO_3^-)$ will increase non-linearly with $\nu(NO_3^-)$. Here, $\nu(NO_3^-)$ and $\rho(NO_3^-)$ were linearly correlated, indicating that no biomass accumulation had occurred. This low realisation of potential new production was also observed at Point Conception in the California current and attributed to strong advection and turbulence (Dugdale et al., 2006). In this study, although the water column was stratified, the positive estuarine circulation that prevails during upwelling causes organic matter export out of the ría (Estrada, 1984; Figueiras et al., 1994), which could explain the low biomass accumulation. Grazing, which is particularly high in the rías due to mussel cultivation (Fernández-Reiriz et al., 2007) and the presence of microheterotrophs during summer (Figueiras & Pazos, 1991b), will also strongly control phytoplankton biomass.

4.3.4. Community structure

4.3.4.1. Comparison between upwelling and downwelling seasons

Results of cluster analyses showed that the upwelling and downwelling phytoplankton communities were statistically distinct at the 50 % similarity level, whereby the downwelling community was dominated by a mixture of dinoflagellates and flagellates, and the upwelling community was dominated by diatoms. This is consistent with the trend observed by Crespo et al. (2006) in a 1-year time-series of phytoplankton community structure in the Ría de Vigo, showing that the 2 surveys carried out in this study were fairly typical of the respective seasons. However, Crespo et al. (2006) reported a much larger dinoflagellate bloom than in this study, with chl-a concentrations reaching 14 $\mu g\ l^{-1}$, whereas in this study they were < 7 $\mu g\ l^{-1}$. The association of diatoms with upwelling is regularly observed in the Iberian (Figueiras & Rios, 1993), NW African, (Estrada & Blasco, 1985), Benguela (Fawcett et al., 2007) and California currents (Lassiter et al., 2006). In the Iberian system, this association has been described by a linear correlation between diatom abundance and the upwelling index (Figueiras & Rios, 1993). Diatoms are thought to be well adapted to the dynamic conditions that prevail in upwelling systems, since they have high nutrient uptake and growth rates and are able to adjust their physiology as a "shift-up" response to increased nutrient concentrations and light (Dugdale et al., 1990; Kudela et al., 1997). Thus, they are able to exploit the windows of opportunity that are created during the upwelling-relaxation-stratification cycles, when these occur at an optimum frequency (Legendre & Le Fèvre, 1989). Furthermore, upwelling favours large diatoms that would otherwise sink out of the euphotic zone (Estrada & Blasco, 1985). Dugdale et al. (1990) found that increased nutrient uptake rates measured in diatom communities in newly upwelled water are proportional to nutrient concentration, and that nutrient exhaustion occurred after 3 days of upwelling relaxation regardless of the initial nutrient concentration (Dugdale et al., 1990).

In contrast, the occurrence of dinoflagellates is generally linked to longer periods of upwelling relaxation and depleted nutrients (Pitcher et al., 1993a; Fawcett et al., 2007) and are generally associated with more stratified offshore waters (Tilstone et al., 1994; Pitcher et al., 1998). In the Galician Rías, dinoflagellate blooms are known to occur during the downwelling season (late summer/autumn) (Figueiras & Rios, 1993). This is

thought to be due to the establishment of dinoflagellate populations in the stratified shelf waters and subsequent advection into the rías where they accumulate at the downwelling front (Fraga et al., 1988; Fraga et al., 1993; Pazos et al., 1995b; Sordo et al., 2000) following wind reversal and the formation of a warm, poleward current (Fraga et al., 1993). A similar mechanism has been proposed for the formation and onshore advection of red tides in the coastal waters of the Benguela current (Pitcher et al., 1998). Furthermore, the reversal of circulation that leads to downwelling is thought to favour selection of highly motile species such as *G. catenatum*, that can maintain themselves in the surface layer (Fraga et al., 1988; Figueiras et al., 1994; Fermin et al., 1996).

4.3.4.2. Spatial and temporal variations in September

In September, nutrient concentrations were relatively high throughout the water column, hence chl-a and phytoplankton cell concentrations were generally high in the top 10 m, where they were not light-limited. Cell concentrations declined rapidly below this depth, particularly concentrations of small flagellates. The decline in chl-a was less pronounced, due to the shift from smaller to larger cells with depth, as was observed in June. The increase in chl-a on 30 September was accompanied by an increase in the proportion of nanoplankton and a decrease in the proportion of microplankton, while the phytoplankton count data revealed that *Prorocentrum* spp. increased by one order of magnitude.

Clusters I and II comprised only shallow samples (<10 m), whereas Clusters III and IV comprised mainly deep samples, but also the shallow samples from 30 September. At the start of the survey, B2 clustered separately from B3 and B5, whereas at the end samples from all 3 stations were found in the same clusters, indicating that community structure became relatively homogeneous along the ría towards the end of the survey. Furthermore, samples from all depths clustered together at the end of the survey, consistent with the occurrence of downwelling and mixing of the water column observed in the hydrographic data.

At the start of the survey, surface samples were divided into Clusters I and II, whereby Cluster I comprised the innermost station B2 and Cluster II comprised the outer stations B5 and B3. This suggests that B2 was characterised by remnants of the phytoplankton community that was present in the ría before reversal of circulation occurred. This is supported by the higher concentrations of diatoms and lower

concentrations of flagellates relative to Cluster II and also by the higher concentrations of PO_4 and Si. The phytoplankton community in Cluster I was characterised by contributions from the diatoms *Chaetoceros* spp. and *Thalassiosira rotula*, as well as the raphidophyte *Heterosigma akashiwo* and the dinoflagellate *Scrippsiella trochoidea*. This mixture of small diatoms and dinoflagellates has been reported for the late upwelling season (June-August) in the Ría de Vigo (Crespo et al., 2006), during periods of weak stratification in between upwelling pulses. This provides evidence that this community had remained from a previous upwelling period.

Cluster II comprised outer stations (B5, B3) from the beginning and middle of the survey as well as the inner station B2 from 29 September, suggesting that an influx of water carried the phytoplankton population into the ría during the survey. This inflow and accumulation of water in the ría could explain why there were little horizontal differences in community structure on 30 September. Cluster II had the lowest proportion of diatoms, the highest proportion of flagellates and was characterised by the presence of *Ceratium fusus* and *Ceratium furca*, suggesting that these species tend to bloom in the shelf waters and are subsequently transported into the ría. This is consistent with a study by Figueiras & Pazos (1991b). *C. fusus* and *C. furca* were also found to reach maximum abundance in late September in the time-series study by Crespo et al. (2006), suggesting that these species are typical members of the downwelling community. The cluster was also characterised by lower NH_4^+, PO_4^{3-} and Si concentrations and the highest DIN:P ratios, consistent with the oceanic origin of these waters.

Cluster III had the highest proportion of diatoms, including the large diatom *Guinardia delicatula*. The nutrient requirements of these large cells were met by high concentrations of NH_4^+, PO_4^{3-} and Si relative to the other clusters. Also, DIN:P ratios were lower and Si:DIN ratios were higher than in the other clusters. This cluster comprised samples from B2 below 20 m on 29 September and from B5 and B3 at ~30 m, suggesting that it could represent water that had downwelled and was exiting the ría along the bottom, consistent with previous studies (Tilstone et al., 1994; Fermin et al., 1996; Crespo et al., 2006).

Cluster IV, on the other hand, had a significantly higher proportion of dinoflagellates relative to Clusters II and III and significantly lower NH_4^+, PO_4^{3-} and Si concentrations than Cluster III but significantly higher DIN:P ratios. Therefore,

dinoflagellates appeared to be more successful at high DIN:P ratios (or to be the cause of these high ratios), whereas the opposite was observed in diatoms.

4.3.4.3. Spatial and temporal variations in June

In June, a subsurface chl-a maximum was observed, as previously reported in the Rías Baixas during periods of moderate upwelling, and is thought to be linked to a deeper (9~50 m) chl-a maximum on the shelf (Figueiras & Pazos, 1991b). However, diatom concentrations and dominance were generally high at the surface despite the low nutrient concentrations. At B2, they were even higher at the surface than at the thermocline, although a chl-a maximum was present, and particularly prominent on 28 June. This discrepancy suggests that the chl-a maximum at B2 was dominated by fewer, larger cells. Indeed, the samples from the surface and from the chl-a maximum clustered separately (Clusters I and II, respectively), although both clusters were numerically dominated by small diatoms (*Skeletonema costatum*, *Leptocyclindrus* spp., *Nitzschia* cf. *americana*). Closer examination of the cell count data from 28 June shows that the giant diatoms *Rhizosolenia stolterfothii* [3-61 μm diameter, 80-168 μm length (Sherer, 1965)] and *Dactyliosolen fragilissimus* [8-70 μm diameter, 42-300 μm length (Hasle & Syvertsen, 1996)] and the relatively large diatom *Eucampia zoodiacus* [8-80 μm length (Syvertsen & Hasle, 1983)] reached concentrations $\geq 10^4$ cells l^{-1} at 12 m, i.e. one order of magnitude higher than at 3 m. Dinoflagellates were also more abundant (~20 %) at 12 m and they also contributed significantly to the microplankton fraction, as shown by the linear correlation between dinoflagellate concentrations and microplankton chl-a. Furthermore, the proportion of microplankton (>20 μm) was always greater at the chl-a maximum than at the surface (data not shown), confirming that the chl-a maximum was formed by large diatoms and, to a lesser extent, dinoflagellates. Thus, diatoms were generally more successful at the thermocline relative to the surface, consistent with a study by Figueiras & Pazos (1991), although small diatoms (e.g. *Nitzschia* cf. *americana* and *Nitzschia longissima*) were sometimes much more abundant at the surface. Their small size and high surface to volume ratio would imply a lower nutrient requirement, as shown by the positive correlation between minimum cell-specific nitrogen quota and cell volume (Aksnes & Egge, 1991; Litchman et al., 2007), which would give them an advantage under nutrient-depleted conditions.

The phytoplankton community present in June was typical of the summer upwelling season (Crespo et al., 2006), characterised by the dominance of small diatoms such as *Chaetoceros* spp., *Skeletonema costatum* and *Leptocylindrus* spp. (but also the giant diatom *Rhizosolenia stolterfothii* in Cluster IV), coexistent with cryptophytes and dinoflagellates such as *Gymnodinium* spp. This type of community was found in the deeper samples of Clusters III and IV (with 6-66 % dinoflagellates), whereas the shallower Clusters I and II were more exclusively dominated by diatoms (77-99 %).

Variability in community structure was linked to spatial (horizontal and vertical) rather than temporal changes since clusters were divided into (I) inner ría, euphotic layer, (II) outer ría, euphotic layer, (III) inner ría, deep water and (IV) outer ría, deep water, with no apparent temporal segregation of the stations. The shallower samples (Clusters I and II) both had significantly higher proportions of diatoms than the deeper samples and a significantly lower percentage of dinoflagellates (with the exception of I vs III). This is somewhat contrary to what one would expect, since the deeper water would have originated from upwelling on the shelf, which is generally thought to contain diatoms, as these are more tolerant of turbulence. However, the presence of high proportions of dinoflagellates in deeper samples from the more stratified outer ría is consistent with previous studies (Tilstone et al., 1994).

Species characterising the deeper clusters included *Nitzschia longissima* and *Pseudo-nitzschia delicatissima*, which were also found below the chl-a maximum in the Rías de Vigo and Arousa (Figueiras & Pazos, 1991b), where it was identified as typical of high nutrient conditions during upwelling. Indeed, these clusters could be linked with high nutrient conditions, since they were associated with higher NH_4^+, PO_4^{3-} and Si concentrations than the outer surface Cluster II (although concentrations were as high in the inner surface Cluster I). Interestingly, NO_3^- concentrations did not seem to have any effect on community structure in either June or September. The DIN:P ratio, however, was higher and the Si:DIN ratios were lower in the deeper samples.

Both inner and outer ria surface clusters were dominated by diatoms, therefore nutrient availability did not appear to affect competition between diatoms and dinoflagellates. H' was lowest for Cluster I, followed by Cluster II, then Clusters III and IV, indicating that diversity increased with depth and towards the mouth of the ría. Therefore, there was no clear link between H' and nutrient availability, although diversity appeared to increase with diminishing irradiance. The high phytoplankton diversity generally observed in natural assemblages has been attributed to the fact that

different species are limited by different resources. Therefore, they can coexist at competitive equilibrium, whereby their relative abundances are controlled by the ratios of the limiting nutrients (Tilman, 1977; Tilman et al., 1982). Chemostat experiments have shown that pulsed nutrient additions can increase the number of species and H' relative to steady state conditions (Sommer, 1984) therefore the higher diversity measured at depth could be linked to weak upwelling pulses that do not affect surface waters. Furthermore, the higher DIN:P ratios were consistently associated with the highest dinoflagellate and lowest diatom contributions and highest H', suggesting that a DIN:P ratio close to Redfield favours dinoflagellates over diatoms, but also increases species diversity. The Redfield ratio is not a universal optimum ratio for phytoplankton, but rather the average of the various N:P requirements of different phytoplankton groups (Klausmeier et al., 2004; Arrigo, 2005). Thus, different groups exhibit different cellular N:P ratios. For example, the red and green phytoplankton superfamilies exhibit ratios of 27 and 10, respectively. Although there is no evidence of lower N:P requirements in diatoms relative to dinoflagellates, diatoms do exhibit lower N:P ratios relative to *Phaeocystis* spp. (Arrigo, 2005), although there is a high degree of interspecific variability within the diatom group (11.1 to 29.2 for 6 diatom species) (Klausmeier et al., 2004). Furthermore, N:P requirements vary under different ecological scenarios (competitive equilibrium and exponential growth) (Klausmeier et al., 2004; Arrigo, 2005).

4.3.4.4. HAB species

HAB species were present during both seasons and included species known to produce toxins in the Rías Baixas and historically known to pose a threat to the mussel farming industry, namely *Dinophysis* spp. and *Gymnodinium catenatum*. *G. catenatum* was only observed during the downwelling season, consistent with its swimming abilities and its adaptation to downwelling conditions (Fraga et al., 1988; Figueiras et al., 1994). While *D. acuta* was observed only in September, *D. acuminata* was more abundant during the upwelling season, showing temporal segregation of the 2 species consistent with previous studies in the rías (Fraga et al., 1988; Figueiras et al., 1994) but also with their spatial segregation (Reguera et al., 1993b). Both *D. acuta* and *G. catenatum* were most abundant in Cluster II, which characterised the inflow of shelf water into the ría. This is consistent with the hypothesis that HAB formation is caused

by advective processes rather than *in situ* growth (Fraga et al., 1993; Pazos et al., 1995b; Sordo et al., 2000). In September, *Dinophysis acuta* was generally restricted to the top 10 m during most of the survey, although on 30 September it was distributed throughout the water column, due to the occurrence of downwelling. Furthermore, the increase in cell concentrations on this date shows that *D. acuta* was favoured by these downwelling conditions. *Dinophysis caudata* was also spatially segregated from *D. acuta*, as it was generally found at deeper depths.

Other HAB species included the ichthyotoxic raphidophyte *Heterosigma akashiwo* in September that was most abundant at B2 at the start of the survey, then throughout the ría at the end. Although they are not toxic, *Ceratium* spp. are also known to form dense blooms that can lead to anoxia and these species also appeared to be advected into the ría and accumulate at the downwelling front. *Pseudo-nitzschia delicatissima* and *P. seriata* are potential domoic acid producers, although they have not been associated with toxic outbreaks in the rías. *P. delicatissima* was present at similar concentrations in September and in June, whereas *P. seriata* was 2 to 3 orders of magnitude higher in June. This suggests that *P. delicatissima* was successful under both upwelling and downwelling regimes, especially since it increased in abundance on 30 September, whereas *P. seriata* was better adapted to the upwelling season, although in both cases they displayed a subsurface maximum.

Since the HAB species were generally a small component of the phytoplankton community, it was difficult to determine whether they displayed particular nitrogen uptake strategies. However, the occurrence of *Dinophysis acuta* and *Gymnodinium catenatum* exclusively during the downwelling season, concurrently with high NH_4^+ concentrations and regeneration rates and very low *f*-ratios, suggests that they require high NH_4^+ concentrations in order to bloom. This study showed that urea is also a significant source of nitrogen supporting the growth of these species.

4.4. Conclusion

The two surveys carried out showed contrasting situations in terms of hydrography, nutrient concentrations, ratios and remineralisation, nitrogen uptake and community structure. In September, circulation in the ría was characterised by downwelling, which intensified during the survey. An influx of lower nutrient water was observed, carrying a dinoflagellate population characterised by *Ceratium* spp. and other dinoflagellates that replaced the existing assemblage of diatoms, *Heterosigma akashiwo* and *Scrippsiella trochoidea*. By the end of the survey, temperature and salinity in the ría were homogeneous, as was community structure, both horizontally and vertically. Ammonium uptake was greater and f-ratios were lower towards the head of the ría, where NH_4^+ concentrations were highest. Furthermore, $\rho(NH_4^+)$ was greater than $\rho(NO_3^-)$, even when NO_3^- concentrations were higher, demonstrating a preference of the phytoplankton assemblage for NH_4^+ over NO_3^- or inhibition of $\rho(NO_3^-)$ by NH_4^+. Urea uptake was also generally greater than $\rho(NO_3^-)$. DIN:P ratios were lower than those characteristic of ENACW (~Redfield), due to high remineralisation rates on the shelf and within the ría itself.

In June, positive estuarine circulation was observed, with upwelled ENACW entering the ría along the bottom and fresher water exiting the ría at the surface. Nutrients were depleted above the thermocline, whereas they were high in the deeper water. DIN: P ratios were on average similar to those of ENACW, although lower ratios were measured in the surface layer. The phytoplankton community was fairly typical of summer upwelling, largely dominated by diatoms in the surface, but including dinoflagellates in the deeper waters. Nitrogen uptake rates and f-ratios were higher than in September, although maximum potential new production was not realised due to organic matter export out of the ría, possibly combined with grazing control. Also, uptake was dominated by NH_4^+, which was preferred over NO_3^- and appeared to be limiting primary production. Two potentially toxic *Pseudo-nitzschia* species were present, as well as *Dinophysis acuminata*, showing that the upwelling season can potentially be conducive to HABs as well as the downwelling season.

5 Distribution and nitrogen nutrition of phytoplankton assemblages comprising *Alexandrium minutum* in the Fal Estuary

5.1. Introduction

5.1.1. General features of the Fal Estuary

The Fal Estuary is a ria, or drowned river valley situated in an area of high relief, which became submerged by post-glacial sea level rise. Situated on the south-east coast of Cornwall (~50°08 to 50°15 N and 5°00 to 5°05 W, Figure 5.1), it covers a total area of 28.4 km^2 and has a length of 18 km. Its entrance is marked by Pendennis Point, to the west, and St Anthony Head to the east. It comprises a number of inner tidal tributaries (Truro, Tresillian and Fal rivers) and an outer tidal basin, known as Carrick Roads, that discharges into Falmouth Bay (Figure 5.1). Maximum water depth is ~34 m in the central channel at the southern end of Carrick Roads, decreasing northwards to 12 m at Turnaware Point and 5 m in King Harry Reach (Figure 2.3). To either side of the channel, depths can be as shallow as 0.3 m. Falmouth Harbour, on the western side of Carrick Roads, is the world's third largest natural deepwater harbour.

The estuary is tidal up to Tresillian, being macrotidal (>4 m tidal range) at Falmouth but mesotidal (2-4 m) at Truro, with maximal spring tidal ranges of 5.3 m and 3.5 m, respectively. Freshwater flows are generally low, as is typical of rias, with maximum measured flow rates of 0.025 m s^{-1} during springs and 0.013 m s^{-1} during neaps. Tidal currents are generally below 0.4 m s^{-1} during springs and 2-3 times lower during neaps [Posford-Duvivier (1992), cited in Percy (2006)].

Two main urban centres are situated on the estuary: Falmouth, on the south-western side, and Truro, at the northern extremity. Both are popular tourist attractions and the estuary is used extensively for recreational activities as well as commercial shipping. Falmouth Docks receive cargo ships and cruise liners and provide a range of services including bunkering and ship repair. As a result, high levels of organotin are present in the water and sediments (Langston et al., 2003). In addition, mining activities carried out since the Bronze Age have resulted in severe heavy metal pollution (Sn, Cu, Pb, Fe), particularly in Restronguet and adjacent creeks (Langston et al., 2003).

Sewage treatment works in the upper estuary are located on the Truro River (Newham and Malpas), the River Fal (Tregony) and the Tresillian River (Ladock Valley) (Figure 5.1) and represent important sources of PO_4^{3-} and NH_4^+. Run-off from surrounding agricultural land (estimated at 719 mm yr^{-1} (Fraser et al., 2000)) represents an important source of NO_3^-. Hence, the estuary is subjected to hypernutrification, particularly in its upper reaches.

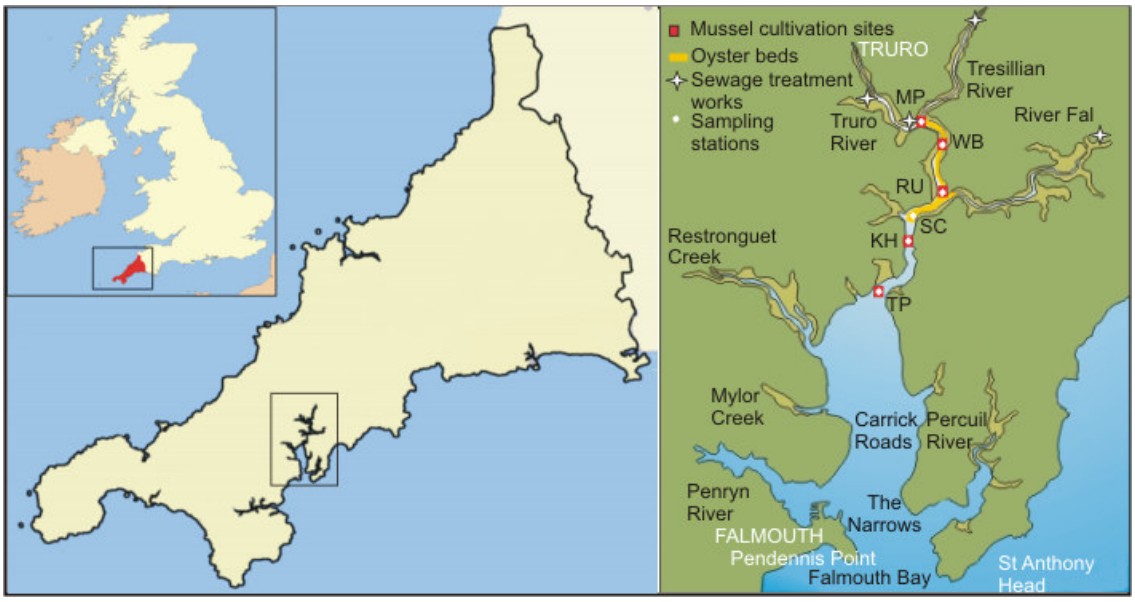

Figure 5.1. Location of the Fal Estuary on the south coast of Cornwall and map of the Fal Estuary showing the location of mussel cultivation sites, oyster beds, sewage treatment works and sampling stations. MP = Malpas; WB = Woodbury; RU = Ruan; SC = Smuggler's Cottage; KH = King Harry Reach; TP = Turnaware Point. N.B. only the oyster beds and sewage treatment works in the upper reaches of the estuary are shown since this is the area of interest to this study.

5.1.2. Shellfish and HABs in the Fal Estuary

The Fal Estuary is used for shellfish farming and harvesting of wild shellfish, both of which are threatened by the occurrence of HABs. The first HAB event in the Fal was reported in 1995 and attributed to *Alexandrium tamarense*, which reached a concentration of 313,000 cells l^{-1} (Reid & Pratt, 1995). A bloom of *Gyrodinium aureolum* (now known as *Karenia mikimotoi*) was observed in 2002 in the Helford River, which resulted in invertebrate mortalities (Langston et al., 2003).

A mussel farm was set up by Cornish Mussels Ltd. at King Harry Reach in 2001, producing 200 t mussels per year. The farm consists of five 20-m long Galician-type mussel rafts and blue mussels (also known as common mussels) *Mytilus edulis* are grown on 8-m ropes that hang from the rafts through the water column. Mussels are also grown on ropes hanging from Malpas, Woodbury, Ruan and Turnaware Pontoons (Figure 5.1). The Fal is also home to wild native European oyster (*Ostrea edulis*) populations that are harvested by Truro Fishery and intended for the international market. Scallop populations also exist in Falmouth Bay and these have been harvested since the late 1970's although the area is under a voluntary protection agreement. A complete ban on scallop dredging was recommended by Natural England in February 2008 and was to become effective in November 2008 (http://www.telegraph.co.uk/earth/earthnews/3335168/Scallop-dredging-to-be-banned-in-Fal-Bay.html).

The Fal estuary is included in the Biotoxin Monitoring Programme for England and Wales, a programme that has been carried out by the Centre for Environment, Fisheries and Aquaculture Science (CEFAS) under the direction of the Food Standards Agency (FSA) since 1999 (Higman & Milligan, 2000). Seawater samples are taken on a regular basis at a number of sites identified as historically prone to algal biotoxins, such as the Fal, and analysed for the presence of toxic phytoplankton species, i.e. *Dinophysis* spp., *Prorocentrum lima*, *Pseudo-nitzschia* spp. and *Alexandrium* spp. At certain sites, samples of shellfish flesh are routinely analysed whereas at others this is only carried out if the concentration of toxic phytoplankton exceeds the action limit. Action limits for the aforementioned species are 100 cells l^{-1} for *Dinophysis* spp. and *P. lima*, 150,000 cells l^{-1} for *Pseudo-nitzschia* spp., and simply the presence of *Alexandrium* spp. Maximum permitted concentrations of DSP, PSP or ASP are 80 µg STX equiv $(100g)^{-1}$, 16 µg OA equiv $(100g)^{-1}$ and 20 µg DA g^{-1}, respectively (Stubbs et al., 2008). If these are exceeded in 2 consecutive weekly samples then the harvesting area is closed until toxin

concentrations drop once again below the permitted concentrations in 2 consecutive samples.

Since 1999, *Alexandrium* spp. has been found regularly at several stations along the Fal between June and October. Maximum reported concentrations were 387,000 cells l^{-1} in July 1999 (Higman & Milligan, 2000), 89,100 cells l^{-1} in June 2000 (Higman et al., 2001) and 130,775 cells l^{-1} in June 2001 (Percy et al., 2004), although concentrations around 10,000 cells l^{-1} are more common during the summer months (Percy, 2006). Highest abundances tend to occur in June/July, followed by a smaller peak in August/September (Percy, 2006). In 2006, *Alexandrium* spp. were observed regularly throughout the summer months and persisted during winter, albeit at lower concentrations (Stubbs et al., 2007). In 2007, lower concentrations were measured throughout the summer (Stubbs et al., 2008).

PSP toxins have been detected in mussels at concentrations as high as 161 μg STX eq $(100g)^{-1}$ in 2000, which resulted in a shellfish fishery closure (Higman et al., 2001). Another closure occurred in July 2006, after toxin concentrations in excess of the regulatory limit were detected in shellfish samples from Malpas and Turnaware Pontoon (Stubbs et al., 2007).

Although the first reported HAB in 1995 was ascribed to *Alexandrium tamarense* (Reid & Pratt, 1995; Geatches, 1997), the species that bloomed in June 2001 was isolated and later identified as *A. minutum*, using molecular techniques as well as microscopy. *A. minutum* is now thought to be the main species occurring in the estuary, although low numbers of *A. tamarense* and *A. ostenfeldii* have also been reported (Percy, 2006).

Pseudo-nitzschia spp. also occur regularly in the Fal Estuary during the summer and have been observed at concentrations up to 10^6 cells l^{-1} in June 2001 (Percy, 2006). A domoic acid concentration of 3 μg g^{-1} was detected in scallops in 2000, which was the highest measured in the monitoring programme that year, although well below the maximum permitted concentration (Higman et al., 2001).

Dinophysis acuminata is generally present during the summer months, at concentrations <1,000 cells l^{-1}, although an unusually high concentration of 950,000 cells l^{-1} was reported in September 2002 in the Percuil River (Percy, 2006). DSP toxins were found in summer 2006 in oyster flesh from the River Penryn (Stubbs et al., 2007) and again in summer 2007 (Stubbs et al., 2008)

Literature on the occurrence of HABs in the Fal is generally scarce and limited to monitoring reports rather than ecological studies. It is thought that HABs may be linked to increased nutrient loading since the late 1980s (Langston et al., 2003) and the 1995 bloom was linked to low freshwater input and high temperatures and nutrient concentrations (Reid & Pratt, 1995). More recently, an intensive survey of the Fal revealed a maximum in "*A. minutum* type" (hereafter *A. minutum*) cell abundance towards the middle of the estuary (Turnaware Pontoon) and at 5-10 m depth in the Narrows (Figure 5.1) and identified the Percuil River as a potential source of cells to the estuary (Percy, 2006). Perez Blanco (2005, cited in Percy, 2006) identified the Percuil and Penryn Rivers and the area around Turnaware Point as potential seed beds. Laboratory studies revealed that cyst germination occurs over a range of irradiances (2 and 20 µmol photons m^{-2} s^{-1}), temperatures (8-24 °C) and salinities (15-30). The study concluded that the sediments provide a constant and rapid supply of vegetative cells to the water column, which under optimal growth conditions can lead to a bloom (Perez Blanco et al., 2009).

Relatively weak southerly winds (<6 m s^{-1}) and reduced rainfall/freshwater flow are conducive to *Alexandrium minutum* blooms, probably due to increased water column stability and reduced flushing rates (Percy, 2006). A study of historical data collected by CEFAS revealed that blooms did not occur in years when river discharge was particularly high in winter or >2 m^3 s^{-1} in summer (Morris, 2006).

A negative correlation between tidal height and *A. minutum* concentration in the Percuil River was also observed over a tidal cycle (Morris, 2006). Irradiance did not appear to limit *A. minutum* growth, since blooms were observed even after 7 days of low irradiance (150-200 W h^{-1} m^{-2}), consistent with the reported adaptation of *A. minutum* to low irradiance (Chang & McClean, 1997) (see section 5.1.3).

Percy (2006) showed that *Pseudo-nitzschia* abundance increased seaward, particularly during spring tides, displaying a maximum in Falmouth Bay (up to 1.1 x 10^7 cells l^{-1}), but reduced concentrations in the Penryn and Percuil tributaries and absence north of Carrick Roads. During neap tides, high concentrations (>1.1 x 10^6 cells l^{-1}) were observed throughout the estuary. These findings suggest that blooms originate at the seaward end of the estuary and are advected into the estuary, where they are more readily retained during neap tides.

5.1.3. *Alexandrium minutum*

Alexandrium minutum was first described in Alexandria Harbour (Halim, 1960) and is a widely distributed species found in coastal waters of Spain, Portugal (as *A. ibericum*) (Balech, 1985), Italy (Montresor et al., 1990), France (Nezan et al., 1989), Ireland (Touzet et al., 2006), Denmark (Hansen et al., 2003), South Australia (Hallegraeff et al., 1988), New Zealand , Malaysia (Usup et al., 2002), Taiwan (Chang et al., 1995b; Hwang et al., 1999), the US east coast (Steidinger & Tangen, 1996) and more recently Cape Town Harbour (Pitcher et al., 2007) and Jamaica (Ranston et al., 2007). Toxin profiles of this species are highly variable between strains. Most strains only produce gonyautoxins, such as the Fal Estuary strain, which produces GTX-II and -III and strains from Spain (Franco et al., 1994), Portugal (Cembella et al., 1987) and Taiwan (Hwang & Lu, 2000) only produce GTX-I and GTX-IV. A strain isolated from the Fleet Lagoon (UK) also produces significant amounts of saxitoxin (Nascimento, 2005). *A. minutum* has been responsible for PSP events in France (Nezan et al., 1989; Erard-Le Denn et al., 2000), the Galician Rias (Franco et al., 1994), New Zealand (Chang et al., 1995b), South Australia (Hallegraeff et al., 1988) and Taiwan (Hwang et al., 1999).

Studies of *A. minutum* blooms have shown that they generally occur in harbours, lagoons and estuaries, where stratification and high freshwater input create favourable conditions for growth (Giacobbe et al., 1996). Blooms in a Sicilian lagoon (Giacobbe et al., 1996) and in a harbour on the Catalan coast (Garcés et al., 2004) were thought to be initiated by cyst germination, triggered by increased solar irradiance, day length and water temperatures. Giacobbe et al (1996) however did not exclude the possibility of an allochthonous mechanism such as transport from coastal waters during the flood tide. Strong winds and water column instability are thought to be responsible for bloom termination (Giacobbe et al., 1996; van Lenning et al., 2007).

A preference for lower salinities (25-30) has been suggested from both field and culture studies (Giacobbe et al., 1996; Grzebyk et al., 2003; Lim & Ogata, 2005) but not corroborated by van Lenning et al. (2007), suggesting the existence of different geographic strains with distinct physiological traits. Significant negative correlations have been observed between *A. minutum* abundance and NH_4^+ concentrations in both the Sicilian lagoon and Catalan harbour (Giacobbe et al., 1996; Bravo et al., 2008). It is not clear however whether this indicates that high NH_4^+ concentrations inhibited *A. minutum*

growth or whether the bloom was drawing down NH_4^+, although the former hypothesis seems to be preferred (Vila et al., 2005; Bravo et al., 2008). Nitrogen uptake measurements in Cape Town Harbour, however, indicated that the bloom was sustained by high rates of NH_4^+ uptake (Pitcher et al., 2007). Culture studies carried out on a French strain have shown higher half-saturation constants (K_s) and maximum cell-specific uptake rates (ν_{max}) for NH_4^+ relative to NO_3^-, indicative of a preference for NH_4^+ over NO_3^-.

In contrast, the estimated NO_3^- requirement of a bloom in the Penzé Estuary (France) was one order of magnitude higher than for NH_4^+ (184 versus 25 μmol l^{-1}), based on ^{15}N uptake rates. Bravo et al. (2008) drew a similar conclusion from their study on the Catalan coast, where they found a positive correlation between *A. minutum* and NO_3^- concentrations. Culture studies have also shown high requirements for NO_3^-, with no growth inhibition observed up to concentrations of 200 μmol N l^{-1}, whereas inhibition occurred at NH_4^+ and urea concentrations of 100 μmol N l^{-1} and 200 μmol N l^{-1}, respectively (Chang & McClean, 1997). Similarly, a study carried out with an Irish strain of *A. minutum* showed no growth inhibition with an initial concentration of up to 1000 μmol N l^{-1} NO_3^- (Touzet et al., 2007).

5.1.4. Aims and objectives

The work carried out in the Fal Estuary aimed to characterise phytoplankton dynamics during the summer dinoflagellate bloom period by comparing two consecutive years (July 2006 and July 2007) that displayed different environmental conditions. Specific objectives were to:

- determine spatial and temporal variations in community structure, with particular focus on *Alexandrium minutum*, *Karenia mikimotoi* and *Pseudo-nitzschia* spp. cell concentrations,
- measure the nutrient uptake rates of different phytoplankton communities and identify possible nitrogen nutrition strategies,
- determine the environmental factors (nutrients, temperature, salinity, tidal state, meteorological conditions) that are conducive to HAB development in the Fal Estuary.

5.2. Results

5.2.1. Meteorological conditions

In 2006, monthly rainfall was highest in autumn (October and November, 115-132 mm) and lowest in early summer (June and July, 20-34 mm) (Figure 5.2). In 2007, rainfall was similar to 2006 in October and November, but was higher than in 2006 between December and February (82-163 mm) and between May and July (94-116 mm).

Minimum and maximum air temperatures were higher in July 2006 (15.0 and 22.3 °C, respectively) relative to July 2007 (12.8 and 17.2°C, respectively) (data not shown).

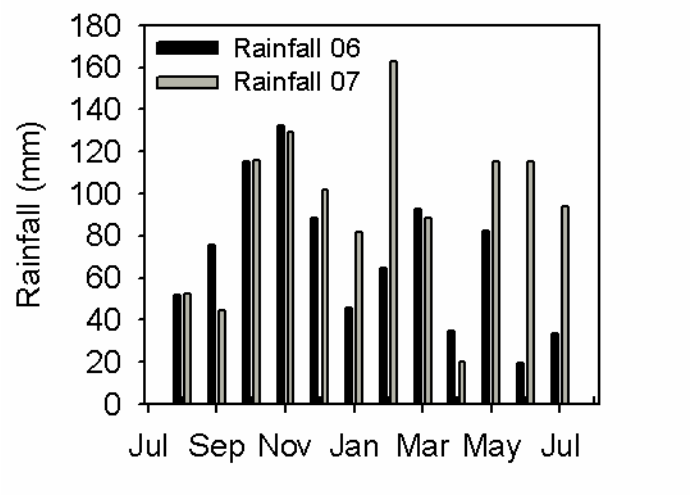

Figure 5.2. Monthly rainfall measured at St Mawgan weather station between August 2005 and July 2006 (black bars) and between August 2006 and July 2007 (grey bars).

5.2.2. Hydrography

5.2.2.1. Tides

In both years the sampling period included both spring and neap tides (Figure 5.3). The neap tidal range was 2.30 m in 2006 (5 July) and 2.85 m in 2007 (10 July), and the spring tidal range was 4.50 m in 2006 and 3.90 m in 2007.

Sampling took place on the ebb tide on 4-5 and 11-16 July 2006 and on 4-6 July 2007, but on the flood tide on 7-9 July 2006 and 10-12 July 2007. Sampling was generally carried out in a seaward direction, therefore against the tide during flood tides but with the tide during ebb flow.

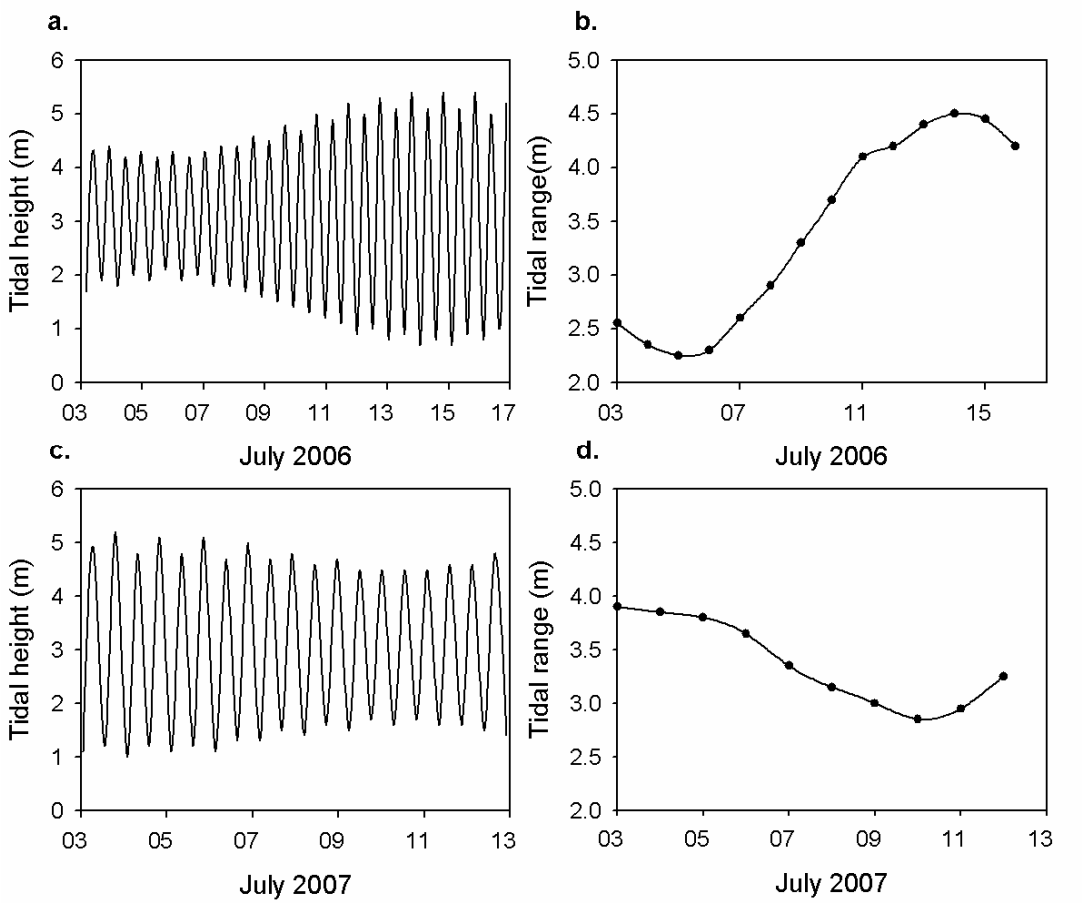

Figure 5.3. Semi-diurnal tidal pattern (data for Falmouth) in (a) 2006 and (c) 2007 and daily averaged tidal ranges in (b) 2006 and (d) 2007.

5.2.2.2. Temperature

Water temperatures were significantly higher at all stations in 2006 relative to 2007 (Student's t-test, $p < 0.001$), ranging from 16.2 to 19.3 °C in 2006 and from 14.2 to 17.4 °C in 2007 (Table 5.2). The lowest surface temperatures in both years were generally measured at the outermost station Turnaware Point (TP) and the highest at the innermost station Malpas (MP). In 2006, temperature variations along the estuary were 1.0-1.4 °C when sampling with the tide and 0.6-1.8 °C when sampling against the tide. In contrast, variations in surface temperature along the estuary in 2007 were small, and fell in the range 0.3-0.7 °C between MP and TP regardless of sampling direction.

Temporal variations in temperature were of the same order as spatial variations in 2006, with differences between 1.0 and 2.1 °C depending on the station. In 2007, they were greater, with surface temperature varying by 1.3 to 3.1 °C. Lowest temperatures were measured during spring tides (14-16 July 2006 and 4-6 July 2007), whereas warmest temperatures were observed during neap tides (4-7 July 2006 and 11-12 July 2007) (Table 5.2). In 2007, temperature was significantly correlated with number of hours before or after high tide ($p < 0.05$, $n = 43$, Figure 5.6), although on 2 occasions very warm temperatures were measured close to high tide, at both MP and TP (7 and 11 July, respectively). This relationship was not observed in 2006.

Temperature generally decreased with depth, with temperature differences between surface and bottom ranging from 0.0 to 2.4 °C in 2006 and from 0.1 to 3.3 °C in 2007. Vertical gradients were strongest during neap tides, whereas the water column was more mixed during spring tides, as shown in Figures 5.4 and 5.5.

	Tidal range (m)	MP	WB	RU	SC	KH	TP
a. 2006							
04/07	2.35	-	-	18.8/ 16.6	*17.8/ 16.5*	*17.5/ 16.6*	17.8
05/07	2.25	-	-	-	*18.2/ 16.8*	18.2/ 16.9	*18.2/ 16.9*
07/07	2.60	19.0/ 17.3	19.3/ 17.0	17.9/ 16.8	18.5/ 16.8	18.7/ 16.5	17.9/ 15.8
08/07	2.90	18.9	18.9	18.1/ 17.0	18.1/ 15.7	*18.0/16.4*	17.1/ 15.4
09/07	3.30	17.9/ 18.1	18.2/ 17.5	18.0/ 17.5	17.9/ 17.6	18.1/ 17.1	17.6/ 17.2
11/07	4.10	19.0/ 18.8	-	18.0/ 17.4	17.5/ 16.7	17.3/ 16.9	17.2/ 15.2
12/07	4.20	-	-	-	17.7/ 16.5	17.6/ 15.9	17.3/ 15.9
14/07	4.50	17.6/ 17.5	17.2/ 17.2	-	16.4/ 16.5	17.7/16.4	16.2/ 15.8
15/07	4.45	18.2/ 17.6	-	-	*17.9/ 17.2*	-	*17.2/ 16.0*
16/07	4.20	17.9/ 17.8	18.0/ 17.0	17.8/ 17.1	-	-	17.0/ 16.6
b. 2007							
04/07	3.85	14.8/ 14.3	14.6/ 13.9	14.8/ 13.7	14.7/ 14.5	15.1/ 13.9	*14.7/ 13.2*
05/07	3.80	14.4/ 14.0	14.5/ 13.8	14.4/ 13.7	14.3/ 13.8	-	14.2/ 13.6
06/07	3.65	14.3/ 13.8	14.3/ 13.5	14.8/ 13.6	*15.0/ 14.4*	14.9/ 14.1	14.8/ 13.6
07/07	3.35	17.4/ 15.3	-	-	-	16.1/ 14.1	15.8/ 13.5
10/07	2.85	14.7/ 14.5	14.6/ 13.9	14.6/ 13.8	14.3/ 13.6	14.8/ 13.5	14.7/ 13.6
11/07	2.95	16.7/ 14.1	14.8/ 13.8	16.0/ 13.6	15.6/ 13.5	-	16.9/ 13.6
12/07	3.25	15.6/ 15.5	15.7/ 14.0	16.1/ 14.3	-	15.9/ 13.8	15.9/ 14.3

Table 5.1. Temperatures measured in (a) 2006 and (b) 2007 at the surface and 2-3 m from the bottom by the YSI probes except values in italic, which were obtained from CTD casts. MP = Malpas, WB = Woodbury, RU = Ruan, SC = Smuggler's Cottage, KH = King Harry Reach, TP = Turnaware Point.

5.2.2.3. Salinity

Salinities were on average 6-19 % higher in 2006 relative to 2007 at stations MP to TP, ranging from 22.3 to 34.6 in 2006 and from 21.5 to 31.7 in 2007 (Table 5.2). The difference was only significant for the outer stations SC (Student's t-test, $p < 0.05$), KH (Student's t-test, $p < 0.001$) and TP (Mann-Whitney U-test, $p < 0.05$).

A salinity gradient was observed along the estuary, with surface salinities as low as 22.3 in 2006 and 21.5 in 2007 at the riverine end (MP) and as high as 34.8 in 2006 and 31.7 in 2007 at the seaward end (TP). However, salinity at MP was highly variable due to the relative influences of tidal and freshwater flows, with values ranging from 21-22 at low tide to 30-34 at high tide. At TP, the salinity range was more restricted, although relatively low salinities of 26-29 were measured at the surface on 11-12 July 2007 (Table 5.2). The salinity gradient between MP and TP was weak when sampling on the ebbing tide (this usually coincided with spring tides, i.e. 14-16 July 2006 and 4-6 July 2007), with high salinities of 33-35 in 2006 and 30-32 in 2007 measured throughout the estuary (Table 5.2). Although a general decrease in salinity was observed with the number of hours since high tide in 2007, the correlation was not significant ($p > 0.05$, n

= 29, Figure 5.6). No relationship between salinity and tidal state was observed in 2006 (data not shown).

Vertical salinity gradients were less pronounced in 2006 relative to 2007, with maximum salinity differences between surface and bottom of 6.5 in 2006 and 13.6 in 2007. In both years, salinity was relatively isohaline throughout the water-column during spring tides, with salinity differences between surface and bottom of 0.7-3.8, whereas a sharper halocline was observed in the top 2 m during neaps (Table 5.2, Figures 5.4 and 5.5).

	Tidal range (m)	MP	WB	RU	SC	KH	TP
a. 2006							
04/07	2.35	-	-	32.3/ 34.6	*32.9/34.9*	*33.7/34.8*	33.7
05/07	2.25	-	-	-	*32.9/34.7*	33.3/34.7	*33.3/34.6*
07/07	2.60	32.2/ 34.5	31.9/ 34.9	34.1/ 34.9	33.4/ 35.0	33.0/ 35.0	34.6/ 35.2
08/07	2.90	28.6	31.0	33.4/ 34.8	32.9/ 35.2	33.3/35.0	34.8/ 35.1
09/07	3.30	23.0/ 29.5	28.0/ 33.6	28.1/ 33.8	30.4/ 33.3	32.0/ 34.3	34.0/ 34.4
11/07	4.10	22.3/ 23.1	-	31.1/ 32.6	30.6/ 34.1	32.7/ 33.6	33.5/ 34.6
12/07	4.20	-	-	-	31.9/ 34.0	32.3/ 34.4	32.9/ 34.4
14/07	4.50	32.9/ 33.0	33.4/ 33.4	-	34.2/ 34.3	34.2/34.2	34.1/ 34.5
15/07	4.45	33.0/ 33.5	-	-	*33.7/34.0*	-	*34.2/34.7*
16/07	4.20	33.6/ 33.7	33.6/ 34.2	33.8/ 34.3	-	-	34.6/ 34.7
b. 2007							
04/07	3.85	30.3/ 32.0	29.8/ 33.6	30.7/ 34.0	31.2/ 31.9	30.8/ 33.5	*31.5/ 34.9*
05/07	3.80	30.4/ 33.2	29.3/ 33.6	30.0/ 33.7	30.7/ 33.5	-	31.7/ 34.0
06/07	3.65	30.5/ 33.6	32.1/ 34.2	31.2/ 34.0	*31.0/ 32.0*	31.2/ 33.2	31.5/ 34.2
07/07	3.35	27.2/ 31.2	-	-	-	30.4/ 33.5	31.0/ 34.5
10/07	2.85	23.2/ 31.7	26.1/ 34.2	30.5/ 34.5	32.4/ 34.8	30.0/ 34.9	29.9/ 35.8
11/07	2.95	21.5/ 34.2	21.1/ 34.7	25.2/ 34.9	27.8/ 34.9	-	26.4/ 35.1
12/07	3.25	24.3/ 28.5	21.1/ 34.3	23.3/ 33.7	-	26.5/ 34.6	28.8/ 33.6

Table 5.2. Salinities in (a) 2006 and (b) 2007 measured at the surface and 2-3 m from the bottom by the YSI probes except values in italic, which were obtained from CTD casts. Station abbreviations are as in Table 5.1.

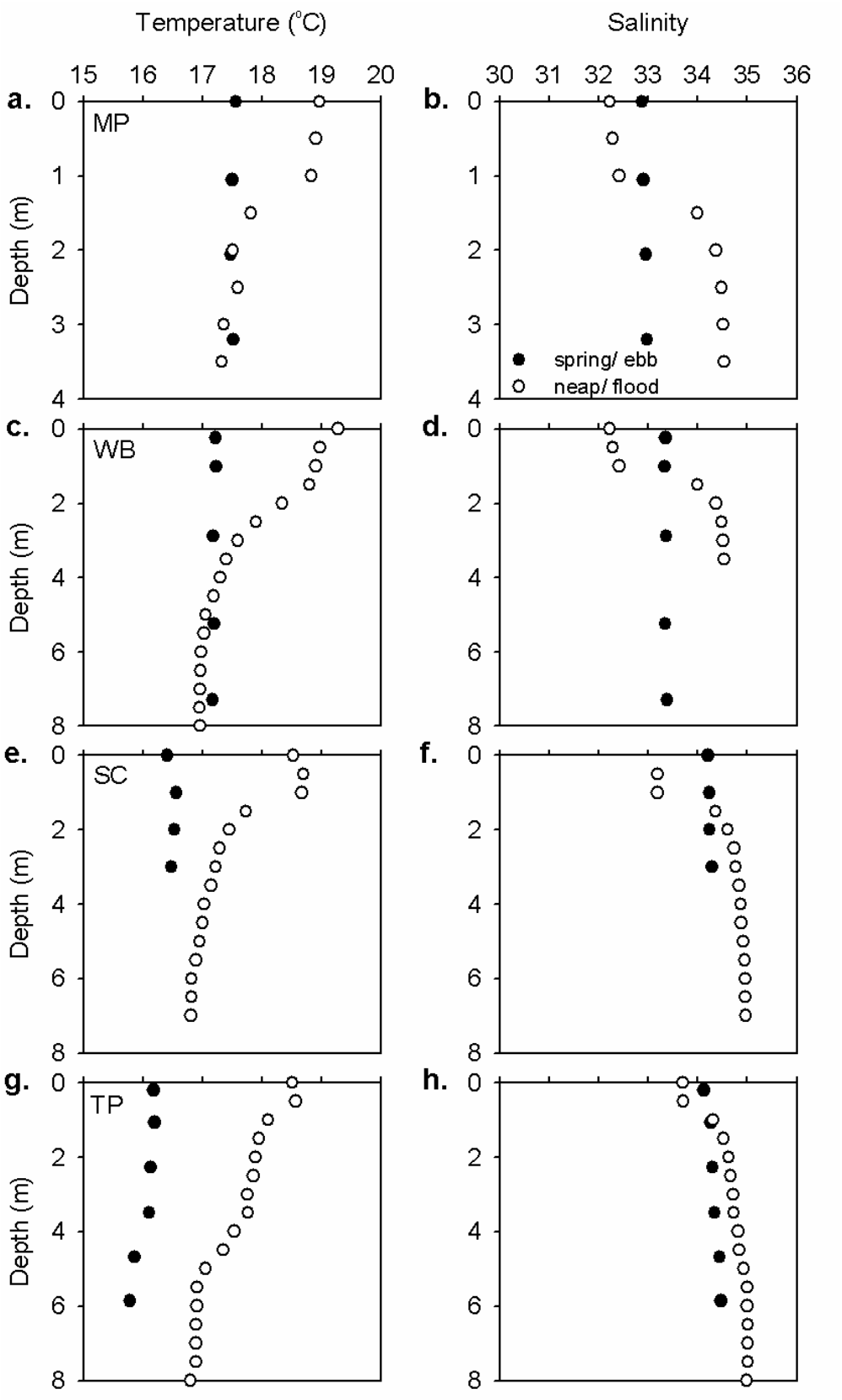

Figure 5.4. Temperature and salinity profiles obtained from YSI casts at stations (a, b) MP, (c, d) WB, (e, f) SC and (g, h) TP on 7 July (neap/flood tide, open circles) and 14 July 2006 (spring/ebb, closed circles).

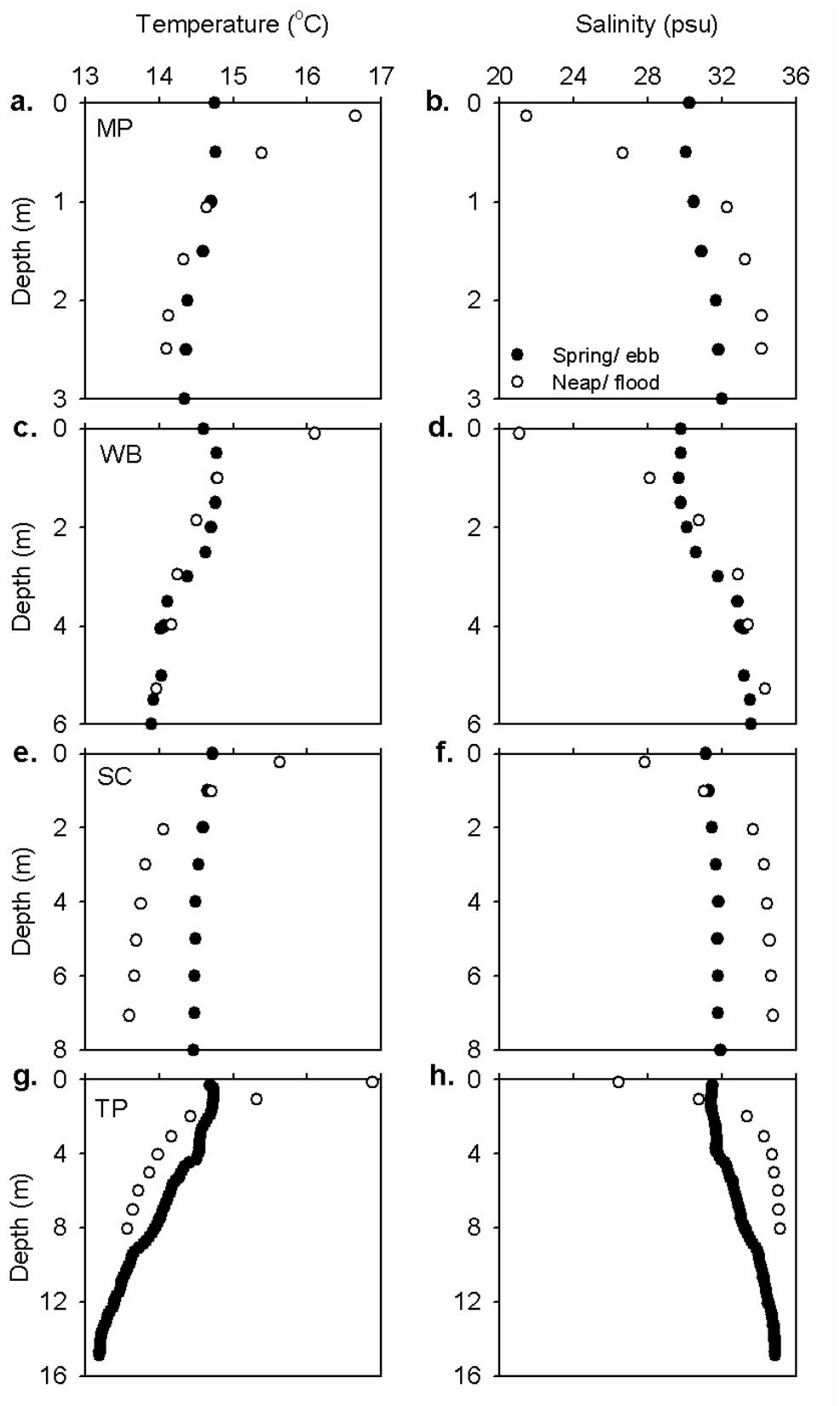

Figure 5.5. Temperature and salinity profiles obtained from YSI casts [or CTD casts for closed circles in (g) and (h)] at stations (a, b) MP, (c, d) WB, (e, f) SC and (g, h) TP on 4 July (spring/ebb, closed circles) and 11 July 2007 (neap/flood, open circles).

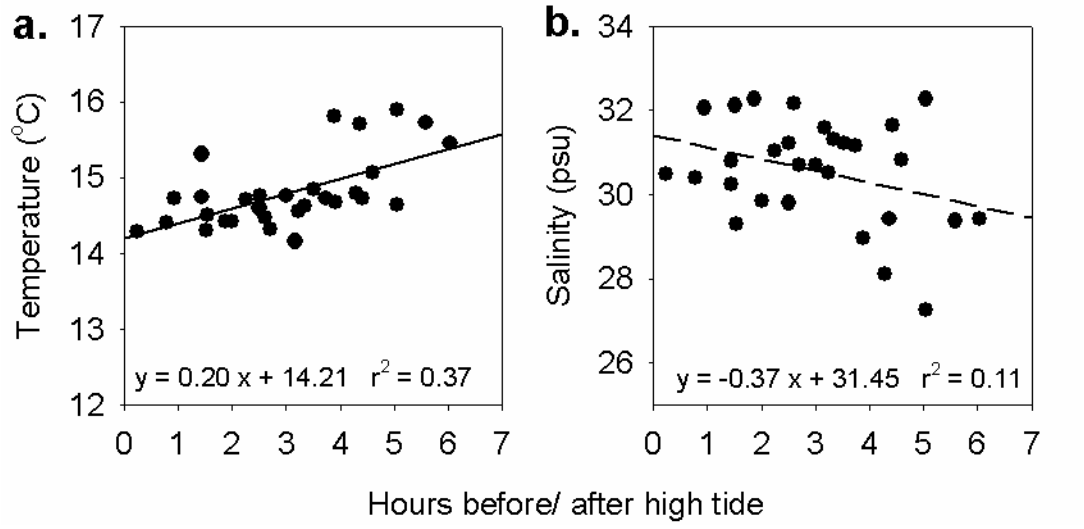

Figure 5.6. Relationships between tidal state and (a) surface temperature and (b) surface salinity. The correlation was significant between tidal state and temperature (solid line, $p < 0.01$, $n = 30$) but not salinity (dashed line, $p > 0.05$, $n = 29$).

5.2.3. Dissolved oxygen

In 2006, DO concentrations were generally measured at MP and TP, whereas in 2007 they were measured at up to 6 stations along the estuary. Also, the YSI probe readings did not correlate with concentrations measured using Winkler titrations in 2006, therefore only measured concentrations are presented for this year.

In 2006, surface water was generally supersaturated, with saturations ranging from 92 to 128 % at MP and from 115 to 127 % at TP. In 2007, DO concentrations were generally close to saturation throughout the water column, with the lowest concentration measured at MP (85 %, spring tide) and the highest at TP (114 %, neap tide) (Table 5.3).

Although a clear pattern along the estuary was not always obvious, a gradient was observed in 2007 when sampling was conducted against the flooding tide (10 July), with saturations increasing seaward. In 2007, DO saturation was generally higher throughout the estuary during neap compared to spring tides, although this trend was not apparent in 2006 (Table 5.3, Figure 5.7). DO saturation generally decreased with depth, with surface values 1-36 % and 1-16 % higher than bottom values in 2006 and 2007, respectively.

DO (%Sat)	Tidal range (m)	MP	WB	RU	SC	KH	TP
a. 2006							
04/07	2.35	-	-	140	-	-	127
05/07	2.25	-	-	-	*139/124*	-	*140/125*
07/07	2.60	128	-	-	*118/87*	-	*117/98*
08/07	2.90	112	-	-	*127*	*110/127*	*109/106*
09/07	3.30	-	-	-	-	116	*121/105*
11/07	4.10	92	-	-	*113/120*	*112/137*	115
12/07	4.20	-	-	-	*116/112*	-	*127/119*
14/07	4.50	125	-	-	*127/126*	*134/119*	*114/115*
15/07	4.45	-	-	-	-	-	-
16/07	4.20	119	-	-	-	100	-
b. 2007							
04/07	3.85	96/ 96	95/ 92	96/ 93	96/ 95	98/ 95	-
05/07	3.80	87/ 85	92/ 86	91/ 86	93/ 87	-	91/ 86
06/07	3.65	99/ 96	100/ 95	100/ 96	-	99/ 97	100/ 94
07/07	3.35	101/ 99	-	-	-	105/ 95	96/ 88
10/07	2.85	101/ 101	102/ 101	104/ 106	109/ 101	111/ 102	114/ 98
11/07	2.95	106/ 100	108/ 101	106/ 98	110/ 97	-	110/ 100
12/07	3.25	92/ 93	98/ 100	94/ 100	-	99/ 99	108/ 108

Table 5.3. (a) Surface DO saturations measured using the Winkler method in 2006, (b) calibrated surface and bottom DO saturations (%) measured using two YSI probes in 2007. Station abbreviations are as in Table 5.1. Italics represent measurements made on *RV Bill Conway*.

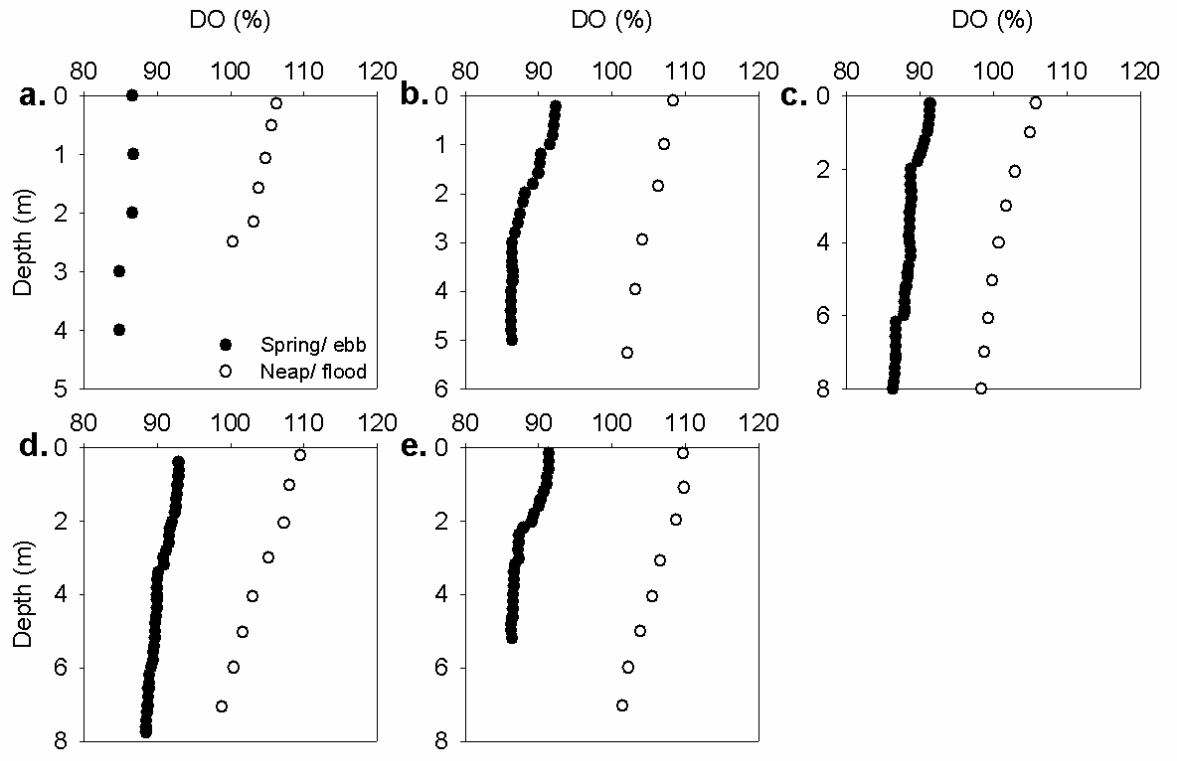

Figure 5.7. DO saturation profiles obtained from YSI deployments on 5 July (closed cicles, spring tide) and 11 July 2007 (open circles, neap tide) at (a) MP, (b) WB, (c) RU, (d) SC and (e) TP. Profile data were not available for 2006 since the YSI DO sensor was unreliable.

5.2.4. Nutrients

5.2.4.1. Nitrate

Surface NO_3^- concentrations ranged from 0.2 to 129.3 μmol l^{-1} in 2006 and from 13.1 to 119.1 μmol l^{-1} in 2007 between stations MP and TP (Table 5.4a). Average concentrations for each station were 34 % to 17-fold higher in 2007 relative to 2006. These differences were significant for all stations except MP (Student's t-test, $p < 0.001$).

A horizontal gradient was consistently observed in 2006, with concentrations decreasing by 3- to 56-fold between MP and TP. In 2007 the gradient was not always observed (e.g. 12 July) and was generally less pronounced, with concentrations decreasing by 1.5- to 5-fold (Table 5.4b).

In 2007, NO_3^- concentrations were measured at depth as well as at the surface and concentrations were significantly lower at depth relative to the surface (paired t-test, $p < 0.05$). The difference was more pronounced during neap tide (66-88 % on 10-11 July) than during spring tide (14-67 % on 6 July), as shown in Figure 5.8d.

Temporal variation was also more pronounced in 2006 relative to 2007, with concentrations as low as 5.3 μmol l^{-1} measured at MP at high tide and as high as 129.3 μmol l^{-1} at low tide whereas in 2007 similar concentrations were measured at both high and low tide (e.g. 5 and 12 July). Significant correlations were observed between NO_3^- concentrations and tidal state (number of hours since/before high tide) in 2007, during neap tides only (Figure 5.9a).

Date	Tidal range (m)	MP	WB	RU	SC	KH	TP
a. 2006							
04/07	2.35	-	-	7.7	-	5.8	2.6
05/07	2.25	-	-	-	-	-	-
07/07	2.60	24.0	13.6	10.1	9.0	-	8.4
08/07	2.90	76.7	34.7	15.6	11.5	*9.2*	*0.8*
09/07	3.30	123.1	63.1	52.1	21.6	12.0	2.2
11/07	4.10	129.3	65.0	25.1	27.9	9.9	2.7
12/07	4.20	-	-	-	*15.0*	*9.9*	*8.1*
14/07	4.50	8.6	8.1	-	2.1	1.7	1.1
15/07	4.45	7.4	-	-	*2.6*	2.5	*0.7*
16/07	4.20	5.3	4.7	2.7	2.2	0.8	0.2
b. 2007							
04/07	3.85	63.6	60.9	51.4	43.6	45.9	*42.0*
05/07	3.80	53.2	61.5	57.4	49.1	-	47.0
06/07	3.65	66.5	45.2	47.1	*45.2*	43.3	39.4
07/07	3.35	119.1	-	-	-	54.2	43.6
10/07	2.85	108.7	56.8	38.7	19.6	19.8	32.3
11/07	2.95	37.7	75.5	52.7	35.6	-	13.1
12/07	3.25	51.6	83.9	77.4	-	58.1	88.2

Table 5.4. Nitrate concentrations (µmol l^{-1}) measured at the surface between MP and TP in (a) 2006 and (b) 2007. Italics represent measurements made on *RV Bill Conway*.

5.2.4.2. Phosphate

Phosphate concentrations were 0.2-2.6 µmol l^{-1} in 2006 and 0.1-1.1 µmol l^{-1} in 2007. Average concentrations for each station were 15-58 % higher in 2006 than in 2007 at the upper stations MP and WB, but 12 % to 2-fold higher in 2007 at the other stations. However, these differences were not statistically significant (Student's t-test, $p > 0.05$).

Phosphate followed the same distribution as NO_3^- along the estuary, with highest concentrations generally measured at MP and lowest concentrations at TP. Horizontal gradients were steeper in 2006 than in 2007, decreasing by 17 % to 10-fold between TP and MP in 2006 and by 10 % to 5-fold in 2007 (Table 5.5).

Concentrations were significantly lower at depth relative to the surface (paired t-test, $p < 0.05$). As with NO_3^-, the difference was more pronounced during neap tides (up to 57 %) than during spring tides (up to 34 %) (Figure 5.8b,e). Significant correlations were observed between PO_4^{3-} concentrations and tidal state (number of hours since/before high tide) in 2007, during neap tides only (Figure 5.9b).

Phosphate concentrations were significantly correlated with NO_3^- concentrations in both years, with a regression coefficient of 45 in 2006 and 73 in 2007, i.e. 3- to 6-fold higher than the Redfield ratio (Figure 5.10a). In 2006, N:P ratios were lowest at TP (1-

23) and highest at MP (13-92) (data not shown). In 2007, N:P ratios were generally high throughout the estuary and were 2.5 to 13-fold higher than in 2006. The difference was statistically significant at stations MP (Student's t-test, $p < 0.01$), WB (Student's t-test, $p < 0.001$), RU (Student's t-test, $p < 0.01$) and TP (Mann-Whitney U-test, $p < 0.05$).

Date	Tidal range (m)	MP	WB	RU	SC	KH	TP
a. 2006							
04/07	2.35	-	-	0.74	-	0.27	0.23
05/07	2.25	-	-	-	-	-	-
07/07	2.60	0.63	0.30	0.24	0.13	-	0.54
08/07	2.90	0.84	0.98	0.60	0.70	*0.50*	*0.50*
09/07	3.30	2.63	1.50	0.77	0.46	0.42	0.26
11/07	4.10	2.04	1.21	0.46	0.38	0.35	0.19
12/07	4.20	-	-	-	0.52	-	0.63
14/07	4.50	0.56	0.47	-	0.24	0.27	0.23
15/07	4.45	0.49	-	-	*0.28*	0.29	*0.24*
16/07	4.20	0.42	0.36	0.29	0.29	0.38	0.24
b. 2007							
04/07	3.85	0.96	0.85	0.79	0.81	0.67	*0.53*
05/07	3.80	0.69	0.70	0.62	1.06	-	0.63
06/07	3.65	0.50	0.65	0.75	*0.61*	1.38	0.53
07/07	3.35	0.82	-	-	-	0.57	0.50
10/07	2.85	0.85	0.71	0.33	0.38	0.32	0.33
11/07	2.95	0.51	0.60	0.43	0.16	-	0.11
12/07	3.25	0.49	0.68	0.57	-	0.39	0.30

Table 5.5. Phosphate concentrations measured at the surface between MP and TP in (a) 2006 and (b) 2007. Italics represent measurements made on *RV Bill Conway*.

5.2.4.3. Silicate

Silicate concentrations were lower than NO_3^- concentrations, ranging from 0.2 to 37.6 μmol l^{-1} at the surface in 2006 and from 5.1 to 19.8 μmol l^{-1} in 2007. Silicate concentrations were significantly higher in 2007 than in 2006 at stations KH and TP only (Student's t-test, $p < 0.01$).

In 2006, concentrations increased up to 12-fold between MP and TP when MP was sampled at low tide, whereas in 2007 they only increased up to 2-fold under the same conditions (Table 5.6). Concentrations were significantly higher at the surface than at depth (paired t-test, $p < 0.01$) and the difference was less pronounced during spring tides (17-46 %) relative to neap tides (67-80 %) (Figure 5.8c,f). Silicate concentrations were significantly correlated with tidal state in 2007, during neap tides only (Figure 5.9c).

Nitrate and Si concentrations were significantly correlated in both years, with a regression coefficient of 2.8 in 2006 and 4.1 in 2007 (Figure 5.10b). N: Si ratios were significantly higher (Student's t-test) in 2007 than in 2006 at MP, WB ($p < 0.05$), RU ($p < 0.01$) and SC ($p < 0.001$).

Date	Tidal range (m)	MP	WB	RU	SC	KH	TP
a. 2006							
04/07	2.35	-	-	2.4	-	3.3	2.0
05/07	2.25	-	-	-	-	-	2.9
07/07	2.60	6.2	12.7	5.3	4.6	-	3.5
08/07	2.90	17.2	11.9	10.1	-	*4.8*	*3.6*
09/07	3.30	29.5	14.0	26.3	11.1	7.2	2.7
11/07	4.10	37.6	18.1	9.4	18.5	7.7	3.1
12/07	4.20	-	-	-	7.1	5.6	4.9
14/07	4.50	6.2	6.2	-	2.4	2.2	1.8
15/07	4.45	2.1	-	-	1.1	0.2	*0.1*
16/07	4.20	3.5	3.2	2.3	1.9	1.6	1.0
b. 2007							
04/07	3.85	17.1	17.9	14.9	13.3	15.2	*11.7*
05/07	3.80	15.2	17.6	16.1	14.8	-	13.9
06/07	3.65	14.7	12.4	14	*13.5*	13.7	12.2
07/07	3.35	24.7	-	-	-	15.4	13.1
10/07	2.85	18.8	11.5	8.4	5.1	5.4	9.3
11/07	2.95	7.8	16.5	14.0	12.0	12.0	9.8
12/07	3.25	9.9	17.1	14.5	-	14.4	19.8

Table 5.6. Silicate concentrations measured at the surface between MP and TP in (a) 2006 and (b) 2007. Italics represent measurements made on *RV Bill Conway*.

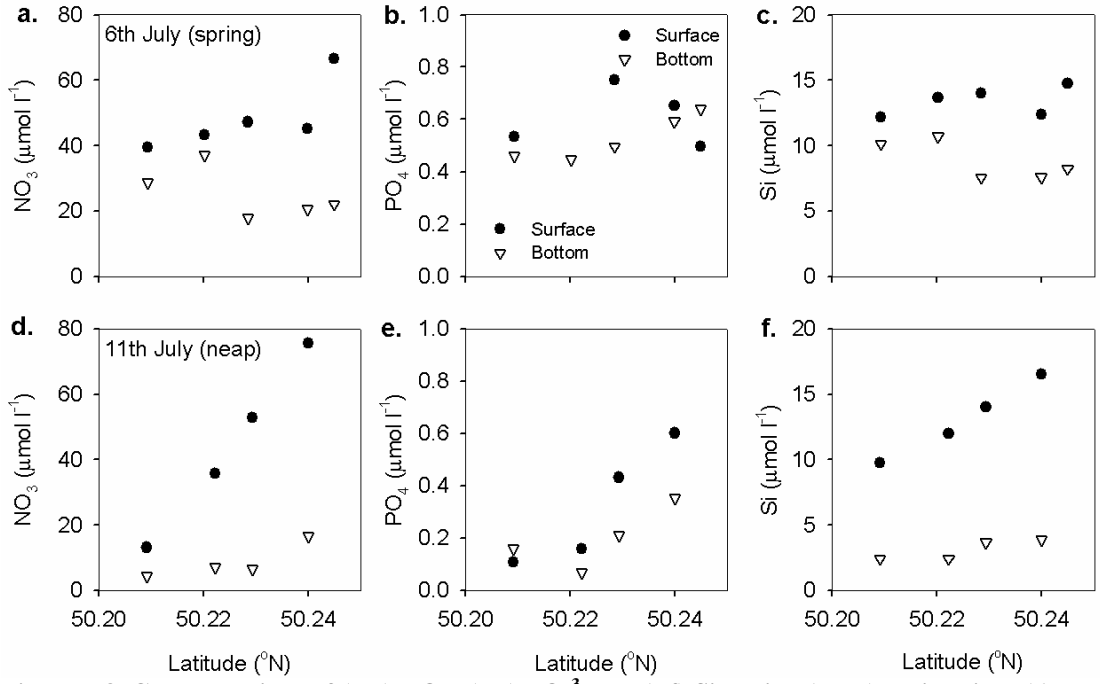

Figure 5.8. Concentrations of (a,d) NO_3^-, (b,e) PO_4^{3-} and (c,f) Si during (a,b,c) spring tides (6 July 2007) and (d,e,f) neap tides (11 July 2007) at the surface (closed symbols) and 2-3 m from the bottom (open symbols).

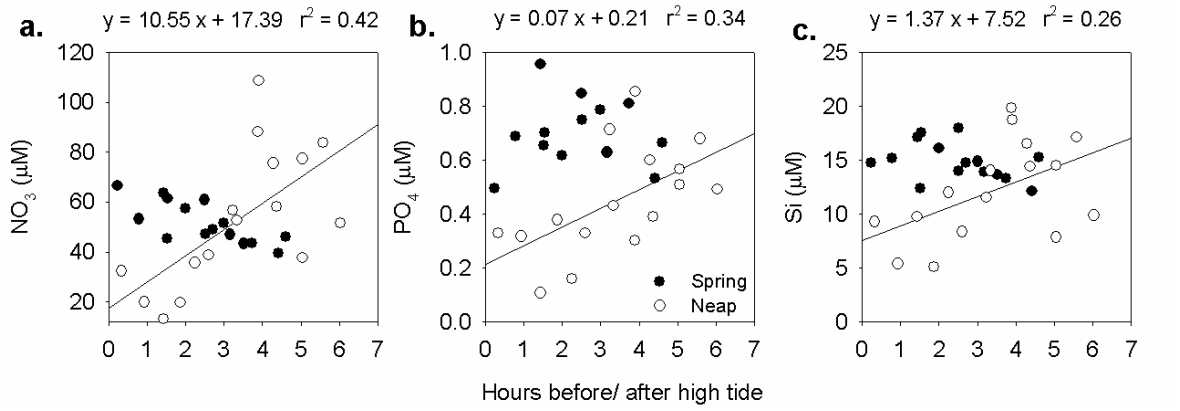

Figure 5.9. Relationships between tidal state and surface concentrations of (a) NO_3^-, (b) PO_4^{3-} and (c) Si during spring (closed circles) and neap tides (open circles) in 2007. Regression lines are drawn where correlations are significant, i.e. for neap tides ($p < 0.01$ for NO_3^-, $p < 0.05$ for PO_4^{3-} and Si, n = 16) but not for spring tides.

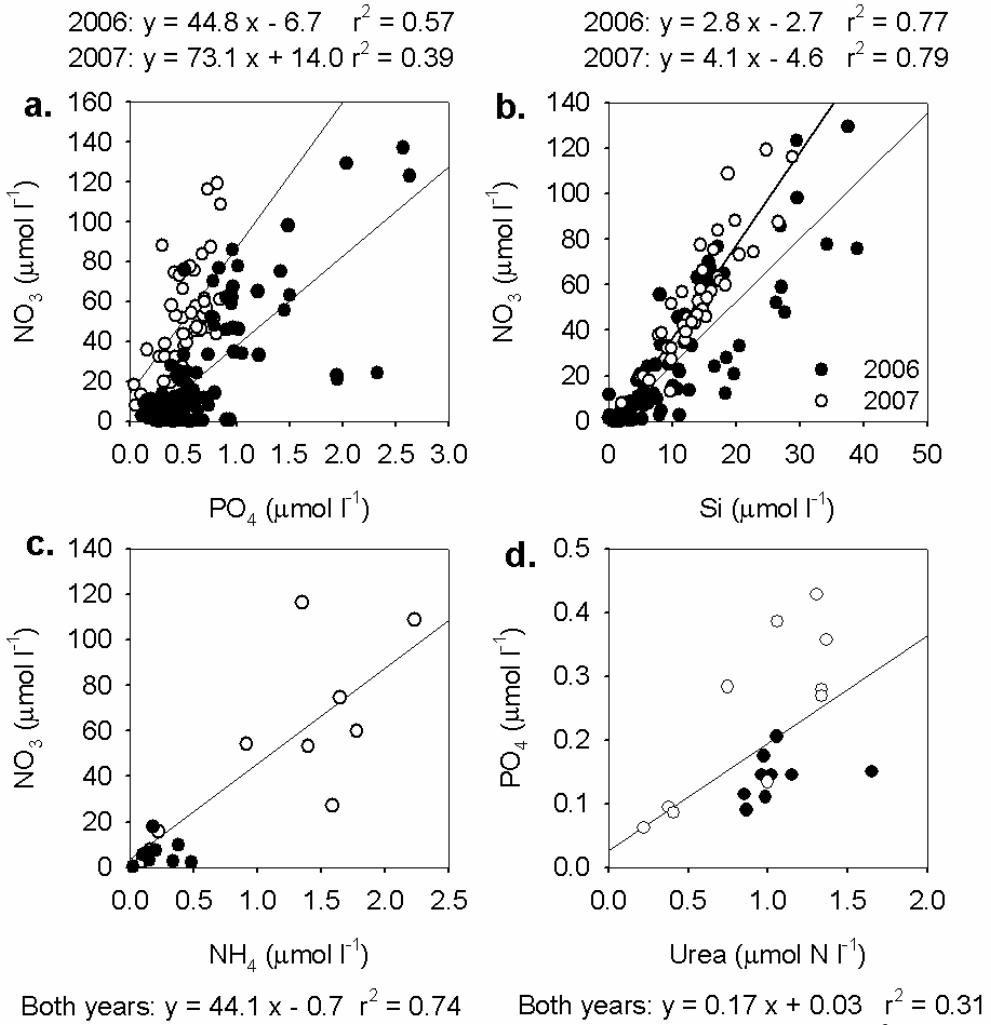

Figure 5.10. Correlations between surface concentrations of (a) NO_3^- and PO_4^{3-}, (b) NO_3^- and Si, (c) NO_3^- and NH_4^+ and (d) PO_4^{3-} and urea, measured in 2006 (closed circles) and 2007 (open circles) at stations listed in Table 5.1. $p < 0.01$ in all cases [n = 111 in 2006 and 45 in 2007 in (a); n = 108 in 2006 and 45 in 2007 in (b); n = 10 in (c); n = 19 in (d)].

5.2.4.4. Ammonium and urea

Ammonium and urea concentrations were only measured in association with nitrogen uptake incubations, therefore spatial coverage of the estuary is limited. Ammonium concentrations ranged from 0.02 to 0.77 µmol N l^{-1} in 2006 and from 0.09 to 2.23 µmol N l^{-1} in 2007. Concentrations were significantly (on average 4-fold) higher in 2007 relative to 2006 (Mann-Whitney U-test, $p < 0.05$). Ammonium concentrations were significantly correlated with NO_3^- concentrations in 2007 but not in 2006, although the correlation was significant for both years combined (Figure 5.10c). Concentrations generally increased towards the head of the estuary although there was a high degree of temporal variability within stations (Figure 5.11).

Urea concentrations were insignificantly different between years, ranging from 0.81 to 1.63 µmol N l^{-1} in 2006 and from 0.13 to 1.34 µmol N l^{-1} in 2007. Concentrations were not correlated with NH_4^+ or NO_3^- (data not shown) but they were significantly correlated with PO_4^{3-} for both years ($p < 0.05$, $n = 18$, Figure 5.10d). Concentrations displayed no particular pattern along the estuary, showing high variability between days at some stations (Figure 5.11). Urea concentrations were significantly higher than NH_4^+ concentrations in 2006 (paired t-test, $p < 0.01$), but not significantly different in 2007.

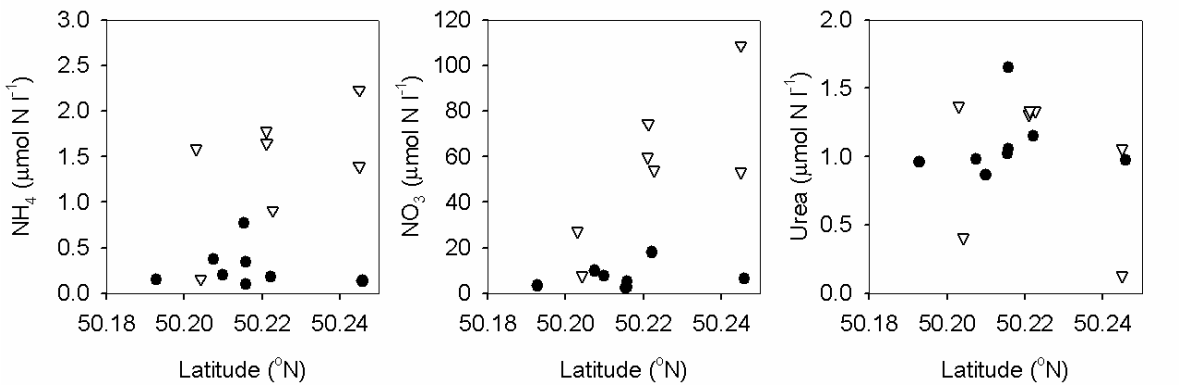

Figure 5.11. Concentrations of (a) NH_4^+, (b) NO_3^- and (c) urea as a function of latitude, measured in association with nutrient uptake incubations on different dates in 2006 (closed symbols) and 2007 (open symbols).

5.2.5. Chl-a

Chl-a concentrations ranged from 2.0 to 19.2 μg l^{-1} in 2006 and from 0.6 to 8.2 μg l^{-1} in 2007. Concentrations were 44 % to 3-fold higher in 2006 than in 2007 depending on the station. These differences were statistically significant (Student's t-test) for stations MP, RU ($p < 0.01$), WB and KH ($p < 0.05$).

Highest concentrations were measured at the head of the estuary in 2006, whereas in 2007 the horizontal distribution of chl-a varied over time. Chl-a was maximal at the mouth of the estuary on 4 and 10 July, in the middle of the estuary on 5, 6 and 11 July and at the head of the estuary on 7 and 12 July. Variations along the estuary were more pronounced in 2006, with concentrations increasing by up to 9-fold between TP and MP but only up to 5-fold in 2007. Higher concentrations were generally measured during neap tides in 2007 (10-12 July), although in 2006 chl-a concentrations were significantly higher at all stations on 9 July, between neap and spring tide (Mann-Whitney U-test or Student's t-test as appropriate, $p < 0.05$).

There was generally little variation in chl-a with depth and chl-a was usually highest at the surface, although occasionally a subsurface maximum was observed (Table 5.7). The difference between surface and bottom in 2006 was more pronounced during neap than during spring tides, although this was not observed in 2007 (Table 5.7).

Chl-a displayed significant positive correlations with NO_3^- ($r^2 = 0.35$, $n = 60$, $p < 0.01$), PO_4^{3-} ($r^2 = 0.22$, $n = 59$, $p < 0.01$) and Si ($r^2 = 0.23$, $n = 59$, $p < 0.01$) in 2006, but no significant correlation with NO_3^- or Si, and a significant negative correlation with PO_4^{3-} in 2007 ($r^2 = 0.14$, $n = 33$, $p < 0.05$) (Figure 5.12).

	Tidal range (m)	MP	WB	RU	SC	KH	TP
a. 2006							
04/07	2.35	-	-	6.2	*11.5/ 4.0*	*6.4/ 2.8*	*6.3/ 2.5*
05/07	2.25	10.9	-	-	*9.6/ 1.9*	12.1	*8.3/ 3.7*
07/07	2.60	11.8	5.6	7.8	*7.4/ 1.6*		*7.4/ 1.9*
08/07	2.90	11.6	7.9	6.6	*5.5/ 2.8*	*9.3/ 3.1*	*2.0/ 2.3*
09/07	3.30	17.8	15.1	6.8	14.2	*10.1/ 7.6*	*7.9/ 6.7*
11/07	4.10	19.2	13.1	8.4	*8.3/ 10.6*	*11.9/ 11.4*	*11.4/ 10.2*
12/07	4.20	-	-	-	*12.1/ 10.3*	*12.7/ 6.2*	*12.9/ 9.1*
14/07	4.50	5.2	5.5	-	*7.0/ 9.1*	*5.8/ 5.7*	*3.8/ 3.5*
15/07	4.45	-	-	-	*10.4/ 10.3*	-	*4.9/ 5.0*
16/07	4.20	-	-	-	-	-	-
b. 2007							
04/07	3.85	1.3	2.2	2.1	*4.5/ 5.0*	3.2	*4.0/ 4.2*
05/07	3.80	3.5	4.6	5.6	*6.1/ 5.2*	-	4.5
06/07	3.65	0.6/ 0.3	1.5/ 1.3	1.6/ 3.5	3.2	2.2/ 3.1	2.0/ 2.6
07/07	3.35	6.2	-	-	*4.3/ 5.1*	2.1/ 4.6	3.1/ 3.6
10/07	2.85	3.4	3.3/ 3.6	3.8/ 4.3	5.9/ 5.7	4.1/ 3.6	7.7/ 6.0
11/07	2.95	5.1	5.5/ 6.3	5.8/ 5.2	8.2/ 5.4	-	6.1/ 5.1
12/07	3.25	6.6	6.2	4.5	-	5.7	5.8

Table 5.7. Chl-a concentrations (µg l^{-1}) measured at the surface (and 2-3 m from the bottom where two values are given) at 6 different stations along the estuary in (a) 2006 and (b) 2007. Italics represent measurements made on *RV Bill Conway*.

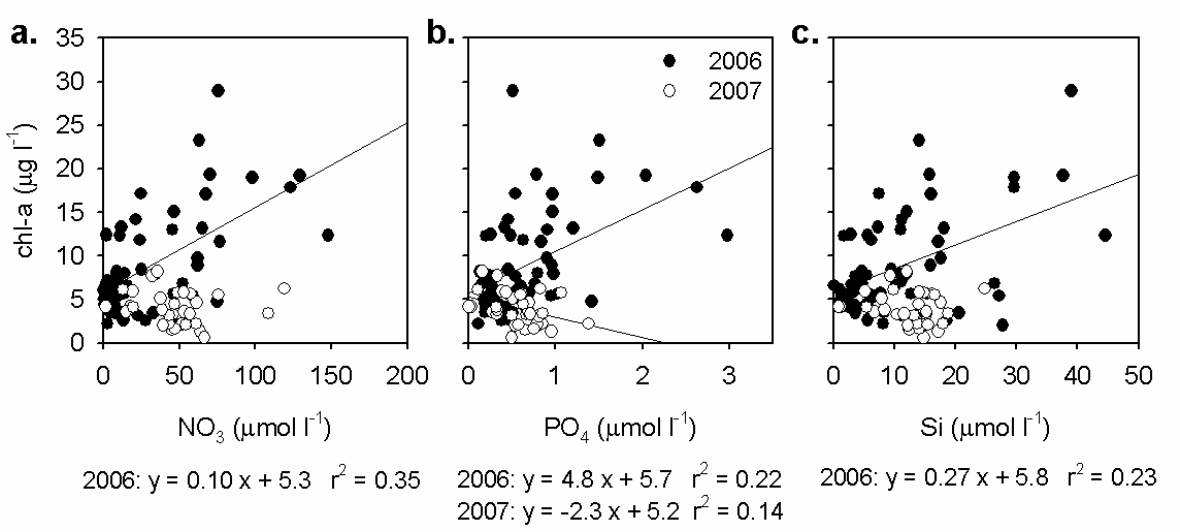

Figure 5.12. Relationships between surface chl-a and (a) NO_3^-, (b) PO_4^{3-} and (c) Si concentrations in 2006 (closed circles) and 2007 (open circles). Regression lines are drawn and equations shown where significant correlations were observed, i.e. 2006 for all nutrients and 2007 for PO_4.

5.2.6. Phytoplankton community structure

5.2.6.1. Cell counts

In 2006, diatoms were dominant, representing up to 99.5 % of total phytoplankton cells, although dinoflagellates dominated (between 50 and 93 %) at some stations (KH on 5 July, SC on 9 July and TP on 8 and 15 July). On these occasions, the main dinoflagellate species were *Alexandrium minutum* type cells (hereafter referred to as *Alexandrium*) at KH and SC, but *Karenia mikimotoi* at TP (Figure 5.13). The main diatom species were *Thalassiosira* spp. (up to 94 % total cells), *Leptocylindrus danicus* (up to 90 %) and *Rhizosolenia setigera* (24 %).

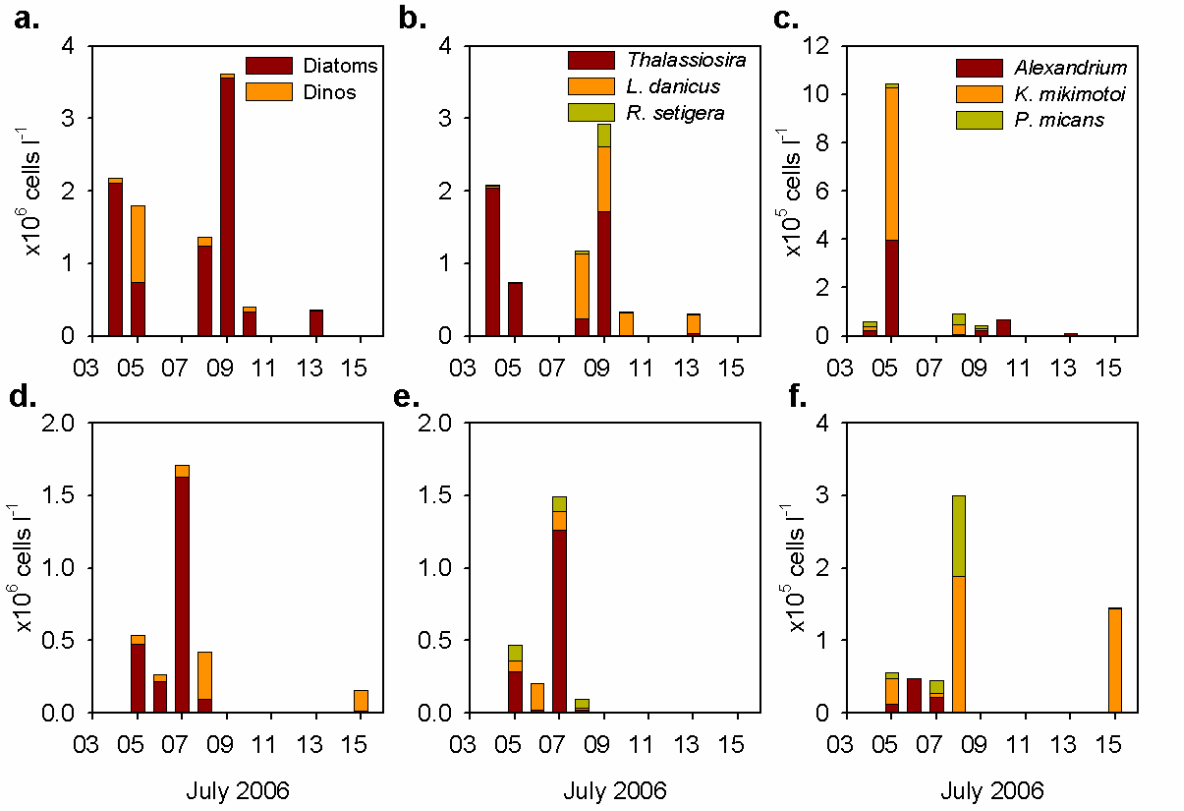

Figure 5.13. Total concentrations of diatoms and dinoflagellates at (a) KH and (d) TP, concentrations of the main diatom species at (b) KH and (e) TP and concentrations of the main dinofagellate species at (c) KH and (f) TP in July 2006.

In 2007, total cell concentrations were one order of magnitude lower and the community was generally dominated by dinoflagellates (up to 99 %), although on 7 and 10 July (Malpas) it was dominated by diatoms (71-94 %) (Figure 5.14). *Alexandrium* was the dominant dinoflagellate, representing 88 to 100 % dinoflagellate cell numbers.

The main diatom species were *Cylindrotheca closterium* (up to 95 % diatom numbers), *Thalassiosira* spp. (up to 30 %) and *Rhizosolenia setigera* (up to 38 %).

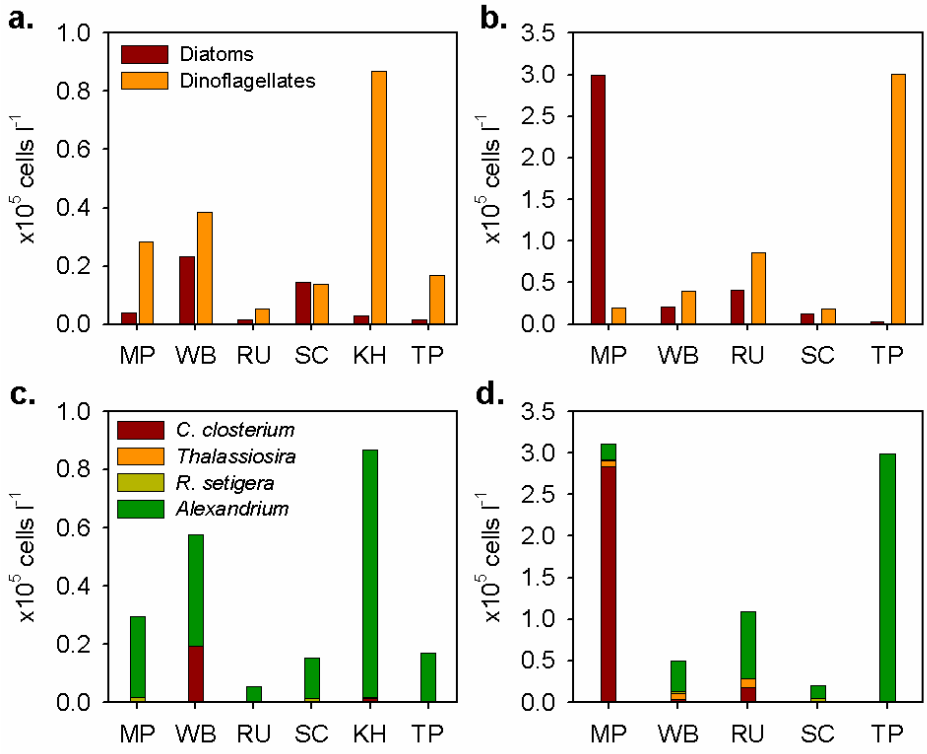

Figure 5.14. Concentrations of (a,b) diatoms and dinoflagellates and (c,d) the main diatom and dinoflagellate species at various stations along the estuary on (a,c) 5 July and (b,d) 10 July 2007.

5.2.6.2. Cluster analysis

Cluster analysis revealed the presence of 5 clusters at the 40 % similarity level, with 2 stations clustering separately. These were omitted from further analyses since the aim of the analysis was to investigate the contributions of different species to between-station similarity within clusters. Cluster I comprised lower estuary (TP) stations from 2006 and was characterised by *Karenia mikimotoi* (Table 5.8). Cluster II comprised stations from various locations along the estuary between 4 and 9 July 2006 and was characterised by a mixture of diatoms, ciliates and *Alexandrium*. Cluster III comprised mid- to lower estuary stations between 6 and 13 July 2006 and was characterised by *Leptocylindrus danicus*. Cluster IV comprised upper estuary stations from both 2006 and 2007 and was characterised by *Cylindrotheca closterium*. Cluster V comprised 2007 stations from all stations along the estuary as well as a 2006 station, and was characterised by *Alexandrium*.

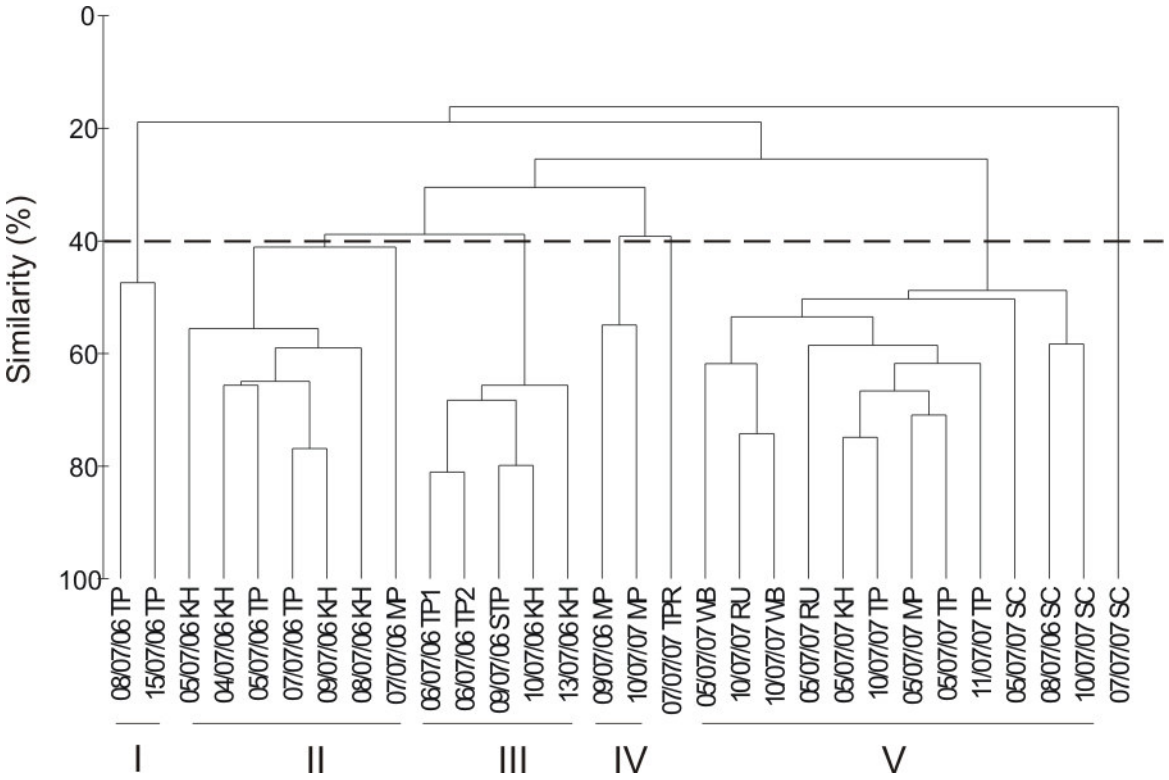

Figure 5.15. Dendrogram derived from calculations of Bray-Curtis similarity indices between stations in 2006 and 2007 combined, using the statistical package PRIMER. Clusters formed at the 40 % similarity level are labelled (I-V) as in the text.

The different clusters displayed, to a certain extent, different hydrographic, chemical and biological properties (Table 5.8). Cluster I was characterised by high temperatures and salinities, very low NO_3^- and PO_4^{3-} but higher Si and low N:P and N:Si ratios and chl-a concentrations. Clusters II and III were both characterised by high temperatures and salinities, moderate nutrient concentrations and high chl-a. Cluster IV occurred at low salinities, high nutrient concentrations and nutrient ratios and high chl-a. Cluster V occurred at low temperatures, intermediate salinities and high nutrient concentrations and ratios (although not as high as Cluster IV), but low chl-a concentrations.

Locations	Species	% contribution to similarity	Temp	Sal	chl-a	% diatoms	H'	NO_3^-	PO_4^{3-}	Si	DIN:P	DIN:Si
TP	*Karenia mikimotoi*	52.1	17.1 (0.05)	34.5 (0.3)	2.5 (1.9)	15.4 (8.3)	1.2 (0.7)	0.7 (0.4)	0.0	5.3	5.3	0.2
TP	*R. setigera*	21.3										
	Naked ciliate	7.8										
KH	*Thalassiosira* spp.	37.2	18.1 (0.06)	33.3 (0.3)	9.8 (1.1)	84.6 (7.6)	1.4 (0.1)	7.0 (1.7)	0.4 (0.1)	5.6 (1.6)	25 (5)	1.2 (0.5)
KH, TP	*Mesodinium* spp.	9.9										
MP, TP	*R. setigera*	9.8										
KH	*L. danicus*	7.2										
KH	*Alexandrium* spp.	7.1										
	P. micans	5.9										
	Naked ciliate	4.7										
TP	*L. danicus*	64.4	17.0 (1.1)	33.3 (0.5)	10.0 (1.5)	90.6 (3.5)	0.8 (0.2)	5.8 (1.3)	0.1 (0.0)	1.7	49 (21)	1.9
STP	*Alexandrium* spp.	14.4										
KH	*Thalassiosira* spp.	10.1										
KH												
MP	*C. closterium*	49.7	16.2 (1.6)	22.0 (1.1)	11.1 (1.2)	96.7 (2.8)	1.3	128.2 (19.6)	1.7 (1.3)	27.7 (16.8)	166 (116)	6.6 (3.3)
MP	Naked ciliate	22.4										
	Thalassiosira spp.	10.8										
MP, WB, RU,	*Alexandrium* spp.	75.5	14.7 (0.2)	30.9 (0.4)	5.4 (0.5)	30.4 (6.4)	0.9 (0.1)	42.7 (5.0)	0.5 (0.1)	11.0 (1.4)	98 (11)	4.4 (0.4)
KH, TP	*R. setigera*	7.0										
SC												
SC												
WB, RU, SC, TP												
TP												

Table 5.8. Main species contributions to total similarity (up to 80 % cumulative percentage) within clusters defined at the 40 % similarity level using the statistical package PRIMER, and mean (standard error) temperature, salinity, chl-a, % diatoms, Shannon diversity index H', NO_3^-, PO_4^{3-} and Si concentrations and DIN:P and DIN:Si ratios for each cluster.

5.2.7. Nitrogen uptake

5.2.7.1. Uptake and regeneration rates

In 2006, $\rho(NH_4^+)$ was significantly lower than both $\rho(NO_3^-)$ (Wilcoxon's test, $p < 0.05$) and ρ(urea) (paired t-test, $p < 0.01$). Nitrate uptake ranged from 0.024 to 0.149 μmol N l^{-1} h^{-1} and ρ(urea) from 0.062 to 0.110 μmol N l^{-1} h^{-1}, whereas $\rho(NH_4^+)$ ranged from 0.018 to 0.089 μmol N l^{-1} h^{-1} (Figure 5.16a). Uptake rates of the various nitrogen sources were not significantly different from one another.

In 2007, both $\rho(NO_3^-)$ and ρ(urea) were significantly lower than in 2006 (Mann-Whitney U-test and Student's t-test, $p < 0.05$ and $p < 0.001$, respectively), but $\rho(NH_4^+)$ was similar to 2006, hence NH_4^+ was generally the most important source of nitrogen. Ammonium uptake ranged from 0.018 to 0.131 μmol N l^{-1} h^{-1}, $\rho(NO_3^-)$ from 0.007 to 0.058 μmol N l^{-1} h^{-1} and ρ(urea) from 0.007 to 0.035 μmol N l^{-1} h^{-1} (Figure 5.16b). Ammonium uptake was significantly higher than ρ(urea) (Wilcoxon's test, $p < 0.01$) but insignificantly different from $\rho(NO_3^-)$. Ammonium uptake increased towards the head of the estuary, whereas $\rho(NO_3^-)$ and ρ(urea) showed little variation, with the exception of one high $\rho(NO_3^-)$ value of 0.058 μmol N l^{-1} h^{-1} measured at the mouth of the estuary (Figure 5.16b).

f-ratios ranged from 0.11 to 0.56 in 2006 (mean 0.41 ± 0.04) and from 0.09 to 0.73 in 2007 (mean 0.23 ± 0.06). They were significantly higher in 2006 relative to 2007 (Student's t-test, $p < 0.05$).

Regeneration rates $r(NH_4^+)$ were on average higher in 2007 (0.079 ± 0.019 μmol N l^{-1} h^{-1}) relative to 2006 (0.038 ± 0.009 μmol N l^{-1} h^{-1}), although the difference was not statistically significant. Ammonium uptake rates displayed a significant positive correlation with $r(NH_4^+)$ for both years combined, with a regression coefficient of 0.52 ($r^2 = 0.47$, $p < 0.01$, $n = 14$, Figure 5.17).

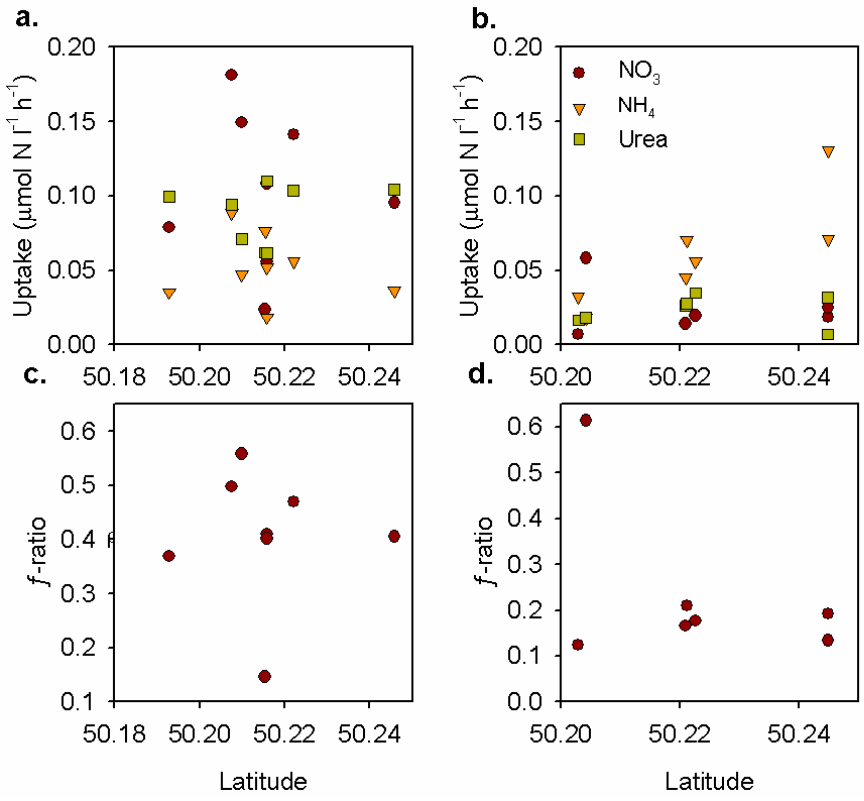

Figure 5.16. $\rho(NO_3^-)$, $\rho(NH_4^+)$ and ρ(urea) in (a) 2006 and (b) 2007 and *f*-ratios in (c) 2006 and (d) 2007 at various stations along the estuary measured on different dates.

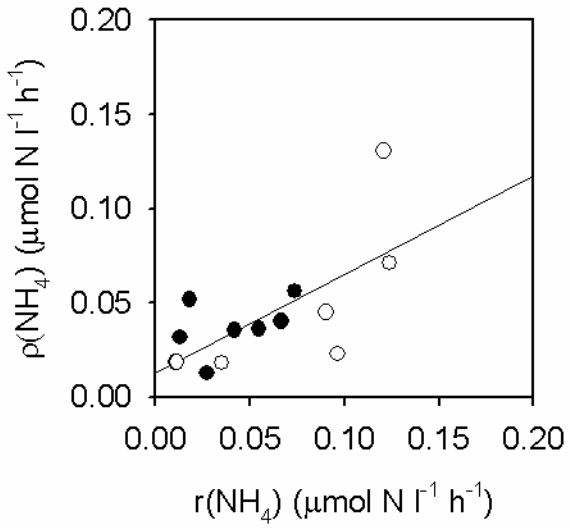

Figure 5.17. Linear regression of $\rho(NH_4^+)$ versus $r(NH_4^+)$ in 2006 (closed circles) and 2007 (open circles) combined; y = 0.52 x + 0.01 (r^2 = 0.47, p < 0.01).

5.2.7.2. Nitrogen uptake kinetics

Two experiments were carried out in 2006 at the same location and were dominated by the same phytoplankton species, *Leptocylindrus danicus*. As a result, the curves and kinetics parameters for NH_4^+ were very similar for both experiments (Figure 5.18, Table 5.9), although they were not determined for NO_3^- in experiment 1. Ammonium was preferred over NO_3^-, with ν_{max} and α 2- and 4-fold higher for NH_4^+ than for NO_3^-, respectively.

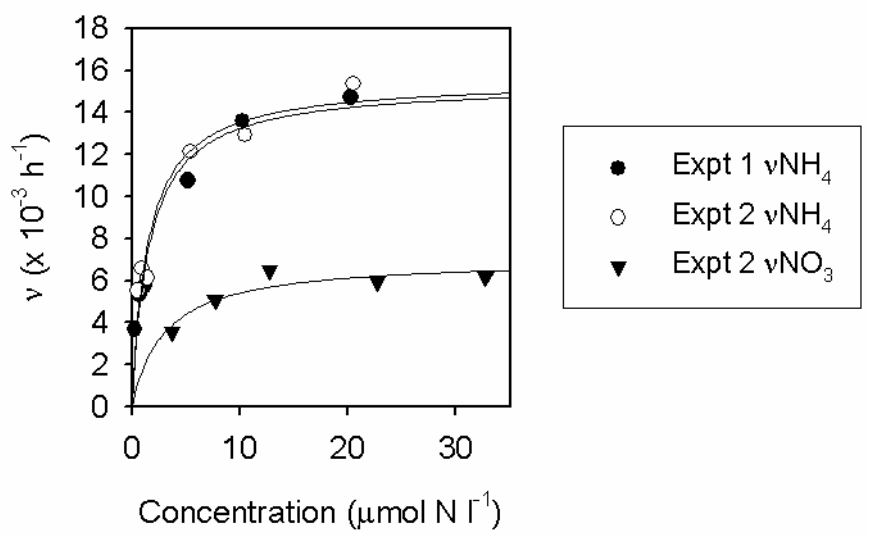

Figure 5.18. PN-specific nitrogen uptake rates versus concentration on 10 July (Expt 1) and 13 July 2006 (Expt 2), fitted to the Michaelis-Menten equation for uptake kinetics using the statistical package SigmaPlot (Jandel Scientific).

Exp.	Dominant	ν_{max}		K_s		α		$\frac{\nu_{max}(NH_4^+)}{\nu_{max}(NO_3^-)}$	$\frac{\alpha(NH_4^+)}{\alpha(NO_3^-)}$
#	species	NO_3^-	NH_4^+	NO_3^-	NH_4^+	NO_3^-	NH_4^+		
1	*L. danicus*	-	15.4 (1.0)*	-	1.61 (0.38)*	-	9.6	-	-
2	*L. danicus*	7.0 (0.6)*	15.6 (1.1)*	3.04 (1.21)	1.50 (0.39)*	2.3	10.4	2.23	4.52

Table 5.9. Nitrogen uptake kinetics parameters ν_{max} (x 10^{-3} h^{-1}), K_s (µmol N l^{-1}) and α (x 10^{-3} h^{-1}(µmol N l^{-1})$^{-1}$) for NO_3^- and NH_4^+ for Experiments 1 and 2 and ratios of the parameters for NH_4^+ to those for NO_3^-, given as indicators of nutrient preference.

5.3. Discussion

5.3.1. Effects of environmental conditions on phytoplankton biomass and community structure

Contrasting meteorological conditions were observed between 2006 and 2007, with 40 %, 6-fold and 3-fold higher rainfall measured in May, June and July 2007, respectively, relative to corresponding months in 2006. Maximum and minimum temperatures were 30 % and 17 % higher, respectively in July 2006, and duration of sunshine was 70 % and 27 % longer in June and July 2006, respectively. The warmer air temperatures in 2006 led to significantly higher water temperatures at all stations, while the lower rainfall led to higher salinities and weaker salinity stratification. Furthermore, NO_3^- concentrations were significantly higher in 2007 at all stations except MP, and Si concentrations were significantly higher at TP and SC. Ammonium concentrations were also significantly higher in 2007 at all stations combined. The higher NO_3^- and Si concentrations in 2007 can be explained by increased runoff. The lack of a significant difference in PO_4^{3-} concentrations between years suggests that PO_4^{3-} was supplied by different sources to NO_3^- and Si, although the increased freshwater flow in 2007 would have acted to reduce PO_4^{3-} concentrations. Sources of NH_4^+ include sewage effluent and *in situ* recycling, therefore NH_4^+ concentrations are not directly related to freshwater input. However, the correlation between NH_4^+ and NO_3^- concentrations (Figure 5.10) indicates that NH_4^+ concentrations may have been indirectly linked to runoff via the relationship between NH_4^+ and NO_3^-. The higher concentrations in 2007 could have been due to the higher regeneration rates (average 0.079 compared to 0.038 μmol N l^{-1} h^{-1} in 2006), which were ~2-fold higher than $\rho(NH_4^+)$.

In 2006, chl-a and nutrient concentrations were positively correlated (Figure 5.12), as observed for a range of estuaries by Monbet (1992), indicating that phytoplankton biomass was probably controlled by nutrient availability. Lower chl-a concentrations in 2007 however were not due to nutrient limitation, since nutrient concentrations were generally higher than in 2006. Irradiance exerts a very strong control on phytoplankton growth (Falkowski & Owens, 1978), therefore the reduced ambient irradiance in 2007 (hence lower surface incident irradiance) were most likely responsible for the reduced biomass. Although wind velocities were not recorded, increased wind in 2007 would

have increased turbidity and thus reduced light penetration through the water column. Tidal mixing and its influence on light availability is also known to play an important role in limiting primary production in estuaries (Monbet, 1992; Gianesella et al., 2000). In this study, the neap tidal range was lower in 2006 (2.30 m) relative to 2007 (2.85 m), however the spring tidal range was higher (4.50 m in 2006 and 3.90 m in 2007). In 2007, higher biomass was observed during neap tides relative to spring tides, however this was not the case in 2006, suggesting that tidal mixing may have been a limiting factor in 2007. Although not measured in this study, grazing pressure may also have played a part in limiting phytoplankton growth. This is supported by the higher $r(NH_4^+)$ in 2007, which suggests that microzooplankton was more abundant in this year.

Marked differences in phytoplankton community structure were observed between years, with diatoms generally dominant in 2006 and dinoflagellates in 2007. Diatoms are traditionally associated with turbulent, high nutrient conditions in spring, whereas dinoflagellates are typically associated with more stratified, nutrient-depleted conditions in summer (Margalef, 1978). This successional pattern is generally observed in temperate coastal waters (Smayda, 1980), although in the Fal Estuary the peak of the diatom bloom has been recorded in June rather than in the early spring (Percy, 2006). This author also reported a higher dominance of diatoms in June 2001 relative to June 2002, when temperatures were ~2 °C higher and dinoflagellates dominated for a period, albeit at lower concentrations.

The lower temperatures and irradiances and higher nutrient concentrations recorded in 2007 are not conditions typically associated with dinoflagellate blooms. However, stronger stratification due to increased rainfall and freshwater runoff most likely favoured dinoflagellates. These are generally more successful in stable environments due to their susceptibility to turbulence (White, 1976; Thomas & Gibson, 1992; Berdalet & Estrada, 1993), although different species display different preferences in terms of water column stability (Holligan et al., 1980). Nutrients and turbulence are positively correlated in the open ocean and dinoflagellates generally occur along a gradient of decreasing turbulence and nutrient availability (Margalef, 1978). However, the "anomalous" combination of high nutrients and high water column stability can occur in coastal environments, and according to Margalef's Mandala these conditions are conducive to HABs (Margalef et al., 1979). This situation was observed in the present study, where increased rainfall, hence freshwater inputs, were responsible for increased

nutrient concentrations and coincided with the dominance of the toxic dinoflagellate *Alexandrium* in 2007.

The dominant diatom species were *Thalassiosira* spp. (37 % similarity within Cluster II), *Leptocylindrus danicus* (64 % similarity within Cluster III) and *Cylindrotheca closterium* (50 % similarity within Cluster IV). Clusters II and III occurred within similar ranges of temperature (17.9-18.3, with the exception of one value of 14.8), salinity (32.0-34.2), NO_3 (2.7-12.0 μmol l^{-1}), PO_4^{3-} (0.09-0.55 μmol l^{-1}), Si (1.7-11.2 μmol l^{-1}), N:P (13.3-89.5) and N:Si ratios(0.2-2.4). These communities were distributed along the estuary, from Malpas to South of Turnaware Point. This wide distribution and the wide range of nutrient concentrations indicates that these communities were able to adapt to fluctuating conditions and were probably carried up and down the estuary with the ebbing and flooding tides. Both *L. danicus* and *Thalassiosira* spp. have been reported as important components of the phytoplankton community in the Fal Estuary, with *L. danicus* dominating in summer and *Thalassiosira* spp. in autumn (Percy, 2006). The low N:Si ratios relative to the other clusters were indicative of these communities' high requirement for Si and their lack of success under Si-limited conditions. In contrast, Cluster IV occurred only on 2 occasions and both times at MP, therefore these species were adapted to low salinities (20.9-23.2) and high nutrient concentrations as well as high N:P and N:Si ratios. This lower requirement for Si is consistent with the morphology of the dominant species *C. closterium*, which is a small, lightly silicified cell.

5.3.2. Factors affecting the spatial and temporal distribution of toxic species

5.3.2.1. Karenia mikimotoi

The ichthyotoxic naked dinoflagellate *Karenia mikimotoi* was present in 2006 and responsible for 52 % similarity within Cluster I. This cluster occurred only on two occasions, at TP (1.4-1.9 x 10^5 cells l^{-1}), where salinities were high (34.2-34.8) and nutrients were low (NO_3^- < 1 μmol l^{-1}, PO_4^{3-} < 0.01 μmol l^{-1}). *K. mikimotoi* was also present in high concentrations (6.3 x 10^5 cells l^{-1}) at KH on one occasion, although it was a smaller component of the phytoplankton community and this station was not included in Cluster I. Interestingly, *K. mikimotoi* was absent from the community in 2007, suggesting that it was better adapted to the warmer temperatures and/or higher

salinities and lower nutrient concentrations in 2006. *K. mikimotoi* has been previously reported in the Fal Estuary in late summer, peaking at a concentration of 1.8 x 10^6 cells l^{-1} in the Percuil River (Percy, 2006). This author reported that cells were first detected at the Narrows and later in the Percuil River, and hypothesised that the cells originated in the English Channel and were then advected into the estuary. The reported occurrence of the blooms in August/September is consistent with an adaptation to warmer temperatures, while their seaward origin confirms their association with more saline waters. Blooms of *K. mikimotoi* (previously known as *Gymnodinium aureolum*) are known to occur in the English Channel (Holligan, 1979; Garcia & Purdie, 1994) and in the Irish Sea (Ottway et al., 1979). Blooms in the western English Channel and off the south coast of Ireland also occurred at very low NO_3^- (<0.5 µmol l^{-1}) and PO_4^{3-} concentrations (<0.1 µmol l^{-1}) (Garcia & Purdie, 1994; Raine et al., 2001), suggesting a preference for nutrient-depleted waters. This is consistent with its presence in 2006 at very low nutrient concentrations (0.2-1.1 µmol l^{-1}) and its absence in 2007, when concentrations were generally higher. Raine et al. (2001) also reported that *K. mikimotoi* blooms develop in stratified waters in the region of the thermocline and are brought to the surface by upwelling, then advected towards the coast during upwelling relaxation. Several authors have also reported the occurrence of *K. mikimotoi* at thermal fronts between upwelled and stratified waters (Holligan et al., 1980; Holligan, 1981; Roden et al., 1981) and blooms are regularly reported at the L4 station off Plymouth (Rodríguez et al., 2000). It therefore seems plausible that in the present study *K. mikimotoi* developed in stratified, nutrient-depleted offshore waters and was then advected into the estuary.

5.3.2.2. Pseudo-nitzschia

Pseudo-nitzschia spp. (hereafter *Pseudo-nitzschia*) was relatively abundant in 2006, reaching 6.1 x 10^5 cells l^{-1}, but representing only 2-45 % total phytoplankton cell numbers. Concentrations were very low in 2007 (<10^3 cells l^{-1}), representing only 0.2-1.6 % total phytoplankton. It was not possible to identify *Pseudo-nitzschia* to species level using light microscopy, but several species were isolated from the Fal and cultured in the study by Percy (2006). These were identified as *Pseudo-nitzschia fraudulenta*, *P.* cf. *pseudodelicatissima*, *P. multiseries* and *P. pungens* and of these, *P. multiseries* was the only one found to produce DA. Although the cells were not identified to species level in the counts of Percy (2006), *P.* cf. *pseudodelicatissima* and *P. fraudulenta* were

identified from samples using Transmission Electron Microscopy (TEM) and were thought to dominate the bloom in June. In the present study, cell sizes were within the range reported by Percy (2006) for *P.* cf. *pseudodelicatissima*.

In 2006, *Pseudo-nitzschia* was observed only at KH and TP, suggesting a seaward source and advection of cells into the estuary. Percy et al. (2006) reported that peaks of *Pseudo-nitzschia* concentrations in the Percuil River and at the Narrows occurred in June-July and September and reached 10^6 cells l^{-1}. The author also reported increased concentrations towards the mouth of the estuary and in Falmouth Bay, suggesting a seaward source and tidal advection of the cells into the estuary. Furthermore, highest domoic acid concentrations were detected in mussels and oysters collected at the seaward end of the estuary (Percy, 2006). As with *Karenia mikimotoi*, the presence of *Pseudo-nitzschia* in 2006 but not in 2007 suggests a preference for warmer, more saline but less stratified water and lower nutrient concentrations.

Blooms of *P. pseudodelicatissima* have been reported on the Washington Coast (USA) in association with shellfish toxicity (Trainer et al., 2002; 2007). They are thought to be initiated in the Juan de Fuca eddy and later transported towards the coast (Trainer et al., 2002). In the eddy, high nutrient concentrations are supplied by a combination of factors, such as upwelling, wind mixing and the outflow of nutrient-rich estuarine water from the Juan de Fuca Strait. However, no link was found between *P. pseudodelicatissima* and Si and NO_3^- concentrations, although it was generally associated with N:Si ratios <1. Blooms occurring in the inland waterways of Washington State, however, were associated with high anthropogenic nutrient concentrations, particularly NH_4^+ (up to 13 μmol l^{-1}) but low NO_3^- concentrations (Trainer et al., 2007). It was hypothesised that the small cell size of *P. pseudodelicatissima*, hence high surface area: volume ratio, gave it an advantage over larger species at limiting NO_3^- concentrations. Other laboratory and field experiments concluded that *Pseudo-nitzschia* was favoured by high N:Si ratios (Sommer, 1994; Dortch et al., 1997; Anderson et al., 2006). In the present study, N:Si ratios ranged from 0.2 to 2.4 when *Pseudo-nitzschia* was present and both NO_3^- and Si concentrations were non-limiting, therefore *Pseudo-nitzschia* was not necessarily favoured by Si limitation. Marchetti et al. (2004) also reported the occurrence of *Pseudo-nitzschia* in the Juan de Fuca eddy in association with high NO_3^- and Si concentrations, although in contrast *Pseudo-nitzschia australis* (a member of the same species complex as *P. fraudulenta*) was associated with low nutrient concentrations (Buck et al., 1992).

Studies have also reported links between *Pseudo-nitzschia* abundance and stratification. In the Washington State waterways, *P. pseudodelicatissima* was associated with increased stratification after a period of high rainfall and river discharge (Trainer et al., 1998; 2007). In Monterey Bay (California), peaks in *P. australis* were associated with periods of wind relaxation and stratification and its abundance was positively correlated with temperature (Buck et al., 1992). Although *Pseudo-nitzschia* in the present study was associated with higher temperatures in 2006, it did not appear to be favoured by the stronger stratification in 2007.

5.3.2.3. Alexandrium

Highest concentrations of *Alexandrium* were observed at KH in 2006, and at TP in 2007. Concentrations were lowest at the two extremities, MP and South of TP. Percy (2006) also reported highest concentrations at Turnaware Point, although sometimes the maximum was further south, between Turnaware Point and the Narrows, or in the Percuil River. The author hypothesised that seed beds situated in the Percuil were a source of *Alexandrium* cells, hence the high concentrations sometimes observed at the Narrows, where the Percuil flows into the main estuary.

Alexandrium was relatively abundant in both 2006 and 2007 (up to 4 x 10^5 and 3 x 10^5 cells l^{-1}, respectively), although the proportion of *Alexandrium* cells was much higher in 2007 (up to 98 %, relative to 50 % in 2006), as few other species were present at that time. Although light microscopy was not sufficient to differentiate between *Alexandrium minutum* and *A. tamarense*, previous studies have shown that *A. minutum* is the dominant species in the Fal Estuary (Percy et al., 2004; Percy, 2006), therefore it is assumed that this was the case in the present study. Furthermore, the sizes of the *Alexandrium* cells were generally closer to those reported for *A. minutum* (~ 25 μm diameter).

The conditions that prevailed in July 2007 (lower temperatures, lower irradiance and stronger stratification) were specifically favourable to *Alexandrium*, thus allowing it to outcompete other species. Cluster analysis confirmed that the cluster dominated by *Alexandrium* occurred under low temperatures (14.1-16.4 °C, mean 14.7 °C) and moderate salinities (28.8-34.5, mean 30.9). Furthermore, a significant negative correlation was observed between the percentage of *Alexandrium* cells and temperature ($r^2 = 0.59$, $n = 26$, $p < 0.01$, Table 5.10). The proportion of *Alexandrium* cells also

decreased linearly with increasing salinity in the range 29-35 ($r^2 = 0.41$, n = 24, $p < 0.01$ for salinity), although it dropped dramatically at salinities below 29 (not included in the regression, Table 5.10). There was no significant relationship between temperature and salinity in the range 29-30, therefore the relationship between *A. minutum* and both parameters was not an artefact of the relationship between temperature and salinity. Although it is difficult to tease apart the relative roles of the different parameters without using multivariate techniques, regression analysis was preferred over multidimensional scaling or principal component analysis because these did not reveal any clear trends. Principal component analysis of temperature, salinity, NO_3^-, PO_4^{3-} and N:P produced principal components PC1 and PC2 that were collectively responsible for 84 % of variation in the data, but neither PC score showed any relationship with % *Alexandrium* (data not shown). Furthermore, the cluster dominated by *Alexandrium* showed a wide range of PC scores.

	a	b	r^2	n
Temp	-16.3	296.3	0.59**	26
Sal	-12.8	450.8	0.41**	24
NO_3	1.2	8.5	0.55**	26
PO_4	61.4	17.9	0.21*	24
N:P	0.36	13.9	0.23*	24

Table 5.10. Parameters from linear regressions (y = ax + b) of % *Alexandrium* in the phytoplankton community and temperature, salinity, NO_3^-, PO_4^{3-} and N:P ratio. n is the number of observations. * p < 0.05. ** p < 0.01.

Alexandrium minutum blooms have been reported within various temperature ranges, e.g. 12-14.5 °C on the Catalan coast of Spain (Vila et al., 2005; Bravo et al., 2008), 16-24 °C in Syracuse Harbour (Sicily) (Vila et al., 2005), 18.3-21.6 °C in Greek coastal waters (Ignatiades et al., 2007), 14.9-18.2 °C in Cape Town Harbour (Pitcher et al., 2007) and 16.3-18.9 in the Penzé Estuary (France) (Maguer et al., 2004). *Alexandrium* in the present study appeared to be favoured by a temperature range within the lower half of that reported for Cape Town Harbour. In a comparative study of the Fal Estuary in 2 consecutive summers, higher *Alexandrium* concentrations were observed in the year when temperatures were between 12 and 16 °C relative to the previous year, when they were <14 °C (Percy, 2006).

Culture experiments have shown that growth of *A. minutum* becomes saturated at relatively low irradiances compared to other species, such as *A. tamiyavanichii* (Lim et al., 2006), *Heterosigma carterae* and *Thalassiosira pseudonana* (Chang & McClean,

1997). This, together with observations of *A .minutum* blooms developing throughout the water column (Cannon, 1990; Chang & Bradford-Grieve, 1994), suggests that this species is generally well adapted to low irradiances. This is consistent with the finding in the present study that *Alexandrium* was more successful in 2007 when irradiances were lower due to meteorological conditions.

Salinities measured for the *Alexandrium*-dominated cluster (Cluster V) in the present study (28.8-34.5) were lower than those reported for *A. minutum* blooms on the Catalan coast and in Syracuse Harbour (32-38, Vila et al. (2005), Bravo et al. (2008)), in Greek waters (35.2-38.2, Ignatiades et al. (2007)) and in Cape Town Harbour (34.1-37.6), but higher than those reported for the Penzé Estuary (26.1-28.0, Maguer et al. (2004)). It was, however, similar to the range reported for Ganzirri Lagoon (29.6-33.4, Giacobbe et al. (1996)). A previous study in the Fal reported the presence of *A. minutum*-type cells at salinities between 21 and 36 (Percy, 2006), although concentrations were reduced at the two extremes, as was the case in the present study.

Culture experiments have demonstrated a high tolerance to fluctuating salinity in *A. minutum*, with no significant difference in growth rate observed at salinities between 5 and 30 in a Malaysian strain (Lim & Ogata, 2005). A similar experiment conducted with a strain isolated from Brittany showed insignificant differences in growth rates in the salinity range 25-37 (Grzebyk et al., 2003), consistent with the range of salinities that appeared favourable to *Alexandrium* in the present study. A negative correlation between *A. minutum* cell concentration and salinity was observed in Ganzirri Lagoon within the range 29-34, suggesting a preference for the lower salinities (Giacobbe et al., 1996). On the Catalan coast, the most intense blooms of *A. minutum* were also observed at the lowest salinities (Bravo et al., 2008). Both of these studies are consistent with the relationship observed in the present study (Table 5.10).

Giacobbe et al. (1996) also reported that maximum *Alexandrium minutum* cell concentrations coincided with highest vertical density gradients, i.e. strongest stratification. This was also the case in the present study, where a higher dominance of *Alexandrium* in 2007 was coincident with sharper salinity gradients. Similarly, a positive correlation between *A. tamarense* blooms, rainfall and river flow was reported in the St. Lawrence Estuary (Weise et al., 2002), although in the Fal *Alexandrium* blooms have previously been associated with reduced freshwater flow (Morris, 2006).

5.3.3. Nitrogen uptake

5.3.3.1. Comparison with other estuaries

An increase in $\rho(NO_3^-)$ and $\rho(NH_4^+)$ was observed with increasing chl-a concentrations up to 10 $\mu g\ l^{-1}$, followed by a decrease at higher concentrations (Figure 5.19). This suggests that self-shading may have occurred at the highest concentrations, which may have caused a reduction in $\rho(NO_3^-)$ and $\rho(NH_4^+)$ as a result of the reduced irradiance. Urea uptake showed a general increase with chl-a, suggesting that ρ(urea) was not as light-dependent as $\rho(NO_3^-)$ and $\rho(NH_4^+)$. In the Humber Estuary, uptake rates of all 3 nitrogen forms increased with irradiance (Shaw et al., 1998) and in a comparative study of 6 European estuaries (Ems, Scheldt, Loire, Gironde, Douro and Rhine), a significant negative correlation was found between DIN uptake and depth of the euphotic zone (Middelburg & Nieuwenhuize, 2000).

Nitrate uptake in the present study was at the lower end of the range reported for Southampton Water (Torres-Valdés & Purdie, 2006), but similar to that reported for the Humber Estuary (Shaw et al., 1998) and for the 6 European estuaries (Middelburg & Nieuwenhuize, 2000). The difference between uptake rates in the Fal and in Southampton Water could be due to lower NO_3^- and chl-a concentrations (Table 5.11). Although NO_3^- concentrations in the Humber, Ems, Loire and Rhine were often much higher than those in the Fal (Table 5.11), $\rho(NO_3^-)$ was similar, possibly because it was limited by light availability in the former estuaries, where turbidity was higher (as shown by higher light attenuation coefficients). Ammonium uptake was at the lower end of the ranges reported for 3 North Carolina estuaries (Fisher et al., 1982), up to 1 order of magnitude lower than in the Ems, Scheldt and Loire estuaries (Middelburg & Nieuwenhuize, 2000) and up to 2 orders of magnitude lower than in Southampton Water (Torres-Valdés & Purdie, 2006). This discrepancy was probably due to the lower NH_4^+ concentrations in the Fal relative to the other estuaries (Table 5.11). The difference in ρ(urea) between the Fal and Southampton Water was less pronounced, presumably due to the similar concentrations (Torres-Valdés & Purdie, 2006).

Shaw et al. (1998) and Torres-Valdés & Purdie (2006) reported higher $\rho(NH_4^+)$ relative to $\rho(NO_3^-)$, consistent with the 2007 dataset in the present study, and Middelburg & Nieuwenhuize (2000) reported a preference for NH_4^+ based on RPI in all

6 estuaries. The importance of urea as a source of nitrogen in the present study was also consistent with results from the Humber (Shaw et al., 1998).

Estuary	Concentration (µmol N l^{-1})			Uptake (µmol N l^{-1} h^{-1})			Source
	NO_3^-	NH_4^+	urea	NO_3^-	NH_4^+	urea	
Fal Estuary	0.2-108.7	0.1-2.2	0.4-1.6	0.0-0.36	0.01-0.13	0.0-0.11	a
Humber Estuary	-	-	-	<0.01-0.06	0.02-0.05	0.01-0.03	b
North Carolina Estuaries	-	0-26	-	-	<0.001-0.5	-	c
Southampton Water	<1-96	<0.2-42	0.1-1.9	0.001-2.6	0.003-5.2	0-0.3	d
6 European estuaries	4-348	0.1-245	-	0.01-1		-	e

Table 5.11. Comparison of ambient N concentrations and N uptake rates in various estuaries. [a] This study; [b] Shaw et al. (1998); [c] Fisher et al. (1982); [d] Torres-Valdes & Purdie (2004); [e] Middelburg & Nieuwenhuize (2000).

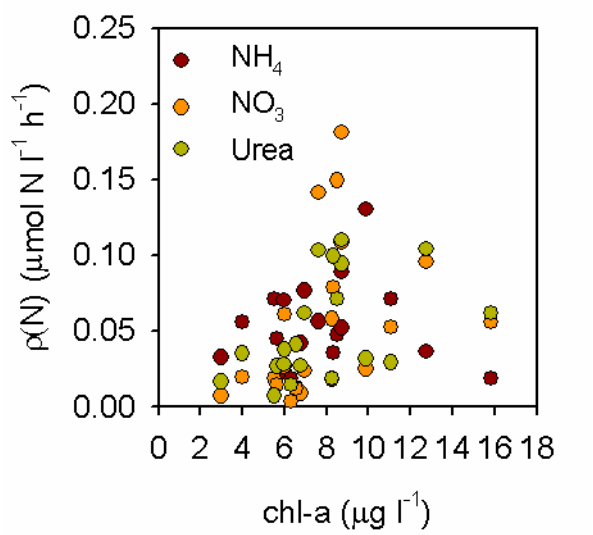

Figure 5.19. Relationships between nitrogen uptake rates and chl-a in both years.

5.3.3.2. Nutrient requirements of *Alexandrium*

In the present study, the dominance of *Alexandrium* in 2007 coincided with high NO_3^- concentrations (7.8-57.4 µmol l^{-1}, average 42.7 µmol l^{-1}) and high DIN:P (46-194, mean 98) and DIN:Si ratios (3.3-6.9, mean 4.4). Furthermore, significant positive correlations were observed between % *Alexandrium* and both NO_3^-, PO_4^{3-} and N:P within the salinity range 29-35 (Table 5.10). Although NH_4^+ concentrations were significantly higher in 2007 relative to 2006, there was no significant correlation between % *Alexandrium* and NH_4^+.

Alexandrium blooms have also been associated with high NO_3^- concentrations on the Catalan coast (Vila et al., 2005; Bravo et al., 2008), in the Bay of Plenty (New Zealand)

and Port River (South Australia) (Cannon, 1990; Chang & Bradford-Grieve, 1994). Several studies have also reported that NO_3 is generally a more important source of nitrogen than NH_4 for *A. minutum* blooms, based on nutrient concentrations on the Catalan coast (Vila et al., 2005; Bravo et al., 2008) and on nitrogen uptake measurements in the Penzé Estuary (Maguer et al., 2004). In the latter study, $\rho(NO_3^-)$ was 7-fold higher relative to $\rho(NH_4^+)$ and the nitrogen requirements of the bloom were calculated at 184 μmol l^{-1} NO_3^- and 25 μmol l^{-1} NH_4^+.

Alexandrium minutum concentrations were negatively correlated with NH_4^+ concentrations in Ganzirri Lagoon (Giacobbe et al., 1996) and on the Catalan coast (Bravo et al., 2008). This may suggest that NH_4^+ was depleted by *A. minutum* growth and accumulated when *A. minutum* growth was limited by other factors such as light, however Bravo et al. (2008) interpreted the results as the inhibition of *A. minutum* growth by high NH_4^+ concentrations. In contrast, *A. minutum* blooms in Syracuse Bay coincided with high NH_4^+ concentrations, and nitrogen uptake measurements in Cape Town Harbour indicated that the bloom was sustained by high $\rho(NH_4^+)$ (up to 1.1 μmol N l^{-1} h^{-1}, representing on average 81 % total ρ(N) (Pitcher et al., 2007). In the present study, $\rho(NH_4^+)$ was between 0.013 and 0.089 μmol N l^{-1} h^{-1} in 2006 and between 0.018 and 0.131 μmol N l^{-1} h^{-1} in 2007, representing 14-54 % total ρ(N) in 2006 and 19-73 % in 2007. Ammonium uptake was generally higher than ρ(urea) and $\rho(NO_3^-)$ in 2007, but lower in 2006, suggesting that the *A. minutum*-dominated communities were sustained predominantly by NH_4^+, consistent with the study in Cape Town Harbour.

Uptake kinetics studies carried out on a French strain of *Alexandrium minutum* have reported a preference for NH_4^+ over NO_3^-, as shown by ~2-fold higher cell-specific ν_{max} and α for NH_4^+ relative to NO_3^- (Maguer et al., 2007). Another study has shown higher maximum growth rates in cultures grown on NH_4^+ and urea, relative to those grown on NO_3^-, although concentrations of 50 μmol N l^{-1} NH_4^+ and urea started to inhibit growth and complete inhibition was observed at 100 and 200 μmol N l^{-1}, respectively (Chang & McClean, 1997). A tolerance to very high concentrations (200-1000 μmol N l^{-1}) of NO_3^- has also been observed (Chang & McClean, 1997; Touzet et al., 2007).

Several studies have demonstrated an increase in PSP toxin content under PO_4^{3-} limitation in various species of *Alexandrium* (Boyer et al., 1987; Anderson et al., 1990), including *A. minutum* (Bechemin et al., 1999; Maestrini et al., 2000; Lippemeier et al., 2003). Bechemin et al. (1999) showed that an N:P ratio of 160 enhanced toxin production 7-fold relative to an N:P ratio of 16, whereas an N:P ratio of 1.6 reduced

toxin production 3-fold. Furthermore, a culture study by Guisande et al. (2002) showed that in mixed species cultures toxin production by *A. minutum* increased under PO_4^{3-} limitation (N:P ~200), as a strategy to redirect grazing pressure towards non-toxic species. In contrast, Flynn et al. (1994) reported that maximum toxin synthesis occurred in *A. minutum* during N-refeeding of N-deprived cells, whereas short-term P stress did not enhance toxin synthesis. They later found that toxin synthesis and content declined during N *or* P deprivation (Flynn et al., 1995). In the present study, the success of Alexandrium in 2007 could have been linked to enhanced toxin production, although it is impossible to conclude whether this would have been linked to higher NO_3^- or higher N:P ratios. In Ganzirri Lagoon, *A. minutum* concentrations were negatively correlated with N:P ratios (Giacobbe et al., 1996) and in a strain isolated from Greek coastal waters, growth rates were negatively correlated with N:P ratios, with optimal N:P ratios being between 15 and 25 (Ignatiades et al., 2007), suggesting that higher N:P ratios were not directly responsible for *Alexandrium* dominance in the present study.

Nutrient kinetics experiments have reported low K_s values for PO_4^{3-} in *A. minutum* cultures, indicative of a high affinity for this nutrient (Frangopulos et al., 2004). These authors also found that K_s was positively correlated with toxin quota, supporting the hypothesis that toxin production is a strategy used to offset the disadvantage of a low affinity for nutrients, as suggested by Smayda (1997).

In both Arenys de Mar and Syracuse, N:Si ratios were >1, indicating potential Si limitation, which would allow *A. minutum* to outcompete diatoms (Vila et al., 2005). This is also consistent with the higher N:Si ratios measured in 2007 relative to 2006 in the present study.

5.4. Conclusion

Phytoplankton biomass in the Fal Estuary was controlled by meteorological and hydrographic conditions, whereby increased sunshine hours and water temperatures enhanced phytoplankton biomass in 2006. In addition, tidal forcing and mixing may have limited primary production in 2007, by interfering with light availability. Furthermore, higher NH_4^+ regeneration rates in 2007 were indicative of higher microzooplankton biomass and potentially higher grazing pressure.

The conditions in 2006 were more favourable to diatoms, the most abundant of which were *Thalassiosira* spp. and *Leptocylindrus danicus*. The potentially toxic species *Karenia mikimotoi* and *Pseudo-nitzschia* were also favoured by the warmer and more saline conditions. Both *K. mikimotoi* and *Pseudo-nitzschia* were particularly adapted to high salinities and low nutrients and appeared to be advected into the estuary from a seaward source, confirming previous findings in the Fal Estuary (Percy, 2006). *Alexandrium minutum* type cells were abundant in both years, although they were more dominant in 2007. Therefore, they seemed to be favoured by the lower irradiances and the combination of stratification and high nutrients, as well as high N:P and N:Si ratios. It is possible that their success under PO_4^{3-} limitation is related to their reported increased toxin quotas under such conditions, used as a strategy to redirect grazing pressure to non-toxic species (Guisande et al., 2002). Furthermore, *Alexandrium* growth was supported primarily by NH_4^+.

6 Culture experiments

6.1. Introduction

Measurements of nitrogen uptake kinetics have shown a high degree of intra-specific variability both in cultures (Carpenter & Guillard, 1971) and in natural populations (Kudela et al., submitted). Furthermore, different geographic strains of the same species can often display very different nutritional requirements, as shown for *Karenia brevis* (Sinclair et al., 2009), *Gambierdiscus toxicus* (Lartigue et al., 2009) and various *Pseudo-nitzschia* species (Thessen et al., 2009), although in the latter case variability was also found between strains isolated from the same water sample.

Furthermore, between-strain variability in toxicity is also frequently observed (Burkholder & Glibert, 2006). This has been shown for example in *Alexandrium minutum*, whereby both the degree of toxicity and the toxin profile differ between geographic strains (Nascimento et al., 2005).

Culture studies carried out on a French strain of *Alexandrium minutum* have shown higher half-saturation constants (K_s) and maximum cell-specific uptake rates (ν_{max}) for NH_4^+ relative to NO_3^-, indicative of a preference for NH_4^+ over NO_3^-. Another study showed high requirements for NO_3^-, with no growth inhibition observed up to concentrations of 200 µmol N l^{-1}, whereas inhibition occurred at NH_4^+ and urea concentrations of 100 µmol N l^{-1} and 200 µmol N l^{-1}, respectively (Chang & McClean, 1997). Similarly, a study carried out with an Irish strain of *A. minutum* showed no growth inhibition with an initial concentration of up to 1000 µmol N l^{-1} NO_3^- (Touzet et al., 2007).

Previous studies have shown links between nitrogen nutrition and toxicity. For example, high NH_4^+ concentrations have been associated with toxicity in *A. minutum* (Flynn et al., 1994) and in *A. tamarense* (Hamasaki et al., 2001). Uptake of organic forms of nitrogen (urea, glycine, leucine and aspartic acid) appear to enhance brevetoxin production in *Gymnodinium breve* (Shimizu & Wrensford, 1993; Shimizu et al., 1995) and growth on urea enhances domoic acid production by *Pseudo-nitzschia australis* (Howard et al., 2007).

The aim of this study was to investigate the differences in (1) nitrogen nutrition, and (2) toxin profile between 3 geographic strains of *Alexandrium minutum*. The 3 chosen strains were isolated from the 2 upwelling systems where field work was carried out and from a UK estuary, in order provide a comparison with the field work. To achieve this, both nitrogen uptake kinetics and growth experiments using different forms of nitrogen were carried out, with the latter involving associated toxicity measurements.

6.2. Methods

Unialgal batch cultures of *Alexandrium minutum* isolated from Cape Town Harbour (AMCT), the Ría de Vigo (AMV) and the Fleet Lagoon (AMF) were grown in L2 medium (Guillard & Hargraves, 1993) using artificial seawater (Harrison et al., 1980) instead of natural seawater. They were maintained in a temperature-controlled incubator at 20 ºC illuminated with tungsten lamps on a 12:12 light:dark cycle. Photon flux density (PFD) was ~100 μE m^{-2} s^{-1}, measured using a Biospherical Instruments Inc. QSL-2000 4π quantum scalar irradiance metre.

Growth experiments were carried out with all 3 strains grown on different nitrogen sources, NO_3^-, NH_4^+ and urea. The cultures were acclimated to the respective nitrogen sources by subculturing them twice into media containing solely NO_3^-, NH_4^+ or urea prior to the experiment. In the first experiment, treatments were duplicated and initial NO_3^- concentrations were 100 μmol N l^{-1}, whereas initial NH_4^+ and urea concentrations were 50 μmol N l^{-1}, except for AMV where NH_4^+ was 25 μmol N l^{-1}. A second experiment was carried out using low nutrient natural seawater collected in the North Atlantic gyre, to determine whether AMV would be more successful than with artificial seawater, and with initial NO_3^-, NH_4^+ and urea concentrations of 100 μmol N l^{-1}.

For experiment 1, two duplicate 50-ml subsamples of culture were collected every 2-3 days and filtered through 25-mm Whatman GF/F filters using a syringe filter. These were immediately frozen for PSP toxin analyses using liquid chromatography coupled with tandem mass spectrometry (LCMS-MS). Unfortunately, due to methodological problems no toxins were detected, therefore, no data on toxicity measurements are shown. The filtrate was collected from one of the duplicate filtrations for nutrient analyses. NH_4^+ samples were analysed immediately, following the fluorometric method of Holmes et al. (1999). Nitrate and urea samples were frozen; NO_3^- was later analysed

on a Burkard Scientific autoanalyser, following the methods of Hydes & Wright (1999) and urea was analysed following the method of Goeyens (1998). Measurements of F_v/F_m were carried out using a Chelsea Instruments Fastracka^{TM} FRRf. For experiment 2, only cell counts were performed.

A nutrient uptake kinetics experiment was carried out for NO_3^-, NH_4^+ and urea on AMCT, AMF and AMV cultures. These were subcultured twice in sterile 1-l borosilicate Schott (Duran) bottles with 25 µmol N l^{-1} of the appropriate nitrogen source to acclimate the cultures to the respective nitrogen sources. In all cases the N:P ratio remained 16. The experiment was conducted during the stationary phase, 11-12 days after inoculation, when nutrients were depleted. Unfortunately, urea was not depleted in any of the cultures, therefore the urea experiment was unsuccessful. Twelve 50 ml samples from each of the nine cultures (3 strains x 3 nutrients) were decanted into 108 x 50-ml polycarbonate bottles, a third of which were to be spiked with $^{15}NH_4Cl$, a third with $K^{15}NO_3$ and a third with $CO(^{15}NH_2)_2$. For each strain and nutrient, different volumes of 1 µmol N l^{-1}, 10 % ^{15}N-enriched stock solutions were added to obtain duplicate sets of six concentrations of NO_3^-, NH_4^+ and urea between 0.1 and 30 µmol N l^{-1}. After spiking, cultures were incubated for ~2 h in normal growth conditions then filtered onto pre-combusted 25-mm Whatman GF/F filters and dried overnight at 60 ºC. Samples were analysed and curves were fitted using the same methods as for the field nutrient uptake kinetics experiments.

6.3. Results

6.3.1. Growth experiments

Alexandrium minutum strains isolated from Cape Town Harbour (AMCT), the Fleet Lagoon (AMF) and the Ria de Vigo (AMV) were able to grow on NO_3^-, NH_4^+ and urea as sole nitrogen source at concentrations of 100 µmol N l^{-1} NO_3^-, 50 µmol N l^{-1} NH_4^+ (25 µmol N l^{-1} for AMV) and 50 µmol N l^{-1} urea (Figure 6.1). For strain AMCT, growth rates on NO_3^- were similar to those using NH_4^+ in both experiments, although growth rates were higher in experiment 2, which used natural rather than artificial seawater (Table 6.1). In experiment 2, AMF also displayed highest growth rates on NO_3^- and NH_4^+, whereas in experiment 1 it grew faster using urea, although it reached lower final concentrations. The NH_4^+ concentration of 100 µmol N l^{-1} used in experiment 2 did not appear to inhibit growth for either AMCT or AMF, since growth rates were 2-fold higher in this experiment.

AMV reached highest growth rates when grown on urea in experiment 1, although cell concentrations were very low in this experiment. This was due to a rapid initial increase in cell concentration, which then reached a plateau on Day 11. In experiment 2, higher final concentrations and higher growth rates were achieved on NO_3^-, but the culture could not grow on NH_4^+ or urea (supplied at 100 µmol N l^{-1}).

Nitrogen and PO_4^{3-} were supplied at the Redfield ratio in all experiments, although PO_4^{3-} was only measured in association with NO_3^-. Nitrate and PO_4^{3-} concentrations were significantly correlated for AMCT and AMV ($p < 0.01$, $n = 5$), but not for AMF. The ratio of NO_3^-: PO_4^{3-} utilisation was 21.5 for AMCT and 24.8 for AMV (data not shown).

Expt		µ (d^{-1})			K (d^{-1})			T (d)		
		NO_3^-	NH_4^+	Urea	NO_3^-	NH_4^+	Urea	NO_3^-	NH_4^+	Urea
1	AMCT	0.27 (0.06)	0.25 (0.002)	0.20 (0.03)	0.39	0.36	0.29	2.6	2.8	3.5
	AMF	0.20 (0.03)	0.18 (0.04)	0.23 (0.005)	0.29	0.26	0.33	3.5	3.9	3.0
	AMV	0.24 (0.01)	0.20 (0.06)	0.37 (0.06)	0.35	0.29	0.53	2.9	3.5	1.9
2	AMCT	0.56	0.49	0.27	0.81	0.71	0.39	1.2	1.4	2.5
	AMF	0.47	0.41	0.22	0.68	0.59	0.32	1.5	1.7	3.2
	AMV	0.48	-	-	0.69	-	-	1.4	-	-

Table 6.1. Growth rates (µ, means of 2 replicate cultures with standard errors in brackets for Experiment 1), doubling rates (K) and doubling times (T) for each *Alexandrium minutum* strain and nutrient treatment in Experiments 1 and 2.

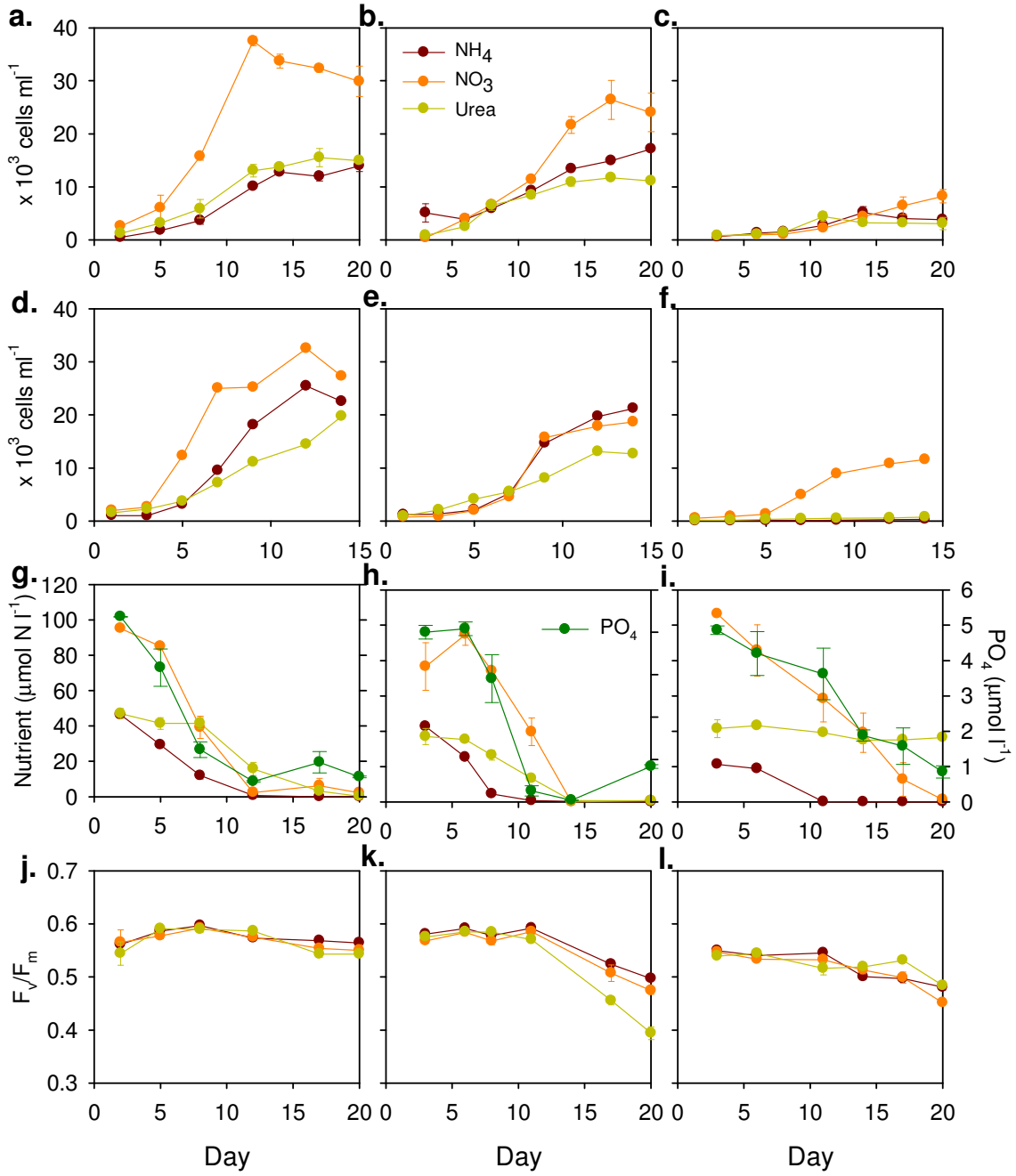

Figure 6.1. Time-series of cell concentrations of *Alexandrium minutum* strains (a) AMCT, (b) AMF and (c) AMV in Experiment 1 and (d,e,f) in Experiment 2. Associated measurements of (g,h,i) nutrient concentrations and (j,k,l) F_v/F_m are reported for Experiment 1 only. Initial concentrations in Experiment 1 were 100 µmol N l^{-1} for NO_3^-, 50 µmol N l^{-1} (AMCT, AMF) or 25 µmol N l^{-1} (AMV) for NH_4^+ and 50 µmol N l^{-1} for urea; in Experiment 2 they were 100 µmol N l^{-1} for all nutrients.

Ammonium was generally exhausted by Day 12 for all strains, whereas NO_3^- was exhausted by Day 12 for AMCT, Day 14 for AMF and Day 20 for AMV. In the NO_3^- experiments, PO_4^{3-} was not completely exhausted by the end of the experiment for AMCT or AMV. Urea was only exhausted by Day 20 for AMCT and by Day 14 for AMF, whereas for AMV, the concentration remained high throughout the experiment (Figure 6.1g-i).

For all strains, F_v/F_m was between 0.54 and 0.58 at the start of the experiment and between 0.45 and 0.56 at the end (Figure 6.1j,k,l). Very little decrease was observed in the AMCT culture over the course of the experiment, whereas F_v/F_m dropped by 0.08-0.18 for AMF and by 0.07-0.15 for AMV. For AMCT and AMV, there were no significant differences between nutrient treatments, whereas for AMF F_v/F_m was significantly higher for NH_4^+ relative to NO_3^- (paired t-test, $p < 0.01$).

6.3.2. Nitrogen uptake kinetics

All 3 strains demonstrated a preference for NH_4^+ over NO_3^- at saturating concentrations in the nitrogen uptake kinetics experiment, with ν_{max} ~2-fold higher for NH_4^+ than for NO_3^- in all cases (Figure 6.2,Table 6.2). At limiting concentrations, AMCT and AMV also showed a preference for NH_4^+, with 2-fold higher α than for NO_3^- although AMF displayed similar α values for NH_4^+ and NO_3^-. AMCT displayed the highest $\nu_{max}(NO_3^-)$ and $\nu_{max}(NH_4^+)$.

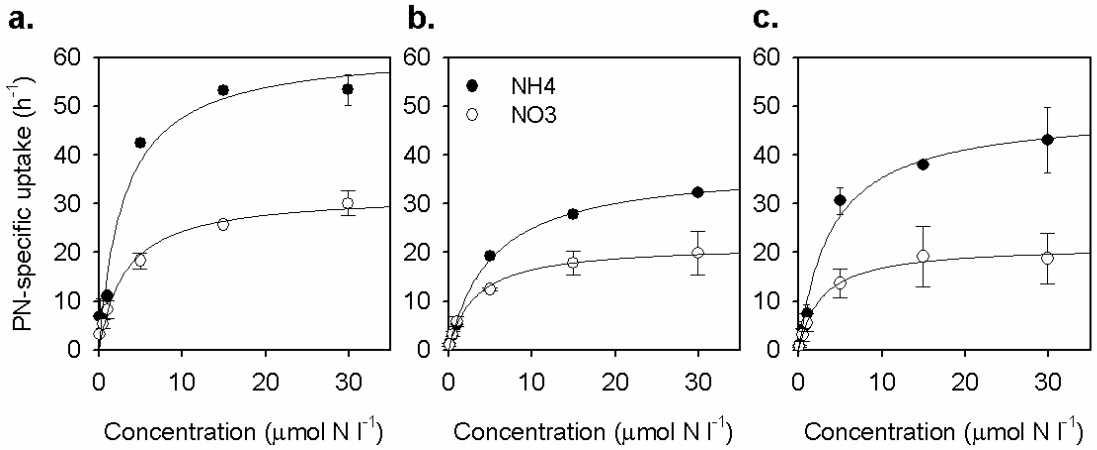

Figure 6.2. PN-specific nitrogen uptake rates versus concentration measured in (a) AMCT, (b) AMF and (c) AMV and fitted to the Michaelis-Menten equation for uptake kinetics.

Strain	ν_{max}		K_s		α		$\nu_{max}(NH_4^+)$ / $\nu_{max}(NO_3^-)$	α(NH_4^+) / α(NO_3^-)
	NO_3^-	NH_4^+	NO_3^-	NH_4^+	NO_3^-	NH_4^+		
AMCT	32.0 (1.9)*	61.9 (4.9)*	3.19 (0.71)*	3.00 (0.92)*	10.0	20.6	1.93	2.06
AMF	21.6 (0.7)*	37.8 (1.1)*	3.16 (0.39)*	5.18 (0.49)*	7.9	7.3	1.75	0.93
AMV	21.4 (0.8)*	49.0 (2.9)*	2.75 (0.39)*	3.89 (0.84)*	7.8	12.6	2.29	1.62

Table 6.2. Nitrogen uptake kinetics parameters ν_{max} (x 10^{-3} h^{-1}), K_s (µmol N l^{-1}) and α (x 10^{-3} h^{-1} (µmol N $l^{-1})^{-1}$) measured in AMCT, AMF and AMV and ratios of the parameters for NH_4^+ to those for NO_3^-, given as indicators of nutrient preference.

6.4. Discussion

The culture experiments showed that all 3 strains were able to grow on NH_4^+ and urea supplied as sole sources of nitrogen. This was also the case for an *Alexandrium minutum* strain isolated from New Zealand (Chang & McClean, 1997), 3 *Karenia brevis* strains isolated from the Gulf of Mexico (Sinclair et al., 2009) and 19 *Pseudo-nitzschia* spp. strains isolated from the mid-Atlantic coast of the US (Thessen et al., 2009). In contrast, it has been reported that the ciguatera toxin-producing dinoflagellate *Gambierdiscus toxicus* is unable to grow on urea (Lartigue et al., 2009). When nitrogen was supplied at 100 μmol N l^{-1} AMCT and AMF displayed highest growth rates when grown on NO_3^- and lowest growth rates with urea. At the lower concentration of 50 μmol N l^{-1}, both AMF and AMV displayed highest growth rates on urea, consistent with results for one of the strains of *Karenia brevis* (Sinclair et al., 2009). Both *K. brevis* and *Pseudo-nitzschia* displayed a high degree of variability in nitrogen preference between strains, as was observed to a certain extent in the present study. AMCT and AMF achieved similar growth rates (~10 %) with 50 μmol N l^{-1} NH_4^+ to the cultures grown on 100 μmol N l^{-1} NO_3^-, indicating that NH_4^+ was a more efficient source of nitrogen, consistent with the lower energetic cost associated with its assimilation (Syrett, 1981). Furthermore, $\rho(NO_3^-)$ requires iron, which was supplied in the same concentration in all treatments, therefore growth at the higher NO_3^- concentration may have been limited by Fe availability. However, when the NH_4^+ concentration was 100 μmol N l^{-1}, growth rate on NH_4^+ did not exceed that on NO_3^-, in fact it became 15 % lower, suggesting that the increase in growth rates between the 2 experiments was due to the use of natural rather than artificial seawater. The effect of the improved seawater medium may therefore have masked an inhibitory effect of increased NH_4^+ concentration.

The nitrogen uptake kinetics experiment showed a preference for NH_4^+ over NO_3^-, as shown by the ~2-fold higher v_{max} values, consistent with the study by Maguer et al. (2007) for a strain isolated from Morlaix Estuary (France). As in their study, AMCT and AMV also displayed 2- and 1.5-fold higher α for NH_4^+ than for NO_3^-, consistent also with the values reported by Maguer et al. (2007), although for AMF α was slightly higher for NO_3^-. Interestingly, although these strains displayed a preference for uptake of NH_4^+, they consistently displayed higher growth rates on NO_3^-, consistent with the review by Dortch (1990). Previously reported K_s values were 2 to 4-fold lower for

growth (Ignatiades et al., 2007) and one order of magnitude lower for uptake (Maguer et al., 2007) relative to those measured in the present study. The strains used in the present study therefore had a lower affinity for both NO_3^- and NH_4^+. Unfortunately, the ν_{max} values reported by Maguer et al. (2007) were cell-specific, therefore it was not possible to compare them with those in the present study, and it was not possible to compare α values, which are known to be more informative than K_s values (Healey, 1980; Aksnes & Egge, 1991).

Temperature can also influence variability in the uptake kinetics of NH_4^+ and NO_3^-, whereby ν_{max} and α for NH_4^+ increase with temperature and α for NO_3^- decreases with temperature (Lomas et al., 1996; Fan et al., 2003). The temperature conditions in Ignatiades et al. (2007) and Maguer et al. (2007) (18-20 °C) were similar to those used in the present study, therefore temperature differences were not responsible for the discrepancies observed. Irradiance was 60 μE m^{-2} s^{-1} for the Greek strain, 200 μE m^{-2} s^{-1} for the French strain and 100 μE m^{-2} s^{-1} in the present study. According to Chang & McClean (1997), K_s for growth decreased with increasing irradiance between 25 and 100 μE m^{-2} s^{-1}, therefore the lower K_s measured by Maguer et al. (2007) may be attributable to the higher irradiance in their experiment, although irradiance could not account for the differences between the values reported by Ignatiades et al. (2007) and those reported in this study. Finally, these differences may be attributable to genetic predispositions to the nutrient concentrations encountered in the respective regions from which the strains were isolated. The total DIN concentration ($NO_3^- + NH_4^+ + NO_2^-$) in Saronikos Gulf, where the Greek strain was isolated, was lower than NO_3^- concentrations in Cape Town Harbour and in the Fleet Lagoon and similar to those in the Ría de Vigo, therefore differences in nutrient concentrations could account for the higher affinity for NO_3 observed in the Greek strain relative to AMCT and AMF, but not AMV. Furthermore, very high inorganic nitrogen concentrations in the Morlaix Estuary (Table 6.3) could not account for the high affinity for NO_3^- and NH_4^+ reported for the French strain.

Maximum PN-specific uptake rates of NO_3^- for all 3 strains in the present study were within the range reported for *A. catenella* and K_s was at the lower end of the range, suggesting that *A. minutum* had a higher affinity for NO_3^- relative to *A. catenella*. *A. minutum* displayed higher $\nu_{max}(NH_4^+)$ relative to *A. catenella*, therefore it was better adapted to higher NH_4^+ concentrations. AMCT also displayed a higher affinity for NH_4^+, as shown by the higher α values relative to *A. catenella*, whereas AMF displayed a lower

affinity and AMV a similar affinity (Table 6.3). These differences were not due to different culture conditions. The higher $\nu_{max}(NH_4^+)$ in AMCT, AMF and AMV may have been due to higher NH_4^+ concentrations in Cape Town Harbour, the Fleet Lagoon and the Ría de Vigo, relative to the Thau Lagoon.

Area of strain isolation	Ambient $[NO_3^-]$	Ambient $[NH_4^+]$	ν_{max}		K_s		α	
			NO_3^-	NH_4^+	NO_3^-	NH_4^+	NO_3^-	NH_4^+
A. minutum								
Cape Town Harbour[a]	7-18[e]	2.5-9.8[e]	32	61.9	3.19	3.00	10.0	20.6
Fleet Lagoon[a]	0-62[f]	0-25[f]	21.6	37.8	3.16	5.18	7.9	7.3
Ria de Vigo[a]	0-3[a]	0-9[a]	21.4	49	2.75	3.89	7.8	12.6
Saronikos Gulf (Greece)[b]	6[b]	-	-	-	1.18	-	-	-
Morlaix Estuary (France)[c]	490-9282[g]	70-1750[g]	0.29-0.40	0.65-0.95	0.22-0.28	0.25-0.38	1.12-1.55	2.48-2.93
A. catenella								
Thau Lagoon (France)[d]	0-4[h]	0-3[h]	3-47	26	0.6-28.1	2.0	-	13.0

Table 6.3. Nitrogen uptake kinetics parameters ν_{max} (x 10^{-3} h^{-1}) , K_s (µmol N l^{-1}) and α (x 10^{-3} h^{-1} (µmol N $l^{-1})^{-1}$) measured in the present study and in other studies using cultures of *A. minutum* and *A. catenella* and ambient NO_3^- and NH_4^+ concentrations reported for the areas where the strains were isolated. NB: ν_{max} in the Morlaix Estuary was reported in pmol cell^{-1} h^{-1}.
[a] This study ; [b] Ignatiades et al (2007); [c] Maguer et al. (2007) ; [d] Collos et al. (2004) ; [e] Pitcher et al. (2007) ; [f] Nascimento (2003) ; [g] Wafar et al. (1989) ; [h] Collos et al. (1997).

6.5. Conclusions

The three strains of *Alexandrium minutum* showed some common nitrogen nutrition characteristics. They were all able to grow on all three sources of N when supplied at concentrations <100 µmol N l^{-1}. When NH_4^+ and urea were supplied at 100 µmol N l^{-1}, AMCT and AMF displayed higher growth rates on NO_3^- relative to NH_4^+ and AMV was only able to grow on NO_3^-. However, all three strains displayed a preference for NH_4^+, as shown by the 2-fold higher ν_{max} for NH_4^+ relative to NO_3^-. Both ν_{max} and K_s were generally higher relative to *A. catenella* isolated from the South of France (Collos et al., 2004), and K_s was higher than in an *A. minutum* strain isolated from Brittany (Maguer et al., 2007), indicating that the strains used in the present study were adapted to higher NO_3^- and NH_4^+ concentrations. Differences in ν_{max} and K_s between the strains used in the present study and *A. minutum* in other studies could hav been attributed to differences in environmental conditions (light, ambient nutrient concentrations), although this was not consistent in all cases. Therefore, it seemed more likely that the differences were due to genetic predispositions.

7 Overall summary and conclusions

7.1. General features of upwelling systems

The sampling sites in the two upwelling regions studied were characterised by very different topography, in that the Lambert's Bay (Benguela) site was on the open shelf whereas the Iberian site was within a coastal indentation, the Ría de Vigo. Although the Rías Baixas act as an extension to the shelf, the circulation patterns within them are different to those observed on the shelf. During upwelling, positive estuarine circulation is observed within the rías and the water column can remain stratified if upwelling is sufficiently weak (Figueiras et al., 1994). This was the case in June 2007 in the present study, and these conditions promoted phytoplankton growth. Nutrients were depleted from the surface layer, hence a chl-a maximum formed near the thermocline. In contrast, on the open shelf in the Benguela, upwelling pulses generated a well-mixed water column and dispersed the phytoplankton biomass accumulated during relaxation. However, the alternation between upwelling pulses supplying nutrients and periods of relaxation enhancing water column stability created "windows of opportunity" for phytoplankton growth.

In the Iberian system, during wind relaxation, surface shelf water is forced into the rías and downwelling occurs, causing the water column to become well-mixed (Figueiras et al., 1994). This was the case in September 2006 in the present study, in which dinoflagellate populations appeared to be advected into the ría. While the circulation patterns promote the advection of HAB populations into the rías (Fraga et al., 1993), downwelling is thought to select motile species that can remain in the surface layer (Figueiras et al., 1995). In Lambert's Bay, relaxation periods lead to stratification and nutrient depletion in the surface layer, although deeper concentrations remained high, whereas in the ría nutrient concentrations were relatively low throughout the water column, although never depleted. In both systems, N:P ratios were higher in recently upwelled water, close to the Redfield ratio in the ría in June, but lower than Redfield in Lambert's Bay, while ratios were very low in the ría in September. In all cases, it appeared that these departures from Redfield stoichiometry could be attributed to an N:P remineralisation ratio lower than Redfield, which was particularly low in the ría in September. In both systems, NH_4^+ regeneration was higher than uptake, resulting in the

accumulation of NH_4^+, which could possibly inhibit NO_3^- uptake. Evidence of such inhibition was provided by the rapid decrease in $\rho(NO_3^-)$ at NH_4^+concentrations above 0.5-1.0 µmol N l^{-1} in both systems.

7.2. Phytoplankton community structure and HAB assemblages

In Lambert's Bay, phytoplankton community structure displayed high short-term as well as interannual variability. Different phytoplankton species or functional groups were favoured by different stages of the upwelling/relaxation cycles. For example, Clusters II (*A. catenella/ Skeletonema costatum*), III (*Scrippsiella trochoidea/ Pseudo-nitzschia* spp.) and IV (*Minidiscus trioculatus*) were favoured by active upwelling, whereas Clusters I (*Dinophysis acuminata/ Gymnodinium* spp.) and V (*Coscinodiscus* spp./ *Gyrodinium zeta*) were associated with warm, stratified, nutrient depleted waters. Clusters VI (*S. costatum/ Chaetoceros* spp.) and VII (*Pseudo-nitzschia* spp./ *Chaetoceros* spp.) occurred in both regimes, and were able to adapt to fluctuating conditions by utilising recycled nitrogen when NO_3^- became limiting.

The lengths of the surveys carried out in the Ría de Vigo did not allow any conclusions on short-term variability and studies were not repeated in the same season to investigate interannual variability. However, a comparison with the literature indicated that the communities present in both seasons were typical "upwelling" and "downwelling" communities (Crespo et al., 2006). For example, the occurrence of *Dinophysis acuta* and *Gymnodinium catenatum* during the downwelling season and *D. acuminata* throughout the year are recurring features (Fraga et al., 1988; Figueiras et al., 1994).

HAB taxa common to both systems included *Dinophysis* spp. and *Pseudo-nitzschia* spp. *D. acuminata* was dominant in Lambert's Bay in 2007, with concentrations up to 31 x 10^3 cells l^{-1}, whereas in the ría it was a minor component of the phytoplankton community, with concentrations up to 15 x 10^3 cells l^{-1}. In both cases, it was associated with nutrient-depleted surface waters, although cell counts were not performed at greater depths, where higher concentrations may have been observed. In 2008, very high concentrations of *D. acuminata* (up to 573 x 10^3 cells l^{-1}) were observed at 5 m, although it was never truly dominant since it co-occurred with *Coscinodiscus* spp. On these occasions, NO_3^- and PO_4^{3-} concentrations were as high as 26.0 and 2.2 µmol l^{-1},

respectively, suggesting that *D. acuminata* was not exclusively adapted to depleted nutrient conditions.

Pseudo-nitzschia consisted of *P. australis* and 2 unidentified species in Lambert's Bay, and of *P. seriata* and *P.* cf. *pseudodelicatissima* in the ría. *P.* cf. *pseudodelicatissima* was abundant in both years, whereas *P. seriata* was only abundant during the upwelling season. In the Benguela, *Pseudo-nitzschia* spp. were most abundant in the year when upwelling-favourable winds were predominant, although biomass tended to accumulate during periods of upwelling relaxation. *Pseudo-nitzschia* appeared to be able to acclimate to rapid fluctuations in the hydrographic and nutrient regime and this was perhaps also the case with *P.* cf. *pseudodelicatissima*, since it was present during both upwelling and downwelling seasons. Since *Pseudo-nitzschia* also forms large blooms in the California current, this tolerance towards upwelling may therefore be an ecological adaptation of *Pseudo-nitzschia* that is specific to upwelling systems.

7.3. Comparison of nutrient uptake strategies

In the Ría de Vigo, growth was supported by regenerated nitrogen in both years, with $\rho(NH_4^+)$ and ρ(urea) generally higher than $\rho(NO_3^-)$, resulting in *f*-ratios <0.5, whereas in the Benguela they ranged from <0.1 to 0.9 depending on the upwelling/relaxation cycles. In the ría, $\rho(NH_4^+)$ increased and *f*-ratios decreased towards the head of the ría, where NH_4^+ concentrations were highest. Absolute total nitrogen uptake was generally higher in Lambert's Bay, reaching a maximum of 0.70 μmol N l^{-1} h^{-1}, relative to 0.44 μmol N l^{-1} h^{-1} in the ría, although specific uptake was generally higher in the ría. This suggests that in the ría the accumulation of biomass was limited by some other external factor, such as grazing or export from the system.

In the ría, the HAB community present during the downwelling season (*Dinophysis acuta*, *Gymnodinium catenatum*) was sustained by NH_4^+, which was supplied by high regeneration rates. In the Benguela, specific nutritional characteristics were attributed to different HAB species that occurred during the 3 surveys. *Alexandrium catenella* bloomed at high NO_3^- concentrations and appeared to have a high requirement for NO_3^- since it disappeared when NO_3^- became depleted. It also displayed the highest surface $\rho(NO_3^-)$ and *f*-ratio measured in all 3 surveys. *Pseudo-nitzschia* was favoured by upwelling and was able to rapidly utilise the high nutrient concentrations supplied by upwelling. However, biomass accumulation occurred during wind relaxation and

Pseudo-nitzschia then switched to NH_4^+ as its main source of nitrogen as NO_3^- became depleted. *Dinophysis acuminata* bloomed during stratified periods, when NO_3^- concentrations were low, and displayed low *f*-ratios indicative of its reliance on recycled nitrogen. In 2008, however, *D. acuminata* was sometimes very abundant at high NO_3^- concentrations, generally forming a thin layer in the pycnocline.

The nitrogen uptake kinetics experiments carried out during the present study in the two upwelling systems, and in other studies in the California system, yielded no apparent trends specific to these systems (Table 7.1). Both ν_{max} and α values varied by one order of magnitude and spanned the same range as that displayed by all ecosystems in Table 6.1. The kinetics experiment carried out on a mixed diatom population in the ría displayed a very strong preference for NH_4^+ over NO_3^-, with a $\nu_{max}(NH_4^+)$: $\nu_{max}(NO_3^-)$ ratio of the same order as those reported for estuaries on the east coast of the US, but at least 3-fold higher than in the Benguela. Furthermore, the Fal Estuary displayed similar ν_{max} and α values and nutrient preferences to the *Dinophysis acuminata* assemblages in the Benguela, therefore differences within upwelling systems were greater than differences between an upwelling system and an estuary.

The different HAB populations displayed a range of nitrogen uptake strategies. *Alexandrium catenella* and the mixed *D. acuminata*/ *Coscinodiscus* spp. assemblage were the only ones to display a $\nu_{max}(NH_4^+)$: $\nu_{max}(NO_3^-)$ ratio <1. In both experiments, the ambient NO_3^- concentration was high, indicating that the high $\nu_{max}(NO_3^-)$ may have been a result of acclimation to high NO_3^- concentration, and that kinetics experiments carrried out when NO_3^- is depleted may not not be applicable to upwelling situations. This is shown by the experiments carried out on *D. acuminata* populations. When NO_3^- was depleted, both Experiments 3 and 5 yielded low $\nu_{max}(NO_3^-)$ and 4-fold higher $\nu_{max}(NH_4^+)$, however in Experiment 4, at a high ambient NO_3^- concentration, $\nu_{max}(NO_3^-)$ was 4-fold higher than $\nu_{max}(NH_4^+)$. *Pseudo-nitzschia* was poised to utilise either source of nitrogen at both saturating and limiting concentrations, as shown by its high ν_{max} and α for both NO_3^- and NH_4^+. Thus, *A. catenella*, the mixed *D. acuminata*/ *Coscinodiscus* spp. assemblage and *Pseudo-nitzschia* were typical of periods of active upwelling and were fairly unique among all the field studies presented in Table 6.1, in that they did not display a preference for NH_4^+ over NO_3^-.

In contrast, the *Dinophysis acuminata* assemblages that occurred during periods of upwelling relaxation displayed a strong preference for NH_4^+ over NO_3^- at both saturating and limiting concentrations. They displayed similar kinetics parameters to the

dinoflagellate species in the California current (*Akashiwo sanguinea*, *Lingulodinium polyedrum*, *Cochlodinium* spp.), that were also associated with upwelling relaxation events. Their ν_{max} and α values were generally lower than for estuarine populations (e.g. Ría de Vigo, Choptank and Neuse Estuaries), but similar to other coastal and open ocean waters (Table 6.1).

Therefore, nitrogen nutrition of HABs in upwelling systems is very much species-dependent, particularly in the Benguela where high interannual and short-term variability in species selection was observed. While there was no obvious difference in nitrogen uptake for HAB species in upwelling systems, it was found that certain species displayed some unique features. For example, *Alexandrium catenella*, that was well adapted to active upwelling, displayed a preference for NO_3^- over NH_4^+, a characteristic that is not generally observed in other ecosystems. A high degree of flexibility in uptake kinetics was also observed in *Dinophysis acuminata*, which may allow it to exploit the fluctuating nutrient regime that is typical of upwelling systems. Although only one experiment was carried out on a *Pseudo-nitzschia*-dominated assemblage, its success during both upwelling and relaxation and ability to switch from new to regenerated production suggests that it may also have had variable uptake kinetics.

Finally, the differences observed between the nutrient kinetics of *Alexandrium catenella* in the Benguela upwelling system and in the Thau Lagoon suggest the existence of different biogeographic strains with different nitrogen uptake strategies. This was also the case for *A. minutum* strains isolated from different geographic locations. Further comparative studies of nutrient kinetics of natural populations and cultures of HAB species are needed to further investigate these differences and to determine whether they are due to selective pressure or acclimation.

Species	Location	ν_{max}			K_s			α			$\nu_{max}(NH_4^+)$ / $\nu_{max}(NO_3^-)$	$\alpha(NH_4^+)$ / $\alpha(NO_3^-)$	ν_{max}(urea) / $\nu_{max}(NO_3^-)$	α(urea) / $\alpha(NO_3^-)$	Reference
		NO_3^-	NH_4^+	Urea	NO_3^-	NH_4^+	Urea	NO_3^-	NH_4^+	Urea					
CULTURES															
Dinoflagellates															
Alexandrium catenella	Thau Lagoon	3-47	26	25	0.6-28.1	2	28.4	nd	13	0.9	nd	nd	nd	nd	a
Gymnodinium catenatum		207.1	107.5	nd	7.59	33.6	nd	27.3	3.2	nd	0.5	0.1	nd	nd	b
Diatoms															
P. australis	California	105.3	80.0	nd	2.82	5.37	nd	37.3	14.9	nd	0.8	0.4	nd	nd	c
Raphidophyte															
Heterosigma akashiwo	California	18.0	28.0	2.9	1.47	1.44	0.42	12.2	19.4	6.9	1.6	1.6	0.1	0.6	d
BLOOMS															
Dinoflagellates															
Akashiwo sanguinea	California	5.2	15.1	7.2	1.00	2.37	0.43	5.2	6.4	16.7	2.9	1.2	1.4	3.2	e
Alexandrium catenella	Benguela	>17.5	14.9	3.5	nd	2.52	0.65	nd	5.9	5.4	<0.9	nd	<0.2	nd	f
A. catenella	Thau Lagoon (S. France)	24.0	64.0	61.0	4.60	8.40	43.90	5.2	7.6	1.4	2.7	1.5	2.5	0.3	a
Cochlodinium spp.	California	0.9	>4.0	2.1*	1.00	nd	4.06*	0.9	0.3	0.8*	4.4	nd	2.3	0.9	g
Dinophysis acuminata	Benguela	3.5	13.9	6.2	0.79	0.67	0.53	4.4	20.7	11.7	4.0	4.7	1.8	2.6	f
Lingulodinium polyedrum	California	3.9	8.1	10.6	0.47	0.59	0.99	8.2	13.7	10.7	2.1	1.7	2.8	1.3	h
Prorocentrum minimum	Choptank Estuary (Chesapeake Bay)	53.8	868.6	492.6	7.12	5.09	16.84	7.6	170.6	29.3	16.2	22.6	9.2	3.9	i
Diatoms															
Pseudo-nitzschia	Benguela	15.0	18.0	4.9	1.21	1.34	nd	12.4	13.4	nd	1.2	1.1	0.3	nd	f
MIXED ASSEMBLAGES															
	Central North Pacific gyre	3.0	16.0	16.0	0.03	0.03	0.02	100.0	533.3	800.0	5.3	5.3	5.3	8.0	j
	Washington coast upwelling	5.8	6.8	4.6	0.05	0.71	0.78	116.0	9.6	5.9	1.2	0.1	0.8	0.1	k
Mixed diatoms	Ría de Vigo	26.2	335.9	67.7	0.37	3.36	0.95	70.8	100.0	71.3	12.8	1.4	2.6	1.0	f
	Western New Zealand	13.8	20.7	12	1.1	0.5	0.5	12.5	41.4	24.0	1.5	3.3	0.9	1.9	l
Mixed dinoflagellates	Neuse Estuary (N. Carolina)	4.0	52.9	5.77	0.54	2.38	0.37	0.6	10.4	0.3	13.3	18.6	1.4	0.6	i
	Benguela (Expt 5)	3.5	14.6	4.4	0.82	0.62	nd	4.3	23.5	nd	4.2	5.5	1.3	nd	f
Diatoms + dinoflagellates	Benguela (Expt 4)	24.0	6.2	3.2	8.24	0.53	0.21	2.9	11.7	15.2	0.3	4.0	0.1	5.2	f
	Fal Estuary	7.0	15.5	nd	3.00	1.55	nd	2.3	10.0	nd	2.2	4.3	nd	nd	f

Table 7.1. Comparison of nitrogen uptake kinetics experiments in upwelling systems (shaded grey) and other ecosystems. References are as in Table 3.7.

Appendix A1
Protocols for nutrient determinations

A1.1. Nitrate (Nydahl, 1976)

1. Reduction of NO_3^- to NO_2^- using cadmium column

Buffers

Tris buffer A (1 M)
- Weigh 30.28 g Tris base (Sigma T-1503) and dissolve in about 210 ml Milli Q.
- Adjust to pH = 8 with concentrated HCl.
- Make up to 250 ml with Milli Q and check pH. Add more HCl if necessary.

Tris buffer B (0.5 M)
- Weigh 6.06g Tris base (T-1503) and 7.90g Tris HCl (T-3253) and dissolve in 100ml Milli Q.
- pH should be around 8.
- Dilute 1:100 for use.

Cadmium preparation

- Wash known weight of granulated cadmium (0.5-1mm size) with acetone, 2 M HCl and methanol, rinsing with water between each. Dry for storage.
- Copperize with 0.08 M $CuSO_4$. For a column which has a bed volume of about 3.9 ml, 16.25g cadmium is required which needs about 40 ml Cu SO_4, i.e. 25ml/10g. Thoroughly wash off colloidal Cu not adhering to cadmium – can lead to highly erratic results. Keep in buffer B or water prior to packing column.
- Plug end of column with glass wool, fill with water or buffer B and add cadmium, tapping occasionally. Finish with plug of glass wool.

Column activation
- Flush column with buffer B to remove air bubbles from lines.
- Activate column with a seawater NO_3^- solution of 50 µmol l^{-1}. Only need to activate newly prepared columns or columns that have been lying idle for some time or re-packed.

Standards

Initial stock (10 µmol N ml^{-1})
- Weigh 0.5055 g KNO_3 and dissolve in 500 ml Milli Q.
- Store in fridge in brown glass bottle.
- Note: according to Strickland and Parsons (1960), chloroform must *not* be used as a preservative as it poisons the copper catalyst and interferes with the reduction.

Working standard (20 µmol N ml^{-1})
- Place 0.1 ml initial stock in a volumetric flask and make up to 50 ml with NO3--free seawater.

- For activation standard make up 0.25 ml of initial stock to 50 ml to obtain a concentration of 50 µmol N ml^{-1}).

Running samples and standards

- Pipette 0.15 ml Tris buffer A into 15 ml test tube and fill with sample/standard.
- Flush column with 7 – 8ml sample at appropriate flow rate to waste beaker.
- Discard this flush water while column is still running and then collect 5 ml for analysis in 10 ml measuring cylinder.
- Stop pump (watch for siphoning action!!), decant reduced sample into test tube.
- Set up new sample/standard.
- Once all samples, standards and blanks have been reduced, NO2- concentration is measured following the protocol described in A1.2.

Sample order (one test tube per sample)

- Run 3 standards - 20 µM
- 10 samples
- Standard
- 10 samples
- Standard etc
- End with 3 blanks (seawater used to make up standard – may not be a real blank).
- Flush and store column filled with buffer B.

NOTES

- Optimal flow rate is crucial to obtaining 100% reduction efficiency (or close) – this should be checked on each new column. For seawater this is around 1.9ml/min with our column set-up (freshwater optimum will be considerably faster). We actually operate at faster than optimal flow rates to speed things up a bit – working on premise that standards will take loss of efficiency into account.
- If the column becomes filled with air bubbles it needs to be repacked (for longer term air contact the column should be re-copperized)
- Following re-packing the column must be re-activated followed by 3 standards. Activation is necessary after long periods without use. Safest to do it each day.

A.1.2. Nitrite (Grasshoff et al., 1999)

Reagents

Sulfanilamide

- Dilute 10 ml concentrated HCl in ~60 ml Milli-Q water.
- Weigh 1 g sulfanilamide and dissolve in the diluted HCl.
- Make up to 100 ml with Milli-Q.

NED

- Weigh 0.1 g N-(1-napthyl)-ethylene-diamine dihydrochloride.
- Dissolve in 100 ml Milli-Q.

Standards

Initial stock (10 µmol N ml^{-1})

- Dry anhydrous sodium nitrite ($NaNO_2$) at 100 °C for 1 h.
- Dissolve 0.345 g $NaNO_2$ in 500 ml Milli-Q.
- Add a few drops of chloroform.
- Store in an amber glass bottle in a refrigerator.

Working standard (4 µmol N l^{-1})

- Place 1 ml initial stock in a 100 ml volumetric flask and make up to 100 ml with Milli-Q to produce a dilute stock of concentration 100 µmol N l^{-1}.
- Place 1 ml of this dilute stock in a 25 ml measuring cylinder and make up to 25 ml with Milli-Q.

Procedure

- Pipette duplicate 5 ml aliquots of Milli-Q (blank), of standard and of each water sample into glass Kimble tubes.
- Add 0.1 ml sulfanilamide and allow about 1 min reaction time.
- Add 0.1 ml NED and allow at least 15 min for colour development.
- Read absorbance on a spectrophotometer at 540 nm within 1 h.
- The same procedure is applied to NO_3 samples (2 seawater blanks, 3 standards and single samples) which have been reduced to NO_2 by passage through a cadmium column.

A1.2. Ammonium

A1.2.1. Colourimetric method (Grasshoff et al., 1999)

Reagents

Citrate
- Weigh 342.8 g trisodium citrate dihydrogen.
- Dissolve in just under 1 l.
- Add 0.4 g (10 mmol) NaOH.
- Boil while stirring on heater-strirrer.
- Cool and make up to 1 l with Milli-Q.
- Store in a glass bottle sealed with a plastic stopper at room temperature. Stable for months.

Phenol
- Weigh 13.58 g phenol and 0.1435 g disodium nitroprusside dihydrate.
- Dissolve in 500 ml Milli-Q.
- Store in an amber glass bottle in a refrigerator. Stable for months.

Trione
- Dissolve 20 g NaOH in 1 l Milli-Q and store in a tightly closed polyethylene bottle.
- Dissolve 0.1833g trione (110 mg Cl) in 100 ml NaOH reagent.
- Store in glass bottle with plastic stopper in fridge. Stable for ~1 week.

Standards

Initial stock (10 μmol N ml^{-1})
- Dissolve 0.2675 g NH_4Cl (dried at 100 °C) in 500 ml Milli-Q.
- Add a few drops of chloroform.

Working standard (4 μmol N l^{-1})
- Place 1 ml initial stock in a 100 ml volumetric flask and make up to 100 ml with Milli-Q to produce a dilute stock of concentration 100 μmol N l^{-1}.
- Place 1 ml of this dilute stock in a 25 ml measuring cylinder and make up to 25 ml with NH_4-free seawater.

Procedure
- Pipette triplicate 5 ml aliquots of standard, NH_4-free seawater and sample
- Add 0.2 ml citrate, followed by 0.2 ml phenol, then 0.2 ml trione, mixing between additions.
- Cover and leave at room temperature in the dark for at least 3 h (generally overnight).
- Measure absorbance on a spectrophotometer at 630 nm.

A.1.2.2. Fluorometric method (Holmes et al., 1999)

Reagents

Sodium sulfite
- Weigh 0.8 g sodium sulfite and place in a 100 ml volumetric flask
- Make up to 100 ml with Milli-Q.

o-Phthaldialdehyde (OPA)
- Weigh 2 g OPA and place in a darkened 50 ml volumetric flask.
- Make up to 50 ml with high grade ethanol.

Sodium tetraborate
- Weigh 40 g sodium tetraborate and place in a 1-l volumetric flask.
- Make up to 1 l with Milli-Q.

Mixed reagent
In a brown 1 l polyethylene bottle mix 5 ml sodium sulfite reagent with OPA and sodium tetraborate reagents. Store at room temperature.

Standards

- Dissolve 53.49 mg of NH_4Cl in 100 ml Milli-Q to produce an initial stock of concentration 10 μmol ml^{-1}.
- Place 0.1 ml of this initial stock in a 100 ml volumetric flask and make up to 100 ml with Milli-Q to obtain a working stock of concentration 10 μmol l^{-1}.
- To obtain standard concentrations of 0.1, 0.5 and 1.0 μmol l^{-1} pipette 0.08, 0.40 and 0.80 ml initial stock into glass Kimble tubes and make up to 8 ml with Milli-Q.

Procedure

- To triplicate 8 ml standards and Milli-Q blanks and duplicate 8 ml samples, add 2 ml mixed reagent and mix.
- Cover and leave at room temperature in the dark for at least 3 h (generally overnight).
- Measure fluorescence on a fluorometer.

A.1.3. Urea

A.1.3.1. Oven method (Grasshoff et al., 1999)

Reagents

Acid reagent

- Dissolve 70 g NaH_2PO_4-H_2O as completely as possible in 60 ml Milli-Q.
- Carefully add 1 l H_2SO_4 (this is done by adding the acid slowly to the solution which is placed in a cold water bath and allowing the solution to cool in between additions).
- Store in a glass bottle. Stable.

Manganous chloride

- Dissolve 40.5 g $MnCl_2$-$4H_20$ and 0.8103 g KNO_3 in 100 ml Milli-Q.
- Store in a glass bottle. Stable.

Mixed reagent

- Dissolve 3.0384 g diacetyl monoxime (CH_3-COC(NOH)-CH_3) and 0.035 g semicarbazide hydrochloride (NH_2-CONH-NH_2-HCl) in 50 ml 50% ethanol.
- Immediately add 50 ml manganous chloride reagent.

Standards

Initial stock (10 µmol N ml^{-1})

- Dissolve 0.15025 g urea in 500 ml Milli-Q. N.B.: the concentration of urea is 5 µmol ml^{-1} because a molecule of urea contains 2 atoms of N.
- Add a few drops of chloroform.
- Store in brown glass bottle.

Working standards

- Place 1 ml initial stock in a 100 ml volumetric flask and make up to 100 ml with Milli-Q to produce a dilute stock of concentration 100 µmol N l^{-1}.
- Place 1 ml of this dilute stock in a 25 ml measuring cylinder and make up to 25 ml with Milli-Q to obtain a standard of concentration 4 µmol N l^{-1}.
- To obtain concentrations of 0.1, 0.5 and 1.0 µmol N l^{-1} dilute 0.1 ml initial stock in 100 ml then pipette volumes of 0.05, 0.25 and 0.50 ml of the dilute stock into glass Kimble tubes and make up to 5 ml with Milli-Q.

Procedure

- To triplicate 5 ml standards, Milli-Q blanks and samples, add 2 ml NaCl and mix. This is a modification of the original method which used 0.55 g dry NaCl.
- Add 0.7 ml sulfuric acid reagent and mix.
- Add 0.2 ml mixed reagent.
- Cover and place in oven (or on a hot plate) at 75 °C for 3 h.
- Cool under running tap water and read at 520 nm within 30 min.

A.1.3.2. Room temperature method (Goeyens, 1998)

Reagents

Acid reagent

- Dilute 300 ml concentrated sulfuric acid in 235 ml Milli-Q (this is done by adding the acid slowly to the solution which is placed in a cold water bath and allowing the solution to cool in between additions).
- Dissolve 0.15 g ferric chloride in 10 ml Milli-Q and add 0.5 ml of this solution to the acid solution.

Mixed reagent

- Dissolve 8.5 g diacetylmonoxime in 250 ml Milli-Q.
- Dissolve 0.95 g thiosemicarbazide in 100 ml and add 10 ml of this solution to the diacetylmonoxime solution.

Procedure

- To each 10 ml standard, blank and sample, add 0.7 ml mixed reagent and mix.
- Add 2.3 ml acid reagent and mix.
- Store the samples at room temperature in the dark for at least 72 h and up to 120 h.
- Measure absorbance at 520 nm, taking care not to expose the samples to light while doing so.

A.1.4. Dissolved inorganic silicate (Grasshoff et al., 1999)

Reagents

Sulfuric acid (4.5 M)

- Carefully add 250 ml concentrated sulfuric acid to 750 ml Milli-Q in a plastic beaker while stirring. Allow to cool and make up to 1 l.
- Store in a polyethylene bottle.

Acid molybdate

- Dissolve 6.335 g ammonium heptamolybdate tetrahydrate [$(NH_4)_6Mo_7O_{24}$-$4H_2O$] in 50 ml Milli-Q.
- Add to 50 ml sulfuric acid reagent (do not add the acid to the molybdate).
- Store in a polyethylene bottle protected from the sun. Stable for months.

Oxalic acid

- Dissolve 10 g oxalic acid dihydrate [$(COOH)_2$-$2H_2O$] in 100 ml Milli-Q.
- Store in a polyethylene bottle at room temperature. Stable indefinitely.

Ascorbic acid

- Dissolve 1.4 g ascorbic acid ($C_6H_3O_6$) in 100 ml pure water.
- Store in an amber polyethylene bottle in the fridge. Effective as long as it remains colourless.

Standards

Initial stock (10 µmol Si ml^{-1})

- Dry standard (Na_2SiF_6) at 105 °C in a platinum or nickel crucible.
- Weigh 0.940 g standard and dissolve in ~100 ml Milli-Q in a plastic beaker, warming carefully if necessary.
- Make up to 500 ml.

Working standard (20 µmol Si l^{-1})

- Pour ~45 ml Milli-Q into a plastic measuring cylinder.
- Add 0.1 ml initial stock then make up to 50 ml with Milli-Q to obtain a standard of concentration 20 µmol Si l^{-1}.

Procedure

- Pipette 5 ml standard, blank and sample into plastic test tubes.
- Add 0.2 ml molybdate reagent and mix.
- Leave for 5-10 min before adding 0.2 ml oxalic acid reagent.
- Immediately add 0.2 ml ascorbic acid and mix.
- Leave for 30-60 min for colour development then measure absorbance at 810 nm.
- Dissolved salts reduce the colour of the blue silicomolybdate complex, therefore a correction factor should be applied to compensate for this matrix effect:

$Si_{cor} = (1 + 0.0045 * salinity) * Si_{uncor}$

A1.5. Dissolved inorganic phosphate (Grasshoff et al., 1999)

Reagents

Sulfuric acid (4.5 M) (same as for Si)

- Carefully add 250 ml concentrated sulfuric acid to 750 ml Milli-Q while stirring. Allow to cool and make up to 1 l.
- Store in a polyethylene bottle.

Mixed reagent

- Dissolve 12.5 g ammonium heptomolybdate tetrahydrate [$(NH_4)6Mo_7O_{24}$-$4H_2O$] in 125 ml Milli-Q.
- Dissolve 0.5 g potassium antinomy tartrate [$K(SbO)C_4H_4O_6$] in 20 ml Milli-Q.
- Add the molybdate solution to 350 ml sulfuric acid reagent, stirring continuously [do not add the acid to the molybdate].
- Add tartrate solution and mix well.
- Store in a glass bottle. Stable for months.

Ascorbic acid

- Dissolve 5 g ascorbic acid in 25 ml Milli-Q, then add 25 ml sulfuric acid reagent.
- Store in a refrigerator in a brown glass bottle. Stable for as long as it remains colourless.

Standards

Initial stock (10 μmol P ml^{-1})

- Dry standard (KH_2PO_4) at 105 °C and cool in a desiccator before use.
- Dissolve 0.6805 g in 500 ml Milli-Q to which 1 ml 4.5 M sulfuric acid has been added.
- Store in a glass bottle in a refrigerator. Stable for months.

Working standard (4 μmol P l^{-1})

- Place 1 ml initial stock in a 100 ml volumetric flask and make up to 100 ml with Milli-Q to produce a dilute stock of concentration 100 μmol P l^{-1}.
- Place 1 ml of this dilute stock in a 25 ml measuring cylinder and make up to 25 ml with Milli-Q to obtain a standard of concentration 4 μmol P l^{-1}.

Procedure

- To 5 ml standards, blanks and samples, add 0.1 ml ascorbic acid and mix.
- Add 0.1 ml mixed reagent and mix.
- Read at 880 nm within 10-30 min.

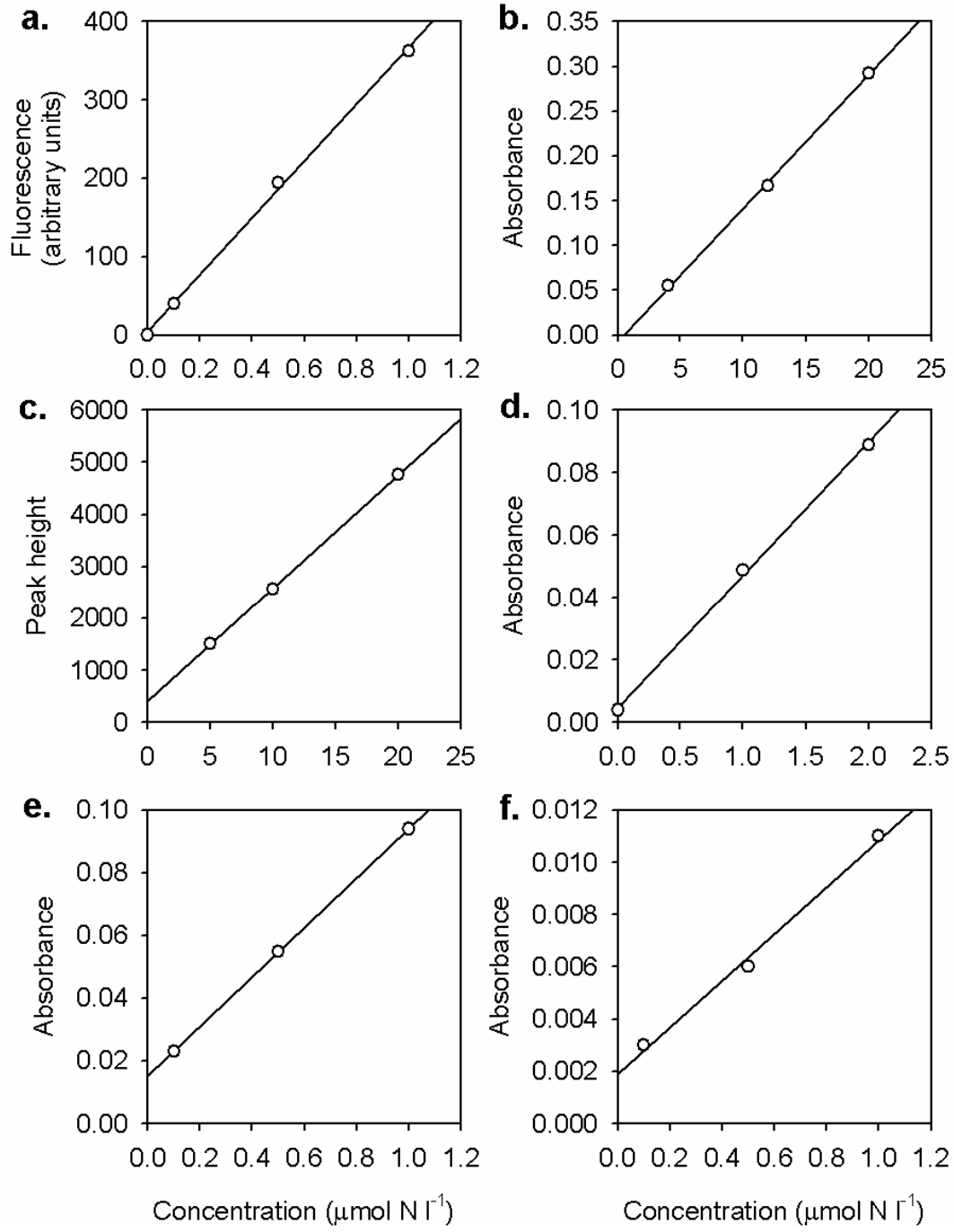

Figure A.1.1. Examples of calibration curves for (a) NH_4 using OPA method, (b) NH_4 using indophenol blue method, (c) NO_3 using flow injection method, (d) NO_2 using manual method, (e) urea using room temperature method and (f) urea using oven method.

Appendix 2

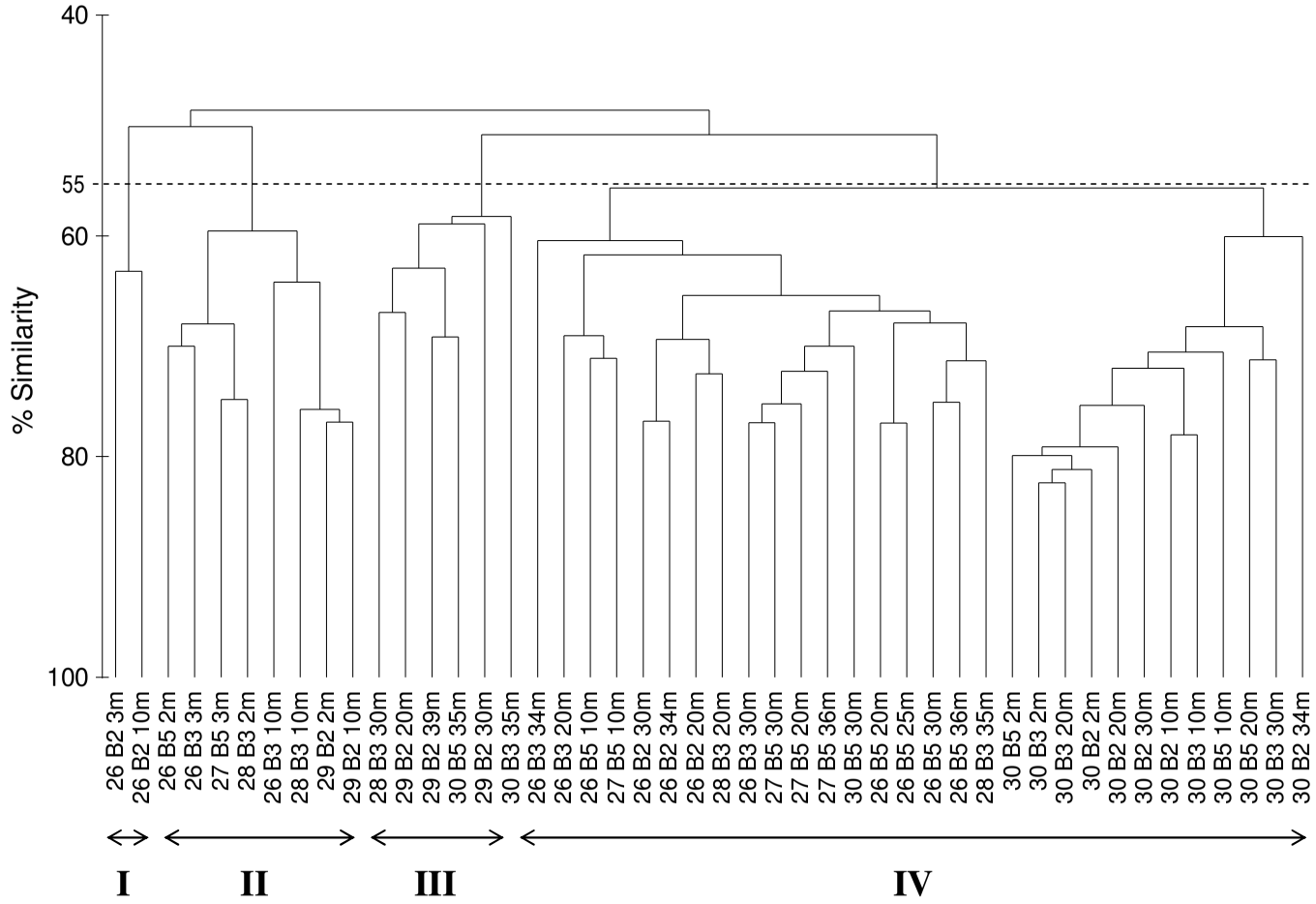

Figure A2.1. Dendrogram derived from Bray-Curtis similarity indices based on phytoplankton counts from all stations and depths sampled in the Ría de Vigo in September 2006 using PRIMER. Counts were standardised and square-root transformed prior to the calculations.

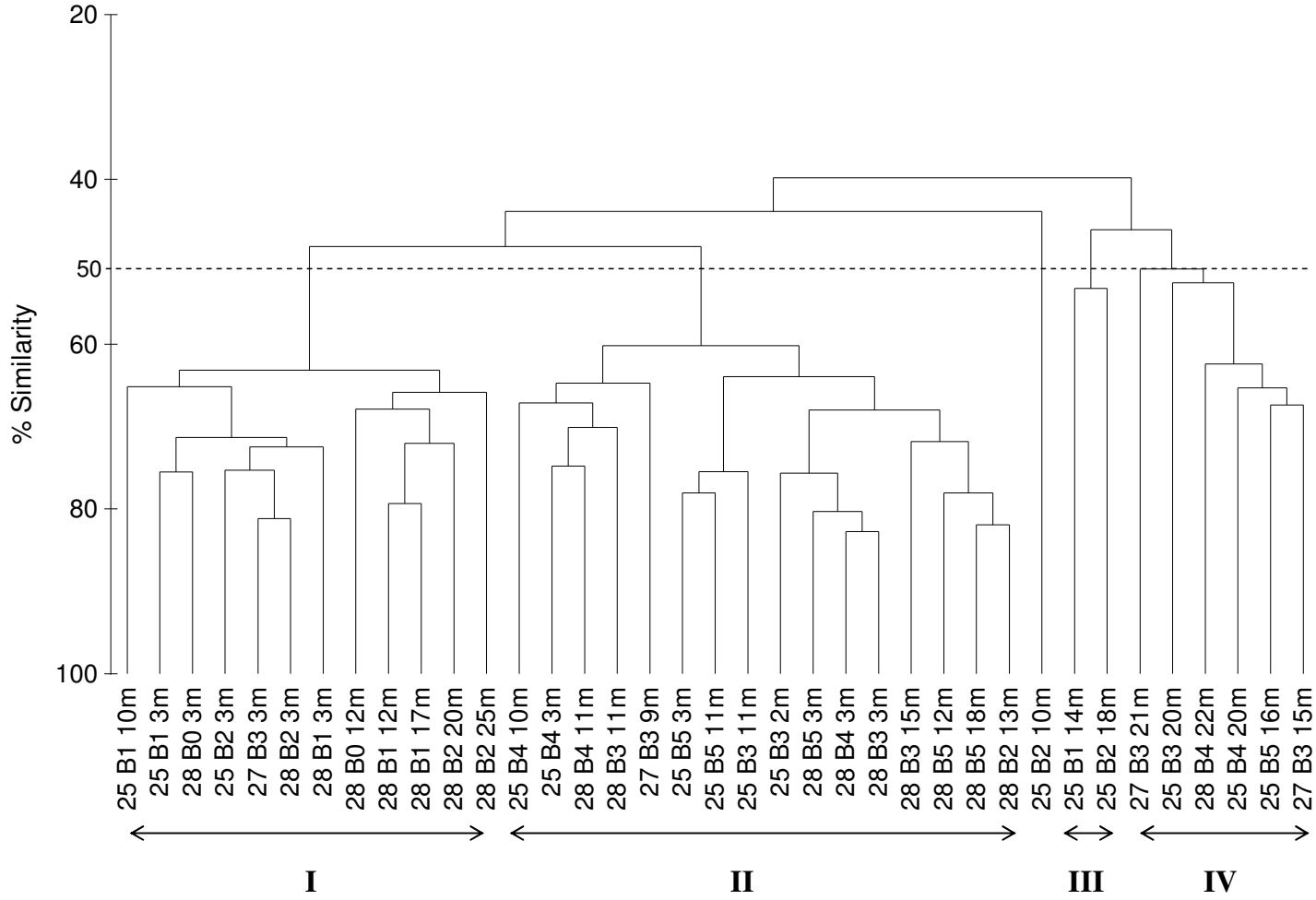

Figure A2.2. Dendrogram derived from Bray-Curtis similarity indices based on phytoplankton counts from all stations and depths sampled in June 2007 using PRIMER. Counts were standardised and square-root transformed prior to the calculations.

References

Adams, N.A., Lesoing, M. and Trainer, V.L. (2000). Environmental influences on domoic acid accumulation in razor clams on the Washington coast. *Journal of Shellfish Research*, 19: 1007-1015.

Aksnes, D.L. and Egge, J.K. (1991). A theoretical model for nutrient uptake in phytoplankton. *Marine Ecology Progress Series*, 70(1): 65-72.

Álvarez-Salgado, X.A., Beloso, S., Joint, I., Nogueira, E., Chou, L., Pérez, F.F., Groom, S., Cabanas, J.M., Rees, A.P. and Elskens, M. (2002). New production of the NW Iberian Shelf during the upwelling season over the period 1982-1999. *Deep-Sea Research Part I*, 49: 1725-1739.

Álvarez-Salgado, X.A., Castro, C.G., Perez, F.F. and Fraga, F. (1997). Nutrient mineralization patterns in shelf waters of the Western Iberian upwelling. *Continental Shelf Research*, 17(10): 1247-1270.

Álvarez-Salgado, X.A., Gago, J., Míguez, B.M., Gilcoto, M. and Pérez, F.F. (2000). Surface waters of the NW Iberian margin: upwelling on the shelf versus outwelling of upwelled waters from the Rías Baixas. *Estuarine, Coastal and Shelf Science*, 51: 821-837.

Álvarez-Salgado, X.A., Labarta, U., Fernandez-Reiriz, M.J., Figueiras, F.G., Rosón, G., Piedracoba, S., Filgueira, R. and Cabanas, J.M. (2008). Renewal time and the impact of harmful algal blooms on the extensive mussel raft culture of the Iberian coastal upwelling system (SW Europe). *Harmful Algae*, 7: 849-855.

Álvarez-Salgado, X.A., Rosón, G., Pérez, F.F. and Pazos, Y. (1993). Hydrographic variability off the Rías Baixas (NW Spain) during the upwelling season *Journal of Geophysical Research*, 98(C8): 14447-14455.

Álvarez–Salgado, X.A., Beloso, S., Joint, I., Nogueira, E., Chou, L., Pérez, F.F., Groom, S., Cabanas, J.M., Rees, A.P. and Elskens, M. (2002). New Production of the NW Iberian Shelf during the Upwelling Season over the period 1982–1999. *Deep Sea Research I* 49: 1725-1739.

Alvarez Salgado, X.A., Castro, C.G., Perez, F.F. and Fraga, F. (1997). Nutrient mineralization patterns in shelf waters of the Western Iberian upwelling. *Continental Shelf Research*, 17(10): 1247-1270.

Anderson, C.R., Brzezinski, M.A., Washburn, L. and Kudela, R.M. (2006). Circulation and environmental conditions during a toxigenic *Pseudo-nitzschia australis* bloom in the Santa Barbara Channel, California. *Marine Ecology Progress Series*, 327: 119-133.

Anderson, D.M., Glibert, P.M. and Burkholder, J.M. (2002). Harmful algal blooms and eutrophication: Nutrient sources, composition, and consequences. *Estuaries*, 25(4B): 704-726.

Anderson, D.M., Kulis, D.M. and Binder, B.J. (1984). Sexuality and cyst formation in the dinoflagellate *Gonyaulax tamarensis* - cyst yield in batch cultures. *Journal of Phycology*, 20(3): 418-425.

Anderson, D.M., Kulis, D.M., Doucette, G.J., Gallagher, J.C. and Balech, E. (1994). Biogeography of toxic dinoflagellates in the genus *Alexandrium* from the northeastern United States and Canada. *Marine Biology*, 120(3): 467-478.

Anderson, D.M., Kulis, D.M., Sullivan, J.J., Hall, S. and Lee, C. (1990). Dynamics and physiology of saxitoxin production by the dinoflagellates *Alexandrium* spp. *Marine Biology*, 104(3): 511-524.

Andrews, W.R.H. and Hutchings, L. (1980). Upwelling in the Southern Benguela current. *Progress in Oceanography*, 9: 1-8.

Antia, N.J., Harrison, P.G. and Oliveira, L. (1991). Phycological reviews 2: The role of dissolved organic nitrogen in phytoplankton nutrition, cell biology and ecology. *Phycologia*, 30: 1-89.

Arístegui, X., Alvarez-Salgado, X.A., Barton, E.D., Figueiras, F.G., Hernandez-Leon, S., Roy, C. and Santos, A.M.P. (2004). *Oceanography and fisheries of the Canary Current/ Iberian region of the eastern North Atlantic*. In: A.R. Robinson and K. Brink (Eds.). The global coastal ocean: interdisciplinary regional studies and syntheses. The sea: ideas and observations on progress in the study of the seas, Harvard University Press, Vol 14.

Armstrong, F.A.J., Stearns, C.R. and Strickland, J.D.H. (1967). The measurement of upwelling and subsequent biological processes by means of the Technicon autoanalyser and associated equipment. *Deep-Sea Research Part II*, 14: 381-389.

Arrigo, K.R. (2005). Marine microorganisms and global nutrient cycles. *Nature*, 437(7057): 349-355.

Auro, M.E. (2007). Nitrogen dynamics and toxicity of the pennate diatom *Pseudo-nitzschia cuspidata*. A field and laboratory based study. MSc Thesis, San Franciso State University.

Avaria, P.S. (1979). Red tides off the coast of Chile. In: D.E. Taylor and H.H. Seliger (Eds). Second International Conference on Toxic Dinoflagellate Blooms, Key Biscayne, Florida. Elsevier, Holland & New York, p. 161-164.

Bailey, G.W. and Chapman, P. (1985). *The nutrient status of the St. Helena Bay region in February 1979*. In: L.V. Shannon (Ed). South African ocean colour and upwelling experiment. Cape Town: Sea Fisheries Research Institute, p. 125-145.

Bakun, A. (1990). Global climate change and intensification of coastal upwelling. *Science*, 247: 198-201.

Balech, E. (1985). *The genus Alexandrium or Gonyaulax of the tamarensis group*. In: D.M. Anderson, A.W. White and D.G. Baden (Eds.). Toxic Dinoflagellates., p. 33-38.

Barlow, R.G. (1982). Phytoplankton ecology in the southern Benguela Current. 1. Biochemical composition. *Journal of Experimental Marine Biology and Ecology*, 63(3): 229-237.

Bates, H.A., Kostriken, R. and Rapoport, H. (1978). The occurrence of saxitoxin and other toxins in various dinoflagellates. *Toxicon*, 16(6): 595-601.

Bates, S.S., Bird, C.J., de Freitas, A.S.W., Foxall, R., Gilgan, M., Hanic, L.A., Johnson, G.R., McCulloch, A.W., Odense, P., Pocklington, R., Quilliam, M.A., Sim, P.G., Smith, J.C., Subba Rao, D.V., Todd, E.C.D., Walter, J.A. and Wright, J.L.C. (1989). Pennate diatom *Nitzschia pungens* as the primary source of domoic acid, a toxin in shellfish from eastern Prince Edward Island, Canada. *Canadian Journal of Fisheries and Aquatic Science*, 48: 1136-1144.

Bates, S.S., Garrison, D.L. and Horner, R.A. (1998). *Bloom dynamics and physiology of domoic acid-producing Pseudo-nitzschia species*. In: D.M. Anderson, A.D. Cembella and G.M. Hallegraeff (Eds.). Physiological Ecology of Harmful Algal Blooms. Berlin: Springer-Verlag.

Bates, S.S., Worms, J. and Smith, J.C. (1993). Effects of ammonium and nitrate on domoic acid production by *Nitzschia pungens* in batch culture. *Canadian Journal of Fisheries and Aquatic Science*, 50: 1248-1254.

Baudinet, D., Alliot, E., Berland, B., Grenz, C., Plante-Cuny, M.R. and Salen-Picard, C. (1990). Incidence of mussel culture on biochemical fluxes at the sediment-water interface. *Hydrobiologia*, 207: 187-196.

Bechemin, C., Grzebyk, D., Hachame, F., Hummert, C. and Maestrini, S.Y. (1999). Effect of different nitrogen/phosphorus nutrient ratios on the toxin content in *Alexandrium minutum*. *Aquatic Microbial Ecology*, 20(2): 157-165.

Berdalet, E. and Estrada, M. (1993). *Effects of turbulence on several dinoflagellate species*. In: T.J. Smayda and Y. Shimizu (Eds.). Toxic phytoplankton blooms in the sea. Amsterdam: Elsevier, p. 737-740.

Berg, G.M., Glibert, P.M., Lomas, M.W. and Burford, M.A. (1997). Organic nitrogen uptake and growth by the chrysophyte *Aureococcus anophagefferens* during a brown tide event. *Marine Biology*, 129: 377-387.

Blackburn, T.H. (1979). Method for measuring rates of $NH4^+$ turnover in anoxic marine sediments, using a ^{15}N-NH_4 dilution technique. *Applied Environmental Microbiology*, 37: 760-765.

Blanton, J.O., Tenore, K.R., Castillejo, F., Atkinson, L.P., Schwing, F.B. and Lavin, A. (1987). The relationship of upwelling to mussel production in the rías on the western coast of Spain. *Journal of Marine Research*, 45: 497-511.

Boczar, B.A., Beitler, M.K., Liston, J., Sullivan, J.J. and Cattolico, R.A. (1988). Paralytic shellfish toxins in *Protogonyaulax tamarensis* and *Protogonyaulax catenella* in axenic culture. *Plant Physiology*, 88(4): 1285-1290.

Bode, A., Gonzalez, N., Rodriguez, C., Varela, M. and Varela, M.M. (2005). Seasonal variability of plankton blooms in the Ria de Ferrol (NW Spain): I. Nutrient concentrations and nitrogen uptake rates. *Estuarine, Coastal and Shelf Science*, 63(1-2): 269-284.

Botes, L., Sym, S.D. and Pitcher, G.C. (2004). *Karenia cristata* sp. Nov. and *Karenia bicuneiformis* sp. Nov. (Gymnodiniales, Dinophyceae): two new *Karenia* species from the South African coast. *Phycologia*, 42(6): 563-571.

Boyer, G.L., Sullivan, J.J., Andersen, R.J., Harrison, P.J. and Taylor, F.J.R. (1987). Effects of nutrient limitation on toxin production and composition in the marine dinoflagellate *Protogonyaulax tamarensis*. *Marine Biology*, 96(1): 123-128.

Bravo, I., Vila, M., Maso, M., Figueroa, R.I. and Ramilo, I. (2008). *Alexandrium catenella* and *Alexandrium minutum* blooms in the Mediterranean Sea: Toward the identification of ecological niches. *Harmful Algae*, 7: 515-522.

Bricelj, V.M. and Lonsdale, D.J. (1997). *Aureococcus anophagefferens*: Causes and ecological consequences of brown tides in U.S. mid-Atlantic coastal waters. *Limnology and Oceanography*, 42: 1023-1038.

Brongersma-Sanders, M. (1957). *Mass mortality in the sea*. In: J.W. Hedgpeth (Ed). Memoirs of the Geological Society of America. Vol 67, p. 941-1010.

Brooks, P.D., Stark, J.M., McInteer, B.B. and Preston, T. (1989). Diffusion method to prepare soil extracts for automated nitrogen-15 analysis. *Soil Science Society of America Journal* 53: 1707-1711.

Buck, K.R., Uttal-Cook, L., Pilskaln, C.H., Roelke, D.L., Villac, M.C., Fryxell, G.A., Cifuentes, L. and Chavez, F.P. (1992). Autecology of the diatom *Pseudonitzschia australis* Frenguelli, a domoic acid producer from Monterey Bay, California. *Marine Ecology Progress Series*, 84: 293-302.

Burkholder, J.M. and Glibert, P.M. (2006). Intraspecific variability: An important consideration in forming generalizations about toxigenic algal species. *South African Journal of Marine Science*, 28: 177-180.

Calvert, S.E. and Price, N.B. (1971). Upwelling and nutrient regeneration in Benguela current, October 1968. *Deep-Sea Research*, 18(5): 505-523.

Cannon, J.A. (1990). *Development and dispersal of red tides in the Port River, South Australia*. In: E. Granéli, B. Sundström, L. Edler and D.M. Anderson (Eds.). Toxic marine phytoplankton., New York: Elsevier, p. 110-115.

Caperon, J. (1968). Population growth response of *Isochrysis galbana* to nitrate variation at limiting concentrations. *Ecology*, 49: 866-872.

Caperon, J. and Meyer, J. (1972). Nitrogen-limited growth of marine phytoplankton. II. Uptake kinetics and their role in nutrient limited growth of phytoplankton. *Deep-Sea Research*, 19(9): 619-632.

Caperon, J., Schell, D., Hirota, J. and Laws, E. (1979). Ammonium excretion rates in Kaneohe Bay, Hawaii, measured by a ^{15}N isotope dilution technique. *Marine Biology*, 54: 33-40.

Carlsson, P., Graneli, E., Finenko, G. and Maestrini, S.Y. (1995). Copepod grazing on a phytoplankton community containing the toxic dinoflagellate *Dinophysis acuminata*. *Journal of Plankton Research*, 17(10): 1925-1938.

Carpenter, E.J. and Guillard, R.R.L. (1971). Intraspecific differences in nitrate half-saturation constants in three species of marine phytoplankton. *Ecology*, 52(1): 183-185.

Carpenter, J.H. (1965). The Chesapeake Bay Institute technique for the Winkler dissolved oxygen method. *Limnology and Oceanography*, 10(1): 141-143.

Cembella, A.D. (1998). *Ecophysiology and metabolism of paralytic shellfish toxins in marine microalgae*. In: D.M. Anderson, A.D. Cembella and G.M. Hallegraeff (Eds.). Physiological Ecology of Harmful Algal Blooms. Berlin: Springer-Verlag, p. 381-426.

Cembella, A.D., Sullivan, J.J., Boyer, G.L., Taylor, F.J.R. and Andersen, R.J. (1987). Variation in paralytic shellfish toxin composition within the *Protogonyaulax tamarensis/catenella* species complex; red tide dinoflagellates. *Biochemical Systematics And Ecology*, 15(2): 171-186.

Cembella, A.D. and Taylor, F.J.R. (1985). *Biochemical variability within the Protogonyaulax catenella/tamarensis species complex*. In: D.M. Anderson, A.W. White and D.G. Baden (Eds.). Toxic Dinoflagellates. New York: Elsevier, p. 55-60.

Chang, F.H. and Bradford-Grieve, J.M. (1994). *Summary of the distribution of toxic dinoflagellates in relation to the physical environment in Bay of Plenty during early 1993 in New Zealand*, A report prepared for the Ministry of Agriculture and Fisheries Regulatory Authority, 69 pp.

Chang, F.H., Bradford-Grieve, J.M., Vincent, W.F. and Woods, P.H. (1995a). Nitrogen uptake by summer size-fractionated phytoplankton assemblages in the Westland, New Zealand, upwelling system. *New Zealand Journal of Marine and Freshwater Research*, 29: 147-161.

Chang, F.H., Mackenzie, L., Till, D., Hannah, D. and Rhodes, L. (1995b). *The first toxic shellfish outbreaks and the associated phytoplankton blooms in early 1993 in New Zealand*. In: P. Lassus, G. Arzul, E. Erard-Le Denn, P. Gentien and C. Marcaillou-Le Baut (Eds.). Harmful Marine Algal Blooms. p. 145-150.

Chang, F.H. and McClean, M. (1997). Growth responses of *Alexandrium minutum* (Dinophyceae) as a function of three different nitrogen sources and irradiance. *New Zealand Journal of Marine and Freshwater Research*, 31(1): 1-7.

Chapman, P. and Shannon, L.V. (1985). The Benguela Ecosystem Part II. Chemistry and Related Processes. *Oceanography and Marine Biology. An Annual Review*, 23: 183-251.

Chretiennot-Dinet, M.J. (1998). Global increase of algal blooms, toxic events, casual species introductions and biodiversity. *Oceanis*, 24(4): 223-238.

Cochlan, W.P. and Harrison, P.J. (1991). Inhibition of nitrate uptake by ammonium and urea in the eukaryotic picoflagellate *Micromonas pusilla* (Butcher) Manton et Parke. *Journal of Experimental Marine Biology and Ecology*, 153: 143-152.

Cochlan, W.P., Herndon, J. and Kudela, R.M. (2008). Inorganic and organic nitrogen uptake by the toxigenic diatom *Pseudo-nitzschia australis* (Bacillariophyceae) *Harmful Algae*, 8: 111-118.

Cochlan, W.P., Herndon, J., Ladizinsky, N.C. and Kudela, R.M. (2006). Nitrogen uptake by the toxigenic diatom *Pseudo-nitzschia australis*. GEOHAB Open Science Meeting on HABs and Eutrophication, Baltimore, MD. Vol 87 (36) suppl.

Collos, Y. (1980). Transient situations in nitrate assimilation by marine diatoms. 1. Changes in uptake parameters during nitrogen starvation. *Limnology and Oceanography*, 26(6): 1075-1081.

Collos, Y. (1982). Transient situations in nitrate assimilation by marine diatoms. 3. Short-term uncoupling of nitrate uptake and reduction. *Journal of Experimental Marine Biology and Ecology*, 62: 285-295.

Collos, Y. (1983). Transient situations in nitrate assimilation by marine diatoms. 4. Non-linear phenomena and the estimation of the maximum uptake rate. *Journal of Plankton Research*, 5(5): 677-691.

Collos, Y. (1989). A linear model of external interactions during uptake of different forms of inorganic nitrogen by microalgae. *Journal of Plankton Research*, 11(3): 521-533.

Collos, Y., Gagne, C., Laabir, M., Vaquer, A., Cecchi, P. and Souchu, P. (2004). Nitrogenous nutrition of *Alexandrium catenella* (Dinophyceae) in cultures and in Thau Lagoon, southern France. *Journal of Phycology*, 40: 96-103.

Collos, Y., Siddiqi, M.Y., Yang, M.Y., Glass, A.D.M. and Harrison, P.J. (1992). Nitrate uptake kinetics by two marine diatoms using the radioactive tracer ^{13}N. *Journal of Experimental Marine Biology and Ecology*, 163: 251-160.

Collos, Y. and Slawyk, G. (1976). Significance of cellular nitrate content in natural populations of marine phytoplankton growing in shipboard cultures. *Marine Biology*, 34: 27-32.

Collos, Y., Vaquer, A., Bibent, B., Slawyk, G., Garcia, N. and Souchu, P. (1997). Variability in nitrate uptake kinetics of phytoplankton communities in a Mediterranean coastal lagoon. *Estuarine, Coastal and Shelf Science*, 44: 369-375.

Collos, Y., Vaquer, A., Laabir, M., Abadie, E., Laugier, T., Pastoureaud, A. and Souchu, P. (2007). Contribution of several nitrogen sources to growth of *Alexandrium catenella* during blooms in Thau lagoon, southern France. *Harmful Algae*, 6: 781-789.

Collos, Y., Vaquer, A. and Souchu, P. (2005). Acclimation of nitrate uptake by phytoplankton to high substrate levels. *Journal of Phycology*, 41: 466-478.

Conway, H.L., Harrison, P.J. and Davis, C.O. (1976). Marine diatoms grown in chemostats under silicate or ammonium limitation. II. Transient response of *Skeletonema costatum* to a single addition of the limiting nutrient. *Marine Biology*, 35: 187-199.

Copenhagen, W.J. (1953). *The periodic mortality of fish in the Walvis region; a phenomenon within the Benguela Current*, Investigational Report: Division of Fisheries, South Africa.

Crespo, B.G., Figueiras, F.G., Porras, P. and Teixeira, I.G. (2006). Downwelling and dominance of autochthonous dinoflagellates in the NW Iberian margin: The example of the Ria de Vigo. *Harmful Algae*, 5: 770-781.

Cullen, J.J. and Horrigan, S.G. (1981). Effects of nitrate on the diurnal vertical migration, carbon to nitrogen ratio and the photosynthetic capacity of the dinoflagellate *Gymnodinium splendens*. *Marine Biology*, 62(2): 81-89.

Dittmar, T. and Birkicht, M. (2001). Regeneration of nutrients in the northern Benguela upwelling and the Angola-Benguela Front areas. *South African Journal of Marine Science*, 97: 239-246.

Dortch, Q. (1990). The interaction between ammonium and nitrate uptake in phytoplankton. *Marine Ecology Progress Series* 61: 183-201.

Dortch, Q. and Postel, J.R. (1989). *Phytoplankton-nitrogen interaction*. In: M.R. Landry and B.M. Hickey (Eds.). Coastal Oceanography of Washington and Oregon. Amsterdam: Elsevier, p. 139-173.

Dortch, Q., Robichaux, R., Pool, S., Milsted, D., Mire, G., Rabalais, N.N., Soniat, T.M., Fryxell, G.A., Turner, R.E. and Parsons, M.L. (1997). Abundance and vertical flux of *Pseudo-nitzschia* in the northern Gulf of Mexico. *Marine Ecology Progress Series*, 146: 249-264.

Doyle, R.W. (1975). Upwelling, clone selection and the characteristic shape of nutrient uptake curves. *Limnology and Oceanography*, 20: 487-489.

Droop, M.R. (1968). Vitamin B_{12} and marine ecology. IV. The kinetics of uptake, growth and inhibition in *Monochrysis lutheri*. *Journal of the Marine Biological Association UK*, 48: 689-733.

Dugdale, R.C. (1967). Nutrient limitation in the sea: Dynamics, identification and significance. *Limnology and Oceanography*, 12: 685-695.

Dugdale, R.C. and Goering, J.J. (1967). Uptake of new and regenerated forms of nitrogen in primary productivity. *Limnology and Oceanography*, 12: 196-206.

Dugdale, R.C., Morel, A., Bricaud, A. and Wilkerson, F.P. (1989). Modeling new production in upwelling centers -a case study of modeling new production from remotely sensed temperature and color. *Journal of Geophysical Research - Oceans*, 94(C12): 18,119-18,132.

Dugdale, R.C. and Wilkerson, F.P. (1986). The use of ^{15}N to measure nitrogen uptake in eutrophic oceans; experimental considerations. *Limnology and Oceanography*, 31(4): 673-689.

Dugdale, R.C., Wilkerson, F.P., Hogue, V.E. and Marchi, A. (2006). Nutrient controls on new production in the Bodega Bay, California, coastal upwelling plume. *Deep-Sea Research Part II* 53: 3049-3062.

Dugdale, R.C., Wilkerson, F.P. and Morel, A. (1990). Realization of new production in coastal upwelling areas: A means to compare relative performance. *Limnology and Oceanography*, 35(4): 822-829.

Eppley, R.W. and Peterson, B.J. (1979). Particulate organic-matter flux and planktonic new production in the deep ocean. *Nature*, 282(5740): 677-680.

Eppley, R.W. and Rogers, J.N. (1970). Inorganic nitrogen assimilation of *Ditylum brightwellii*, a marine plankton diatom. *Journal of Phycology*, 6: 344-351.

Eppley, R.W., Rogers, J.N. and McCarthy, J.J. (1969). Half-saturation constants for uptake of nitrate and ammonium by marine phytoplankton. *Limnology and Oceanography*, 14: 912-920.

Erard-Le Denn, E., Chretiennot-Dinet, M.J. and Probert, I. (2000). First report of parasitism on the toxic dinoflagellate *Alexandrium minutum* Halim. *Estuarine, Coastal and Shelf Science*, 50(1): 109-113.

Estrada, M. (1984). Phytoplankton distribution and composition off the coast of Galicia (northest of Spain). *Journal of Plankton Research*, 6: 417-434.

Estrada, M. (1995). *Dinoflagellate assemblages in the Iberian upwelling area*. In: P. Lassus, G. Arzul, E. Erard, P. Gentien and C. Marcaillou-Le Baut (Eds.). Harmful Marine Algal Blooms. Paris: Lavoisier.

Estrada, M. and Blasco, D. (1985). Phytoplankton assemblages in upwelling areas. In: C. Bas, R. Margalef and P. Rubies (Eds). International Symposium on the Upwelling Areas off Western Africa, Barcelona. Vol 1, p. 379-402.

Estrada, M., Sanchez, F.J. and Fraga, S. (1984). *Gymnodinium catenatum* (Graham) en las rias gallegas (NO de España). *Investigaciones Pesqueras* 48: 31-40.

Etheridge, S.M. and Roesler, C.M. (2005). Effects of temperature, irradiance and salinity on photosynthesis, growth rates, total toxicity and toxin composition for *Alexandrium fundyense* isolates from the Gulf of Maine and Bay of Fundy. *Deep-Sea Research II*, 52: 2491-2500.

Falkowski, P.G. and Owens, T.G. (1978). Effects of light intensity on photosynthesis and dark respiration in six species of marine phytoplankton. *Marine Biology*, 45(4): 289-295.

Fan, C., Glibert, P.M. and Burkholder, J.M. (2003). Characterization of the affinity for nitrogen, uptake kinetics and environmental relationships for *Prorocentrum minimum* in natural blooms and laboratory cultures. *Harmful Algae*, 2(4): 283-299.

Fawcett, A., Pitcher, G.C., Bernard, S., Cembella, A.D. and Kudela, R.M. (2007). Contrasting wind patterns and toxigenic phytoplankton in the southern Benguela upwelling system. *Marine Ecology Progress Series*, 348: 19-31.

Fermin, E.G., Figueiras, F.G., Arbones, B. and Villarino, M.L. (1996). Short time-scale development of a *Gymnodinium catenatum* population in the Ria de Vigo (NW Spain). *Journal of Phycology*, 32: 212-221.

Fernández-Reiriz, M.J., Duarte, P. and Labarta, U. (2007). *Modelos de comportamiento alimentario en el mejillon de las Rias Gallegas*, Biologia y cultivo del mejillon (*Mytilus galloprovincialis*) en Galicia: CSIC, 195-223.

Figueiras, F.G., Alvarez-Salgado, X.A., Castro, C.G. and Villarino, M.L. (1998). *Accumulation of Gymnodinium catenatum Graham cells in western Iberian shelft waters in response to poleward flowing slope currents*. Harmful Algae. Xunta de Galicia and Intergovernmental Oceanographic Commission of UNESCO, p. 114-117.

Figueiras, F.G. and Fraga, F. (1990). *Vertical nutrient transport during proliferation of Gymnodinium catenatum Graham in Ria de Vigo, Northwest Spain*. In: E. Granéli, B. Sundström, L. Edler and D.M. Anderson (Eds.). Toxic marine phytoplankton. New York: Elsevier, p. 144-148.

Figueiras, F.G., Jones, K.J., Mosquera, A.M., Álvarez–Salgado, X.A., Edwards, A. and MacDougall, N. (1994). Red tide assemblage formation in an estuarine upwelling ecosystem: Ria de Vigo. *Journal of Plankton Research*, 16(7): 857-878.

Figueiras, F.G., Labarta, U. and Fernandez-Reiriz, M.J. (2002). Coastal upwelling, primary production and mussel growth in the Rias Baixas of Galicia. *Hydrobiologia*, 484: 121-131.

Figueiras, F.G. and Pazos, Y. (1991a). Hydrography and phytoplankton of the Ría de Vigo before and during a red tide of *Gymnodinium catenatum* Graham. *Journal of Plankton Research*, 13: 589-608.

Figueiras, F.G. and Pazos, Y. (1991b). Microplankton assemblages in 3 Rias Baixas, Vigo, Arosa and Muros, Spain, with a subsurface chlorophyll maximum. Their relationships to hydrography. *Marine Ecology Progress Series*, 76(3): 219-233.

Figueiras, F.G. and Rios, A.F. (1993). *Phytoplankton succession, red tides and the hydrographic regime in the Rias Bajas of Galicia*. In: T.J. Smayda and Y. Shimizu (Eds.). Toxic Phytoplankton Blooms. New York: Elsevier, p. 239-244.

Figueiras, F.G., Wyatt, T., Alvarez-Salgado, X.A. and Jenkinson, Y.R. (1995). *Advection, diffusion and patch development in the Rias Baixas*. In: P. Lassus, G. Arzul, E. Erard-Le Denn, P. Gentien and C. Marcaillou-Le Baut (Eds.). Harmful Marine Algal Blooms. Paris: Lavoisier, p. 579-584.

Fisher, T.R., Carlson, P.R. and Barber, R.T. (1981). Some problems in the interpretation of ammonium uptake kinetics. *Marine Biology Letters*, 2: 33-44.

Fisher, T.R., Carlson, P.R. and Barber, R.T. (1982). Carbon and nitrogen primary productivity in three North Carolina Estuaries. *Estuarine, Coastal and Shelf Science*, 15: 621-644.

Flynn, K., Franco, J., Fernandez, P., Reguera, B., Zapata, M. and Flynn, K.J. (1995). *Nitrogen and phosphorus limitation in cultured Alexandrium minutum Halim does not promote toxin production*. In: P. Lassus, G. Arzul, E. Erard-Le Denn, P. Gentien and C. Marcaillou-Le Baut (Eds.). Harmful Marine Algal Blooms. Paris: Lavoisier, p. 439-444.

Flynn, K., Franco, J.M., Fernandez, P., Reguera, B., Zapata, M., Wood, G. and Flynn, K.J. (1994). Changes in toxin content, biomass and pigments of the dinoflagellate *Alexandrium minutum* during nitrogen refeeding and growth into nitrogen or phosphorus stress. *Marine Ecology Progress Series*, 111(1-2): 99-109.

Fraga, F., Reguera, B. and Bravo, I. (1990). *Gymnodinium catenatum bloom formation in the Spanish Rías*. In: E. Granéli, B. Sundström, L. Edler and D.M. Anderson (Eds.). Toxic marine phytoplankton. New York: Elsevier.

Fraga, S. (1981). *Upwelling off the Galician coast, Northwest Spain*. In: F.A. Richards (Ed). Coastal Upwelling. Washington: American Geophysical Union, p. 176-182.

Fraga, S. (1989). *Las purgas de mar en las Rías Bajas gallegas*. In: S. Fraga and F.G. Figueiras (Eds.). Las purgas de mar como fenomeno natural. Las mareas rojas. Cuadernos da Área do Ciencias Mariñas, Vol 4, p. 95-104.

Fraga, S., Anderson, D.M., Bravo, I., Reguera, B., Steidinger, K.A. and Yentsch, C.M. (1988). Influence of upwelling relaxation on dinoflagellates and shellfish toxicity in Ria de Vigo, Spain. *Estuarine, Coastal and Shelf Science*, 27(4): 349-361.

Fraga, S., Bravo, I. and Reguera, B. (1993). *Poleward surface current at the shelf break and blooms of Gymnodinium catenatum in Ria de Vigo (NW Spain)*. In: T.J. Smayda and Y. Shimizu (Eds.). Toxic Phytoplankton Blooms in the Sea. New York: Elsevier, p. 245-249.

Franco, J.M., Fernandez, P. and Reguera, B. (1994). Toxin profiles of natural populations and cultures of *Alexandrium minutum* Halim from Galician (Spain) coastal waters. *Journal of Applied Phycology*, 6(3): 275-279.

Frangopulos, M., Guisande, C., deBlas, E. and Maneiro, I. (2004). Toxin production and competitive abilities under phosphorus limitation of *Alexandrium* species. *Harmful Algae*, 3(2): 131-139.

Fraser, A.I., Butterfield, D., Uncles, R., Johnes, P. and Harrod, T.R. (2000). *Fal and Helford Special Areas of Conservation (cSAC) and the Tamar Estuaries complex cSAC/ Special Protection Area (pSPA): Estimation of diffuse and point-source nutrient inputs*, SSLRC report to the EA.

Garber, J.H. (1984). Laboratory study of nitrogen and phosphorous remineralization during the decomposition of coastal plankton and seston. *Estuarine, Coastal and Shelf Science*, 18: 685-702.

Garcés, E., Bravo, I., Vila, M., Figueroa, R.I., Maso, M. and Sampedro, N. (2004). Relationship between vegetative cells and cyst production during *Alexandrium minutum* bloom in Arenys de Mar harbour (NW Mediterranean). *Journal of Plankton Research*, 26(6): 637-645.

Garcia, V.M.T. and Purdie, D.A. (1994). Primary production studies during a *Gyrodinium* cf *aureolum* (Dinophyceae) bloom in the western English Channel. *Marine Biology*, 119(2): 297-305.

Geatches, T. (1997). *Update of Upper Fal Estuary Urban Wastewater Treatment Directive Sensitive Area (Eutrophic) Designation*, Environment Agency Report COR/97/022.

GEOHAB (2001). *Global Ecology and Oceanography of Harmful Algal Blooms, Science Plan*, Baltimore and Paris: Scientific Committee on Oceanographic Research and Intergovernmental Oceanographic Commission of UNESCO.

Giacobbe, M.G., Oliva, F.D. and Maimone, G. (1996). Environmental factors and seasonal occurrence of the dinoflagellate *Alexandrium minutum*, a PSP potential producer, in a Mediterranean lagoon. *Estuarine, Coastal and Shelf Science*, 42(5): 539-549.

Gianesella, S.M.F., Saldahna-Corrêa, F.M.P. and Teixeira, C. (2000). Tidal effects on nutrients and phytoplankton distribution in Bertioga Channel, São Paulo, Brazil. *Aquatic Ecosystem Health and Management*, 3: 533-544.

Gilchrist, J.D.F. (1914). An enquiry into fluctuations in fish supply on the South African coast. *Marine Biology Report, Cape Town*, 2: 8-35.

Glibert, P.M. and Goldman, J.C. (1981). Rapid ammonium uptake by marine phytoplankton. *Marine Biology Letters*, 2: 25-31.

Glibert, P.M., Goldman, J.C. and Carpenter, E.J. (1982a). Seasonal variations in the utilization of ammonium and nitrate by phytoplankton in Vineyard Sound, Massachusetts, USA. *Marine Biology*, 70: 237-250.

Glibert, P.M., Lipschulz, F., McCarthy, J.J. and Altabet, M.A. (1982b). Isotope dilution models of uptake and remineralization of ammonium by marine plankton. *Limnology and Oceanography*, 27(4): 639-650.

Goering, J.J., Wallen, D.D. and Naumann, R.A. (1970). Nitrogen uptake by phytoplankton in the discontinuity layer of the eastern subtropical Pacific Ocean. *Limnology and Oceanography*, 15: 789-796.

Goeyens, L., Kindermans, N., Abu Yusuf, M. and Elskens, M. (1998). A room temperature procedure for the manual determination of urea in seawater. *Estuarine, Coastal and Shelf Science*, 47(4): 415-418.

Goldman, J.C. and Glibert, P.M. (1982a). Comparative rapid ammonium uptake by four marine phytoplankton species. *Limnology and Oceanography*, 27: 814-827.

Goldman, J.C. and Glibert, P.M. (1982b). *Kinetics of inorganic nitrogen uptake by phytoplankton*. In: E.J. Carpenter and D.G. Capone (Eds.). Nitrogen in the Marine Environment. New York: Academic Press, p. 233-274.

Goldman, J.C., McCarthy, J.J. and Peavy, D.G. (1979). Growth rate influence on the chemical composition of phytoplankton in oceanic waters. *Nature*, 279: 210-215.

Grasshoff, K., Kremling, K. and Ehrhardt, M. (1999). *Methods of seawater analysis*. Weinheim, Germany: Wiley-Verlag Chemie.

Gregg, W.W., Casey, N.W. and McClain, C.R. (2005). Recent trends in global ocean chlorophyll. *Geophysical Research Letters*, 32(L03606): doi:10.1029/2005JC003140.

Grill, E.V. and Richards, F.A. (1964). Nutrient regeneration from phytoplankton decomposing in seawater. *Journal of Marine Research*, 22: 51-69.

Grime, J.P. (1974). Vegetation classification by reference to strategies. *Nature*, 242: 344-347.

Grindley, J.R. and Taylor, F.J.R. (1962). Red water and mass-mortality of fish near Cape Town. *Nature*, 195(4848): 1324.

Grzebyk, D., Bechemin, C., Ward, C.J., Verite, C., Codd, G.A. and Maestrini, S.Y. (2003). Effects of salinity and two coastal waters on the growth and toxin content of the dinoflagellate *Alexandrium minutum*. *Journal of Plankton Research*, 25: 1185-1199.

Guillard, R.R.L. and Hargraves, P.E. (1993). *Stichochrysis immobilis* is a diatom, not a chrysophyte. *Phycologia*, 32(3): 234-236.

Guisande, C., Frangopulos, M., Maneiro, I., Vergara, A.R. and Riveiro, I. (2002). Ecological advantages of toxin production by the dinoflagellate *Alexandrium minutum* under phosphorus limitation. *Marine Ecology Progress Series* 225: 169-176.

Guisande, C., Vergara, A.R., Riveiro, I. and Cabanas, J.M. (2004). Climate change and abundance of the Atlantic Iberian sardine (*Sardina pilchardus*). *Fisheries Oceanography*, 13: 91-101.

Guzman, L., Pacheco, H., Pizarro, G. and Alarcon, C. (2002). *Alexandrium catenella y veneno paralizante de los mariscos en Chile*. In: E.A. Sar, M.E. Ferrario and B. Reguera (Eds.). Floraciones Algales Nocivas en el Cono Sur Americano. Madrid: Instituto Espanol de Oceanographia, p. 235-256.

Halim, Y. (1960). *Alexandrium minutum* nov. g., nov. sp., a dinoflagellate causing 'red water'. *Vie et Milieu*, 11(1): 102-105.

Hallegraeff, G.M. (1993). A review of harmful algal blooms and their apparent global increase. *Phycologia*, 32: 79-99.

Hallegraeff, G.M., Steffensen, D.A. and Wetherbee, R. (1988). Three estuarine Australian dinoflagellates that can produce paralytic shellfish toxins. *Journal of Plankton Research*, 10(3): 533-541.

Hamasaki, K., Horie, M., Tokimitsu, S., Toda, T. and Taguchi, S. (2001). Variability in toxicity of the dinoflagellate *Alexandrium tamarense* isolated from Hiroshima Bay, western Japan, as a reflection of changing environmental conditions. *Journal of Plankton Research*, 23(3): 271-278.

Hansen, G., Daugbjerg, N. and Franco, J.M. (2003). Morphology, toxin composition and LSU rDNA phylogeny of *Alexandrium minutum* (Dinophyceae) from Denmark, with some morphological observations on other European strains. *Harmful Algae*, 2: 317-335.

Harrison, P.J., Parslow, J.S. and Conway, H.L. (1989). Determination of nutrient uptake kinetic parameters: a comparison of methods. *Marine Ecology Progress Series*, 52: 301-312.

Harrison, P.J., Waters, R.E. and Taylor, F.J.R. (1980). A broad spectrum artificial seawater medium for coastal and open ocean phytoplankton. *Journal of Phycology*, 16: 28-35.

Harrison, W.G. (1976). Nitrate metabolism of the red tide dinoflagellate *Gonyaulax polyedra* Stein. *Journal of Experimental Marine Biology and Ecology*, 21(199-209).

Harrison, W.G. (1980). *Nutrient regeneration and primary production in the sea*. In: P.G. Falkowski (Ed). Primary productivity in the sea. New York: Plenum Press, p. 433-460.

Harvey, J. (1982). θ-S relationship and water masses in the Eastern North Atlantic. *Deep-Sea Research*, 29: 1021-1033.

Hasle, G.R. and Syvertsen, E.E. (1996). *Marine Diatoms*. In: C.R. Tomas (Ed). Identifying Marine Diatoms and Dinoflagellates. San Diego: Academic Press, p. 5-385.

Haynes, R. and Barton, E.D. (1990). A poleward flow along the Atlantic coast of the Iberian Peninsula. *Journal of Geophysical Research*, 95(C7): 11,425-11,441.

Healey, F.P. (1980). Slope of the Monod equation as an indicator of advantage in nutrient competition. *Microbial Ecology*, 5: 281-286.

Herndon, J. and Cochlan, W.P. (2007). Nitrogen utilization by the raphidophyte *Heterosigma akashiwo*: Growth and uptake kinetics in laboratory cultures. *Harmful Algae*, 6(2): 260-270.

Higman, W., Gubbins, M. and Milligan, S. (2001). The marine biotoxin monitoring programme for England and Wales 2000-2001. *Shellfish News*(11): 34-36.

Higman, W. and Milligan, S. (2000). The biotoxin monitoring programmes for England and Wales. *Shellfish News*(9): 27-28.

Hildebrand, M. and Dahlin, K. (2000). Nitrate transporter genes from the diatom *Cylindrotheca fusiformis* (Bacillariophyceae): mRNA levels controlled by nitrogen source and by the cell cycle. *Journal of Phycology*, 36: 702-713.

Hillebrand, H., Durselen, C.-D., Kirschtel, D., Pollingher, U. and Zohary, T. (1999). Biovolume calculation for pelagic and benthic microalgae. *Journal of Phycology*, 35: 403-424.

Holden, C.J. (1985). *Currents in St Helena Bay inferred from radio-tracked drifters*. In: L.V. Shannon (Ed). South African ocean colour and upwelling experiment. Cape Town: Sea Fisheries Research Institute, p. 97-109.

Holligan, P.M. (1979). *Dinoflagellate blooms associated with tidal fronts around the British Isles*. In: D.E. Taylor and H.H. Seliger (Eds.). Toxic dinoflagellate blooms. New York: Elsevier, p. 249-256.

Holligan, P.M. (1981). *Biological implications of fronts on the northwest European continental shelf*, Philosophical Transactions of the Royal Society, London, No A302, 547-562.

Holligan, P.M., Maddock, L. and Dodge, J.D. (1980). The distribution of dinoflagellates around the British Isles in July 1977: a multivariate analysis. *Journal of the Marine Biological Association UK*, 60(4): 851-867.

Holmes, R.M., Aminot, A., Kerouel, R., Hooker, B.A. and Peterson, B.J. (1999). A simple and precise method for measuring ammonium in marine and freshwater ecosystems. *Canadian Journal of Fisheries and Aquatic Science*, 56(1801-1808).

Honjo, T. (1993). *Overview on bloom dynamics and physiological ecology of Heterosigma akashiwo*. In: T.J. Smayda and Y. Shimizu (Eds.). Toxic Phytoplankton Blooms in the Sea. Amsterdam: Elsevier Science Publishers, p. 33-41.

Horner, R.A., Hickey, B.M. and Postel, J.R. (2000). *Pseudo-nitzschia* blooms and physical oceanography off Washington State, USA. *South African Journal of Marine Science*, 22: 299-308.

Horstman, D.A. (1981). Reported red tide outbreaks and their effects on fauna of the West coast and South coast of South Africa 1959-1980. *Fisheries Bulletin South Africa*(15): 71-88.

Horstman, D.A., McGibbon, S., Pitcher, G.C., Calder, D., Hutchings, L. and Williams, P. (1991). Red tides in False Bay, 1959-1989, with particular reference to recent blooms of *Gymnodinium* sp. *Transactions of the Royal Society of South Africa*, 47(4-5): 611-628.

Howard, M.D.A., Cochlan, W.P., Ladizinsky, N. and Kudela, R.M. (2007). Nitrogenous preference of toxigenic *Pseudo-nitzschia australis* (Bacillariophyceae) from field and laboratory experiments. *Harmful Algae*, 6(2): 206-217.

Howarth, R. and Marino, R. (2006). Nitrogen as the limiting nutrient for eutrophication in coastal marine ecosystems: evolving views over three decades. *Limnology and Oceanography*, 51: 364-376.

Hutchings, L., Pitcher, G.C., Probyn, T.A. and Bailey, G.W. (1995). *The chemical and biological consequences of coastal upwelling*. In: C.P. Summerhayes, K.-C. Emeis, M.V. Angel, R.L. Smith and B. Zeitzschel (Eds.). Upwelling in the oceans: modern processes and ancient records. New York: John Wiley & Sons, p. 65-81.

Hwang, D.F. and Lu, Y.H. (2000). Influence of environmental and nutritional factors on growth, toxicity, and toxin profile of dinoflagellate *Alexandrium minutum*. *Toxicon*, 38(11): 1491-1503.

Hwang, D.F., Tsai, Y.H., Liao, H.J., Matsuoka, K., Noguchi, T. and Jeng, S.S. (1999). Toxins of the dinoflagellate *Alexandrium minutum* halim from the coastal waters and aquaculture ponds in Southern Taiwan. *Fisheries Science Tokyo*, 65(1): 171-172.

Hydes, D.J. and Wright, P.N. (1999). *SONUS, The SOuthern NUtrients Study 1995-1997* Final Report to the Department for the Environment, Transport and the Regions, No 7.

Ignatiades, L., Gotsis-Skretas, O. and Metaxatos, A. (2007). Field and culture studies on the ecophysiology of the toxic dinoflagellate *Alexandrium minutum* (Halim) present in Greek coastal waters. *Harmful Algae*, 6(2): 153-165.

Jacobson, D.M. and Anderson, D.M. (1994). The discovery of mixotrophy in photosynthetic species of *Dinophysis* (Dinophyceae): light and electron microscopical observations of food vacuoles of *Dinophysis acuminata*, *D. norvegica* and two heterotrophic dinophysoid dinoflagellates. *Phycologia*, 33: 97-110.

Jiménez, C., Niell, F.X., Figueiras, F.G., Clavero, V., Algarrra, P. and Buela, J. (1992). Green mass aggregations of *Gyrodinium aureolum* (Hulbert) in the Ría of Pontevedra, Northwest Spain. *Journal of Plankton Research*, 14(5): 705-720.

John, E.H. and Flynn, K.J. (1999). Amino acid uptake by the toxic dinoflagellate *Alexandrium fundyense*. *Marine Biology*, 133(1): 11-19.

Johnson, K. and Petty, R.L. (1983). Determination of nitrate and nitrite in seawater by flow injection analysis. *Limnology and Oceanography*, 28: 1260-1266.

Johnson, M., Sanders, R., Avgoustidi, V., Lucas, M., Brown, L., Hansell, D., Moore, M., Gibb, S., Liss, P. and Jickells, T. (2007). Ammonium accumulation during a silicate-limited diatom bloom indicates the potential for ammonia emission events. *Marine Chemistry*, 106: 63-75.

Jones, P.G.W. (1971). The Southern Benguela Current region in February 1966: Part I. Chemical observations with particular reference to upwelling. *Deep-Sea Research*, 18: 193-208.

Joyce, L.B. and Pitcher, G.C. (2004). Encystment of *Zygabikodinium lenticulatum* (Dinophyceae) during a summer bloom of dinoflagellates in the southern Benguela upwelling system. *Estuarine, Coastal and Shelf Science*, 59(1): 1-11.

Klausmeier, C.A., Litchman, E., Daufresne, T. and Levin, S.A. (2004). Optimal nitrogen-to-phosphorus stoichiometry of phytoplankton. *Nature*, 429: 171-174.

Kodama, M. (1990). *Possible links between bacteria and toxin production in algal blooms*. In: E. Granéli, B. Sundström, L. Edler and D.M. Anderson (Eds.). Toxic marine phytoplankton. New York: Elsevier, p. 52-61.

Kodama, M., Fukuyo, Y., Ogata, T., Igarashi, T., Kamiya, H. and Matsuura, F. (1982). Comparison of toxicities of *Protogonyaulax* cells of various sizes. *Bulletin of the Japanese Society of Scientific Fisheries*, 48(4): 567-571.

Kudela, R.M. and Cochlan, W.P. (2000). Nitrogen and carbon uptake kinetics and the influence of irradiance for a red tide bloom off southern California. *Aquatic Microbial Ecology*, 21: 31-47.

Kudela, R.M., Cochlan, W.P. and Dugdale, R.C. (1997). Carbon and nitrogen uptake response to light by phytoplankton during an upwelling event. *Journal of Plankton Research*, 19: 609-630.

Kudela, R.M., Lane, J.Q. and Cochlan, W.P. (2008a). The potential role of anthropogenically derived nitrogen in the growth of harmful algae in California, USA. *Harmful Algae*, 8: 103-110.

Kudela, R.M., Pitcher, G.C., Probyn, T.A., Figueiras, F.G., Moita, M.T. and Trainer, V. (2005). Harmful Algal Blooms in Coastal Upwelling Systems. *Oceanography*, 18(2): 184-197.

Kudela, R.M., Ryan, J.P., Blakely, M.D., Lane, J.Q. and Peterson, T.D. (2008b). Linking the physiology and ecology of *Cochlodinium* to better understand harmful algal bloom events: A comparative approach. *Harmful Algae*, 7: 278-292.

Kudela, R.M., Seeyave, S. and Cochlan, W.P. (submitted). The role of nutrients in regulation and promotion of harmful algal blooms in upwelling systems. *Progress in Oceanography*.

Kuypers, M.M.M., Lavik, G., Woebken, D., Schmid, M., Fuchs, B.M., Amann, R., Jorgensen, B.B. and Jetten, M.S.M. (2005). Massive nitrogen loss from the Benguela upwelling system through anaerobic ammonium oxidation. *Proceedings of the National Academy of Sciences of the United States of America*, 102(18): 6478-6483.

L' Helguen, S., Maguer, J.-F. and Caradec, J. (2008). Inhibition kinetics of nitrate uptake by ammonium in size-fractionated oceanic phytoplankton communities: implications for new production and f-ratio estimates. *Journal of Plankton Research*, 30(10): 1179-1188.

Labarta, U., Fernandez-Reiriz, M.J., Perez-Camacho, A. and Perez Corbacho, E. (2004). *Bateeiros, mar, mejillon. Una perspectiva bioeconomica*, CIEF. Fundacion Caixagalicia, Santiago de Compostela.

Lancelot, C., Billen, G., Sournia, A., Weisse, T., Colijn, F., Veldhuis, M.J.W., Davies, A. and Wassman, P. (1987). *Phaeocystis* blooms and nutrient enrichment in the continental coast zones of the North Sea. *Ambio*, 16(1): 38-46.

Langston, W.J., Chesman, B.S., Burt, G.R., Hawkins, S.J., Readman, J. and Worsfold, P. (2003). *Site characterisation of the south west European marine sites. The Fal and Helford (candidate) Special Area of Conservation*, Marine Biological Association Occasional Publication, Plymouth, Devon: Marine Biological Association of the UK, No 8.

Lartigue, J., Jester, E.L.E., Dickey, R.W. and Villareal, T.A. (2009). Nitrogen source effects on the growth and toxicity of two strains of the ciguatera-causing dinoflagellate *Gambierdiscus toxicus*. *Harmful Algae*, 8: 781-791.

Lassiter, A.M., Wilkerson, F.P., Dugdale, R.C. and Hogue, V.E. (2006). Phytoplankton assemblages in the CoOP-WEST coastal upwelling area. *Deep-Sea Research Part II*, 53: 3063-3077.

Lassus, P., Bardouil, M., Truquet, I., Truquet, P., Marcaillou, C. and Pierre, M.J. (1985). *Dinophysis acuminata distribution and toxicity along the southern Brittany coast (France): correlation with hydrological parameters*. In: D.M. Anderson, A.W. White and D.G. Baden (Eds.). Toxic Dinoflagellates. New York: Elsevier, Vol 18, p. 159-164.

Le Corre, P. and L' Helguen, S. (1993). Nitrogen source for uptake by *Gyrodinium* cf. *aureolum* in a tidal front. *Limnology and Oceanography*, 38(2): 446-451.

Legendre, L. and Le Fèvre, J. (1989). *Hydrodynamic singularities as controls of recycled versus export production in oceans*. In: W.H. Berger, V.S. Smetacek and G. Weger (Eds.). Productivity of the Ocean: Present and Past. Dahlem Workshop Report LS44. Chichester: Wiley, p. 49-63.

Lewis, N.D. (1984). *Ciguatera in the Pacific: Incidence and implications for marine resource development*. In: E.P. Ragelis (Ed). Seafood Toxins. American Chemical Society Symposium Series, Washington D.C., Vol 262, p. 289-306.

Lim, P.-T., Leaw, C.-P., Usup, G., Kobiyama, A., Koike, K. and Ogata, T. (2006). Effects of light and temperature on growth, nitrate uptake and toxin production of two tropical dinoflagellates *Alexandrium tamiyavanichii* and *Alexandrium minutum* (Dinophyceae). *Journal of Phycology*, 42: 786-799.

Lim, P.-T. and Ogata, T. (2005). Salinity effect on growth and toxin production of four tropical *Alexandrium* species (Dinophyceae). *Toxicon*, 46: 699-710.

Lippemeier, S., Frampton, D.M.F., Blackburn, S.I., Geier, S.C. and Negri, A.P. (2003). Influence of phosphorus limitation on toxicity and photosynthesis of *Alexandrium minutum* (Dinophyceae) monitored by in-line detection of variable chlorophyll fluorescence. *Journal of Phycology*, 38: 320-331.

Litchman, E., Klausmeier, C.A., Schofield, O.M. and Falkowski, P.G. (2007). The role of functional traits and trade-offs in structuring phytoplankton communities: scaling from cellular to ecosystem level. *Ecology Letters*, 10: 1170-1181.

Lomas, M.W. and Glibert, P.M. (1999). Temperature regulation of nitrate uptake: a novel hypothesis about nitrate uptake and reduction in cool-water diatoms. *Limnology and Oceanography*, 44: 556-572.

Lomas, M.W. and Glibert, P.M. (2000). Comparison of nitrate uptake, storage and reduction in marine diatoms and flagellates. *Journal of Phycology*, 36: 903-913.

Lomas, M.W., Glibert, P.M., Berg, G.M. and Burford, M. (1996). Characterization of nitrogen uptake by natural populations of *Aureococcus anophagefferens* (Chrysophyceae) as a function of incubation duration, substrate concentration, light, and temperature. *Journal of Phycology*, 32(6): 907-916.

López-Jamar, E., Cal, R.M., González, G., Hanson, R.B., Rey, J., Santiago, G. and Tenore, K.R. (1992). Upwelling and outwelling effects on the benthic regime of the continental shelf off Galicia, NW Spain. *Journal of Marine Research*, 50: 465-488.

Lundholm, N., Skov, J., Pocklington, R. and Moestrup, O. (1994). Domoic acid, the toxic amino acid responsible for amnesic shellfish poisoning, now in *Pseudo-nitzschia seriata* (Bacillariophyceae) in Europe. *Phycologia*, 33: 475-478.

MacIsaac, J.J. and Dugdale, R.C. (1969). The kinetics of nitrate and ammonia uptake by natural populations of marine phytoplankton. *Deep-Sea Research*, 14: 45-57.
MacIsaac, J.J., Dugdale, R.C., Barber, R.T., Blasco, D. and Packard, T. (1985). Primary production cycle in an upwelling center. *Deep-Sea Research*, 32: 503-529.
Maestrini, S.Y., Bechemin, C., Grzebyk, D. and Hummert, C. (2000). Phosphorus limitation might promote more toxin content in the marine invader dinoflagellate *Alexandrium minutum*. *Plankton Biology and Ecology*, 47(1): 7-11.
Maestrini, S.Y. and Bonin, D.J. (1981). *Competition among phytoplankton based on inorganic macronutrients*. In: T. Platt (Ed). Physiological Bases of Phytoplankton Ecology. Canadian Bulletin of Fisheries and Aquatic Science, Vol 210, p. 211-233.
Maguer, J.-F., L' Helguen, S., C., M., Labry, C. and Le Corre, P. (2007). Nitrogen uptake and assimilation kinetics in *Alexandrium minutum* (Dinophyceae): effect of N-limited growth rate on nitrate and ammonium interactions. *Journal of Phycology*, 43: 295-303.
Maguer, J.-F., Wafar, M., Madec, C., Morin, P. and Erard-Le Denn, E. (2004). Nitrogen and phosphorous requirements of an *Alexandrium minutum* bloom in the Penze Estuary, France. *Limnology and Oceanography*, 49(4): 1108-1114.
Marchetti, A., Trainer, V.L. and Harrison, P.J. (2004). Environmental conditions and phytoplankton dynamics associated with *Pseudo-nitzschia* abundance and domoic acid in the Juan de Fuca eddy. *Marine Ecology Progress Series*, 281: 1-12.
Margalef, R. (1978). Life-forms of phytoplankton as survival alternatives in an unstable environment *Oceanologica Acta*, 1: 493-509.
Margalef, R., Estrada, M. and Blasco, D. (1979). *Functional morphology of organisms involved in red tides, as adapted to decaying turbulence*. In: D. Taylor and H.H. Seliger (Eds.). Toxic dinoflagellate blooms. New York: Elsevier, p. 89-94.
Matsuda, A., Nishijima, T. and Fukami, K. (1999). Effects of nitrogenous and phosphorus nutrients on the growth of toxic dinoflagellate *Alexandrium catenella*. *Nippon Suisan Gakkaishi*, 65(5): 847-855.
Matthews, S.G. and Pitcher, G.C. (1996). *Worst recorded marine mortality on the South African coast*. In: T. Yasumoto, Y. Oshima and Y. Fukuyo (Eds.). Harmful and Toxic Algal Blooms. Paris: UNESCO, p. 89-92.
McCarthy, J.J. (1981). *The kinetics of nutrient utilization*. In: T. Platt (Ed). Physiological Bases of Phytoplankton Ecology. Canadian Bulletin of Fisheries and Aquatic Science, Vol 210, p. 211-233.
McCarthy, J.J., Taylor, W.R. and Taft, J.L. (1977). Nitrogenous nutrition of the plankton in the Chesapeake Bay. Part I. Nutrient availability and phytoplankton preferences. *Limnology and Oceanography*, 22: 996-1011.
McGregor, H.V., Dima, M., Fischer, H.W. and Mulitza, S. (2007). Rapid 20th-century increase in coastal upwelling off northwest Africa. *Science*, 315: 637-639.
Menden-Deuer, S. and Lessard, E.J. (2000). Carbon to volume relationships for dinoflagellates, diatoms and other protist plankton. *Limnology and Oceanography*, 45(3): 569-579.
Michaelis, L. and Menten, M. (1913). The kinetics of the inversion effect. *Biochemische Zeitschrift*, 49: 333-369.
Middelburg, J.J. and Nieuwenhuize, J. (2000). Uptake of dissolved inorganic nitrogen in turbid, tidal estuaries. *Marine Ecology Progress Series*, 192: 79-88.

Moita, M.T. (1993). *Development of toxic dinoflagellates in relation to upwelling patterns off Portugal*. In: T.J. Smayda and Y. Shimizu (Eds.). Toxic phytoplankton blooms in the sea. New York: Elsevier, p. 299-304.

Moita, M.T. and da Silva, A.J. (2000). *Dynamics of Dinophysis acuta, D. acuminata, D. tripos and Gymnodinium catenatum during an upwelling event off the Northwest coast of Portugal*. In: G.M. Hallegraeff, S.I. Blackburn, C.J. Bolch and R.J. Lewis (Eds.). Harmful Algal Blooms. Paris: Intergovernmental Oceanographic Commission of UNESCO, p. 169-173.

Monbet, Y. (1992). Control of phytoplankton biomass in estuaries: a comparative analysis of microtidal and macrotidal estuaries. *Estuaries*, 15(4): 563-571.

Monod, J. (1942). *Recherches sur la croissance des cultures bacteriennes*. Paris: Hermann.

Monteiro, P.M.S. and van der Plas, A.K. (2006). *Low Oxygen Water (LOW) variability in the Benguela System: Key processes and forcing scales relevant to forecasting*. In: V. Shannon, G. Hempel, P. Malanotte-Rizzoli, C. Moloney and J. Woods (Eds.). Benguela: predicting a large marine ecosystem. Large marine ecosystems, Amsterdam: Elsevier, Vol 14.

Montresor, M., Marino, D., Zingone, A. and Dafnis, G. (1990). *Three Alexandrium species from coastal Tyrrhenian waters (Mediterranean Sea)*. In: E. Granéli, B. Sundström, L. Edler and D.M. Anderson (Eds.). Toxic marine phytoplankton., New York: Elsevier, p. 82-87.

Morris, J. (2006). Is the occurrence of *Alexandrium minutum* in the Fal Estuary related to environmental and meteorological forcing? 3rd year undergraduate project, University of Southampton

Morris, J.G., Jr. (1999). *Pfiesteria*, "The cell from hell," and other toxic algal nightmares. *Clinical Infectious Diseases*, 28(6): 1191-1198.

Mulholland, M.R., Glibert, P.M., Berg, G.M., van Heukelem, L., Pantoja, S. and Lee, C. (1998). Extracellular amino acid oxidation by microplankton: A cross-ecosystem comparison. *Aquatic Microbial Ecology*, 15: 141-152.

Mulholland, M.R., Lee, C. and Glibert, P.M. (2003). Extracellular enzyme activity and uptake of carbon and nitrogen along an estuarine salinity and nutrient gradient. *Marine Ecology Progress Series*, 258: 3-17.

Muller, G., van Zyl, J., Hoffman, B. and Pitcher, G.C. (1998). Paralytic shellfish Poisoning (PSP): report of a major outbreak in the Western Cape. 13th European Symposium on Animal, Plant and Microbial Toxins, London.

Mulvenna, P.F. and Savidge, G. (1992). A modified manual method for the determination of urea in seawater using diacetylmonoxime reagent. *Estuarine, Coastal and Shelf Science*, 34(5): 429-438.

Murphy, J. and Riley, J.P. (1962). A modified single solution method for the determination of phosphate in natural waters. *Analytica Chimica Acta*, 27: 31-36.

Nascimento, S.M. (2003). Phytoplankton blooms and water quality of the Fleet Lagoon, Dorset, UK, including studies of isolated toxic strains of *Alexandrium minutum* and *Prorocentrum lima*. PhD Thesis, University of Southampton.

Nascimento, S.M., Purdie, D.A., Lilly, E.L., Larsen, J. & Morris, S. (2005). Toxin profile, pigment composition and large subunit rDNA phylogenetic analysis of an *Alexandrium minutum* (Dinophyceae) strain isolated from the Fleet lagoon, United Kingdom. *Journal of Phycology*, 41: 343-353.

Nelson, G. and Hutchings, L. (1983). The Benguela upwelling area. *Progress in Oceanography*, 12: 333-356.

Nezan, E., Belin, C., Lassus, P., Piclet, G. and Berthome, J.P. (1989). *Alexandrium minutum*: first PSP species occurrence in France. In: E. Granéli (Ed). 4th International Conference on Toxic Marine Phytoplankton, Lund, Sweden.

Nishitani, L. and Chew, K. (1988). PSP toxins in the Pacific coast states USA monitoring programs and effects on bivalve industries *Journal of Shellfish Research*, 7(4): 653-670.

Nogueira, E., Pérez, F.F. and Ríos, A.F. (1997). Seasonal patterns and long-term trends in an estuarine upwelling ecosystem (Ría de Vigo, NW Spain). *Estuarine, Coastal and Shelf Science*, 44: 285-300.

Nydahl, F. (1976). On the optimum conditions for the reduction of nitrate to nitrite by cadmium. *Talanta*, 23: 349-357.

Oshima, Y., Blackburn, S.I. and Hallegraeff, G.M. (1993). Comparative study on paralytic shellfish toxin profiles of the dinoflagellate *Gymnodinium catenatum* from three different countries. *Marine Biology*, 116(3): 471-476.

Ottway, B., Parker, M., McGrath, D. and Crowley, M. (1979). *Observations on a bloom of Gyrodinium aureolum Hulbert on the south coast of Ireland, summer 1976, associated with mortalities of littoral & sub-littoral organisms*, Irish Fisheries Investigations Series B, No 18, 1-9.

Palenik, B. and Morel, F.M.M. (1990). Comparison of cell-surface L-amino acid oxidases from several marine phytoplankton. *Marine Ecology Progress Series*, 59: 195-201.

Parsons, T.R., Maita, Y. and Lalli, C.M. (1984). *A manual of chemical and biological methods for seawater analysis*. Oxford: Pergamon Press.

Pazos, Y., Figueiras, F.G., Alvarez-Salgado, X.A. and Roson, G. (1995a). *The control of succession in red tide species in the Ria de Arousa (NW Spain) by upwelling and stability*. In: P. Lassus, G. Arzul, E. Erard-Le Denn, P. Gentien and C. Marcaillou-Le Baut (Eds.). Harmful Marine Algal Blooms. Paris: Lavoisier.

Pazos, Y., Figueiras, F.G., Alvarez Salgado, X.A. and Roson, G. (1995b). *Hydrographic situations and species associated with the appearance of Dinophysis acuta and their probable cysts in the Ria de Arousa*. In: P. Lassus, G. Arzul, E. Erard-Le Denn, P. Gentien and C. Marcaillou-Le Baut (Eds.). Harmful Marine Algal Blooms. Paris: Lavoisier, p. 651-656.

Percy, L. (2006). An investigation of the phytoplankton of the Fal Estuary, UK and the relationship between the occurrence of potentially toxic species and associated algal toxins in shellfish. PhD Thesis, University of Westminster.

Percy, L., Higman, W. and Lewis, J. (2004). The relationship between phytoplankton and algal toxins in shellfish, Fal Estuary UK. *Shellfish News*, 17: 21-22.

Perez Blanco, E., Lewis, J. and Aldridge, J. (2009). The germination characteristics of *Alexandrium minutum* (Dinophyceae), a toxic dinoflagellate from the Fal estuary (UK). *Harmful Algae*, 8: 518-522.

Pérez, F.F., Mouriño, C. and Fraga, F. (1986). *Influencia de los effluentes terrestres en los nutrientes de la Ría de Vigo*, Seminario de Quimica Marina: Servicio de Publicaciones, Universidad de Cadíz, 73-82.

Pérez, F.F., Mouriño, C., Fraga, F. and Ríos, A.F. (1993). Displacement of water masses and remineralization rates off the Iberian Peninsula by nutrient anomalies. *Journal of Marine Research*, 51: 869-892.

Pieterse, F. and van der Post, D.C. (1967). *Oceanographical conditions associated with red tides and fish mortalities in the Walvis Bay region*, Investigational Report of the Administration of South West Africa Marine Research Laboratory, No 14.

Pitcher, G.C., Bernard, S. and Ntuli, J. (2008). Contrasting bays and red tides in the Southern Benguela upwelling system. *Oceanography*, 21(3): 82-91.

Pitcher, G.C. and Boyd, A.J. (1996). *Across-shelf and alongshore dinoflagellate distributions and the mechanisms of red tide formation within the southern Benguela upwelling system*. In: T. Yasumoto, Y. Oshima and Y. Fukuyo (Eds.). Harmful and Toxic Algal Blooms. Paris: Intergovernmental Oceanographic Commission of UNESCO, p. 243-246.

Pitcher, G.C., Boyd, A.J., Horstman, D.A. and Mitchell-Innes, B.A. (1998). Subsurface dinoflagellate populations, frontal blooms and the formation of red tide in the southern Benguela upwelling system. *Marine Ecology Progress Series*, 172: 253-264.

Pitcher, G.C. and Calder, D. (2000). Harmful algal blooms of the southern Benguela current: a review and appraisal of monitoring from 1989 to 1997. *South African Journal of Marine Science*, 22: 255-271.

Pitcher, G.C., Cembella, A.D., Joyce, L.B., Larsen, J., Probyn, T.A. and Sebastian, C.R. (2007). The dinoflagellate *Alexandrium minutum* in Cape Town harbour (South Africa): Bloom characteristics, phylogenetic analysis and toxin composition. *Harmful Algae*, 6: 823-836.

Pitcher, G.C. and Cockcroft, A. (1998). *Low oxygen, rock lobster strandings and PSP*, Harmful Algal News, Paris: Intergovernmental Oceanographic Commission of UNESCO, 1-3.

Pitcher, G.C., Horstman, D.A. and Calder, D. (1993a). *Formation and decay of red tide blooms in the southern Benguela upwelling system during the summer of 1990/91*. In: T.J. Smayda and Y. Shimizu (Eds.). Toxic phytoplankton blooms in the sea. New York: Elsevier, p. 317-322.

Pitcher, G.C., Horstman, D.A., Calder, D., De Bruyn, J.H. and Post, B.J. (1993b). The first record of diarrhetic shellfish poisoning on the South African coast. *South African Journal of Science*, 89(10): 512-514.

Pitcher, G.C. and Matthews, S.G. (1996). *Noxious Gymnodinium species in South African waters*, Harmful Algae News, Paris: Intergovernmental Oceanographic Commission of UNESCO, 1-3.

Pitcher, G.C. and Nelson, G. (2006). Characteristics of the surface boundary layer important to the development of red tide on the southern Namaqua shelf of the Benguela upwelling system. *Limnology and Oceanography*, 51(6): 2660-2674.

Pitcher, G.C. and Weeks, S.J. (2006). *The variability and potential for prediction of Harmful Algal Blooms in the Southern Benguela Ecosystem*. In: V. Shannon, G. Hempel, P. Malanotte-Rizzoli, C. Moloney and J. Woods (Eds.). Benguela: Predicting a Large Marine Ecosystem. Large Marine Ecosystems, Amsterdam: Elsevier, Vol 14, p. 125-146.

Pollard, R.T. and Pu, S. (1985). Structure and ventilation of the upper Atlantic Ocean northeast of the Azores. *Progress in Oceanography*, 14: 443-462.

Pollingher, U. and Zemel, E. (1981). *In situ* and experimental evidence of the influence of turbulence on cell division processes of *Peridinium cinctum* forma *westii* (Lemm.) Lefevre. *British Phycological Journal*, 16: 281-287.

Popkiss, M.E.E., Horstman, D.A. and Harpur, D. (1979). Paralytic shellfish poisoning. A report of 17 cases in Cape Town. *South African Medical Journal*, 55(25): 1017-1023.

Prego, R. (1993). Biogeochemical patterns of phosphate in a Galician ria (Northwestern Iberian Peninsula). *Estuarine, Coastal and Shelf Science*, 37: 437-451.

Preston, T. and Owens, N.J.P. (1983). Interfacing an automatic elemental analyser with an isotope ratio mass spectrometer: the potential for fully automated total nitrogen and nitrogen-15 analysis. *Analyst*, 108: 971-977.

Probyn, T.A. (1985). Nitrogen uptake by size-fractionated phytoplankton populations in the southern Benguela upwelling system. *Marine Ecology Progress Series*, 22: 249-258.

Probyn, T.A. (1987). Ammonium regeneration by microplankton in an upwelling environment. *Marine Ecology Progress Series*, 37(1): 53-64.

Probyn, T.A. (1992). *The inorganic nitrogen nutrition of phytoplankton in the Southern Benguela: New production, phytoplankton size and implications for pelagic foodwebs*. In: A.I.L. Payne, K.H. Brink, K.H. Mann and R. Hilborn (Eds.). Benguela Trophic Functioning. South African Journal of Marine Science, Vol 12, p. 411-420.

Probyn, T.A., Pitcher, G.C., Monteiro, P.M.S., Boyd, A.J. and Nelson, G. (2000). Physical processes contributing to Harmful Algal Blooms in Saldanha Bay, South Africa. *South African Journal of Marine Science*, 22: 285-297.

Probyn, T.A., Pitcher, G.C., Pienaar, R.N. and Nuzzi, R. (2001). Brown tides and mariculture in Saldanha Bay. *Marine Pollution Bulletin*, 42(5): 405-408.

Proctor, N.H., Chan, S.L. and Trevor, A.J. (1975). Production of saxitoxin by cultures of *Gonyaulax catanella*. *Toxicon*, 13(1): 1-10.

Radan, R.L. (2008). Nitrogen uptake and domoic acid production by the toxigenic diatom *Pseudo-nitzschia multiseries*. MSc Thesis, San Francisco State University.

Raine, R., O'Boyle, S., O'Higgins, T., White, M., Patching, J., Cahill, B. and McMahon, T. (2001). A satellite and field portrait of a *Karenia mikimotoi* bloom off the South coast of Ireland, August 1998. *Hydrobiologia*, 465: 187-193.

Ranston, E.R., Webber, D.F. and Larsen, J. (2007). The first description of the potentially toxic dinoflagellate, *Alexandrium minutum* in Hunts Bay, Kingston Harbour, Jamaica. *Harmful Algae*, 6: 29-47.

Redfield, A.C. (1934). *On the proportion of organic derivatives in sea water and their relation to the composition of plankton*. James Johnston Memorial Volume. Liverpool: University Press of Liverpool, p. 176-192.

Reguera, B., Bravo, I., Marcaillou-Le Baut, C., Masselin, P., Fernandez, M.L., Miguez, A. and Martinez, A. (1993a). *Monitoring of Dinophysis spp. and vertical distribution of okadaic acid on mussel rafts in Ria de Pontevedra (NW Spain)*. In: T.J. Smayda and Y. Shimizu (Eds.). Toxic phytoplankton blooms in the sea. Amsterdam: Elsevier, p. 553-558.

Reguera, B., Marino, J., Campos, M.J., Bravo, I., Fraga, S. and Carbonell, A. (1993b). *Trends in the occurrence of Dinophysis spp. in Galician waters*. In: T.J. Smayda and Y. Shimizu (Eds.). Toxic Phytoplankton Blooms in the Sea., p. 559-564.

Reid, P.C. and Pratt, S. (1995). *A red tide event in the Fal Estuary, Cornwall*, Contract Report for the National Rivers Authority: Sir Alistair Hardy Foundation for Ocean Science.

Reynolds, C.S. (1980). Phytoplankton assemblages and their periodicity in stratifying lake systems. *Holarctic Ecology*, 3: 141-159.

Reynolds, C.S. (1984). Phytoplankton periodicity: the interactions of form, function and environmental variability. *Freshwater Biology*, 14: 111-142.

Reynolds, C.S. (1987). Community organization in the freshwater plankton. *Symposium of the British Ecological Society*, 27: 297-325.

Reynolds, C.S. (1988). *Functional morphology and the adaptive strategies of freshwater phytoplankton*. In: C.D. Sandgren (Ed). Growth and reproductive strategies of freshwater phytoplankton. Cambridge University Press, p. 388-433.

Reynolds, C.S. (1995). *Successional changes in the planktonic vegetation: species, structures, scales*. In: I. Joint (Ed). The molecular ecology of aquatic microbes. Berlin: Springer-Verlag, p. 115-132.

Rhodes, L., White, D., Syhre, M. and Atkinson, M. (1996). *Pseudo-nitzschia species isolated from New Zealand coastal waters: domoic acid production in vivo and links with shellfish toxicity*. In: T. Yasumoto, Y. Oshima and Y. Fukuyo (Eds.). Harmful and Toxic Algal Blooms. Paris: Intergovernmental Oceanographic Commission of UNESCO, p. 155-158.

Ríos, A.F. (1992). El Fitoplancton en la Ría de Vigo y sus Condiciones Ambientales. PhD Thesis, University of Santiago.

Rios, A.F., Fraga, F., Figueiras, F.G. and Perez, F.F. (1995). *New and regenerated production in relation to proliferations of diatoms and dinoflagellates in natural conditions*. In: P. Lassus, G. Arzul, E. Erard-Le Denn, P. Gentien and C. Marcaillou-Le Baut (Eds.). Harmful Marine Algal Blooms. Paris: Lavoisier, p. 663-668.

Ríos, A.F., Pérez, F.F. and Fraga, S. (1992). Water masses in the upper and middle North Atlantic Ocean east of the Azores. *Deep-Sea Research I*, 39: 645-658.

Roden, C.M., Lennon, H.J., Mooney, E., Leahy, P. and Lart, W. (1981). Red tides, water stratification and phytoplankton species succession around Sherkin Island, south-west Ireland. *Journal of Sherkin Island*, 1: 50-68.

Rodríguez, F., Fernández, E., Head, R.N., Harbour, D.S., Bratbak, G., Heldal, M. and Harris, R.P. (2000). Temporal variability of viruses, bacteria, phytoplankton and zooplankton in the Western English Channel off Plymouth. *Journal of the Marine Biological Association UK*, 80(4): 575-586.

Rowe, G.T., Clifford, C.H., Smith, K.L. and Hamilton, P.L. (1977). Regeneration of nutrients in sediments off Cape Blanc, Spanish Sahara. *Deep-Sea Research*, 24: 57-64.

Ryther, J.H. (1969). Photosynthesis and fish production in the sea. *Science*, 166: 72-76.

Ryther, J.H. and Dunstan, W.M. (1971). Nitrogen, phosphorous and eutrophication in the coastal marine environment. *Science*, 171: 1008-1013.

Sahlsten, E. (1987). Nitrogenous nutrition in the euphotic zone of the central North Pacific gyre. *Marine Biology*, 96: 433-439.

Sapeika, N. (1948). Mussel poisoning. *South African Medical Journal*, 22: 337-338.

Sapeika, N. (1958). Mussel poisoning: a recent outbreak. *South African Medical Journal*, 32: 527.

Satake, M., Ichimura, T., Sekiguchi, K., Yoshimatsu, S. and Oshima, Y. (1999). Confirmation of yessotoxin and 45,46,47-trinoryessotoxin production by *Protoceratium reticulatum* collected in Japan. *Natural Toxins*, 7(4): 147-150.

Satake, M., Ofuji, K., Naoki, H., James, K.J., Furey, A., McMahon, T., Silke, J. and Yasumoto, T. (1998). Azaspiracid, a new marine toxin, having unique spiro ring assemblies, isolated from Irish mussels, *Mytilus edulis*. *Journal of the American Chemical Society* 9967-9968.

Scatasta, S., Stolte, W., Granéli, E., Weikard, H.P. and van Ierl, E. (2003). *Harmful algal blooms in European marine water: socio-economic analysis of selected case studies*, Thrid deliverable for the EU-funded project ECOHARM.

Schnitzler-Parker, M. and Armbrust, E.V. (2005). Synergistic effects of light, temperature and nitrogen source on transcription of genes for carbon and

nitrogen metabolism in the centric diatom *Thalassiosira pseudonana* (Bacillariophyceae). *Journal of Phycology*, 41: 1142-1153.

Schoemann, V., Becquevort, S., Stefels, J., Rousseau, V. and Lancelot, C. (2005). *Phaeocystis* blooms in the global ocean and their coontrolling mechanisms: a review. *Journal of Sea Research*, 53: 43-66.

Scholin, C.A., Gulland, F., Doucette, G.J., Benson, S., Busman, M., Chavez, F.P., Cordaro, J., DeLong, R., De Vogelaere, A., Harvey, J., Haulena, M., Lefebvre, K., Lipscomb, T., Loscutoff, S., Lowenstine, L.J., Marin, R., Miller, P.E., McLellan, W.A., Moeller, P.D.R., Powell, C.L., Rowles, T., Silvagni, P., Silver, M., Spraker, T., Trainer, V. and Van Dolah, F.M. (2000). Mortality of sea lions along the central California coast linked to a toxic diatom bloom. *Nature*, 403(6765): 80-84.

Serra, J.L., Llama, M.J. and Cadenas, E. (1978). Nitrate utilization by the diatom *Skeletonema costatum*. I. Kinetics of nitrate uptake. *Plant Physiology*, 62: 987-990.

Shannon, C.E. (1948). A mathematical theory of communication. *Bell System Technical Journal*, 27: 379-423 and 623-656.

Shannon, L.V. (1966). *Hydrology of the South and West coasts of South Africa*, Investigational Report of the Division of Sea Fisheries South Africa, No 58.

Shannon, L.V. (1985a). The Benguela Ecosystem Part I. Evolution of the Benguela, physical features and processes. *Oceanography and Marine Biology. An Annual Review*, 23: 105-182.

Shannon, L.V. (1985b). The Benguela Ecosystem Part II. Chemistry and related processes. *Oceanography and Marine Biology. An Annual Review*, 23: 183-251.

Shannon, L.V. (2001). *Benguela Current*. In: J. Steele, S. Thorpe and K. Turekian (Eds.). Encyclopedia of Ocean Sciences. London: Academic Press, Vol 1, p. 255-267.

Shannon, L.V. and Anderson, F.P. (1982). Applications of satellite ocean colour imagery in the study of the Benguela current system. *South African Journal of Photogrammetry, Remote Sensing and Cartography*, 13: 153-169.

Shaw, P.J., Purdie, D.A., de Frietas, P.S., Rees, A.P. and Joint, I. (1998). Nutrient uptake in a highly turbid estuary (th Humber, United Kingdom) and adjacent coastal waters. *Estuaries*, 21(4A): 507-517.

Sherer, C. (1965). *Rhizosolenia stolterfothii Peragallo*, Leaflet Series: Plankton, St. Petersburg, Florida: Florida Board of Conservation, Division of Salt Water Fisheries, Marine Laboratory, No Vol. 1, No. 7.

Shimizu, Y., Watanabe, N. and Wrensford, G. (1995). *Biosynthesis of brevetoxins and heterotrophic metabolism in Gymnodinium breve*. In: P. Lassus, G. Arzul, E. Erard-Le Denn, P. Gentien and C. Marcaillou-Le Baut (Eds.). Harmful marine algal blooms. Paris: Lavoisier, p. 351-358.

Shimizu, Y. and Wrensford, G. (1993). *Peculiarities in the biosynthesis of brevetoxins and metabolism of Gymnodinium breve*. In: T.J. Smayda and Y. Shimizu (Eds.). Toxic Phytoplankton Blooms in the Sea. New York: Elsevier, p. 919-923.

Sinclair, G., Kamykowski, D. and Glibert, P.M. (2009). Growth, uptake and assimilation of ammonium, nitrate, and urea, by three strains of *Karenia brevis* grown under low light. *Harmful Algae*, 8: 770-780.

Siu, G.K.Y., Young, M.L.C. and Chan, D.K.O. (1997). Environmental and nutritional factors which regulate population dynamics and toxin production in the dinoflagellate *Alexandrium catenella*. *Hydrobiologia*, 352(1-3): 117-140.

Smaal, A.C. and Prins, T.C. (1993). *The uptake of organic matter and the release of inorganic nutrients by bivalve suspension feeder beds*, NATO ASI Series, Springer-Verlag, Berlin, No G33, 271-298.

Smayda, T.J. (1980). *Phytoplankton species succession*. In: I. Morris (Ed). Studies in Ecology. Oxford: Blackwell, Vol 7, p. 493-570.

Smayda, T.J. (1997). Harmful algal blooms: Their ecophysiology and general relevance to phytoplankton blooms in the sea. *Limnology and Oceanography*, 42(5): 1137-1153.

Smayda, T.J. (2000). Ecological features of harmful algal blooms in coastal upwelling ecosystems. *South African Journal of Marine Science*, 22: 219-253.

Smayda, T.J. and Reynolds, C.S. (2001). Community assembly in marine phytoplankton: application of recent models to harmful dinoflagellate blooms. *Journal of Plankton Research*, 23(5): 447-461.

Smayda, T.J. and Trainer, V. (submitted). Distribution, adaptation and selection of harmful algal bloom species in upwelling systems. *Progress in Oceanography*.

Sobrino Buhigas, R. (1918). La purga de mar o hematotalasia. *Memorias de la Real Sociedad Espanola de Historia Natural*, 10: 407-458.

Sommer, U. (1984). The paradox of the plankton - fluctuations of phosphorus availability maintain diversity of phytoplankton in flow-through cultures. *Limnology and Oceanography*, 29(3): 633-636.

Sommer, U. (1989). *The role of competition for resources in phytoplankton succession*. In: U. Sommer (Ed). Plankton ecology: Succession in phytoplankton communities. Springer, p. 57-106.

Sommer, U. (1994). Are marine diatoms favoured by high Si:N ratios? *Marine Ecology Progress Series*, 115: 309-315.

Sordo, I.S., Pazos, Y., Triñanes, J.A. and Maneiro, J. (2000). *The advection of a toxic bloom of Gymnodinium catenatum to the Galician Rias, detected from SST satellite images*. In: G.M. Hallegraeff, S.I. Blackburn, C.J. Bolch and R.J. Lewis (Eds.). Harmful Algal Blooms. Intergovernmental Oceanographic Commission of UNESCO.

Stark, J.M. and Hart, S.C. (1996). Diffusion technique for preparing salt solutions, Kjeldahl digests, and persulfate digests for nitrogen-15 analysis. *Soil Science Society of America Journal*, 60(6): 1846-1855.

Steidinger, K.A. and Tangen, K. (1996). *Dinoflagellates*. In: C.R. Tomas (Ed). Identifying Marine Diatoms and Dinoflagellates. New York: Academic Press, p. 387-598.

Steidinger, K.A., Vargo, G.A., Tester, P.A. and Tomas, C.R. (1998). *Bloom dynamics and physiology of Gymnodinium breve with emphasis on the Gulf of Mexico*. In: D.M. Anderson, A.D. Cembella and G.M. Hallegraeff (Eds.). Physiological ecology of Harmful Algal Blooms. Vol 41, p. 133-153.

Stolte, W. and Riegman, R. (1996). The relative preference index (RPI) for phytoplankton nitrogen use is only weakly related to physiological preference. *Journal of Plankton Research*, 18(6): 1041-1045.

Stubbs, B., Coates, L., Milligan, S., Morris, S., Higman, W. and Algoet, M. (2008). *Biotoxin monitoring programme for England and Wales -1st April 2007 to 31st March 2008*, Shellfish News: CEFAS, 35-38.

Stubbs, B., Milligan, S., Morris, S. and Algoet, M. (2007). *Biotoxin monitoring programme for England and Wales 1st June 2006 to 31st March 2007*, Shellfish News: CEFAS, 48-51.

Sverdrup, H.U., Johnson, M.W. and Fleming, R.H. (1942). *The Oceans*. Englewood Cliffs, NJ: Prentice-Hall.

Syrett, P.J. (1981). *Nitrogen metabolism of microalgae*. In: T. Platt (Ed). Physiological bases of phytoplankton ecology. Canadian Bulletin of Fisheries and Aquatic Science, Vol 210, p. 182-210.

Syrett, P.M. and Morris, I. (1963). The inhibition of nitrate assimilation by ammonium in *Chlorella*. *Biochimica et Biophysica Acta*, 67: 566-575.

Syvertsen, E.E. and Hasle, G.R. (1983). The diatom genus *Eucampia*: Morphology and taxonomy. *Bacillaria*, 6: 169-210.

Thessen, A.E., Bowers, H.A. and Stoeker, D.K. (2009). Intra- and interspecies differences in growth and toxicity of *Pseudo-nitzschia* whie using different nitrogen sources. *Harmful Algae*, 8: 792-810.

Thomas, W.H. (1970a). Effect of ammonium and nitrate concentration on chlorophyll increases in natural tropical Pacific phytoplankton populations. *Limnology and Oceanography*, 15: 386-394.

Thomas, W.H. (1970b). On nitrogen deficiency in tropical Pacific oceanic phytoplankton: Photosynthetic parameters in poor and rich water. *Limnology and Oceanography*, 15: 380-385.

Thomas, W.H. and Gibson, C.H. (1990). Quantified small-scale turbulence inhibits a red-tide dinoflagellate *Gonyaulax polyedra* Stein. *Deep-Sea Research Part I*, 37: 1583-1593.

Thomas, W.H. and Gibson, C.H. (1992). Effects of quantified small-scale turbulence on the dinoflagellate, *Gymnodinium sanguineum* (*splendens*): Contrasts with *Gonyaulax* (*Lingulodinium*) *polyedra*, and the fishery implication. *Deep-Sea Research*, 39(7-8A): 1429-1437.

Tilman, D. (1977). Resource competition between planktonic algae: An experimental and theoretical approach. *Ecology*, 58: 338-348.

Tilman, D., Kilham, S.S. and Kilham, P. (1982). Phytoplankton community ecology: The role of limiting nutrients. *Annual Review of Ecology and Systematics*, 13: 349-372.

Tilstone, G.H., Figueiras, F.G. and Fraga, F. (1994). Upwelling-downwelling sequences in the generation of red tides in a coastal upwelling system. *Marine Ecology Progress Series*, 112: 241-253.

Torres-Valdés, S. and Purdie, D.A. (2006). Nitrogen removal by phytoplankton uptake through a temperate non-turbid estuary. *Estuarine, Coastal and Shelf Science*, 70(473-486).

Touzet, N., Franco, J.M. and Raine, R. (2007). Influence of inorganic nutrition on growth and PSP toxin production of *Alexandrium minutum* (Dinophyceae) from Cork Harbour, Ireland. *Toxicon*, 50: 106-119.

Touzet, N., Paz Pino, B., Riobo Agulla, P., Franco, J.M. and Raine, R. (2006). *Morphology, phylogeny and PSP toxin composition of Alexandrium spp. isolated from Irish coastal waters*. Proceedings of the Fifth International Conference on Molluscan Shellfish Safety. p. 248-252.

Toyoshima, T., M., S., Ozaki, H.S., Okaichi, T. and Murakami, T.H. (1989). *Histological alterations to gills of the yellowtail Seriola quinqueradiata, following exposure to the red tide species Chattonella antiqua* In: T. Okaichi, D.M. Anderson and T. Nemoto (Eds.). Red Tides, Biology, Environmental Science, and Toxicology. Amsterdam: Elsevier, p. 439-442.

Trainer, V., Adams, N.G., Bill, B.D., Anulacion, B.F. and Wekell, J.C. (1998). Concentration and dispersal of a *Pseudo-nitzschia* bloom in Penn Cove, Washington, USA. *Natural Toxins*, 6: 1-13.

Trainer, V.L., Adams, N.G. and Wekell, J.C. (2001). *Domoic acid- producing Pseudo-nitzschia species off the US West coast associated with toxification events* In: G.M. Hallegraeff, S.I. Blackburn, C.J. Bolch and R.J. Lewis (Eds.). Harmful Algal Blooms. Intergovernmental Oceanographic Commission of UNESCO, p. 46-49.

Trainer, V.L., Cochlan, W.P., Erickson, A., Bill, B.D., Cox, F.H., Borchert, J.A. and Lefebvre, K.A. (2007). Recent domoic acid closures of shellfish harvest areas in Washington State inland waterways. *Harmful Algae*, 6(3): 449-459.

Trainer, V.L., Hickey, B.M. and Horner, R.A. (2002). Biological and physical dynamics of domoic acid production off the Washington coast. *Limnology and Oceanography*, 47(5): 1438-1446.

Treguer, P. and Le Corre, P. (1979). The ratios of nitrate, phosphate and silicate during uptake and regeneration phases of the Moroccan upwelling regime. *Deep-Sea Research*, 26: 163-184.

Tyrrell, T. and Law, C.S. (1997). Low nitrate:phosphate ratios in the global ocean. *Nature*, 387: 793-796.

Tyrrell, T. and Lucas, M.I. (2002). Geochemical evidence of denitrification in the Benguela upwelling system. *Continental Shelf Research*, 22: 2497-2511.

Utermöhl, H. (1958). Zur vervollkommung der quantitative phytoplankton metodik. *Mitteilungen Internationale Vereinigung für Theoretische und Angewandte Limnologie*, 9: 1-38.

van Egmond, H.P., van Apeldoorn, M.E. and Speijers, G.J.A. (2004). *Marine Biotoxins*, Food and Nutrition Paper, Rome: Food and Agriculture Organisation of the United Nations, No 80.

van Lenning, K., Vila, M., Maso, M., Garces, E., Angles, S., Sampedro, N., Morales-Blake, A. and Camp, J. (2007). Short-term variations in development of a recurrent toxic *Alexandrium minutum*- dominated dinoflagellate bloom induced by meteorological conditions. *Journal of Phycology*, 43: 892-907.

Varela, D.E. and Harrison, P.J. (1999). Effect of ammonium on nitrate utilization by *Emiliania huxleyi*, a coccolithophore from the oceanic northeastern Pacific. *Marine Ecology Progress Series*, 186: 67-74.

Vila, M., Giacobbe, M.G., Maso, M., Gangemi, E., Penna, A., Sampedro, N., Azzaro, F., Camp, J. and Galluzzi, L. (2005). A comparative study on recurrent blooms of *Alexandrium minutum* in two Mediterranean coastal areas. *Harmful Algae*, 4(4): 673-695.

Wafar, M.V.W., Le Corré, P. and Birrien, J.L. (1989). Transport of carbon, nitrogen and phosphorous in a Brittany River, France. *Estuarine, Coastal and Shelf Science*, 29(489-500).

Walz, P.M., Garrison, D.L., Graham, W.M., Cattey, M.A., Tjeerdema, R.S. and Silver, M.W. (1994). Domoic acid-producing diatoms in Monterey Bay, California: 1991-1993. *Natural Toxins*, 2: 271-279.

Weeks, S.J., Currie, B., Bakun, A. and Peard, K.R. (2004). Hydrogen sulphide eruptions in the Atlantic Ocean off southern Africa: implications of a new view based on SeaWiFS satellite imagery. *Deep-Sea Research Part I*, 51: 153-157.

Weise, A.M., Levasseur, M., Saucier, F.J., Senneville, S., Bonneau, E., Roy, S., Sauvé, G., Michaud, S. and Fauchot, J. (2002). The link between precipitation, river

runoff and blooms of the toxic dinoflagellate *Alexandrium tamarense* in the St. Lawrence. *Canadian Journal of Fisheries and Aquatic Science*, 59(3): 464-473.

Weiss, R.F. (1970). Solubility of nitrogen, oxygen and argon in water and seawater. *Deep-Sea Research*, 17(4): 721-735.

Welschmeyer, N.A. (1994). Fluorometric Analysis of Chlorophyll-a in the Presence of Chlorophyll-B and Pheopigments. *Limnology and Oceanography*, 39(8): 1985-1992.

Wheeler, P.A., Glibert, P.M. and McCarthy, J.J. (1982). Ammonium uptake and incorporation by Chesapeake Bay phytoplankton: Short-term uptake kinetics. *Limnology and Oceanography*, 27: 1113-1128.

Wheeler, P.A. and Kokkinakis, S.A. (1990). Ammonium recycling limits nitrate use in the oceanic subarctic Pacific. *Limnology and Oceanography*, 35: 1267-1278.

White, A. (1976). Growth inhibition caused by turbulence in the toxic marine dinoflagellate *Gonyaulax excavata*. *Journal of the Fisheries Research Board of Canada*, 33: 2598-2602.

White, A.W. (1978). Salinity effects on growth and toxin content of *Gonyaulax excavata* - a marine dinoflagellate causing paralytic shellfish poisoning. *Journal of Phycology*, 14(4): 475-479.

Work, T.M., Beale, A.M., Fritz, L., Quilliam, M.A., Silver, M.W., Buck, K.R. and Wright, J.L. (1992). Domoic acid intoxification in brown pelicans and cormorants in Santa Cruz, California. In: T.J. Smayda (Ed). Fifth International Conference on Toxic Phytoplankton, Elsevier, p. 643.

Wyatt, T. and Reguera, B. (1989). Historical trends in the red tide phenomenon in the Rias Bajas of Northwest Spain. In: T. Okaichi, D.M. Anderson and T. Nemoto (Eds). Red Tides: Biology, Environmental Science, and Toxicology. Proceedings of the First International Symposium On Red Tides, Takamatsu, Kagawa Prefecture, Japan. p. 33-36.

Yamamoto, T., Oh, S.J. and Yakaoka, Y. (2004). Growth and uptake kinetics for nitrate, ammonium and phosphate by the toxic dinoflagellate *Gymnodinium catenatum* isolated from Hiroshima Bay, Japan. *Fisheries Science*, 70: 108-115.

Yool, A., Martin, A.P., Fernandez, C. and Clark, D.R. (2007). The significance of nitrification for oceanic new production. *Nature*, 447: 999-1002.

Yoshida, T., Sako, Y. and Uchida, A. (2001). Geographic differences in paralytic shellfish poisoning toxin profiles among Japanese populations of *Alexandrium tamarense* and *A. catenella* (Dinophyceae). *Phycological Research*, 49(1): 13-21.